USGS
science for a changing world

Prepared in cooperation with the U.S. Army Corps of Engineers and in collaboration with the State of Alabama and the National Fish and Wildlife Foundation

Predicting Barrier Island Habitats and Oyster and Seagrass Habitat Suitability for Various Restoration Measures and Future Conditions for Dauphin Island, Alabama

Open-File Report 2020–1003

U.S. Department of the Interior
U.S. Geological Survey

Predicting Barrier Island Habitats and Oyster and Seagrass Habitat Suitability for Various Restoration Measures and Future Conditions for Dauphin Island, Alabama

Edited by Nicholas M. Enwright, Hongqing Wang, P. Soupy Dalyander, and Elizabeth Godsey

Chapter A

Landscape-Position-Based Habitat Modeling for the Alabama Barrier Island Restoration Feasibility Assessment at Dauphin Island

By Nicholas M. Enwright, Lei Wang, Hongqing Wang, P. Soupy Dalyander, Michael J. Osland, Spencer J. Stelly, Rangley C. Mickey, Laura C. Feher, Sinéad M. Borchert, and Richard H. Day

Chapter B

Oyster Habitat Suitability Modeling for the Alabama Barrier Island Restoration Feasibility Assessment at Dauphin Island

By Hongqing Wang, Nicholas M. Enwright, Thomas M. Soniat, Jason E. Herrmann, Megan K. La Peyre, Sung-Chan Kim, Barry Bunch, Spencer J. Stelly, P. Soupy Dalyander, and Rangley C. Mickey

Chapter C

Seagrass Habitat Suitability Modeling for the Alabama Barrier Island Restoration Feasibility Assessment at Dauphin Island

By Hongqing Wang, Nicholas M. Enwright, Kelly M. Darnell, Megan K. La Peyre, Just Cebrian, Sung-Chan Kim, Barry Bunch, Spencer J. Stelly, Brady R. Couvillion, P. Soupy Dalyander, Rangley C. Mickey, and Martha Segura

Prepared in cooperation with the U.S. Army Corps of Engineers and in collaboration with the State of Alabama and the National Fish and Wildlife Foundation

Open-File Report 2020–1003

U.S. Department of the Interior
U.S. Geological Survey

U.S. Department of the Interior
DAVID BERNHARDT, Secretary

U.S. Geological Survey
James F. Reilly II, Director

U.S. Geological Survey, Reston, Virginia: 2020

Suggested citation:
Enwright, N.M., Wang, H., Dalyander, P.S., and Godsey, E., eds., 2020, Predicting barrier island habitats and oyster and seagrass habitat suitability for various restoration measures and future conditions for Dauphin Island, Alabama: U.S. Geological Survey Open-File Report 2020–1003, 99 p., https://doi.org/10.3133/ofr20201003.

Associated data for this publication:
Enwright, N.M., Wang, L., Wang, H., Dalyander, P.S., Osland, M.J., Stelly, S.J., Mickey, R.C., Feher, L.C., Borchert, S.M., and Day, R.H., 2020, Landscape position-based habitat modeling for the Alabama Barrier Island feasibility assessment at Dauphin Island: U.S. Geological Survey data release, https://doi.org/10.5066/P9PK0EH0.

Wang, H., Enwright, N.M., Darnell, K.M., LaPeyre, M.K., Cebrian, J., Kim, S.-C., Bunch, B., Stelly, S.J., Couvillion, B.R., Dalyander, P.S., Mickey, R.C., and Segura, M., 2020, Seagrass habitat suitability modeling for the Alabama Barrier Island restoration assessment at Dauphin Island: U.S. Geological Survey data release, https://doi.org/10.5066/P9B32VTE.

Wang, H., Enwright, N.M., Soniat, T.M., Hermann, J.E., LaPeyre, M.K., Kim, S.-C., Bunch, B., Stelly, S.J., Dalyander, P.S., and Mickey, R.C., 2020, Oyster habitat suitability modeling for the Alabama Barrier Island restoration assessment at Dauphin Island: U.S. Geological Survey data release, https://doi.org/10.5066/P9O30XMZ.

ISSN 2331-1258 (online)

Acknowledgments

This effort was one component of a larger effort funded by the National Fish and Wildlife Foundation (project identifier 45719) to investigate viable, sustainable restoration options that protect and restore the natural resources of Dauphin Island, Alabama. This effort was completed in cooperation with the U.S. Army Corps of Engineers and in collaboration with the State of Alabama and the National Fish and Wildlife Foundation. We thank Yi Qiang from the University of Hawaii and Nina Lam from Louisiana State University for guidance on using MATLAB for machine learning with geospatial datasets. We thank Claudia Laurenzano from Cherokee Nation Technologies for her assistance with formatting and data processing for this report.

We also thank Stephen Hartley, Michelle Fischer, Sarai Piazza, Ann Hijuelos, Holly Beck, and Simeon Yurek from the U.S. Geological Survey for reviewing sections of this report.

Contents

Figures

Tables

Conversion Factors

International System of Units to U.S. customary units

Multiply	By	To obtain
	Length	
meter (m)	3.281	foot (ft)
kilometer (km)	0.6214	mile (mi)
	Area	
square meter (m^2)	0.0002471	acre
square meter (m^2)	10.76	square foot (ft^2)
hectare (ha)	2.471	acre
hectare (ha)	0.003861	square mile (mi^2)
square kilometer (km^2)	247.1	acre
square kilometer (km^2)	0.3861	square mile (mi^2)

Temperature in degrees Celsius (°C) may be converted to degrees Fahrenheit (°F) as °F = (1.8 × °C) + 32.

Temperature in degrees Fahrenheit (°F) may be converted to degrees Celsius (°C) as °C = (°F – 32) / 1.8.

Datum

Vertical coordinate information is referenced to the North American Vertical Datum of 1988 GEOID 12a (NAVD 88 Geoid 12a), unless otherwise noted. Horizontal coordinate information is referenced to the North American Datum of 1983 Universal Transverse Meter Zone 16 North (NAD 83 UTM 16N). Elevation, as used in this report, refers to distance above the vertical datum, unless otherwise noted.

Supplemental Information

Concentrations of chemical constituents in water are given in either milligrams per liter (mg/L) or micrograms per liter (µg/L).

Abbreviations

>	greater than
≥	greater than or equal to
<	less than
≤	less than or equal to
ADCNR	Alabama Department of Conservation and Natural Resources
CE–QUAL–ICM	U.S. Army Corps of Engineers Integrated Compartment Water Quality Model
CH3D–WES	Curvilinear Hydrodynamics in 3 Dimensions—Waterway Experiment Station version
CoNED	Coastal National Elevation Database
DEM	digital elevation model
DO	dissolved oxygen
EHWS	extreme high water springs tide level
GULN	Gulf Coast Inventory and Monitoring Network
HSI	habitat suitability index
lidar	light detection and ranging
LSU	Louisiana State University
NAVD 88	North American Vertical Datum of 1988
NPS	National Park Service
ppt	parts per thousand
REI	relative wave exposure index
SLR	sea-level rise
TBDEM	topobathymetric digital elevation model
TPI	topographic position index
USACE	U.S. Army Corps of Engineers
USGS	U.S. Geological Survey

Predicting Barrier Island Habitats and Oyster and Seagrass Habitat Suitability for Various Restoration Measures and Future Conditions for Dauphin Island, Alabama

Executive Summary

By Nicholas M. Enwright and Hongqing Wang

Barrier islands are subaerial landforms consisting of wave-, wind-, and (or) tide-deposited sediments located along parts of coasts on every continent except Antarctica. These systems provide numerous invaluable ecosystem services including storm damage reduction and erosion control to the mainland, habitat for fish and wildlife, carbon sequestration in marshes, water catchment and purification, recreation, and tourism. Barrier islands also are critical to estuarine seagrass and oyster habitats because of their ability to indirectly regulate salinity in the adjacent estuarine water bodies and limit the exposure to high-energy waves. These islands are dynamic environments that are gradually shaped by currents, waves, and tides under quiescent conditions yet can evolve in the time scale of hours to days during hurricanes and other extreme storms. The ecosystems associated with these islands also face numerous other hazards, including accelerated sea-level rise (SLR), oil spills, and anthropogenic stressors, with climate-related threats predicted to likely increase in the future.

Hurricane Katrina in 2005 and the Deepwater Horizon oil spill in 2010 are two major events that have affected habitats and natural resources on Dauphin Island, Alabama. The latter event prompted a collaborative effort between the U.S. Geological Survey, the U.S. Army Corps of Engineers, and the State of Alabama, funded by the National Fish and Wildlife Foundation, to investigate viable, sustainable restoration measures that reduce degradation and enhance the natural resources of Dauphin Island, Ala. The overarching goal of the Alabama Barrier Island Restoration Feasibility Assessment project was to document baseline conditions and forecast potential conditions under varying sea-level change and storm scenarios for a no-action alternative along with a variety of restoration measures including beach and dune restoration, marsh and back-barrier restoration, and placement of sand in the littoral zone.

Restoration and engineering (that is, development of seawalls, groins, and breakwaters; beach and dune nourishment vegetation planting; and marsh restoration) are often executed to limit issues associated with natural hazards to populated areas or restore and enhance habitat for fish and wildlife and (or) recreational use. Typically, the goal for any restoration effort is to meet a suite of desired objectives while also ensuring natural coastal processes can continue, which can help maximize the sustainability of the system. Because climate-related threats to barrier islands are expected to increase in the future, it is imperative to make decisions about restoration measures based on the best available knowledge regarding possible sustainability. In response, the modeling component of the Alabama Barrier Island Restoration Feasibility Assessment project used decadal hydrodynamic geomorphic, water quality, and habitat modeling to understand how the various restoration measures may affect the habitat composition, sustainability, and resiliency of Dauphin Island under varying potential future scenarios.

Many abiotic factors affect the performance of foundation plant species, including wave energy, salinity, inundation frequency, sea spray, Aeolian transport, and nutrient availability. The spatial distribution of these characteristics is a function of island geomorphology, which therefore plays a critical role in the distribution of barrier island habitats because foundation species, such as *Spartina patens* (Aiton) Muhl. (saltmeadow cordgrass), *Uniola paniculata* L. (sea oats), and *Pinus elliottii* (slash pine), tend to thrive in certain topographic settings and (or) disturbance regimes. Although researchers have studied the relation between landscape position, such as elevation and distance from shoreline and barrier island habitats, little work has been done to leverage habitat-landscape-position linkages for barrier island habitat prediction. The initial step in the habitat modeling effort was developing a baseline habitat map to better understand current conditions and use these data to help understand the relation between landscape position and contemporary barrier island habitats. This related effort was covered in U.S. Geological Survey Open-File Report 2017–1083.

Geocomputational models were developed for each tidal regime (that is, subtidal, intertidal, supratidal/upland) to predict barrier island habitats from landscape-position

information, including elevation, relative topography, and distance from shore. The habitat modeling effort involved a three-step process. First, a contemporary habitat model was developed using landscape information from the best available high-resolution topography information. Second, the contemporary habitat model was calibrated from contemporary high-resolution topography data to modeled topobathymetry developed using hydrodynamic geomorphic modeling. Finally, this calibrated model was used to forecast habitats for future conditions using simulated decadal hydrodynamic geomorphic model outputs.

Habitat suitability index (HSI) models can be used as a screening or risk assessment tool by coastal restoration and resource managers to efficiently manage restoration activities to achieve barrier island restoration while also reducing degradation and (or) enhancing the habitat suitability for critical estuarine and marine species. In addition to spatially explicit habitat predictions, we used HSI models to forecast habitat suitability for oysters and seagrass based on water quality model predictions and information extracted or produced from the hydrodynamic geomorphic model outputs. We used literature and expert opinion to develop the initial HSI models. Both models were calibrated and validated using in situ ecological field data and water quality data.

Results from this effort are included in three chapters (chapters A–C). Any action in ecosystem restoration, including the no-action alternative, often has tradeoffs. Another component of the Alabama Barrier Island Restoration Feasibility Assessment project, presented elsewhere, integrates these habitat model results into a structured decision-making framework that accounts for competing objectives to determine the most appropriate barrier island restoration measures based on any given suite of objectives or desired outcomes. Collectively, this information provides insights to natural resource managers and planners on how a restoration measure may maintain or impede natural coastal processes and provides information critical for making future-focused decisions regarding barrier island restoration.

Chapter A. Landscape-Position-Based Habitat Modeling for the Alabama Barrier Island Restoration Feasibility Assessment at Dauphin Island

A barrier island habitat prediction model was used to forecast barrier island habitats (for example, beach, dune, intertidal marsh, and woody vegetation) for Dauphin Island, Ala. Forecasts were made to estimate habitat coverage for future potential island configurations associated with a variety of restoration measures and varying future conditions of storminess and sea levels. The habitat model framework was loosely coupled with decadal hydrodynamic geomorphic model outputs to forecast habitats for 2 potential future conditions related to storminess (that is, “medium” storminess and “high” storminess based on storm climatology data) and 4 sea-level scenarios (that is, an increase in sea level of 0.3 meter [m] between 2030 and 2050 and about 1.0 m between 2070 and 2128). These SLR scenarios followed two SLR curves: the U.S. Army Corps of Engineers intermediate SLR curve (0.7 m by 2100) and high SLR curve (1.7 m by 2100). The hydrodynamic geomorphic modeling was quasi-static, using an elevated offshore water level to capture effects of future sea-level increases, and as such did not account for the dynamic effects of rising sea levels; however, for intertidal marshes, it was important to factor in the timing of the SLR because the SLR rate is important for the ability of an intertidal marsh to keep pace with SLR. Thus, we used literature-based assumptions related to the rate of SLR to account for potential vertical accretion in intertidal marshes.

We found that restoration measures had the potential to reduce island breaching and, therefore, maintain acreage of subaerial habitat types. Intertidal marsh tended to keep pace with sea level for habitat predictions for scenarios with the intermediate curve, whereas intertidal marsh was often converted to intertidal flat or open water for habitat predictions for scenarios with the high SLR curve. The modeling results indicated that areas restored under the marsh restoration measure were converted to intertidal flat under the scenario with faster SLR, which indicates that regular nourishment may be necessary to maintain marsh restoration areas, especially if storm frequency is low and overwash depth is low (that is, minimal elevation gain through sedimentation from overwash).

Chapter B. Oyster Habitat Suitability Modeling for the Alabama Barrier Island Restoration Feasibility Assessment at Dauphin Island

A spatially explicit oyster HSI model was developed for estuarine waters near Dauphin Island, Ala., for several potential future island configurations over a decadal period. The model parameters include salinity, dissolved oxygen, total suspended solid, water depth, and water temperature, which have all been found to affect oyster growth and mortality. The oyster HSI model was calibrated and validated using available in situ oyster monitoring data and continuous water quality data. The oyster HSI model was used to assess the possible effects of a variety of restoration measures including beach and dune restoration, marsh restoration, placement of sand in the littoral zone, and the no-action alternative on habitat suitability for oysters near Dauphin Island waters for the aforementioned future conditions related to storminess and sea level. Modeling results indicated that the proposed Dauphin Island restoration projects tend to have little or no effects on oyster habitat under the medium storminess and 0.3 m sea-level scenario. In contrast, the restoration actions, especially beach/dune restoration in front of Katrina Cut (that is, the side facing the Gulf of Mexico), could positively influence oyster habitat suitability by reducing the breaching potential under the high storminess and 1.0 m sea-level scenario. Modeling results indicated that

these restoration actions could maintain barrier island integrity while also enhancing oyster habitat.

Chapter C. Seagrass Habitat Suitability Modeling for the Alabama Barrier Island Restoration Feasibility Assessment at Dauphin Island

A seagrass HSI model was developed for estuarine waters near Dauphin Island, Ala., for several potential future island configurations over a decadal period. *Halodule wrightii* (shoal grass) was used as a representative seagrass because this is the dominant species of seagrass community along the barrier islands of the Mississippi Sound. Model variables include water quality parameters (salinity, temperature, water depth, and total suspended solids or turbidity) and geomorphological variable (exposure to wind and waves). The HSI model was calibrated and validated using available in situ seagrass monitoring data (height and present cover) and continuous water quality data. This seagrass HSI model was used to assess the possible effect of a variety of restoration measures including beach and dune restoration, marsh restoration, placement of sand in the littoral zone, and a no-action alternative on seagrass habitat suitability for two potential future conditions related to the aforementioned storminess and sea-level scenarios. Model results indicated that the beach/dune restoration project in front of Katrina Cut has the potential to largely enhance and preserve seagrass suitability under the high storminess and 1.0 m sea-level scenario because of the predicted prevention of breaches. Other barrier island restoration projects did not tend to affect the overall habitat suitability and distribution of seagrass.

Chapter A. Landscape-Position-Based Habitat Modeling for the Alabama Barrier Island Restoration Feasibility Assessment at Dauphin Island

By Nicholas M. Enwright,[1] Lei Wang, Hongqing Wang,[2] P. Soupy Dalyander,[1] Michael J. Osland,[1] Spencer J. Stelly,[3] Rangley C. Mickey,[1] Laura C. Feher,[1] Sinéad M. Borchert,[4] and Richard H. Day[1]

Abstract

Barrier islands are dynamic environments because of their position along the marine-estuarine interface. Geomorphology affects habitat distribution on barrier islands by regulating exposure to harsh abiotic conditions. Researchers have identified linkages between habitat and landscape position, such as elevation and distance from shore, yet these linkages have not been fully leveraged to develop predictive habitat models. Here, our aim was to deploy a contemporary barrier island habitat model that used machine learning algorithms, including *K*-nearest neighbor and random forest, to predict barrier island habitats (for example, beach, dune, intertidal marsh, and woody vegetation) using landscape-position information (for example, elevation, relative topography, and distance from shore) for Dauphin Island, Alabama. This model framework was loosely coupled with decadal hydrodynamic geomorphic model outputs to forecast habitats for two potential future conditions related to storminess and sea level (that is, 0.3 meter [m] and 0.96 m above the contemporary sea level). In addition to the potential future conditions, we explored habitat coverage for a variety of restoration measures including beach and dune restoration, marsh restoration, placement of sand in the littoral zone, and a no-action alternative. The hydrodynamic geomorphic modeling was static and did not account for island evolution from the contemporary sea level to future sea levels; however, for intertidal marshes, it was important to factor in the timing of the sea-level rise (SLR) because the SLR rate is important for the ability of an intertidal marsh to keep pace with SLR. Thus, we predicted habitats under future sea levels using two SLR curves (that is, the U.S. Army Corps of Engineers intermediate SLR curve [0.69 m by 2100] and high SLR curve [1.7 m by 2100]) and used literature-based assumptions to account for potential vertical accretion in intertidal marshes.

In addition to understanding the habitat composition of Dauphin Island without restoration, we compared each scenario to the future without action to gauge the relative effect of the restoration effort. We determined that restoration measures had the potential to reduce island breaching and, therefore, maintain acreage of subaerial habitat types. Intertidal marsh tended to keep pace with sea level for habitat predictions for scenarios with the U.S. Army Corps of Engineers intermediate SLR curve, whereas intertidal marsh often was converted to intertidal flat or open water for habitat predictions for scenarios with the U.S. Army Corps of Engineers high SLR curve. Along those lines, the modeling results indicated that areas restored under the marsh restoration measure were converted to intertidal flat under the scenario with faster SLR, which indicates that regular nourishment may be necessary to maintain marsh restoration areas, especially if storm frequency is low and overwash depth is low. These results can be integrated into a structured decision-making process to include information about how restoration measures could positively or negatively affect habitat resources over time. This information can also provide insights to natural resource managers and planners on how a restoration project may maintain or impede natural coastal processes and provide information critical for making future-focused decisions regarding barrier island restoration.

Introduction

Barrier island habitats, such as beach, dune, woody vegetation, and intertidal marsh, provide numerous important ecosystem services including storm surge reduction, wave attenuation, erosion control to the mainland, habitat for fish and wildlife, carbon sequestration in marshes, water catchment

[1]U.S. Geological Survey.

[2]Louisiana State University.

[3]Stelly Consulting at the U.S. Geological Survey.

[4]Borchert Consulting at the U.S. Geological Survey.

and purification, recreation, and tourism (Sallenger, 2000; Feagin and others, 2010; Barbier and others, 2011). Barrier islands are dynamic environments that are gradually shaped by currents, waves, and tides under quiescent conditions yet can evolve in the time scale of hours to days during hurricanes and other extreme storms. The ecosystems associated with these islands also face numerous additional hazards, including accelerated sea-level rise (SLR), oil spills, and anthropogenic stressors (Pilkey and Cooper, 2014), with climate-related threats predicted to likely increase in the future (Knutson and others, 2010; Hansen and others, 2016). Therefore, natural resource managers tasked with making future-focused management decisions often rely on scientific models that predict what barrier island systems may look like in the future, especially with regard to morphology (Gutierrez and others, 2015; Passeri and others, 2018) and habitat for fish and wildlife (Foster and others, 2017).

Many abiotic factors influence the performance of foundation plant species, including wave energy, salinity, inundation frequency, sea spray, Aeolian transport, and nutrient availability (Young and others, 2011). The spatial distribution of these characteristics is a function of island geomorphology, which therefore plays a critical role in the distribution of barrier island habitats because foundation species (Dayton, 1972), such as *Spartina patens* (Aiton) Muhl. (saltmeadow cordgrass), *Uniola paniculata* L. (sea oats), and *Pinus elliottii* (slash pine), tend to thrive in certain topographic settings and (or) disturbance regimes (Zinnert and others, 2017). Researchers have established linkages between barrier island habitats and landscape-position information, such as distance from shoreline (Young and others, 2011) and elevation (Young and others, 2011; Anderson and others, 2016; Foster and others 2017; Halls and others, 2018). In a prior study, we built on these efforts by using machine learning algorithms, such as *K*-nearest neighbor and random forest, to develop a geocomputational model to make spatially explicit predictions of barrier island habitats (for example, beach, dune, woody vegetation, and intertidal marsh) using landscape-position information from 2015 for Dauphin Island, Alabama (Enwright and others, 2019b). The model was validated using deterministic accuracy, fuzzy accuracy, and hindcasting (Enwright and others, 2019b). We found machine learning algorithms were well suited for predicting barrier island habitats using landscape position. For the contemporary model outputs, deterministic overall accuracy was nearly 70 percent, and fuzzy overall accuracy was more than 80 percent. For the hindcast model outputs, the deterministic overall accuracy was nearly 80 percent, and fuzzy overall accuracy was more than 90 percent.

Purpose and Scope

Here, we expand on this work by using the Dauphin Island habitat model (Enwright and others, 2019b) to predict habitats using landscape-position information extracted from the suite of decadal hydrodynamic geomorphic model outputs. The objective of this effort was to forecast habitat coverage under future sea levels (0.3 m and about 1.0 m above the contemporary sea level) and simulated storms for a variety of restoration measures, including beach and dune restoration, marsh restoration, placement of sand in the littoral zone, and a no-action alternative. For more information on the hydrodynamic geomorphic modeling associated with this effort, see Mickey and others (2020).

Methods

Study Site and Model Domain

Dauphin Island, Alabama (fig. A1), is on the eastern end of a 105-kilometer (km) long Mississippi-Alabama, wave-dominated (McBride and others, 2013) barrier island chain. The island provides important salinity regulation to the Mississippi Sound, north of the island, in addition to the Mobile Bay estuary to the northeast. In 2015, the length of Dauphin Island was about 25 km, and the subaerial part of the island was estimated to be about 15.8 square kilometers (km^2; Enwright and others, 2019b). Dauphin Island has diurnal tides with a mean tidal range of about 0.36 m (that is, mean low water to mean high water), based on observations during the most recent North American Tidal Datum Epoch (1983 to 2001) from a National Oceanic and Atmospheric Administration tide gauge (station identifier 8735180) located on the eastern end of the island. We developed the modeling domain for this study (fig. A1) by buffering the maximum extent of Dauphin Island shorelines from 1940 to 2015 (Henderson and others, 2017) by 2.5 km. The rationale for buffering historical shorelines by this distance was so that the subaerial island footprint would remain within the model domain even with restoration measures and storm effects, such as island transgression. We used Esri ArcMap 10.5.1 (Redlands, California) for all spatial analyses.

Barrier Island Habitats

We set our model response variable to be generalized habitat classes from a geomorphology-based habitat classification scheme that was developed for a 2015 Dauphin Island habitat map (Enwright and others, 2019a; fig. A2; table A1). The generalizations of the mapping classification scheme involved combining habitat classes that occupy the same geomorphic setting but are regulated by factors we did not include in our model, such as disturbance and habitat succession. These included combining meadow and unvegetated barrier flat habitats into a single habitat class (that is, barrier flat), combining dunes with various vegetative states into a single class (that is, dune), and, likewise, combining forest and

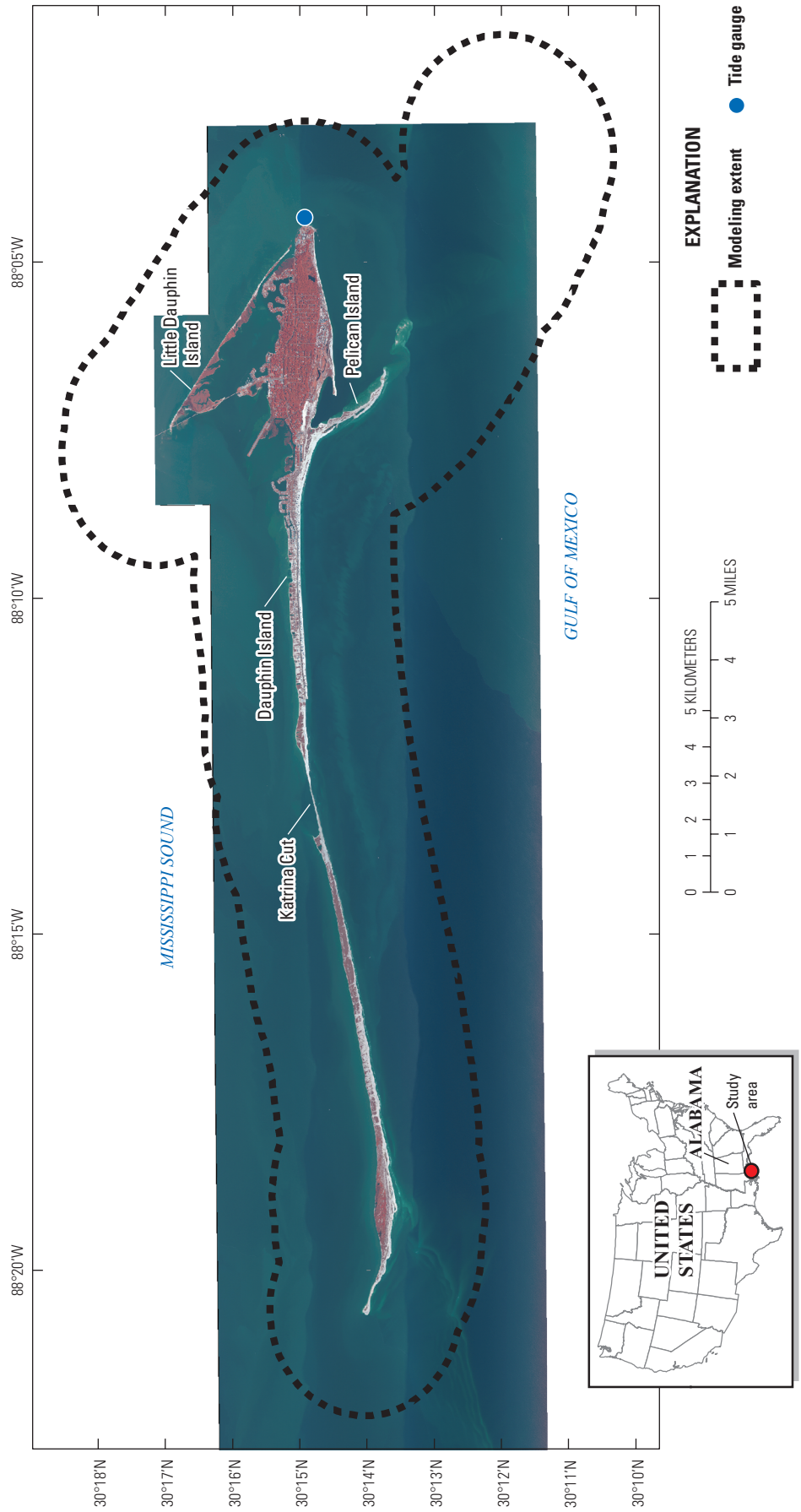

Figure A1. Model domain for landscape-position-based habitat prediction for the Barrier Island Restoration Feasibility Assessment project, Dauphin Island, Alabama. Modified from Enwright and others (2019b) with permission.

Figure A2. Examples of the habitat classes for landscape-position-based habitat prediction for the Barrier Island Restoration Feasibility project for Dauphin Island, Alabama. The classes are linked to tidal regime (see explanation in lower left corner of the figure). Reprinted from Enwright and others (2019b) with permission.

scrub/shrub into a single habitat class (that is, woody vegetation). Each habitat class in the model classification scheme fell within a specific tidal zone (that is, subtidal, intertidal, supratidal/upland; fig. A2). In this effort, we did not make any predictions of changes to developed areas. Instead, we assumed these areas were constant regardless of morphologic change. The underlying assumption that developed areas would remain constant was based on historical trends at Dauphin Island; namely, that currently developed land has not been abandoned after storm events (that is, housing is rebuilt after damage) and that currently unoccupied areas (for example, the western terminus of the island and Pelican Island) have not been developed over the past several decades. In other words, model outputs contained the current footprint for developed areas. We set the spatial resolution of the habitat prediction model to be 10 m (that is, a grid with cells that were 100 square meters [m^2]). The rationale for selecting 10 m for the model resolution was to use a spatial resolution that would limit the loss of narrow habitats and would be compatible with the spatial resolution of the hydrogeomorphic numerical models that were used for forecasting geomorphology (Passeri and others, 2018; Mickey and others, 2020).

Model Runs

We predicted habitat coverage for 43 island configurations corresponding to different island states associated with various environmental scenarios evolving over time. These configurations corresponded to the 2015 modeled topobathymetric digital elevation model (TBDEM), which was used to calibrate the model framework, along with 12 model outputs per restoration measure (table A2) for 2 potential scenarios related to storminess and sea level (Mickey and others, 2020). The storminess bins included realizations with a "medium" storminess (that is, ST2) and a "high" storminess (that is, ST3). As previously mentioned, we predicted habitats under two future sea levels. These included a sea level of 0.3 m above the contemporary sea level (that is, SL1) and a sea level of about 1.0 m above the contemporary sea level (that is, SL3). Specifically, ST2 was paired with SL1 (that is, ST2SL1) and ST3 was paired with SL3 (that is, ST3SL3). For more information on how the storminess and sea-level bins were selected, see Mickey and others (2020).

The geomorphic modeling effort captured the potential effects of changes in sea level through the addition of a static increase in water level for the duration of each decadal modeling period, thereby decoupling the imposed sea-level increase from any specific SLR rate prediction (Mickey and others, 2020). For example, we added 0.3 m to the contemporary sea level for the SL1 scenario rather than letting that SLR happen

Table A1. Descriptions of the classes included in the habitat model for the Barrier Island Restoration Feasibility Assessment project, Dauphin Island, Alabama. Adapted from Enwright and others (2019a, b) with permission.

Habitat[1]	Description	Source
Barrier flat	Barrier flat includes flat or gently sloping supratidal/upland areas that are located on the backslope of dunes, unvegetated washover fans, and areas along estuarine shorelines. Barrier flat habitat can be unvegetated or vegetated (that is, meadow).	Leatherman (1979), Lucas and Carter (2010)
Beach	Beach includes bare or sparsely vegetated supratidal areas that are located upslope of the intertidal beach and marine-water habitats. These habitats are located along shorelines with high wave energy.	Cowardin and others (1979)
Developed[1]	Developed includes areas dominated by constructed materials (that is, transportation infrastructure, residential, and commercial areas).	Homer and others (2015)
Dune	Dunes are supratidal features developed via Aeolian processes with a well-defined relative elevation. Dune habitat can be vegetated or unvegetated.	Acosta and others (2005)
Intertidal beach	Intertidal beach includes bare or sparsely vegetated intertidal wetlands located along the ocean-facing side of the island that are adjacent to high-energy shorelines.	Cowardin and others (1979)
Intertidal flat	Intertidal flat includes bare or sparsely vegetated intertidal wetlands that are adjacent to estuarine water and along low-energy shorelines.	Cowardin and others (1979)
Intertidal marsh	Intertidal marsh includes all intertidal wetlands with 30 percent or greater areal cover by erect, rooted, herbaceous hydrophytes.	Cowardin and others (1979)
Water, estuarine	Water, estuarine, includes all areas of subtidal water and ponds on the back-barrier side of the island. These areas rarely have salinity greater than 30 parts per thousand and generally have less than 30-percent cover of vegetation.	Cowardin and others (1979)
Water, fresh	Water, fresh, includes all areas of supratidal/upland water that generally have less than 30-percent cover of vegetation.	Cowardin and others (1979)
Water, marine	Water, marine, includes all areas of subtidal water located offshore of the ocean-facing side of the island. These areas are located along high-energy coastlines and (or) are areas that occasionally experience salinity levels greater than or equal to 30 parts per thousand and generally have less than 30-percent cover of vegetation.	Cowardin and others (1979)
Woody vegetation	Woody vegetation includes supratidal/upland scrub/shrub and forested areas where woody vegetation height is greater than about 0.5 meter. Woody vegetation coverage should generally be greater than 30 percent.	Cowardin and others (1979), Homer and others (2015)
Woody wetland	Woody wetland includes all supratidal/upland wetlands dominated by woody vegetation with a vegetation height greater than about 0.5 meter. Woody vegetation coverage should generally be greater than 30 percent.	Cowardin and others (1979)

[1]Developed habitat was not modeled in this effort. We assumed there were no changes in developed areas from the 2015 habitat map.

over a gradual process; however, for intertidal marshes, it was important to factor in the timing of the SLR because the rate of increase is important for the ability of an intertidal marsh to keep pace with the rise in sea level. For each future SL, habitat predictions were made assuming that the SLR followed the U.S. Army Corps of Engineers (USACE) high SLR curve (that is, SLR of 1.7 m by 2100 [not shown]) or USACE intermediate SLR curve (that is, SLR of 0.7 m by 2100; fig. A3). For example, habitats were predicted for the ST2SL1 scenario for a given restoration measure for the USACE high and intermediate curves, respectively (table A3; fig. A3). For context, a recent report by the National Oceanic and Atmospheric Administration included six global mean SLR scenarios for 2100: low, intermediate-low, intermediate, intermediate-high, high and extreme, which correspond to a global mean SLR of 0.3 m, 0.5 m, 1.0 m, 1.5 m, 2.0 m, and 2.5 m, respectively (Sweet and others, 2017). In summary, our effort made habitat predictions based on potential island configurations for 2 storminess scenarios that were paired with 4 sea-level scenarios (that is, an increase in sea level of 0.3 m by around 2030 [high curve] and 2050 [intermediate curve] and about 1.0 m by around 2070 [high curve] and 2128 [intermediate curve]). Besides the baseline condition (that is, the 2015 modeled TBDEM), habitats were predicted from geomorphic data for year 0, year 5, and year 10 for each potential state of the island under simulated storms and sea level with and without various restoration measures (Mickey and others, 2020).

Table A2. Restoration measures for the Alabama Barrier Island Restoration Feasibility Assessment project, Dauphin Island, Alabama. For more information see Mickey and others (2020).

[R, restoration measure; km, kilometer; m, meter]

Restoration measure	Description
Future without action (R0)	No restoration action.
Katrina Cut structure sand berm (R1)	Sensitivity testing related to the Katrina Cut structure (habitat modeling was not completed for this measure).
Pelican Island southeast nourishment (R2)	Pelican Island nourishment that extended the island by about 2.6 km to the south of the present tip of Pelican Island.
Sand Island platform nourishment and sand bypassing (R3)	Nourishment of the submerged Sand Island platform that is designed to increase the elevation to 2 m below mean sea level, which is 5 m higher than some current bed-elevation levels in this area.
West and east end beach and dune nourishment (R4)	Nourishment of the beach east of the Katrina Cut and the shorefront area east of Pelican Island to raise beach and dune elevations by a maximum of about 3.7 m.
Back-barrier tidal flats and marsh habitat restoration (R5)	Marsh restoration and filling of burrow pits along the back-barrier area of Dauphin Island.
West end beach and dune nourishment (R6)	Modified version of the R4 measure, which moved the restored dune area landward with no sediment nourishment east of Pelican Island.
West end and Katrina Cut beach and dune nourishment (R7)	Modified version of the R6 measure extends these changes west to the front side of the Katrina Cut rubble wall structure.

Sea-Level Rise and Intertidal Marsh Accretion

Intertidal marshes have the ability to adjust to SLR through vertical and (or) horizontal adjustments to their position in the landscape. Changes in vertical position (that is, elevation and inundation frequency) can result from biogeomorphic feedbacks among inundation, plant growth, and sedimentation (Morris and others, 2002; Kirwan and Murray, 2007). Changes in horizontal position can result from landward migration (that is, transgression) of intertidal marshes into upslope or upriver ecosystems or seaward migration onto newly deposited sediments (Williams and others, 1999; Enwright and others, 2016; Woodroffe and others, 2016). To account for the role of these two adaptation mechanisms under accelerated SLR for the various alternative restoration measures, we used our intertidal marsh habitat model in combination with assumptions regarding the potential for vertical elevation adjustments, erosion, and sedimentation. Dauphin Island intertidal marshes are dominated by species from different plant functional groups, including *Fimbristylis spadicea*, *Juncus roemerianus*, *Spartina alterniflora*, *Paspalum vaginatum*, and various succulent salt marsh plant species (Enwright and others, 2017). On barrier islands, marsh responses to SLR are greatly influenced by geomorphic processes that result in the erosion, transport, and (or) deposition of barrier island sediments (Morton, 2008; Moore and others, 2014; Walters and others, 2014; Vinent and Moore, 2015). Hurricanes and other storms greatly influence the delivery and accumulation of inorganic sediments in these marshes (McKee and Cherry, 2009; Smith and others, 2013). Ellis and others (2018) studied the sedimentological characteristics of 11 push cores from marshes on Dauphin Island and found these marshes had a compaction-corrected linear sedimentation rate of about 0.3 centimeter per year (cm/yr) with an interquartile range of 0.2 cm/yr. The Dauphin Island geomorphic model was used to account for storm-induced sediment deposition and erosion during the decadal simulations (Mickey and others, 2020). We used accretion assumptions to predict future landward migration of intertidal marshes into adjacent upslope ecosystems for SLR increments (that is, moving from current sea level to 0.3 m or about 1.0 m) and seaward migration onto newly deposited sediments from overwash events during decadal geomorphic model runs. Our threshold rate of SLR for marsh persistence was 1 cm/yr. This rate was selected using information contained in Kirwan and others (2010, 2016) and Parkinson and others (2015). The ability of intertidal marshes to adjust vertically to SLR is lower in microtidal settings like those present along the northern Gulf of Mexico (Kirwan and others, 2010, 2016). To account for the potential for existing intertidal marshes to adjust to SLR via biogeomorphic feedbacks, we assumed that (1) restoration measures for the Alabama Barrier Island Restoration Feasibility Assessment project the elevation of existing marshes would adjust to keep up with SLR at rates of as much as 1 cm/yr (that is, cumulative accretion in marshes would be the same as the cumulative SLR); and (2) marsh accretion would not occur once the SLR rate exceeded 1 cm/yr.

We used the USACE high and intermediate SLR curves (fig. A3; U.S. Army Corps of Engineers, 2014) to account for the rate of SLR change. The base year for the SLR curve was 1992. We determined the rate of SLR per year for each curve to determine when the 1 cm/yr threshold was exceeded.

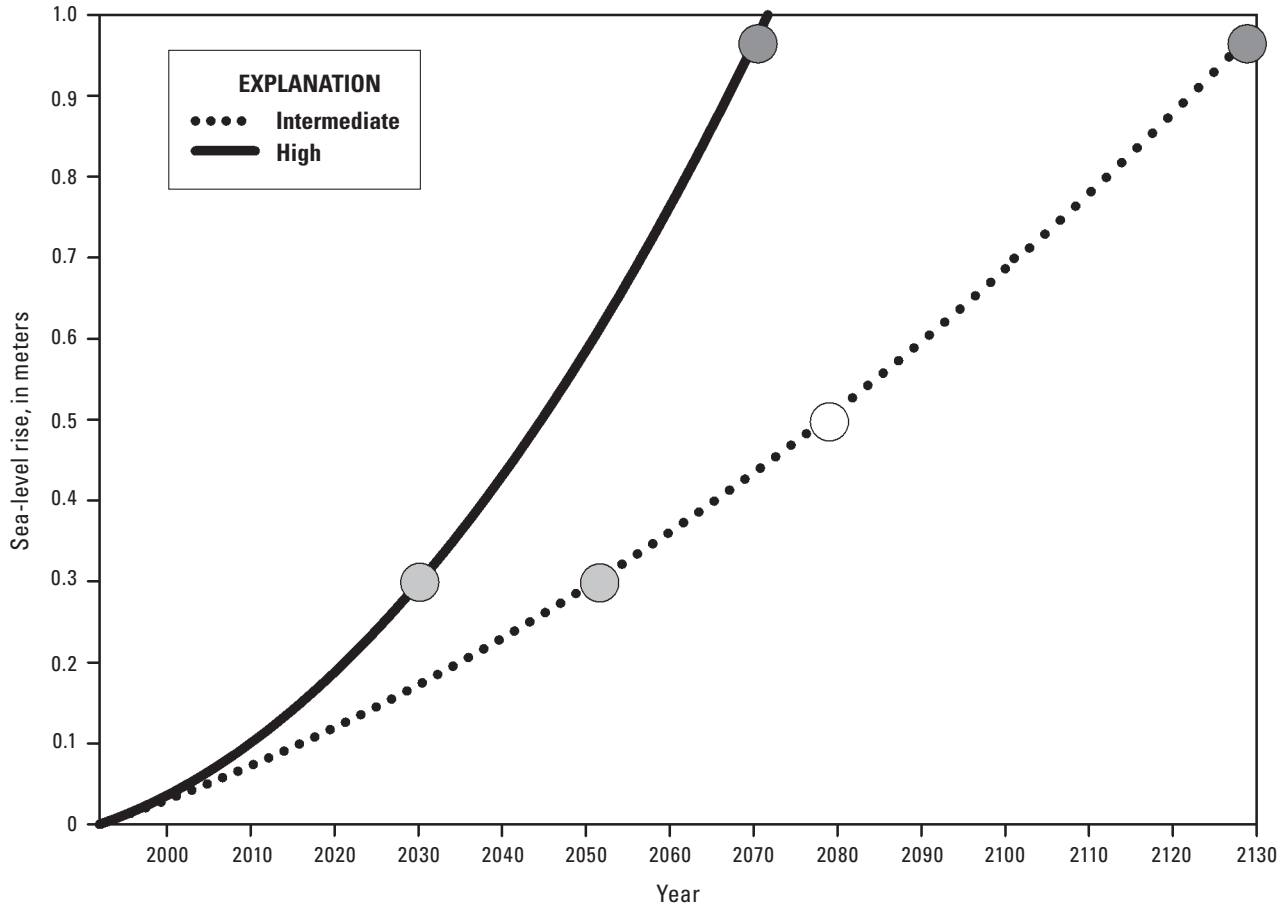

Figure A3. Sea-level scenarios along the U.S. Army Corps of Engineers high and intermediate sea-level rise curves used for the habitat model for the Barrier Island Restoration Feasibility Assessment project, Dauphin Island, Alabama. The light gray points depict the 0.3-meter (m) sea-level scenario (that is, SL1). The white point depicts a 0.5-m sea-level scenario along the intermediate curve, which was used to estimate intertidal marsh migration potential along the intertidal curve. The dark gray points depict the ~1.0-m sea-level scenario (that is, SL3).

Because of a rapid SLR rate, the USACE high curve only had accretion through 2022, whereas intertidal marshes kept pace with SLR through accretion for nearly the entirety of the USACE intermediate curve. For scenario nomenclature in this report, the last letter will be "H" for the high curve and "I" for the intermediate curve (for example, ST2SL1H would be the "medium" storminess scenario with a 0.3-m SLR using the USACE high curve). All plots were developed using SigmaPlot 14.0.

We developed spatially explicit layers for the application of accretion. First, we developed an accretion mask for areas predicted as intertidal marsh for the 2015 modeled TBDEM (Mickey and others, 2020). Next, we identified "newly" created intertidal marsh areas via landward migration under future SLs (that is, areas that were previously supratidal/upland but are now intertidal because of SLR). Although our assessment focused on a 0.3-m and 1.0-m SLR, we also modeled habitats for year 0 for the future without action case with an SLR of 0.5 m for the intermediate curve to identify intertidal marsh landward migration while moving along this curve (that is, from 0.3 m to about 1.0 m; fig. A3). In other words, for habitat prediction for the 1.0-m SLR event using the intermediate SLR curve, intertidal marsh from 2015 accreted about 0.7 m, upslope areas that transitioned to intertidal marsh for an SLR of 0.3 m accreted about 0.5 m, and upslope areas that transitioned to intertidal marsh for an SLR of 0.5 m accreted about 0.3 m. When modeling habitats for the back-barrier tidal flats and marsh habitat restoration measure (R5), we added the marsh creation footprints associated with this restoration measure (Mickey and others, 2020) to the marsh accretion mask.

Topobathymetric Digital Elevation Model Processing

The geomorphic model predictions are represented using an irregular Delft3D grid (Mickey and others, 2020). This grid had a cross-shore spatial resolution of about 5 m for subaerial areas of the island to about 300 m for subaqueous areas. For alongshore resolution, the grid had a spatial resolution of

Table A3. Model runs for the habitat model for the Barrier Island Restoration Feasibility Assessment project, Dauphin Island, Alabama. For more information on measures, see Mickey and others (2020).

[ST/SL, storminess and sea-level bins; SLR, sea-level rise; R, restoration measure; --, not applicable; ST2SL1, "medium" storminess bin was paired with the 0.3-meter SLR; ST3SL3, "high" storminess bin was paired with the 1.0-meter SLR]

Restoration measure	ST/SL	SLR curves	Time
Katrina Cut structure sand berm (R1)	--	--	--
Pelican Island southeast nourishment (R2)	ST2SL1 ST3SL3	High and Intermediate High and Intermediate	Years 0, 5, and 10 Years 0, 5, and 10
Sand Island platform nourishment and sand bypassing (R3)	ST2SL1 ST3SL3	High and Intermediate High and Intermediate	Years 0, 5, and 10 Years 0, 5, and 10
West and east end beach and dune nourishment (R4)	ST2SL1 ST3SL3	High and Intermediate High and Intermediate	Years 0, 5, and 10 Years 0, 5, and 10
Back-barrier tidal flats and marsh habitat restoration (R5)	ST2SL1 ST3SL3	High and Intermediate High and Intermediate	Years 0, 5, and 10 Years 0, 5, and 10
West end beach and dune nourishment (R6)	ST2SL1 ST3SL3	High and Intermediate High and Intermediate	Years 0, 5, and 10 Years 0, 5, and 10
West end and Katrina Cut beach and dune nourishment (R7)	ST2SL1 ST3SL3	High and Intermediate High and Intermediate	Years 0, 5, and 10 Years 0, 5, and 10

about 40 m for subaerial areas and about 100 m for subaqueous areas. These data were used to estimate the elevation to the habitat model points (that is, points with a 10-m spacing) for each scenario and time step for which habitats were modeled using linear interpolation. We converted these point data to a 10-m TBDEM. The baseline morphology data were modified by including the template of the restoration measure(s) run, as necessary.

The vertical datum for the elevation from the TBDEM was the North American Vertical Datum of 1988 (NAVD 88). We transformed the vertical datum from NAVD 88 to mean sea level using relative height differences from the National Oceanic and Atmospheric Administration tide gauge during the current North American Tidal Datum Epoch. In doing so, we assumed the relative difference between NAVD 88 tidal datums would be similar under future sea-level conditions. For forecasting habitats for island configurations with potential future sea levels, we added accretion based on the SLR increment using the previously described spatially explicit accretion layers.

We extracted the extreme high water springs (EHWS) shoreline from each TBDEM. The EHWS represents the upper elevation contour for the intertidal zone (Cowardin and others, 1979). These shoreline data were generalized to only include exterior shorelines and converted to points with a 10-m spacing. A semiautomated process was used to label shorelines as ocean facing or back-barrier facing. The Delft3D grid was used to develop points that estimated the center of the island. These data were developed by analyzing the midpoint of each cross-shore profile based on island subaerial area. We used these points to determine whether an area was north of the island or south of the island. To do this, we calculated the Euclidean direction from the center variable, recoded this variable to 1 for directions between 90 and 270 degrees, and set the value to 0 otherwise. These data were used to assign the shoreline type (that is, ocean facing or back-barrier facing) to the shoreline points. The shoreline type was checked and manually edited, as needed.

Probabilistic Surface Generation

The baseline TBDEM was the result of using Delft3D to predict geomorphology in 2015 (Mickey and others, 2020). The TBDEM was validated using light detection and ranging (lidar) acquired with Leica ALS70 and ALS80 sensors in January 2015 by Digital Aerial Solutions, LLC (Riverview, Florida), and the U.S. Geological Survey (USGS; see references within Mickey and others, 2020). Tidal regimes can be extracted from TBDEMs; however, elevation uncertainty should be treated before conducting automated extraction of elevation-dependent habitats. The level of uncertainty from data collected with conventional aerial linear lidar systems is considerable within intertidal areas and can be as high as 60 cm in densely vegetated emergent wetlands (Buffington and others, 2016; Medeiros and others, 2015). Because of the lack of detailed error information, the uncertainty of DEMs is often left unaddressed for habitat mapping efforts, yet the level of uncertainty becomes critical when studying low-relief environments where centimeters can make a difference in the exposure to physically demanding abiotic conditions (for example, inundation, salt spray, wave energy; Young and others, 2011; Anderson and others, 2016). We used relative accuracy information from the 2015 lidar DEM and Real-Time Kinematic Global Position System observations for Monte Carlo simulations to develop probability surfaces that indicated the likelihood that a pixel in the TBDEM is either in an intertidal geomorphic setting or above an extreme water level,

respectively. For more details on the relative error assessment and the Monte Carlo simulations, see Enwright and others (2018, 2019a).

Tidal Zone Determination

As previously mentioned, habitat classes were linked to tidal zones (fig. A2). We developed an automated process that used the intertidal probability surfaces to separate the model domain by tidal zone. First, subtidal areas were those areas that had an elevation below mean sea level and less than a 50-percent probability of being intertidal. Intertidal areas were areas with greater than or equal to a 50-percent probability of being intertidal. We used the connectivity of the raster cells as defined by the queen's move rule, which searches for interconnected cells in cardinal and diagonal directions, to remove isolated low-lying areas from the intertidal zone (Poulter and Halpin, 2008). Once subtidal and intertidal areas were identified, the remaining areas, which included the isolated low-lying areas, were assumed to be supratidal/upland.

Predictor Variables

For each TBDEM, we developed numerous landscape-position predictor variables based on literature-derived linkages of landscape position to barrier island ecology and habitat distribution (Young and others, 2011; Anderson and others, 2016; Foster and others, 2017; Halls and others, 2018). These predictor variables were related to elevation and X, Y coordinates (such as proximity and direction; fig. A4). We determined the value of these predictor variables for each 10-m pixel in the TBDEM.

We developed direct linkages from the geomorphic model outputs for three of the predictor variables. The first linkage was the previously described identification of points as north or south of the island based on the position relative to the island centerline. The second linkage from the geomorphic model outputs was the elevation per model cell. This elevation parameter was interpolated to the 10-m habitat model grid from the irregular Delft3D grid (Mickey and others, 2020). The third linkage with geomorphic model outputs was for the development of the topographic position index (TPI; fig. A4), which was first proposed by Weiss (2001). The TPI provides a scale-dependent measure of relative topography that has been found to be effective in dune extraction (Enwright and others, 2019b; Halls and others, 2018; Wernette and others, 2016). The TPI was calculated for each point within the TBDEM but used the Delft3D grid to take advantage of increased cross-shore resolution (Mickey and others, 2020). Specifically, TPI is a measure of local elevation relative to the elevation of grid cells within a fixed distance (d) of the reference point (x, y) and is calculated as

$$TPI_d(x_0,y_0) = Z(x_0,y_0) - \frac{\sum_{i=1}^{N} Z(x_i,y_i)}{N} \quad \text{(A1)}$$

The number of grid cells within distance d of the reference point is denoted by N. For the purposes of subaerial habitat characterization, only those grid cells with an elevation greater than −0.5 m were included. The TPI at Dauphin Island was calculated for d values of 30 m and 100 m. The rationale to use a scale of 30 m was based on visual inspection when developing the 2015 habitat map (Enwright and others, 2019a) and the 100-m TPI could be helpful for identifying ridges and upper slopes that are broader. Values of TPI_{30} and TPI_{100} were then interpolated to the habitat grid and exported to ArcGIS format for inclusion in the habitat model. In some cases, the exclusion of elevations of −0.5 m left gaps in the TPI for freshwater ponds. These areas were added to the 10-m TPI predictor variable layers by calculating the TPI for each scale using the TBDEM in ArcGIS. We determined the elevation to the south (that is, the high-energy shoreline) by taking the median of the maximum elevation for three 22-degree wedge-shaped kernels radiating to the south with radii of 1 km and 8 km. We used hydrological analyses to identify depressions in the TBDEM by identifying sink depth. Sinks are areas in the TBDEM where flow is interrupted because of a depression or noise (O'Callaghan and Mark, 1984).

We determined the Euclidean distance from the back-barrier shoreline and the ocean-facing shoreline, respectively. We used the mean sea level for the contemporary habitat modeling effort (Enwright and others, 2019b), but for this effort we used the EHWS instead because distance from the shoreline tends to differ from the 2015 modeled TBDEM. This is most likely from smoothing over Delft3D decadal model runs. The distance from the Mobile-Tensaw River Delta was a cost distance, which restricted the distance calculation to subtidal areas identified from the TBDEMs. To do this, we created a cost surface that only included subtidal areas (that is, intertidal and supratidal/upland areas were set to "NoData").

Habitat Modeling

For each island configuration (table A3), we predicted the habitat for each 10-m cell using the model framework outlined in Enwright and others (2019b). The model components for this framework, including the habitats, predictor variables with supporting literature, and algorithm used per tidal zone, are outlined in table A4. This initial model development was focused on a proof of concept using landscape predictors that were extracted from actual, best available lidar elevation and bathymetry data for 2015; thus, the first step was to calibrate this model framework to the 2015 modeled TBDEM developed using Delft3D (Mickey and others, 2020). We used MathWorks MATLAB 2016b (Natick, Massachusetts) for model fitting and prediction. Similar to the initial framework, we trained 100 models per tidal zone from 70 percent of the training set selected by random permutations to avoid overfitting a single model. For each cell, the majority habitat class of the 100 predictions was chosen as the final prediction. The intertidal zone and the supratidal/upland zone models were

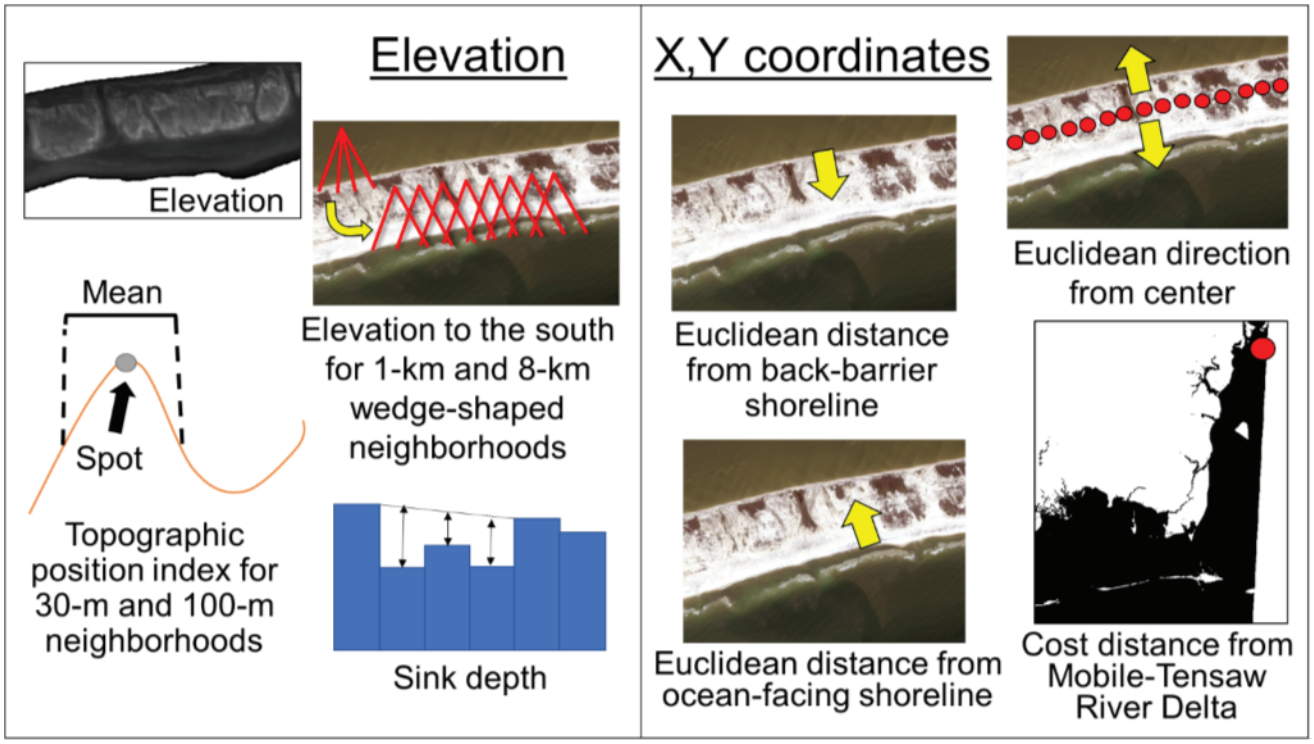

Figure A4. Predictor variables for the habitat model for the Barrier Island Restoration Feasibility project, Dauphin Island, Alabama. Reprinted from Enwright and others (2019b) with permission. [km, kilometer; m, meter]

applied to each cell in the 10-m raster; however, to increase efficiency of the subtidal zone models, we made predictions for a 100-m raster and then converted these data to a 10-m raster using inverse distance weighted interpolation.

Similar to the initial Dauphin Island habitat model framework (Enwright and others, 2019b), the final step of our modeling process was the application of a suite of postprocessing routines. The first step in this process was smoothing noise by using a majority filter. The majority filter changes the pixel value to be the majority value if three of its four orthogonal neighbors have the same value. In addition to noise reduction, the postprocessing steps also included several user-defined constraints based on our theoretical understanding of barrier island habitats from the literature regarding elevation and X, Y coordinates (Cowardin and others, 1979; Leatherman, 1979; Young and others, 2011); for example, relative topography often differs between restored and natural dunes. Initially, restored dunes may be less well defined at a 30-m scale compared to natural dunes. For this reason, we added an additional step to the original model framework postprocessing steps (Enwright and others, 2019b) to better capture restored dunes. Although dunes were still predicted using the machine learning algorithm, we also recoded areas that were upper slopes and ridges, as defined by the TPI values, to dunes if they were above the extreme storm water level. This followed a similar method used by Enwright and others (2019a) for dune habitat mapping. We only applied this approach to the area south of the island centerline because of the focus of dune restoration on the front half of the island and noisy elevation data on the back half of the island. Additionally, on nonfetch-limited barrier islands, emergent marsh vegetation typically occurs where wave energy is lower, whereas unvegetated intertidal mudflats or intertidal beach habitats are more common where wave energy is higher (Roland and Douglass, 2005). Therefore, intertidal marsh habitats located along the ocean-facing shore were changed to intertidal beach habitats. Dune habitats that were predicted by the habitat model that had a probability of less than 0.5 for being above the extreme storm water level were recoded to barrier flats (Enwright and others, 2019a). These rules were applied in a stepwise fashion (table A5). Some of the thresholds used were directly related to tidal datums (for example, EHWS), whereas others, such as sink depth, were determined by trial and error with the final value being selected by visual inspection. Lastly, this process also included the application of a four-pixel minimum mapping unit (400 m^2). For more details on the modeling development and validation, see Enwright and others (2019b).

The overall objective of our effort was to understand how habitat coverage changed with and without various restoration measures under potential future alternative states of the island related to storminess and sea level. To provide insights to the relative effect of each restoration measure, we outlined the habitat coverage, produced maps for each island configuration, and summarized the percentage change of selected habitat types (that is, all but water classes and woody vegetation)

Table A4. Response variables (that is, habitat classes), predictor variables with supporting literature, and algorithm per tidal zone for the habitat model for the Barrier Island Restoration Feasibility project, Dauphin Island, Alabama. Modified from Enwright and others (2019b) with permission.

[km, kilometer; m, meter]

Tidal zone	Habitat	Predictor variables	Source	Algorithm
Subtidal	Water, estuarine, water, marine	(1) Distance from Mobile-Tensaw River Delta (2) Direction from center	(1–2) Cowardin and others (1979)	Coarse *K*-nearest neighbor
Intertidal	Intertidal flat, intertidal beach, intertidal marsh	(1) Elevation (2) Elevation to the south (8 km) (3) Distance from ocean-facing shoreline (4) Distance from back-barrier shoreline	(1) Anderson and others (2016), Cowardin and others (1979), Foster and others (2017), Young and others (2011) (2) Zinnert and others (2017) (3–4) Young and others (2011)	Random forest
Supratidal/ upland	Barrier flat, beach, dune, water, fresh; woody vegetation; woody wetland	(1) Elevation (2) Elevation to the south (1 km) (3) Topographic position index (30 m) (4) Topographic position index (100 m) (5) Distance from ocean-facing shoreline (6) Distance from back-barrier shoreline	(1) Anderson and others (2016), Cowardin and others (1979), Foster and others (2017), Young and others (2011) (2) Zinnert and others (2017) (3–4) Halls and others (2018), Enwright and others (2019b), Wernette and others (2016) (5–6) Young and others (2011)	Random forest

compared to the respective scenario for the future without action case.

Habitat Model Results

Model data, including the model inputs with landscape-position predictor variables and model outputs, have been made available as a USGS data release that accompanies this report (Enwright and others, 2020). A map of predicted habitats for the 2015 modeled TBDEM is shown in figure A5, and the predicted habitats for potential future island configurations related to restoration measure, storminess, and sea level are shown in figures A6–A8 (at the end of this chapter) and figures A1.1–A1.4. Each restoration measure map shows how the restoration measure may evolve over the decadal hydrodynamic geomorphic model run (that is, from year 0 to year 10) and, more importantly, how this restoration measure may influence the response of the island over time. For instance, model runs for year 10 of the ST3SL3 scenarios had breaching on either side of Katrina Cut for the future without action measure (figs. A6*G*, A1.1*G*, A1.2*G*, A1.3*G*), except for the west and east end beach and dune design measure (R4; fig. A7*G*) and the west end beach and dune measure (R6; fig. A1.4*G*), which had breaching only on the western end of Katrina Cut. There were no breaches near Katrina Cut for the runs for the west end and Katrina Cut beach and dune restoration measure (R7; fig. A8). The maps also depict how upslope tidal saline wetland migration occurs with SLR. As expected, intertidal marsh from the 2015 modeled TBDEM (fig. A6) tends to keep pace with SLR for habitat predictions for island configurations with the USACE intermediate curve (for example, figs. A6*B* and *E*), whereas intertidal marsh often was converted to intertidal flat or water, estuarine, for habitat predictions for island configurations with the USACE high curve (for example, figs. A6*A* and *D*).

The areal coverage, in hectares, per habitat for all potential future island configurations is shown in tables A6–A9. In figure A9, the way each restoration measure (R2 to R7) compared to the future without action for the intertidal habitat classes (that is, intertidal beach, intertidal flat, and intertidal marsh) and several supratidal/upland habitat classes (that is, beach, barrier flat, and dune) is shown. For all future island configurations, there were no detectable differences for any of the habitats for island configurations for R3. Although this section focuses on the initial year and year 10, the variability among the three years for a given restoration measure highlights the dynamic nature of barrier island systems (fig. A9).

For intertidal habitats, the percentage change from R0 varied for each scenario and USACE curve (fig. A9). Intertidal beach had a high percentage increase (that is, a percentage change with a magnitude greater than 10 percent) for R2 for all the potential future scenarios and for R6 and R7 for both of the ST2SL1 scenarios. For the initial year, the maximum percentage increase was 32 percent, which was for R2 for the

Table A5. The type, condition, and order for user-defined rules applied to model results via postprocessing by habitat class for the habitat model for the Barrier Island Restoration Feasibility project, Dauphin Island, Alabama. Adapted from Enwright and others (2019b) with permission.

[m, meter; km, kilometer; EHWS, extreme high water springs tide level]

Type of correction	Habitat	Condition	Order
Elevation	Dune	Dune areas that had a probability of less than 0.5 for being above the extreme storm water level were changed to barrier flat.	2
Elevation—depressional habitats	Barrier flat	Barrier flat areas that had a sink depth greater than or equal to 0.5 m were changed to water, fresh.	11
	Intertidal beach	Intertidal beach areas that had a sink depth greater than or equal to 0.01 m should be commonly inundated with standing water and were changed to water, marine.	8
	Intertidal flat	Intertidal flat areas that had a sink depth greater than or equal to 0.01 m should be commonly inundated with standing water and were changed to water, estuarine.	9
	Water, fresh	Water, fresh, areas that did not have a sink depth greater than or equal to 0.5 m were changed to barrier flat.	12
	Woody wetland	Woody wetland areas that did not have a sink depth greater than or equal to 0.1 m were recoded to be woody vegetation.	1
X,Y coordinates	Intertidal beach	Intertidal beach areas that were found to be closer to the back-barrier shoreline than the ocean-facing shoreline were changed to intertidal flat.	3
	Barrier flat	Barrier flat areas that had intertidal beach within a 5-by-5 pixel neighborhood were changed to beach because of the proximity to the ocean-facing shoreline.	10
	Intertidal beach	Intertidal beach areas that are located behind supratidal areas with an elevation to the south for 1 km greater than or equal to 0.6 m and located on the southern half of the island were changed to intertidal flat.	5
	Intertidal flat	Intertidal flat areas that were closer to water, marine, than water, estuarine, and were found to be closer to the back-barrier shoreline than the ocean-facing shoreline were changed to intertidal beach.	6
	Intertidal marsh and intertidal flat	Intertidal marsh areas should be sheltered from high-energy areas (Roland and Douglass, 2005). These areas that did not have an elevation to the south for 8 km greater than or equal to 0.448 m (that is, EHWS) were changed to intertidal beach. This rule was also applied to intertidal flat.	4, 7 (repeated for intertidal flat)

ST3SL3I scenario for the initial year. There were no restoration measures with a high percentage increase for intertidal beach for the year 10 runs. For the initial year, intertidal beach had a high percentage decrease for R6 for ST3SL3H and for all the potential future scenarios for R7 for the ST3SL3 scenarios. For year 10, R7 had a percent decrease of about 11 percent for both ST3SL3 scenarios. The maximum percent decrease was 19 percent, which was for R7 of ST3SL3H for Y0. For the initial year, intertidal flat had a high percent increase for R5 for all potential future conditions except for the scenario with the ST2SL1I scenario. The maximum percent increase was around 23 percent, which was for the ST2SL1H scenario. None of the island restoration measures led to a high percent decrease for any intertidal flat for the initial year. For year 10, R5 of the ST2SL1H and R7 of the ST3SL3H both had a high percentage increase, and a maximum increase of 17 percent for the R5. Similar to the initial year, none of the restoration measures had a high percentage decrease for any intertidal flat for year 10. Intertidal marsh increased for the initial year for R5 for ST2SL1I with a percentage increase of 16 percent. For the initial year, no restoration measure had a high percentage decease for intertidal marsh. Intertidal marsh increased in year 10 for R5 of the ST2SL1I and ST3SL3I scenarios, R6 of the ST3SL3H scenario, and R7 of both ST3SL3 scenarios. The maximum percentage change for year 10 was 19 percent, which was for the R5 of the ST2SL1I scenario. Areas associated with marsh restoration sites were converted to intertidal flat or open water for both scenarios with the high curve (fig. A1.3*A* and *D*).

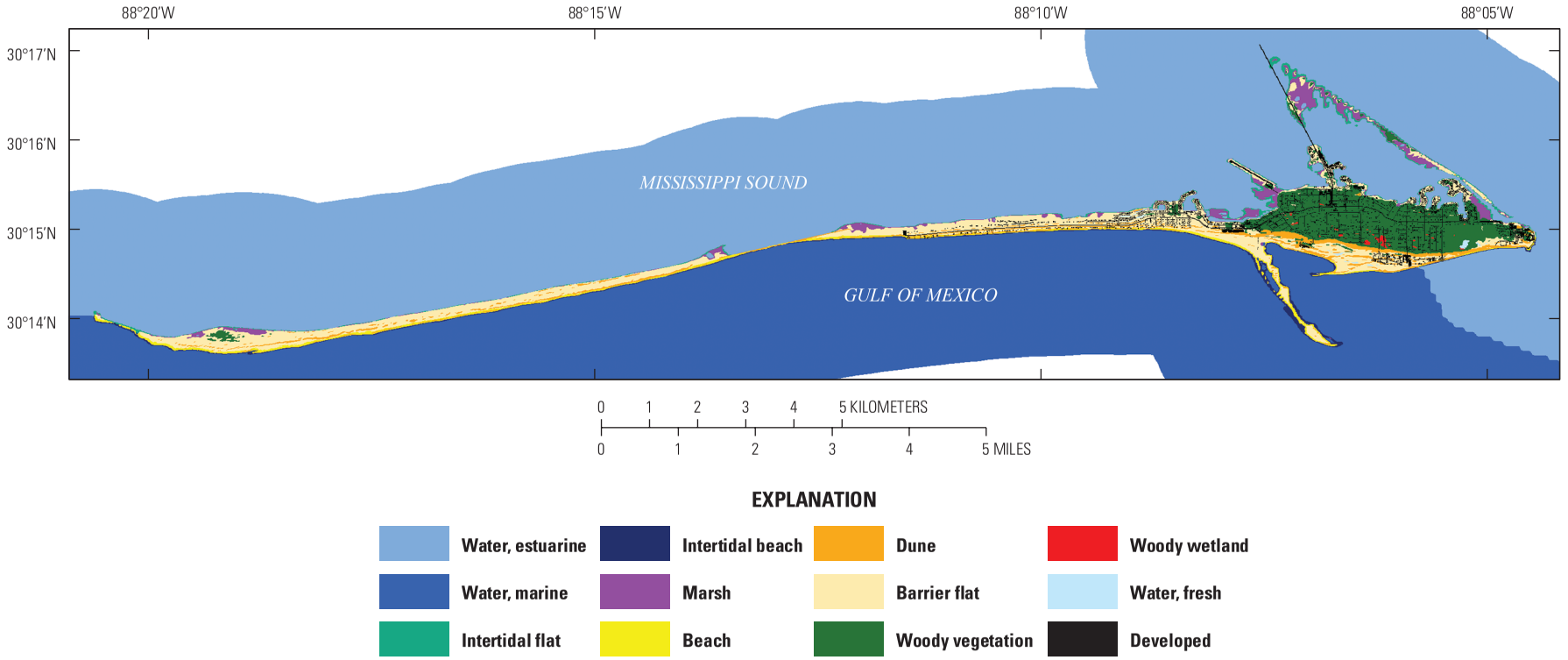

Figure A5. Habitat model results for the 2015 modeled topobathymetric digital elevation model for the Barrier Island Restoration Feasibility Assessment project, Dauphin Island, Alabama.

Table A6. Areal coverage, in hectares, by habitat class for the 2015 modeled topobathymetric digital elevation model and restoration measures with "medium" storminess (ST2) and a sea level 0.3 meter above the contemporary sea level (SL1) using the U.S. Army Corps of Engineers high sea-level rise curve (H) for the Barrier Island Restoration Feasibility Assessment project, Dauphin Island, Alabama.

[ha, hectare; WE, water, estuarine; WM, water, marine; IF, intertidal flat; IB, intertidal beach; IM, intertidal marsh; B, beach; D, dune; BF, barrier flat; WV, woody vegetation; WW, woody wetland; WF, water, fresh; TBDEM, topobathymetric digital elevation model; --, not applicable; R, restoration measure; Y, year]

Restoration measure	Year	Areal coverage (ha) by habitat class										
		WE	WM	IF	IB	IM	B	D	BF	WV	WW	WF
2015 modeled TBDEM	--	10,674.00	11,204.10	84.17	65.30	115.86	95.28	128.39	501.99	356.61	6.35	5.62
Future without action (R0)	Y0	10,701.40	11,215.80	156.23	101.79	115.05	98.05	100.49	417.98	317.24	8.23	6.09
	Y5	10,794.50	11,108.10	184.04	163.56	100.07	73.22	106.12	384.52	310.86	6.71	6.56
	Y10	10,794.40	11,116.30	188.24	171.00	99.39	59.94	108.00	377.06	309.73	6.69	7.47
Pelican Island southeast nourishment (R2)	Y0	10,701.60	11,147.30	156.17	115.81	115.13	114.59	96.68	459.59	317.02	8.35	6.05
	Y5	10,805.10	11,040.30	183.73	179.84	99.86	83.12	106.73	414.35	311.48	7.17	6.61
	Y10	10,806.50	11,052.80	188.08	184.85	98.59	73.98	103.30	405.25	310.88	6.64	7.43
Sand Island platform nourishment and sand bypassing (R3)	Y0	10,701.60	11,215.80	156.13	101.64	114.91	99.17	96.33	421.39	316.98	8.35	5.99
	Y5	10,806.00	11,096.20	184.32	164.45	99.42	72.81	106.29	384.29	311.16	6.78	6.56
	Y10	10,819.20	11,088.20	187.97	174.78	98.86	60.37	108.20	376.73	309.86	6.67	7.48
West and east end beach and dune (R4)	Y0	10,685.40	11,147.60	156.19	102.93	115.55	96.17	114.45	464.34	340.59	8.76	6.39
	Y5	10,800.80	11,033.60	182.16	161.40	104.70	77.52	113.87	425.24	325.53	7.18	6.27
	Y10	10,815.00	11,033.20	186.63	167.42	104.20	61.14	124.59	410.12	322.50	6.64	6.89
Back-barrier tidal flats and marsh habitat restoration (R5)	Y0	10,658.10	11,216.00	192.69	101.72	111.35	97.48	98.68	430.60	317.36	8.35	5.99
	Y5	10,763.60	11,097.50	217.33	162.94	99.11	70.79	104.15	398.22	310.85	7.24	6.54
	Y10	10,777.60	11,093.30	219.79	170.12	99.23	57.07	112.56	384.37	310.06	6.69	7.48
West end beach and dune nourishment (R6)	Y0	10,702.20	11,167.00	156.05	99.26	115.32	95.07	106.53	460.68	322.15	8.34	5.73
	Y5	10,818.40	11,051.30	182.34	161.73	104.06	76.42	107.04	407.05	316.86	7.19	5.92
	Y10	10,820.40	11,061.80	186.55	166.42	103.69	62.78	115.70	393.32	313.99	6.65	7.02
West end and Katrina Cut beach and dune nourishment (R7)	Y0	10,701.50	11,075.40	151.74	97.43	119.29	93.66	119.76	543.38	322.08	8.30	5.72
	Y5	10,808.20	10,988.40	182.10	150.17	105.87	83.90	115.25	474.30	317.00	7.22	5.91
	Y10	10,822.00	10,994.60	188.55	152.59	103.72	62.58	128.83	457.71	314.09	6.65	7.02

Table A7. Areal coverage, in hectares, by habitat class for the 2015 modeled topobathymetric digital elevation model and restoration measures with "medium" storminess (ST2) and a sea level 0.3 meter above the contemporary sea level (SL1) using the U.S. Army Corps of Engineers intermediate sea-level rise curve (I) for the Barrier Island Restoration Feasibility Assessment project, Dauphin Island, Alabama.

[ha, hectare; WE, water, estuarine; WM, water, marine; IF, intertidal flat; IB, intertidal beach; IM, intertidal marsh; B, beach; D, dune; BF, barrier flat; WV, woody vegetation; WW, woody wetland; WF, water, fresh; TBDEM, topobathymetric digital elevation model; --, not applicable; R, restoration measure; Y, year]

Restoration measure	Year	Areal coverage (ha) by habitat class										
		WE	WM	IF	IB	IM	B	D	BF	WV	WW	WF
2015 modeled TBDEM	--	10,674.00	11,204.10	84.17	65.30	115.86	95.28	128.39	501.99	356.61	6.35	5.62
Future without action (R0)	Y0	10,699.10	11,215.70	99.90	101.86	174.09	98.12	100.69	417.39	317.08	8.24	6.07
	Y5	10,794.20	11,108.20	138.94	162.68	145.16	73.08	99.95	391.44	310.89	7.20	6.53
	Y10	10,793.70	11,116.30	147.51	170.91	139.64	60.47	107.98	378.10	309.33	6.84	7.47
Pelican Island southeast nourishment (R2)	Y0	10,699.50	11,147.20	99.84	115.85	173.82	114.69	96.67	459.25	317.08	8.29	6.07
	Y5	10,804.80	11,040.40	138.42	179.11	144.83	83.30	106.65	415.58	311.39	7.18	6.60
	Y10	10,817.10	11,041.70	147.21	184.77	138.76	74.33	103.35	406.39	310.50	6.81	7.43
Sand Island platform nourishment and sand bypassing (R3)	Y0	10,699.40	11,215.70	99.90	101.80	173.77	99.06	96.33	420.90	317.07	8.29	6.01
	Y5	10,805.90	11,096.20	139.36	163.69	144.11	73.30	100.13	390.91	310.87	7.22	6.53
	Y10	10,818.60	11,088.00	147.33	174.88	139.16	60.50	108.34	377.38	309.78	6.87	7.48
West and east end beach and dune (R4)	Y0	10,683.60	11,147.40	99.65	103.05	173.93	96.04	114.45	464.33	340.75	8.71	6.39
	Y5	10,801.10	11,033.70	137.66	160.70	148.97	77.60	113.85	426.01	325.29	7.17	6.29
	Y10	10,814.40	11,033.00	146.93	167.49	143.92	61.09	124.62	410.83	322.30	6.81	6.89
Back-barrier tidal flats and marsh habitat restoration (R5)	Y0	10,669.20	11,202.60	104.71	104.90	202.42	93.94	98.65	429.96	317.54	8.29	6.01
	Y5	10,761.90	11,097.50	144.03	162.35	172.16	70.85	104.16	400.45	311.09	7.24	6.53
	Y10	10,775.40	11,093.30	151.33	169.89	166.74	57.40	112.72	387.34	309.86	6.87	7.48
West end beach and dune nourishment (R6)	Y0	10,700.10	11,166.90	100.01	99.31	173.77	95.17	106.50	460.46	322.08	8.30	5.72
	Y5	10,818.80	11,051.40	137.67	160.80	148.54	76.41	107.06	407.48	317.12	7.18	5.91
	Y10	10,819.80	11,061.60	147.05	166.53	143.32	62.71	115.87	393.88	313.66	6.86	7.05
West end and Katrina Cut beach and dune nourishment (R7)	Y0	10,698.90	11,075.30	95.89	97.65	177.93	97.82	119.69	538.97	322.16	8.29	5.73
	Y5	10,807.80	10,988.50	135.57	150.27	152.49	83.24	116.56	474.00	316.79	7.21	5.92
	Y10	10,821.80	10,994.60	147.33	152.56	144.68	62.41	129.87	457.21	313.96	6.86	7.05

Table A8. Areal coverage, in hectares, by habitat class for the 2015 modeled topobathymetric digital elevation model and restoration measures with "high" storminess (ST3) and a sea level of about 1.0 meter above the contemporary sea level (SL3) using the U.S. Army Corps of Engineers high sea-level rise curve (H) for the Barrier Island Restoration Feasibility Assessment project, Dauphin Island, Alabama.

[ha, hectare; WE, water, estuarine; WM, water, marine; IF, intertidal flat; IB, intertidal beach; IM, intertidal marsh; B, beach; D, dune; BF, barrier flat; WV, woody vegetation; WW, woody wetland; WF, water, fresh; TBDEM, topobathymetric digital elevation model; --, not applicable; R, restoration measure; Y, year]

Restoration measure	Year	Areal coverage (ha) by habitat class										
		WE	WM	IF	IB	IM	B	D	BF	WV	WW	WF
2015 modeled TBDEM	--	10,674.00	11,204.10	84.17	65.30	115.86	95.28	128.39	501.99	356.61	6.35	5.62
Future without action (R0)	Y0	10,867.50	11,251.60	267.82	209.90	137.51	65.90	59.33	163.92	208.32	2.90	3.57
	Y5	10,926.00	11,220.80	232.04	267.19	129.56	63.23	41.61	151.45	200.61	2.47	3.30
	Y10	10,846.90	11,336.50	272.86	241.79	113.53	62.88	32.13	155.39	175.48	0.77	0.00
Pelican Island southeast nourishment (R2)	Y0	10,866.00	11,192.80	267.42	270.50	137.61	65.65	59.91	163.86	208.01	2.90	3.62
	Y5	10,923.10	11,192.80	230.75	290.79	130.76	65.21	41.59	155.14	202.05	2.69	3.36
	Y10	10,857.30	11,322.20	274.60	237.62	112.71	63.65	33.50	159.81	176.07	0.78	0.00
Sand Island platform nourishment and sand bypassing (R3)	Y0	10,854.50	11,264.70	267.18	210.30	137.86	62.76	61.86	164.57	207.98	2.90	3.62
	Y5	10,921.60	11,224.80	227.99	270.70	131.10	61.63	43.13	150.99	200.51	2.51	3.32
	Y10	10,847.20	11,330.90	272.38	244.50	113.23	61.77	34.61	157.50	175.45	0.81	0.00
West and east end beach and dune (R4)	Y0	10,851.90	11,184.60	270.03	191.84	142.05	82.18	70.45	224.55	213.47	3.39	3.80
	Y5	10,936.30	11,144.70	257.78	242.72	141.73	67.02	56.24	180.76	204.99	2.85	3.23
	Y10	10,869.20	11,229.20	297.28	237.24	124.16	67.50	34.93	181.67	193.48	0.79	2.85
Back-barrier tidal flats and marsh habitat restoration (R5)	Y0	10,823.10	11,252.20	311.16	210.10	137.79	62.65	62.50	164.09	208.08	2.90	3.62
	Y5	10,891.10	11,224.10	260.81	259.37	134.67	64.94	43.14	153.57	201.41	1.77	3.34
	Y10	10,829.80	11,324.00	291.33	236.58	121.00	63.67	33.70	162.27	175.19	0.78	0.00
West end beach and dune nourishment (R6)	Y0	10,868.40	11,200.50	270.56	189.05	138.62	76.19	67.24	213.11	208.07	2.91	3.59
	Y5	10,946.50	11,165.30	251.37	243.21	134.32	68.92	48.14	173.93	200.72	2.53	3.32
	Y10	10,871.70	11,261.50	285.63	235.16	128.78	66.47	33.58	179.64	174.99	0.83	0.01
West end and Katrina Cut beach and dune nourishment (R7)	Y0	10,869.80	11,107.50	279.70	169.23	140.89	89.74	74.39	292.60	207.92	2.91	3.61
	Y5	10,973.10	11,056.50	265.09	223.45	152.78	78.74	47.84	234.45	200.64	2.47	3.32
	Y10	10,906.80	11,140.40	302.46	245.41	133.44	68.09	37.90	227.99	174.97	0.84	0.01

Table A9. Areal coverage, in hectares, by habitat class for the 2015 modeled topobathymetric digital elevation model and restoration measures with "high" storminess (ST3) and a sea level of about 1.0 meter above the contemporary sea level (SL3) using the U.S. Army Corps of Engineers intermediate sea-level rise curve (I) for the Barrier Island Restoration Feasibility Assessment project, Dauphin Island, Alabama.

[ha, hectare; WE, water, estuarine; WM, water, marine; IF, intertidal flat; IB, intertidal beach; IM, intertidal marsh; B, beach; D, dune; BF, barrier flat; WV, woody vegetation; WW, woody wetland; WF, water, fresh; TBDEM, topobathymetric digital elevation model; --, not applicable; R, restoration measure; Y, year]

Restoration measure	Year	Areal coverage (ha) by habitat class										
		WE	WM	IF	IB	IM	B	D	BF	WV	WW	WF
2015 modeled TBDEM	--	10,674.00	11,204.10	84.17	65.30	115.86	95.28	128.39	501.99	356.61	6.35	5.62
Future without action (R0)	Y0	10,854.90	11,266.30	126.66	196.38	286.38	66.42	59.31	167.18	208.22	2.93	3.57
	Y5	10,877.00	11,215.00	228.27	214.16	175.79	84.77	41.76	194.98	200.72	2.47	3.42
	Y10	10,775.20	11,334.70	275.65	223.13	142.58	78.96	32.63	198.72	175.77	0.85	0.12
Pelican Island southeast nourishment (R2)	Y0	10,853.50	11,204.20	126.49	258.92	290.86	66.07	59.93	163.52	208.20	2.89	3.62
	Y5	10,871.10	11,188.80	227.87	237.09	176.70	88.59	41.62	198.32	202.11	2.53	3.49
	Y10	10,790.70	11,316.70	275.85	216.86	143.67	80.27	33.98	203.06	176.27	0.84	0.12
Sand Island platform nourishment and sand bypassing (R3)	Y0	10,853.70	11,264.40	126.18	199.22	290.72	63.20	61.92	164.15	208.28	2.89	3.62
	Y5	10,871.60	11,219.20	227.99	214.24	175.86	84.57	43.17	195.07	200.61	2.57	3.43
	Y10	10,776.00	11,327.70	277.02	225.79	141.55	77.46	35.06	201.07	175.63	0.87	0.12
West and east end beach and dune (R4)	Y0	10,843.10	11,196.10	120.60	182.05	298.44	82.15	70.44	224.71	213.55	3.37	3.78
	Y5	10,888.60	11,144.20	219.27	206.60	225.77	82.19	56.37	204.48	204.81	2.84	3.22
	Y10	10,799.00	11,230.00	272.63	233.28	160.84	86.01	35.09	224.22	193.54	0.88	2.89
Back-barrier tidal flats and marsh habitat restoration (R5)	Y0	10,807.90	11,264.70	152.84	199.09	305.38	63.87	62.49	167.14	208.23	2.89	3.70
	Y5	10,835.20	11,217.40	233.60	210.16	198.44	89.55	43.12	204.33	200.54	2.51	3.46
	Y10	10,730.40	11,342.00	280.01	222.36	158.61	83.00	33.95	211.84	175.20	0.83	0.12
West end beach and dune nourishment (R6)	Y0	10,860.00	11,212.00	120.81	179.18	294.64	76.35	67.20	213.28	208.25	2.94	3.59
	Y5	10,896.70	11,164.30	217.27	203.65	210.23	84.80	48.24	206.47	200.82	2.51	3.36
	Y10	10,800.00	11,261.60	276.71	225.31	150.89	80.92	33.85	233.06	175.06	0.89	0.05
West end and Katrina Cut beach and dune nourishment (R7)	Y0	10,868.50	11,111.40	115.09	164.89	306.98	89.62	74.33	293.01	208.01	2.86	3.65
	Y5	10,922.90	11,059.90	215.50	201.79	226.02	89.89	48.03	267.97	200.57	2.48	3.32
	Y10	10,836.80	11,141.00	278.91	239.58	162.6	73.25	39.45	291.08	174.53	1.06	0.09

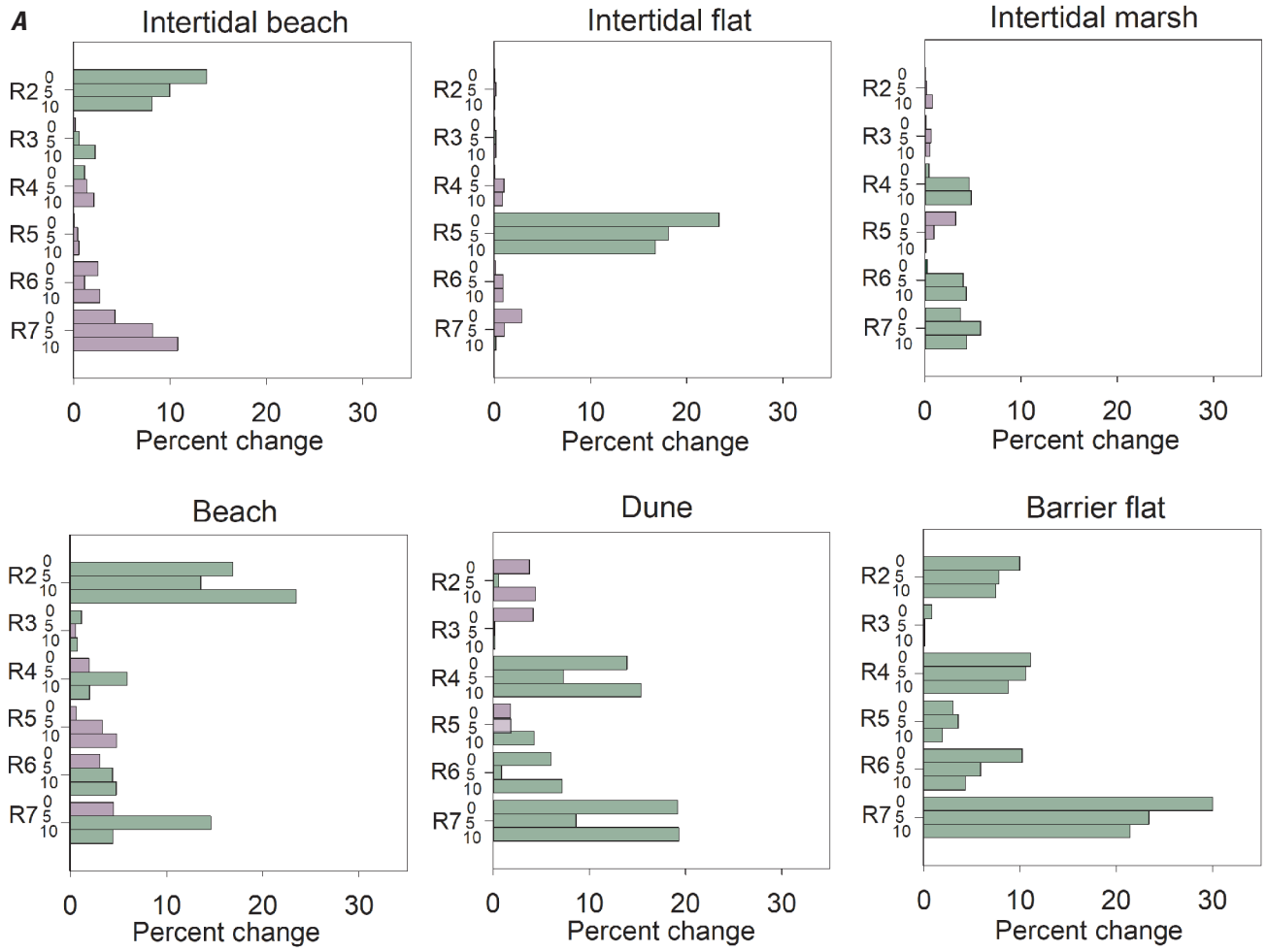

Figure A9. Percentage change for selected habitat classes for restoration measures relative to the future without action (R0) measure for the Barrier Island Restoration Feasibility Assessment project, Dauphin Island, Alabama. *A*, "medium" storminess (ST2) and a sea level 0.3 meter above the contemporary sea level (SL1) using the U.S. Army Corps of Engineers (USACE) high sea-level rise (SLR) curve (H); *B*, ST2SL1 using the USACE intermediate SLR curve (I); *C*, "high" storminess (ST3) and a sea level of about 1.0 meter above the contemporary sea level (SL3) using the USACE high SLR curve (H); *D*, ST3SL3I. [Green bars indicate a percentage increase and purple bars indicate a percentage decrease. R2, Pelican Island southeast nourishment; R3, Sand Island platform nourishment and sand bypassing; R4, west and east end beach and dune nourishment; R5, back-barrier tidal flats and marsh habitat restoration; R6, west end beach and dune restoration; R7, west end and Katrina Cut beach and dune restoration. Numbers on the y-axis indicate the year of the run]

For supratidal/upland habitats (fig. A2), the percentage change from R0 was similar for both USACE curves (fig. A9). In contrast to intertidal habitats, no restoration measure led to a high percentage decrease of beach, dune, or barrier flat habitat. For the initial year, beach had a high percentage increase in R2 for both ST2SL1 scenarios R4, R6, and R7 for both of the ST3SL3 scenarios. The maximum percent increase was around 36 percent, which was for R7 of the ST3SL3H scenario. For year 10, R2 had a high percent increase of around 23 percent in both ST2SL1 scenarios. For the initial year, dune habitat had a high percent increase for R4 and R7 in all scenarios and for R6 of the ST3SL3H scenario. The maximum percent increase was around 22 percent, which was for R7 in the ST3SL3H scenario. In year 10, dune habitat had a high percent increase for R4 of the ST2SL1 scenarios and R7 in all scenarios. The maximum percent increase in year 10 for dune was 21 percent, which was R7 in the ST3SL3I scenario. For the initial year, barrier flat had a high percentage increase for R2 of both ST2SL1 scenarios and for R4, R6, and R7 in all scenarios. The maximum percentage increase was around 79 percent, which was for R7 of the ST3SL3H scenario. For year 10, barrier flat had a high percentage increase for R4

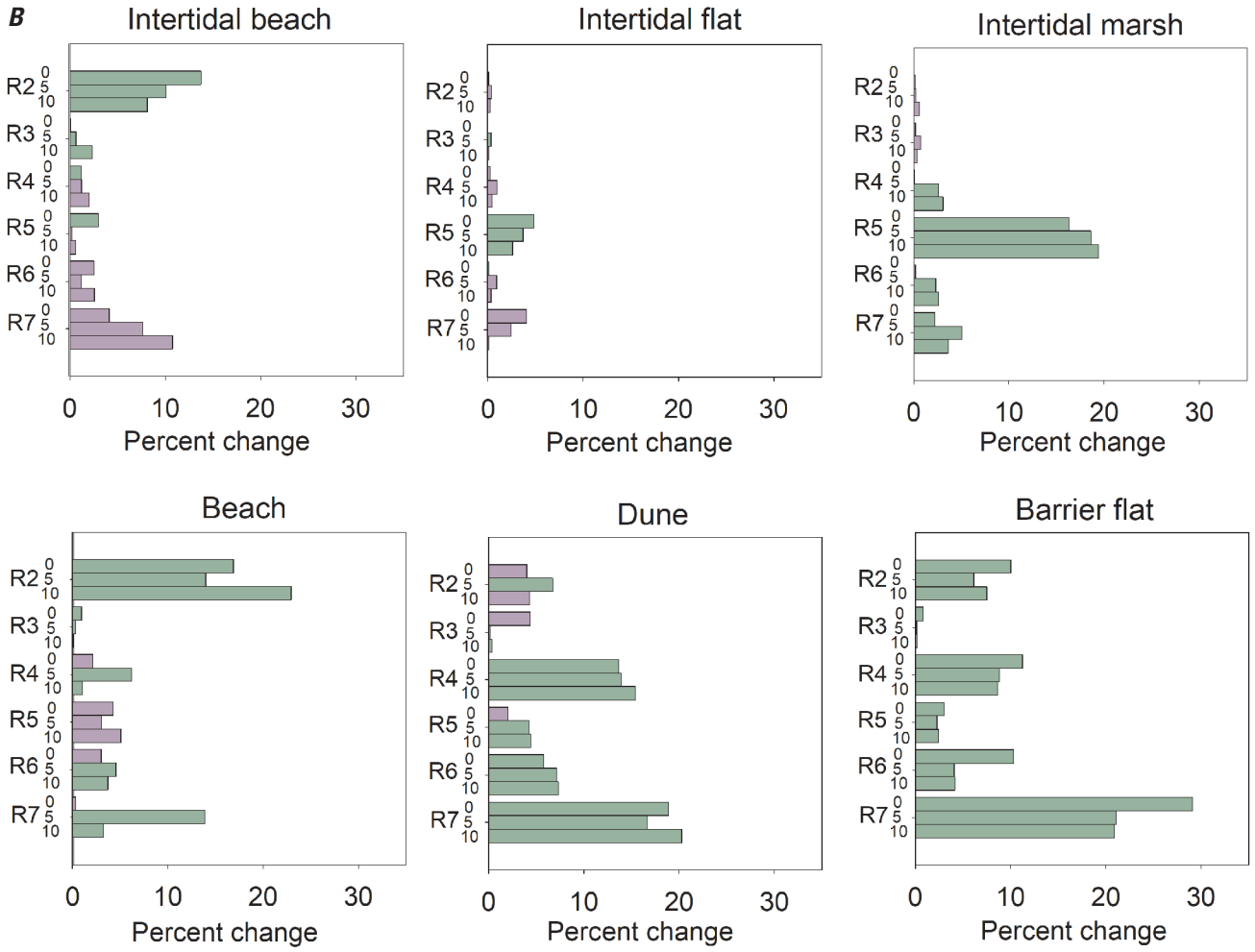

Figure A9. —Continued

and R6 of both ST3SL3 scenarios and for R7 of all island configurations. The maximum percentage increase for barrier flat in year 10 was 47 percent, which was R7 of the ST3SL3H scenario.

Discussion

In this effort, we extended a machine learning-based barrier island habitat model framework (Enwright and others, 2019b) to predict barrier island habitats under potential future alternative states of Dauphin Island, Ala. To our knowledge, this effort is the first model that predicts barrier island-specific habitats based on linkages to a hydrodynamic geomorphic model. Some limitations specific to the model development along with suggested next steps are discussed in Enwright and others (2019b). These limitations included (1) estimating habitat-geomorphology linkages from a single snapshot; (2) difficulty with estimating vegetation coverage on the barrier flat; (3) development of a single model compared to developing a model specific to island orientation and wave energy setting (for example, Little Dauphin Island and Pelican Island); and (4) spatial resolution.

The application of this model to predicted geomorphology introduces some additional limitations. First, the quiescent period hydrodynamic geomorphic model will have increased uncertainty along the back barrier because local winds were not incorporated (Mickey and others, 2020). Along these lines, a separate effort is underway by the USACE and the USGS St. Petersburg Coastal and Marine Science Center to update geomorphic models for Little Dauphin Island. Second, although our analyses allowed for tidal saline wetland migration, the hydrodynamic geomorphic models were not run for an end-to-end simulation when moving from current sea level to the future sea levels because of computational limitations. Because of this, our results may miss some overwash events that could have provided critical sediments to marshes and other potential dynamic effects of SLR. Despite these uncertainties and assumptions, our results suggest that regular

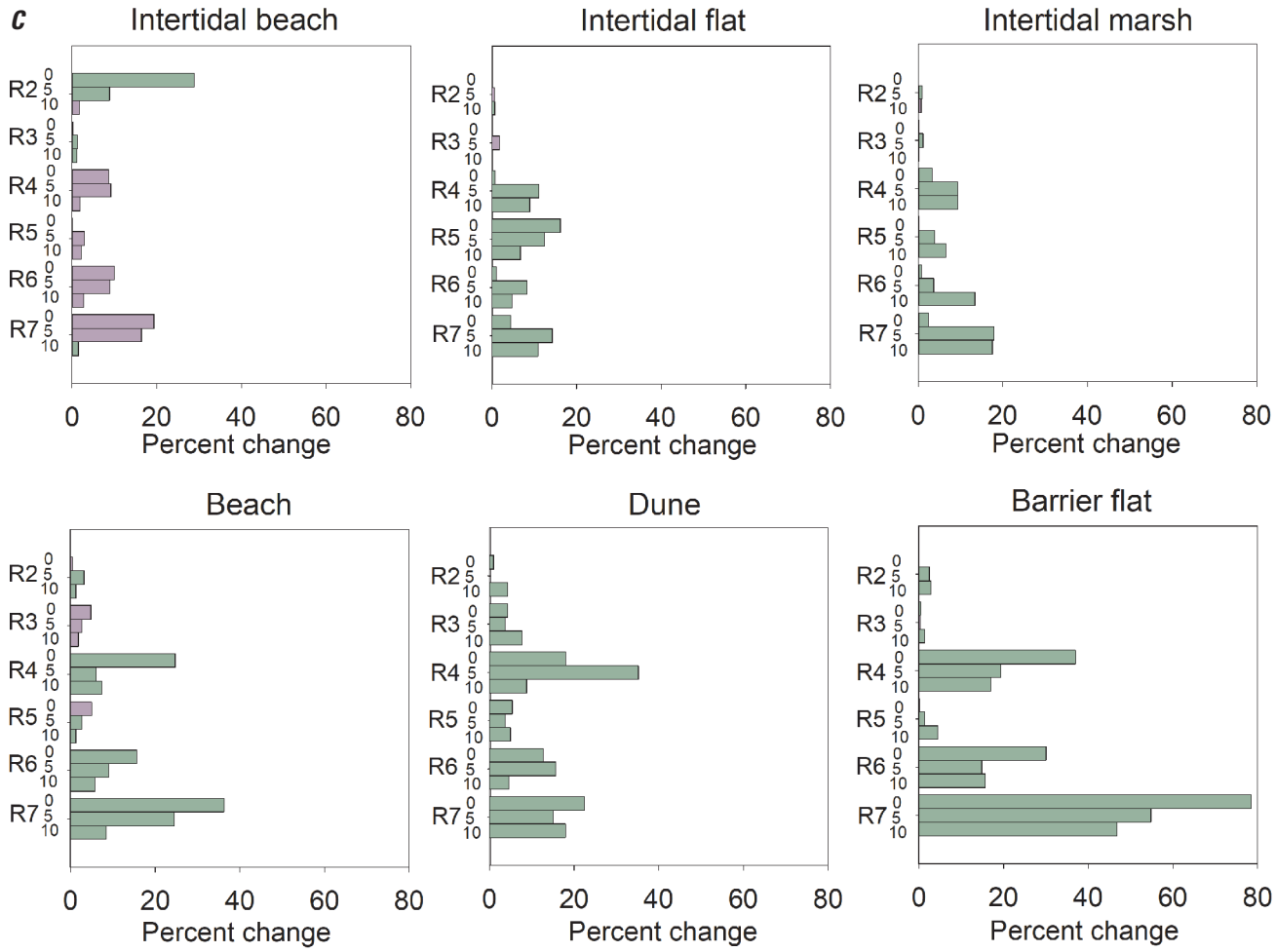

Figure A9. —Continued

maintenance of intertidal marsh may be warranted under accelerated SLR, especially under conditions with infrequent storms and low overwash depth, which is in line with other studies, such as Walters and Kirwan (2016). Future applications of a barrier island habitat model framework similar to this one could explore the incorporation of a more dynamic coastal wetland response using an approach similar to Alizad and others (2016). This approach would require TBDEM correction using a regression-based approach to correct the DEM similar to ones used by Medeiros and others (2015) and Buffington and others (2016), which was beyond the scope of this effort. Although our approach did not include TBDEM correction, we did include probabilistic outputs related to tidal zones, which are important for enhancing the automated extraction of intertidal areas (Enwright and others, 2018). Along those lines, researchers could also explore using a hydrodynamic geomorphic model for insights into how the tidal range is changing under alternative sea levels (Passeri and others, 2016) rather than assuming the tidal range would be similar in the future. Third, although the results included changes in woody wetlands, it is likely that these changes are a result of model smoothing rather than actual topographic changes. Finally, for future efforts, researchers should explore treating restored dune extraction differently from natural dune extraction to account for broader topography that is commonly associated with the initial phases of dune restoration efforts.

The results from our modeling effort provide insights to natural resource managers and planners on how a restoration project may maintain or impede the occurrence of natural coastal processes and provide information critical for making future-focused decisions regarding barrier island restoration. The interpretation of these results can hinge on numerous management objectives, many of which could have tradeoffs; therefore, the results from this effort could be analyzed using a structured decision-making process, such as the one used by Dalyander and others (2016), to provide planners with an understanding of how restoration actions could positively or negatively affect habitat resources over time. In this kind of decision-making framework, the results from this study could be coupled with habitat suitability predictions for oysters

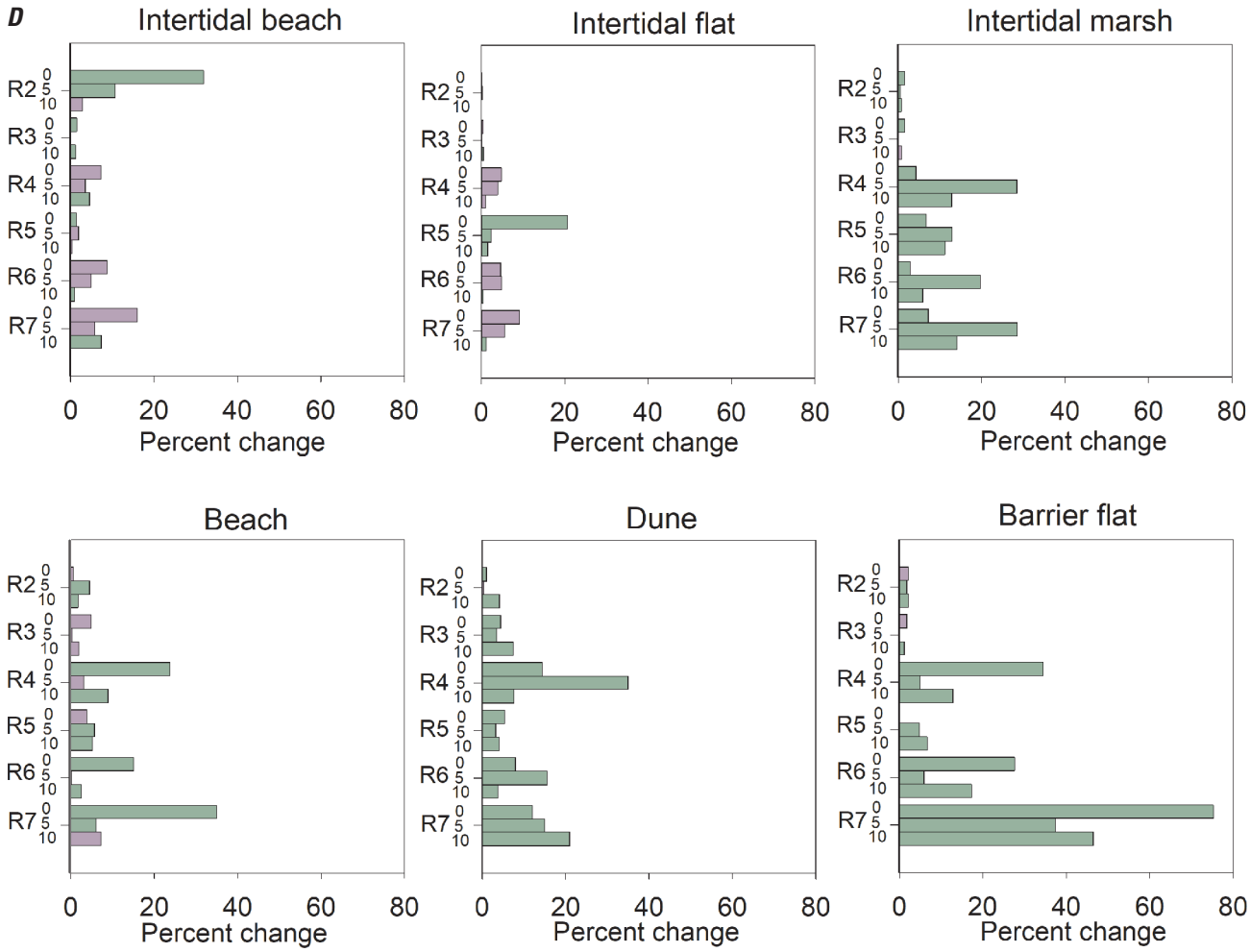

Figure A9. —Continued

and seagrass (chapters B and C) and (or) linkages of how the restoration measure may benefit specific fish and wildlife such as *Acipenser oxyrinchus*, Mitchill (Gulf sturgeon); shorebirds; neotropical migrants; and sea turtles and restoration cost to make an informed decision on tradeoffs for the various restoration measures.

Conclusion

A machine learning-based barrier island habitat model framework (Enwright and others, 2019b) was used in this study to predict barrier island habitats under potential future alternative states of Dauphin Island. We predicted habitat coverage for 43 island configurations, which included the 2015 modeled DEM along with 12 model outputs per restoration measure for two potential conditions related to storminess and sea level. Our results provide valuable insights into the sustainability of Dauphin Island along with how various restoration measures may alter habitat coverage. The future without action measure provided helpful information on the sustainability of Dauphin Island for several future conditions related to storminess and SLR. Comparing habitat model results for various restoration measures provided quantitative information on how a restoration project may maintain or impede the occurrence of natural coastal processes and how these restoration measures may influence the sustainability of the island resources. For example, we found that restoration measures had the potential to reduce island breaching and, therefore, maintain acreage of subaerial habitat types. Intertidal marsh marsh tended to keep pace with SLR for scenarios with the USACE intermediate curve, whereas intertidal marsh often was converted to intertidal flat or open water for scenarios with the USACE high SLR curve. Along those lines, the modeling results indicated that areas restored for the back-barrier marsh restoration measure were converted to intertidal flat under the scenario with faster SLR, which indicates that regular nourishment may be necessary to maintain marsh restoration areas, especially if storm frequency is low

and overwash depth is low. This information can be used as one component in a multifaceted, structured decision-making process, such as the one used by Dalyander and others (2016) to make future-focused decisions regarding barrier island restoration.

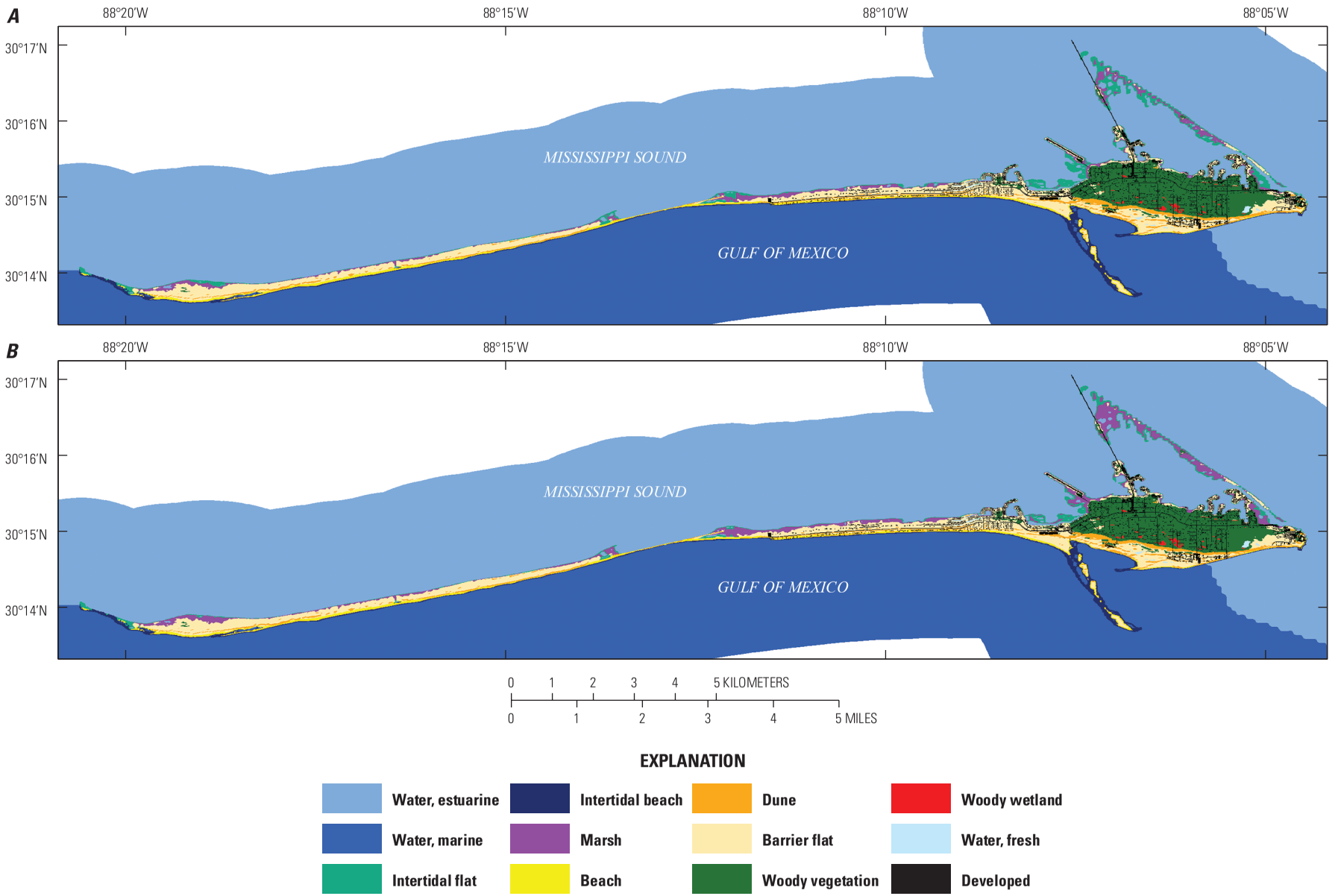

Figure A6. Habitat model results for the future without action restoration measure (R0) for the Barrier Island Restoration Feasibility Assessment project, Dauphin Island, Alabama. *A*, year 0 for "medium" storminess (ST2) and a sea level 0.3 meter (m) above the contemporary sea level (SL1) using the U.S. Army Corps of Engineers (USACE) high sea-level rise (SLR) curve (H); *B*, year 0 for ST2SL1 using the USACE intermediate SLR curve (I); *C*, year 10 for ST2SL1H; *D*, year 10 for ST2SL1I; *E*, year 0 for "high" storminess (ST3) and a sea level of about 1.0 m above the contemporary level (SL3) using the USACE high SLR curve (H); *F*, year 0 for ST3SL3 using the USACE intermediate SLR curve (I); *G*, year 10 for ST3SL3H; *H*, year 10 for ST3SL3I.

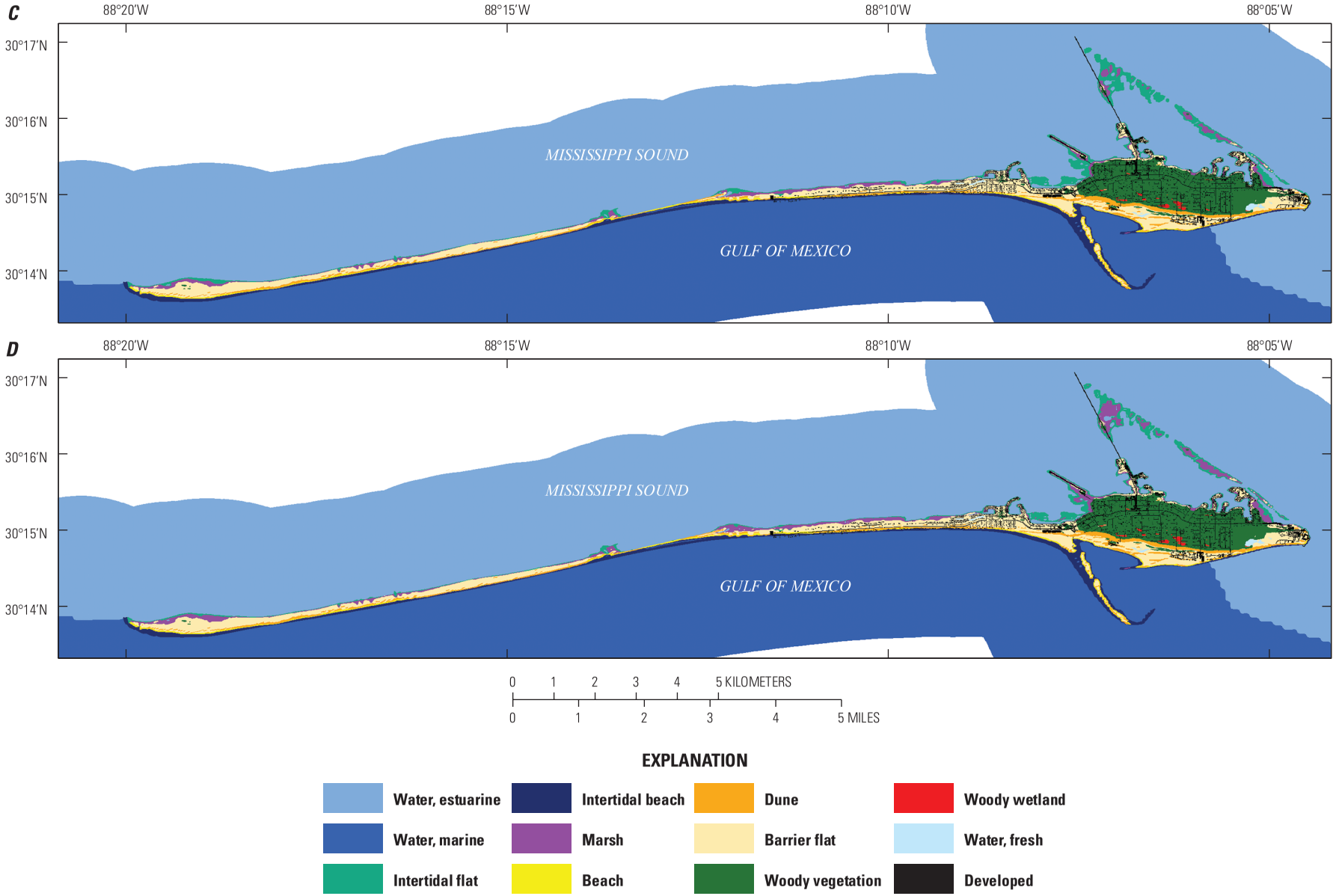

Figure A6. —Continued

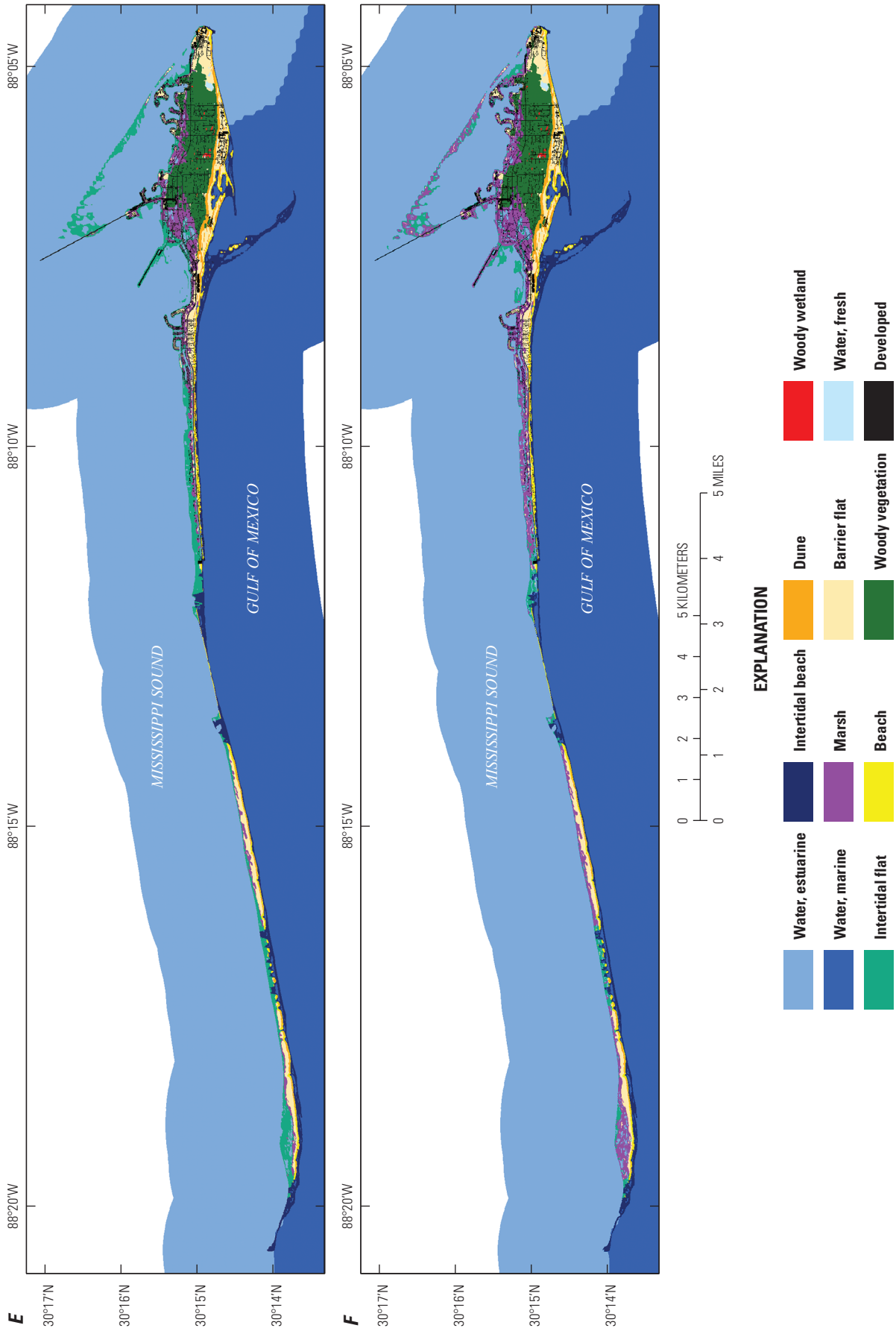

Figure A6. —Continued

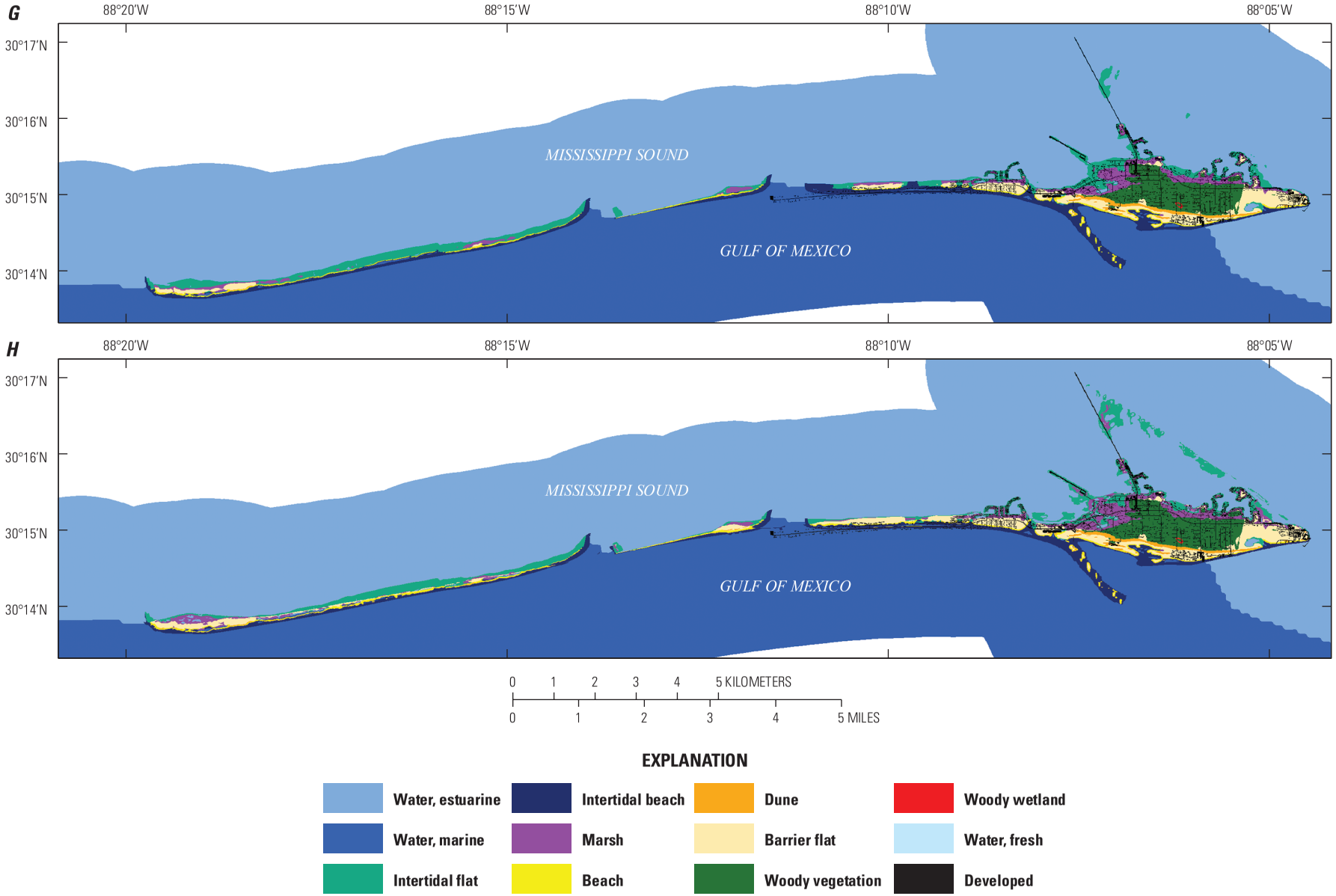

Figure A6. —Continued

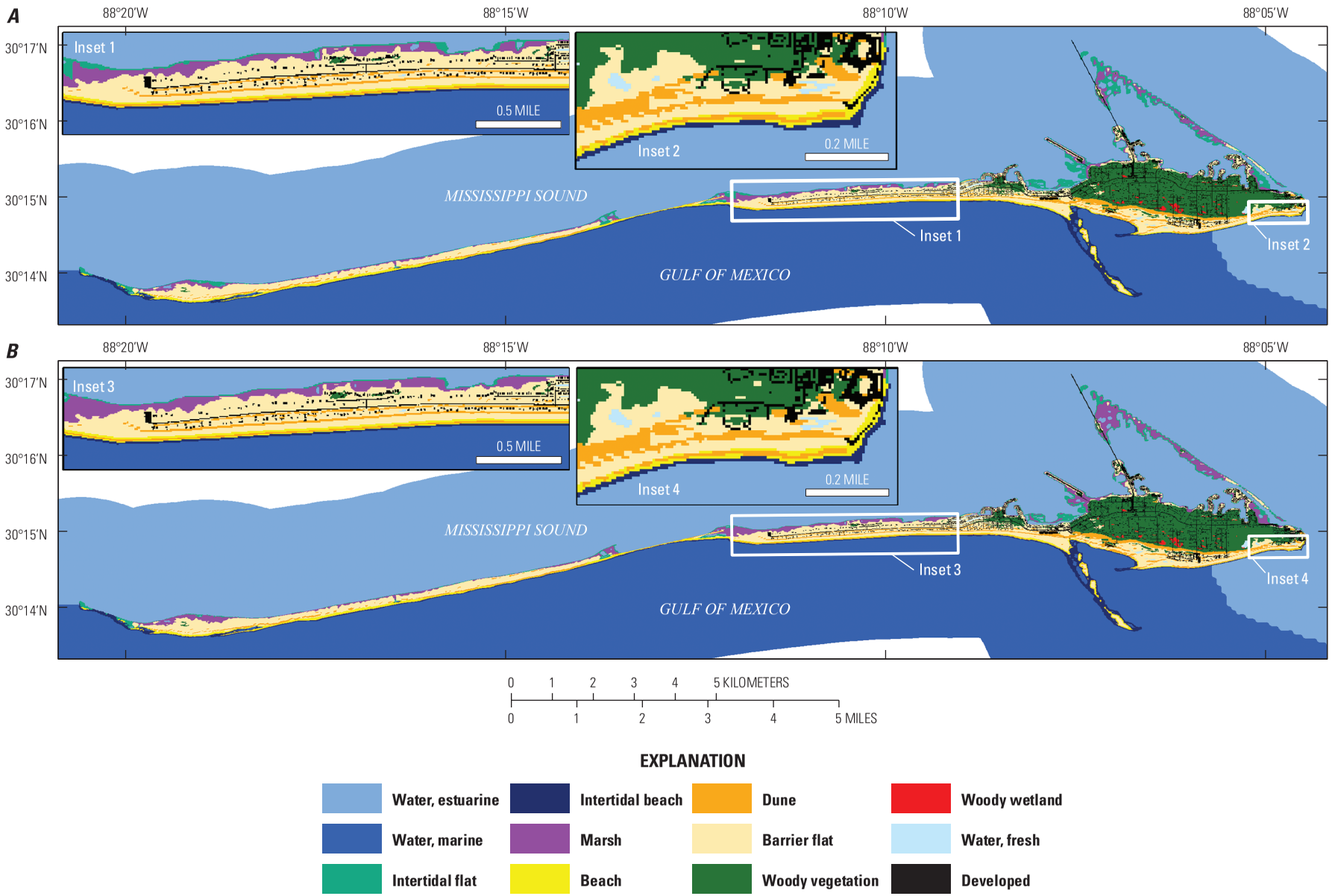

Figure A7. Habitat model results for the west and east end beach and dune nourishment restoration measure (R4) for the Barrier Island Restoration Feasibility Assessment project, Dauphin Island, Alabama. *A*, year 0 for "medium" storminess (ST2) and a sea level 0.3 meter (m) above the contemporary sea level (SL1) using the U.S. Army Corps of Engineers (USACE) high sea-level rise (SLR) curve (H); *B*, year 0 for ST2SL1 using the USACE intermediate SLR curve (I); *C*, year 10 for ST2SL1H *D*, year 10 for ST2SL1I; *E*, year 0 for "high" storminess (ST3) and a sea level of about 1.0 m above the contemporary level (SL3) using the USACE high SLR curve (H), *F*, year 0 for ST3SL3 using the USACE intermediate SLR curve (I), *G*, year 10 for ST3SL3H, *H*, year 10 for ST3SL3I. The dashed pink box indicates the general area of the restoration measure.

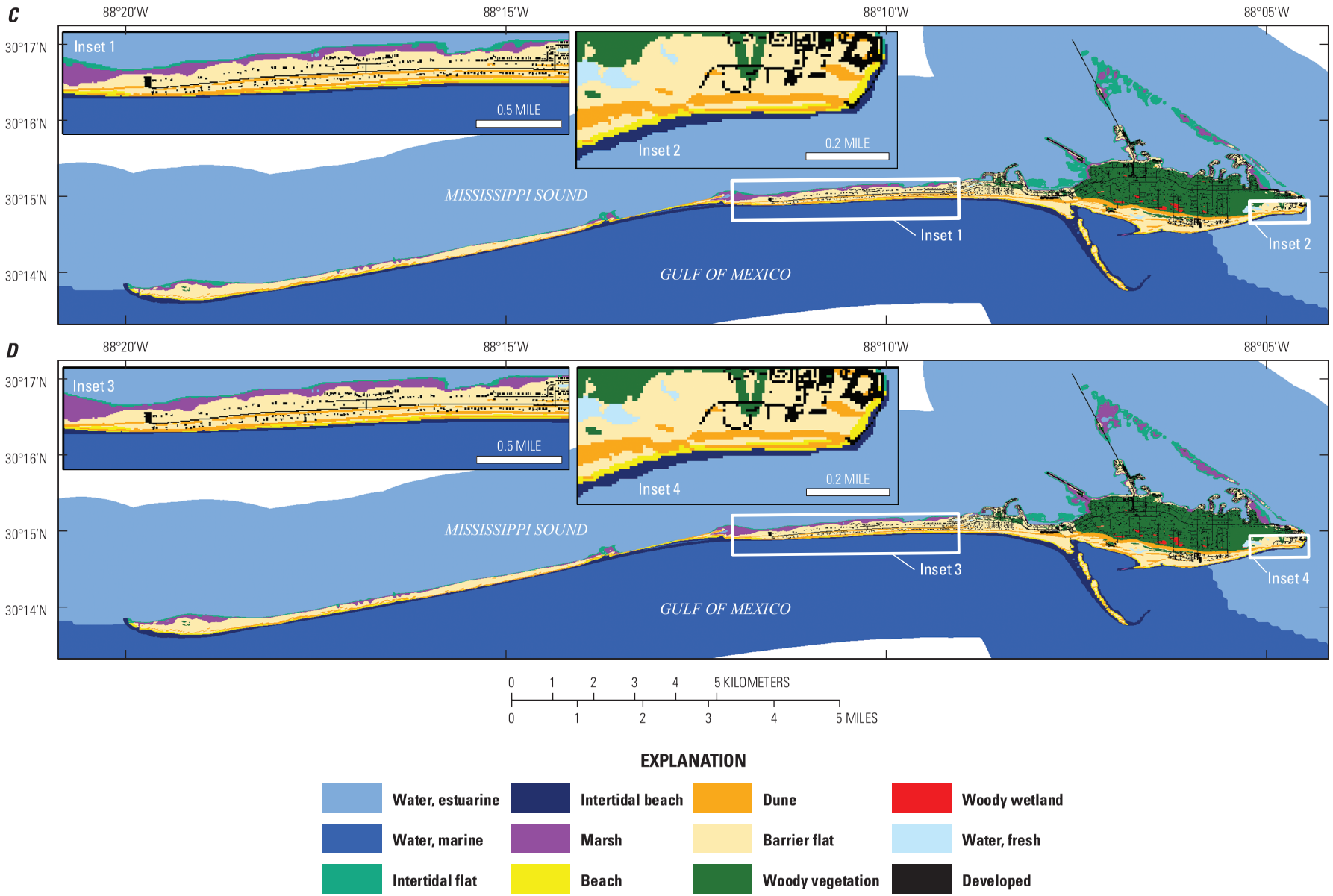

Figure A7. —Continued

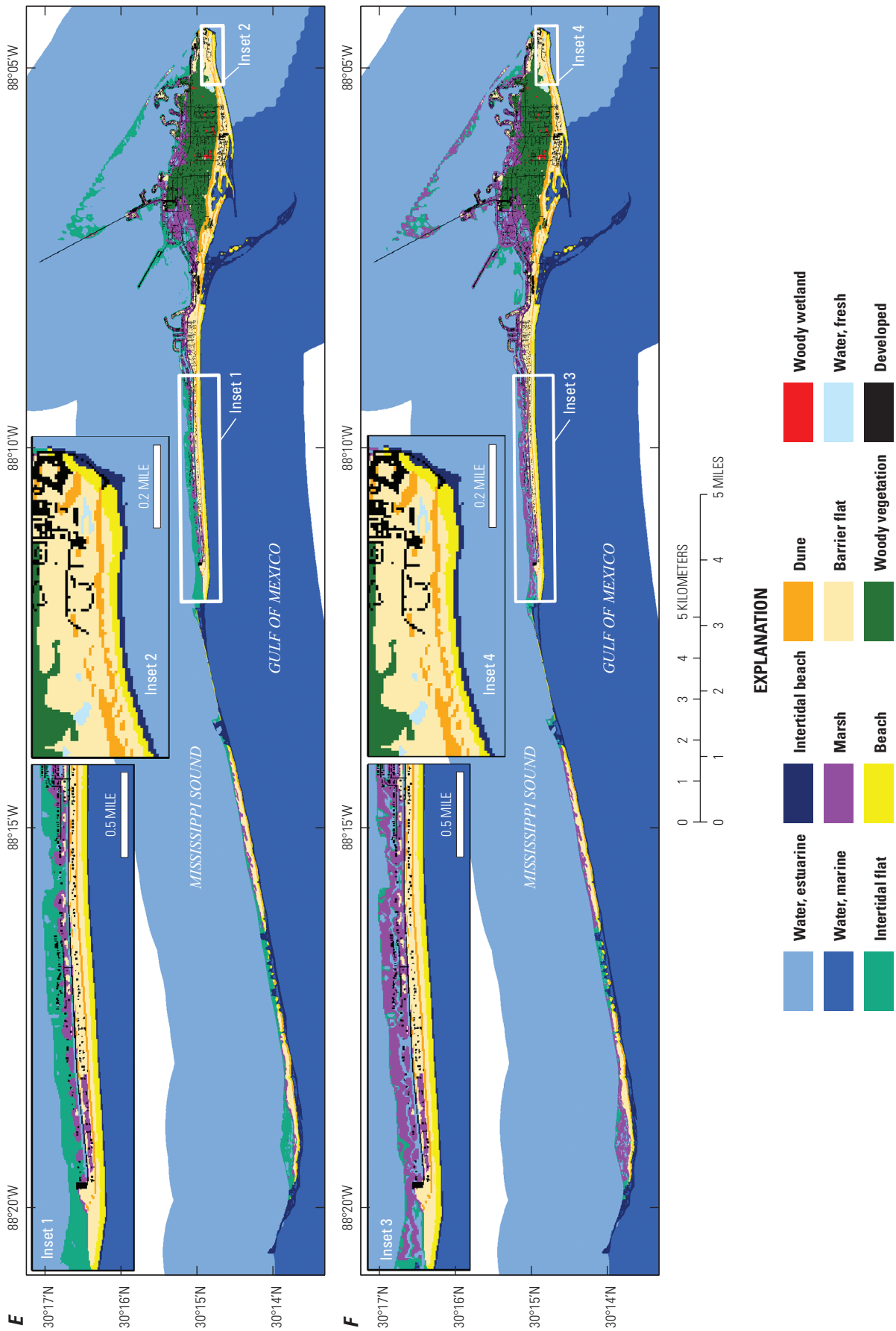

Figure A7. —Continued

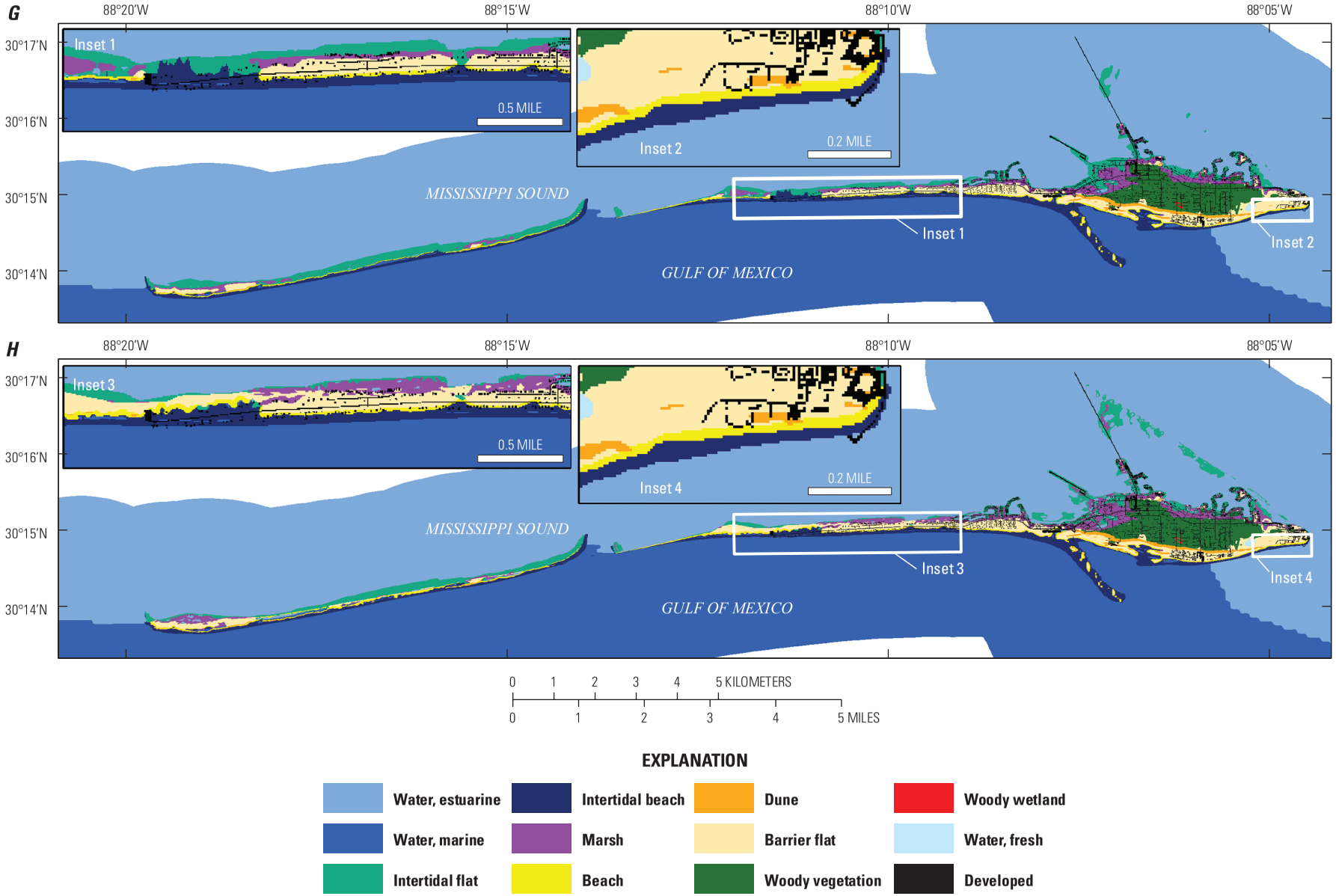

Figure A7. —Continued

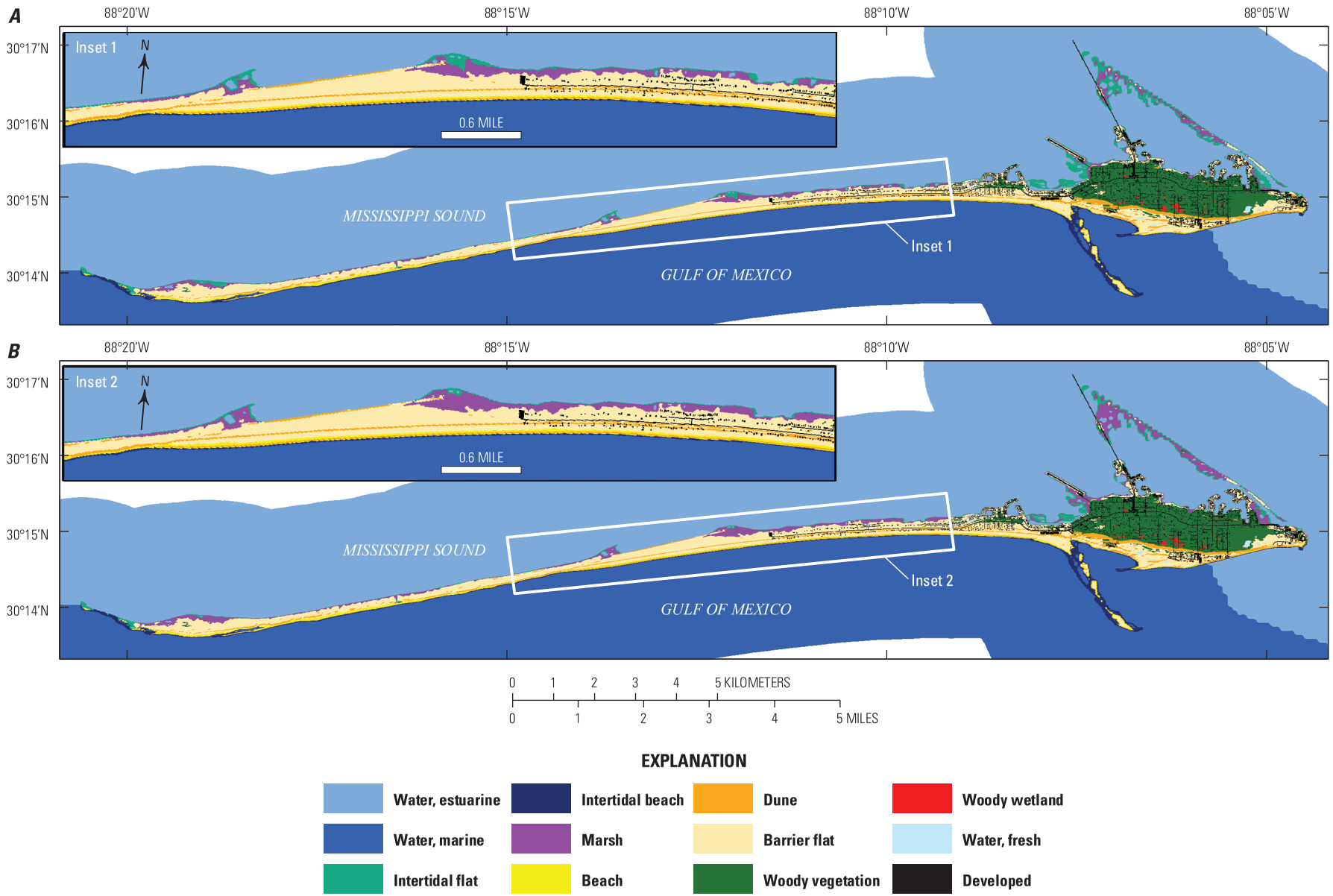

Figure A8. Habitat model results for the west end and Katrina Cut beach and dune nourishment restoration measure (R7) for the Barrier Island Restoration Feasibility Assessment project, Dauphin Island, Alabama. *A*, year 0 for "medium" storminess (ST2) and a sea level 0.3 meter (m) above the contemporary sea level (SL1) using the U.S. Army Corps of Engineers (USACE) high sea-level rise (SLR) curve (H); *B*, year 0 for ST2SL1 using the USACE intermediate SLR curve (I); *C*, year 10 for ST2SL1H; *D*, year 10 for ST2SL1I; *E*, year 0 for "high" storminess (ST3) and a sea level of about 1.0 m above the contemporary level (SL3) using the USACE high SLR curve (H); *F*, year 0 for ST3SL3 using the USACE intermediate SLR curve (I); *G*, year 10 for ST3SL3H; *H*, year 10 for ST3SL3I. The solid white box indicates the general area of the restoration measure.

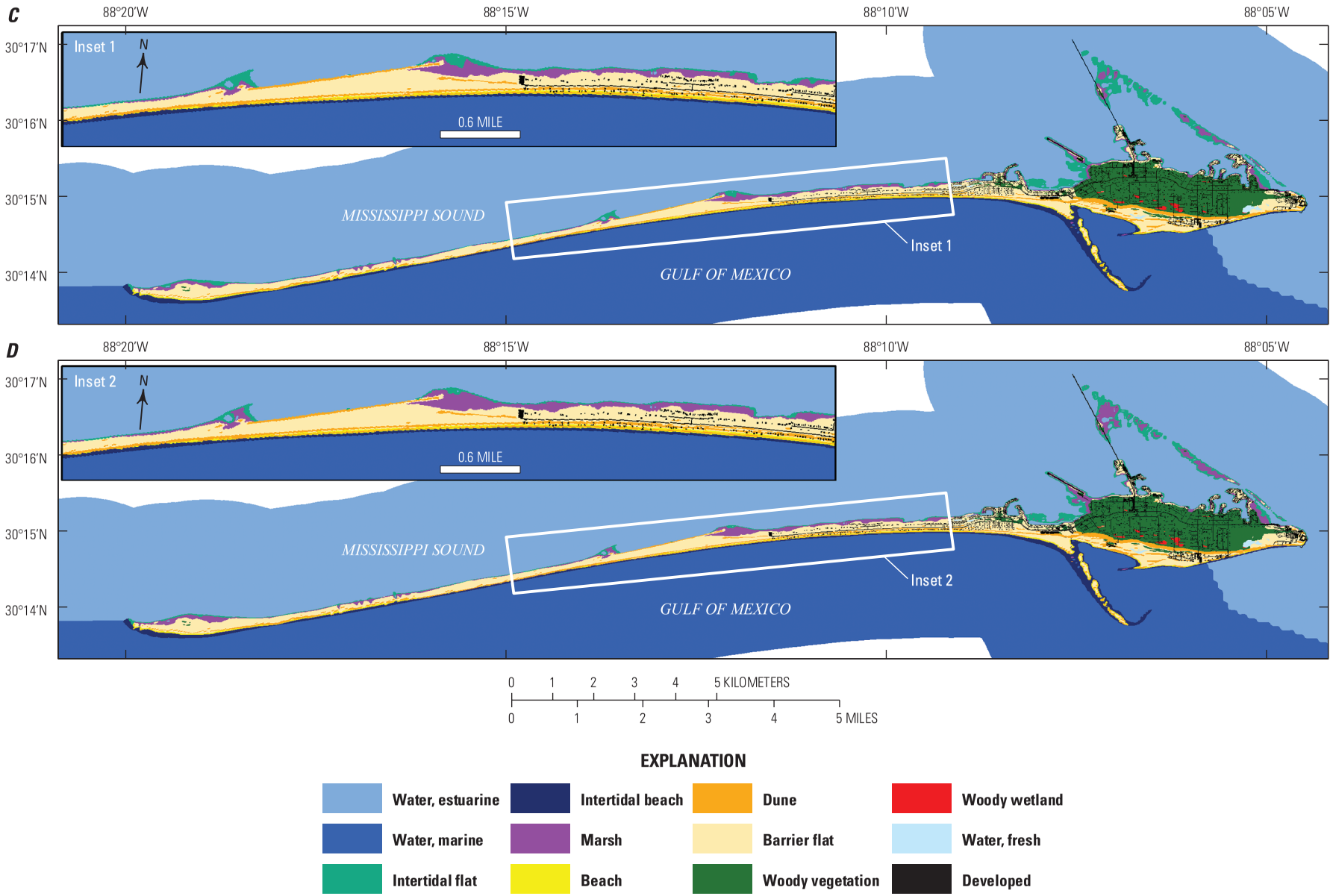

Figure A8. —Continued

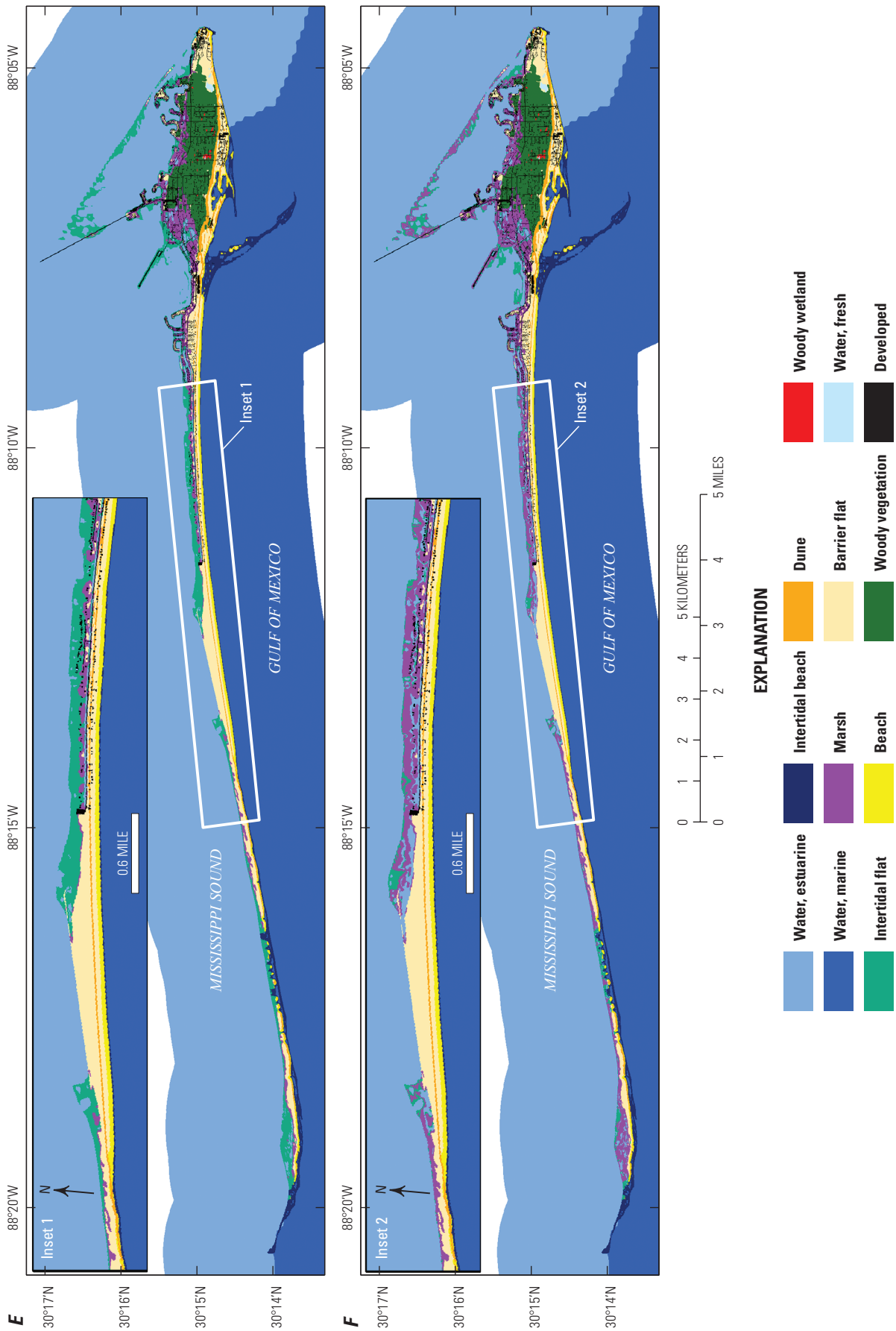

Figure A8. —Continued

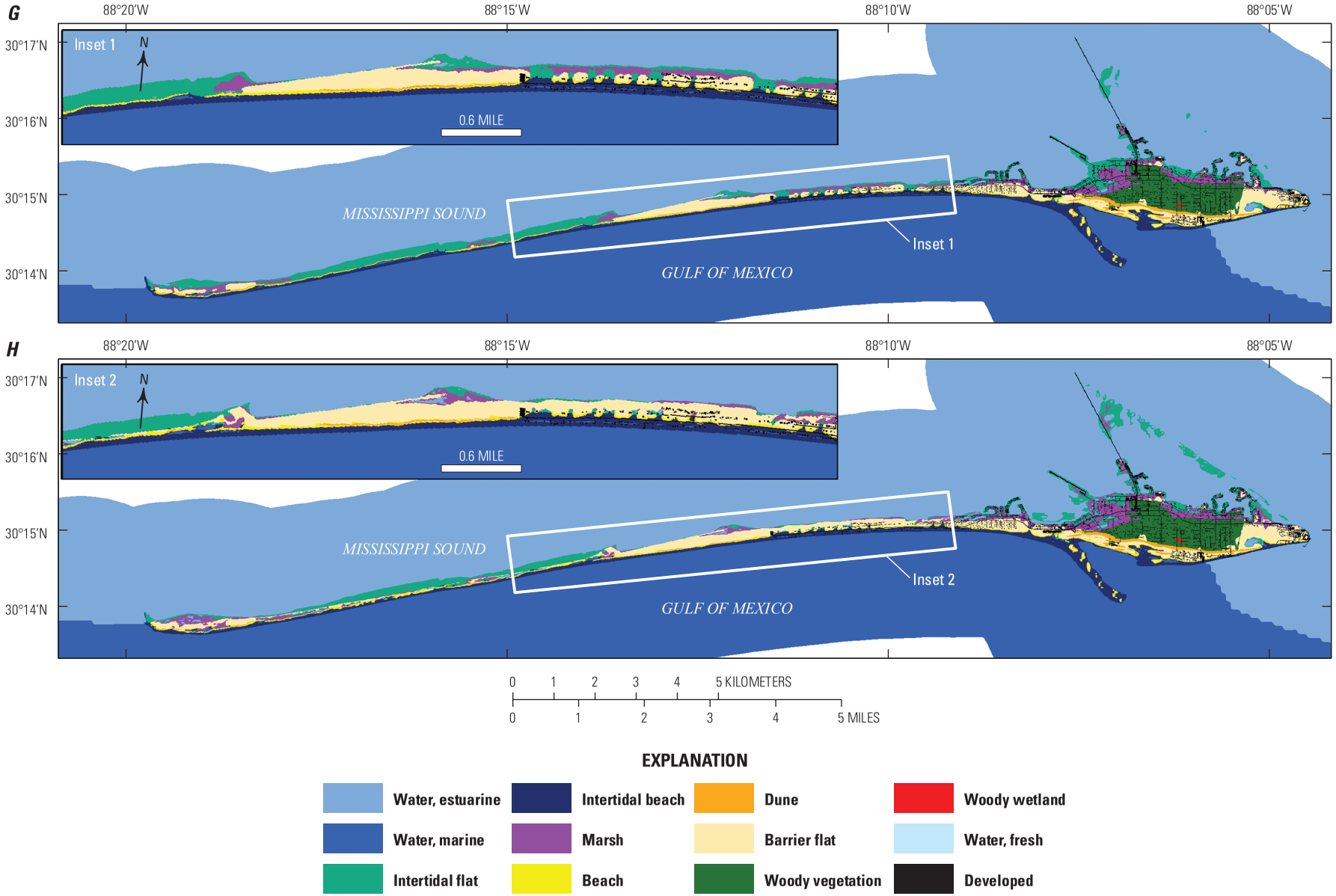

Figure A8. —Continued

References Cited

Acosta, A., Carranza, M.L., and Izzi, C.F., 2005, Combining land cover mapping of coastal dunes with vegetation analysis: Applied Vegetation Science, v. 8, no. 2, p. 133–138. [Also available at https://doi.org/10.1111/j.1654-109X.2005.tb00638.x.]

Alizad, K., Hagen, S.C., Morris, J.T., Medeiros, S.C., Bilskie, M.V., and Weishampel, J.F., 2016, Coastal wetland response to sea-level rise in a fluvial estuarine system: Earth's Future, v. 4, no. 11, p. 483–497. [Also available at https://doi.org/10.1002/2016EF000385.]

Anderson, C.P., Carter, G.A., and Funderburk, W.A., 2016, The use of aerial RGB imagery and LIDAR in comparing ecological habitats and geomorphic features on a natural versus man-made barrier island: Remote Sensing, v. 8, no. 7, 17 p. [Also available at https://doi.org/10.3390/rs8070602.]

Barbier, E.B., Hacker, S.D., Kennedy, C., Koch, E.W., Stier, A.C., and Silliman, B.R., 2011, The value of estuarine and coastal ecosystem services: Ecological Monographs, v. 81, no. 2, p. 169–193. [Also available at https://doi.org/10.1890/10-1510.1.]

Buffington, K.J., Dugger, B.D., Thorne, K.M., and Takekawa, J.Y., 2016, Statistical correction of lidar-derived digital elevation models with multispectral airborne imagery in tidal marshes: Remote Sensing of Environment, v. 186, p. 616–625. [Also available at https://doi.org/10.1016/j.rse.2016.09.020.]

Cowardin, L.M., Carter, V., Golet, F.C., and LaRoe, E.T., 1979, Classification of wetlands and deepwater habitats of the United States: U.S. Fish and Wildlife Service, Report FWS/OBS–79/31, 131 p.

Dalyander, P.S., Meyers, M.B., Mattsson, B., Steyer, G., Godsey, E., McDonald, J., Byrnes, M.R., and Ford, M., 2016, Use of structured decision-making to explicitly incorporate environmental process understanding in management of coastal restoration projects—Case study on barrier islands of the northern Gulf of Mexico: Journal of Environmental Management, v. 183, p. 497–509. [Also available at https://doi.org/10.1016/j.jenvman.2016.08.078.]

Dayton, P.K., 1972, Toward an understanding of community resilience and the potential effects of enrichments to the benthos at McMurdo Sound, Antarctica, *in* Proceedings of the Colloquium on Conservation Problems in Antarctica: Lawrence, Kans., Allen Press, p. 81–96.

Ellis, A.M., Smith, C.G., and Marot, M.E., 2018, The sedimentological characteristics and geochronology of the marshes of Dauphin Island, Alabama: U.S. Geological Survey Open-File Report 2017–1165, accessed November 2019 at https://doi.org/10.3133/ofr20171165.

Enwright, N.M., Borchert, S.M., Day, R.H., Feher, L.C., Osland, M.J., Wang, L., and Wang, H., 2017, Barrier island habitat map and vegetation survey—Dauphin Island, Alabama, 2015: U.S. Geological Survey Open-File Report 2017–1083, 17 p., accessed October 2018 at https://doi.org/10.3133/ofr20171083.

Enwright, N.M., Griffith, K.T., and Osland, M.J., 2016, Barriers to and opportunities for landward migration of coastal wetlands with sea-level rise: Frontiers in Ecology and the Environment, v. 14, no. 6, p. 307–316. [Also available at https://doi.org/10.1002/fee.1282.]

Enwright, N.M., Wang, L., Borchert, S.M., Day, R.H., Feher, L.C., and Osland, M.J., 2018, The impact of lidar elevation uncertainty on mapping intertidal habitats on barrier islands: Remote Sensing, v. 10, no. 1, p. 1–18. [Also available at https://doi.org/10.3390/rs10010005.]

Enwright, N.M., Wang, L., Borchert, S.M., Day, R.H., Feher, L.C., and Osland, M.J., 2019a, Advancing barrier island habitat mapping using landscape position information: Progress in Physical Geography: Earth and Environment, v. 43, no. 3, p. 425–450. [Also available at https://doi.org/10.1177/0309133319839922.]

Enwright, N.M., Wang, L., Wang, H., Osland, M.J., Feher, L.C., Borchert, S.M., and Day, R.H., 2019b, Modeling barrier island habitats using landscape position information: Remote Sensing, v. 11, no. 8, 24 p. [Also available at https://doi.org/10.3390/rs11080976.]

Enwright, N.M., Wang, L., Wang, H., Dalyander, P.S., Osland, M.J., Stelly, S.J., Mickey, R.C., Feher, L.C., Borchert, S.M., and Day, R.H., 2020, Landscape position-based habitat modeling for the Alabama Barrier Island Restoration Assessment at Dauphin Island: U.S. Geological Survey data release, https://doi.org/10.5066/P9PK0EH0.

Feagin, R.A., Smith, W.K., Psuty, N.P., Young, D.R., Martínez, L.M., Carter, G.A., Lucas, K.L., Gibeaut, J.C., Gemma, J.N., and Koske, R.E., 2010, Barrier islands—Coupling anthropogenic stability with ecological sustainability: Journal of Coastal Research, v. 26, p. 987–992. [Also available at https://doi.org/10.2112/09-1185.1.]

Foster, T.E., Stolen, E.D., Hall, C.R., Schaub, R., Duncan, B.W., Hunt, D.K., and Drese, J.H., 2017, Modeling vegetation community responses to sea-level rise on barrier island systems—A case study on the Cape Canaveral barrier island complex, Florida, USA: PLoS One, v. 12, no. 8, 22 p. [Also available at https://doi.org/10.1371/journal.pone.0182605.]

Gutierrez, B.T., Plant, N.G., Thieler, E.R., and Turecek, A., 2015, Using a Bayesian network to predict barrier island geomorphologic characteristics: Journal of Geophysical Research. Earth Surface, v. 120, no. 12, p. 2452–2475. [Also available at https://doi.org/10.1002/2015JF003671.]

Halls, J.N., Frishman, M.A., and Hawkes, S.C., 2018, An automated model to classify barrier island geomorphology using lidar data and change analysis (1998–2014): Remote Sensing, v. 10, no. 7, p. 1109. [Also available at https://doi.org/10.3390/rs10071109.]

Hansen, J., Sato, M., Hearty, P., Ruedy, R., Kelley, M., Masson-Delmotte, V., Russell, G., Tselioudis, G., Cao, J., Rignot, E., Velicogna, I., Tormey, B., Donovan, B., Kandiano, E., von Schuckmann, K., Kharecha, P., Legrande, A.N., Bauer, M., and Lo, K.-W., 2016, Ice melt, sea level rise and superstorms—Evidence from paleoclimate data, climate modeling, and modern observations that 2 °C global warming could be dangerous: Atmospheric Chemistry and Physics, v. 16, no. 6, p. 3761–3812. [Also available at https://doi.org/10.5194/acp-16-3761-2016.]

Henderson, R.E., Nelson, P.R., Long, J.W., and Smith, C.G., 2017, Vector shorelines and associated shoreline change rates derived from lidar and aerial imagery for Dauphin Island, Alabama: 1940–2015: U.S. Geological Survey data release, accessed September 2018 at https://doi.org/10.5066/F7T43RB5.

Homer, C.G., Dewitz, J.A., Yang, L., Jin, S., Danielson, P., Xian, G., Coulston, J., Herold, N.D., Wickham, J.D., and Megown, K., 2015, Completion of the 2011 National Land Cover Database for the conterminous United States—Representing a decade of land cover change information: Photogrammetric Engineering and Remote Sensing, v. 81, no. 5, p. 345–354.

Kirwan, M.L., Guntenspergen, G.R., D'Alpaos, A., Morris, J.T., Mudd, S.M., and Temmerman, S., 2010, Limits on the adaptability of coastal marshes to rising sea level: Geophysical Research Letters, v. 37, no. 23, L23401. [Also available at https://doi.org/10.1029/2010GL045489.]

Kirwan, M.L., and Murray, A.B., 2007, A coupled geomorphic and ecological model of tidal marsh evolution: Proceedings of the National Academy of Sciences of the United States of America, v. 104, no. 15, p. 6118–6122. [Also available at https://doi.org/10.1073/pnas.0700958104.]

Kirwan, M.L., Temmerman, S., Skeehan, E.E., Guntenspergen, G.R., and Fagherazzi, S., 2016, Overestimation of marsh vulnerability to sea level rise: Nature Climate Change, v. 6, no. 3, p. 253–260. [Also available at https://doi.org/10.1038/nclimate2909.]

Knutson, T.R., McBride, J.L., Chan, J., Emanuel, K., Holland, G., Landsea, C., Held, I., Kossin, J.P., Srivastava, A.K., and Sugi, M., 2010, Tropical cyclones and climate change: Nature Geoscience, v. 3, no. 3, p. 157–163. [Also available at https://doi.org/10.1038/ngeo779.]

Leatherman, S.P., 1979, Barrier Island Handbook—National Park Service Cooperative Research Unit: Amherst, Mass., The Environmental Institute, University of Massachusetts at Amherst, 101 p.

Lucas, K.L., and Carter, G.A., 2010, Decadal changes in habitat-type coverage on Horn Island, Mississippi, U.S.A: Journal of Coastal Research, v. 26, no. 6, p. 1142–1148. [Also available at https://doi.org/10.2112/JCOASTRES-D-09-00018.1.]

McBride, R.A., Anderson, J.B., Buynevich, I.V., Cleary, W., Fenster, M.S., FitzGerald, D.M., Harris, M.S., Hein, C.J., Klein, A.H.F., Liu, B., de Menezes, J.T., Pejrup, M., Riggs, S.R., Short, A.D., Stone, G.W., Wallace, D.J., and Wang, P., 2013, Morphodynamics of barrier systems—A synthesis, *in* Sherman, D.J., ed., Treatise on Geomorphology, Coastal Geomorphology: San Diego, Calif., Academic Press, p. 166–244. [Also available at https://doi.org/10.1016/B978-0-12-374739-6.00279-7.]

McKee, K.L., and Cherry, J.A., 2009, Hurricane Katrina sediment slowed elevation loss in subsiding brackish marshes of the Mississippi River delta: Wetlands, v. 29, no. 1, p. 2–15. [Also available at https://doi.org/10.1672/08-32.1.]

Medeiros, S., Hagen, S., Weishampel, J., and Angelo, J., 2015, Adjusting lidar-derived digital terrain models in coastal marshes based on estimated aboveground biomass density: Remote Sensing, v. 7, no. 4, p. 3507–3525. [Also available at https://doi.org/10.3390/rs70403507.]

Mickey, R.C., Godsey, E., Dalyander, P.S., Gonzalez, V., Jenkins, R.L., III, Long, J.W., Thompson, D.M., and Plant, N.G., 2020, Application of decadal modeling approach to forecast barrier island evolution, Dauphin Island, Alabama: U.S. Geological Survey Open-File Report 2020–1001, 45 p., https://doi.org/10.3133/ofr20201001.

Moore, L.J., Patsch, K., List, J.H., and Williams, S.J., 2014, The potential for sea-level-rise-induced barrier island loss—Insights from the Chandeleur Islands, Louisiana, USA: Marine Geology, v. 355, p. 244–259. [Also available at https://doi.org/10.1016/j.margeo.2014.05.022.]

Morris, J.T., Sundareshwar, P.V., Nietch, C.T., Kjerfve, B., and Cahoon, D.R., 2002, Responses of coastal wetlands to rising sea level: Ecology, v. 83, no. 10, p. 2869–2877. [Also available at https://doi.org/10.1890/0012-9658(2002)083[2869:ROCWTR]2.0.CO;2].

Morton, R.A., 2008, Historical changes in the Mississippi-Alabama barrier-island chain and the roles of extreme storms, sea level, and human activities: Journal of Coastal Research, v. 24, no. 6, p. 1587–1600. [Also available at https://doi.org/10.2112/07-0953.1.]

O'Callaghan, J.F., and Mark, D.M., 1984, The extraction of drainage networks from digital elevation data: Computer Vision Graphics and Image Processing, v. 28, no. 3, p. 323–344. [Also available at https://doi.org/10.1016/S0734-189X(84)80011-0.]

Parkinson, R.W., Harlem, P.W., and Meeder, J.F., 2015, Managing the Anthropocene marine transgression to the year 2100 and beyond in the State of Florida USA: Climatic Change, v. 128, no. 1–2, p. 85–98. [Also available at https://doi.org/10.1007/s10584-014-1301-2.]

Passeri, D.L., Hagen, S.C., Plant, N.G., Bilskie, M.V., Medeiros, S.C., and Alizad, K., 2016, Tidal hydrodynamics under future sea level rise and coastal morphology in the Northern Gulf of Mexico: Earth's Future, v. 4, no. 5, p. 159–176. [Also available at https://doi.org/10.1002/2015EF000332.]

Passeri, D.L., Long, J.W., Plant, N.G., Bilskie, M.V., and Hagen, S.C., 2018, The influence of bed friction variability due to land cover on storm-driven barrier island morphodynamics: Coastal Engineering, v. 132, p. 82–94. [Also available at https://doi.org/10.1016/j.coastaleng.2017.11.005.]

Pilkey, O.H., and Cooper, J.A.G., 2014, The last beach: Durham, N.C., Duke University Press Books, 256 p. [Also available at https://doi.org/10.1215/9780822375944.]

Poulter, B., and Halpin, P.N., 2008, Raster modelling of coastal flooding from sea-level rise: International Journal of Geographical Information Science, v. 22, no. 2, p. 167–182. [Also available at https://doi.org/10.1080/13658810701371858.]

Roland, R.M., and Douglass, S.L., 2005, Estimating wave tolerance of *Spartina alterniflora* in coastal Alabama: Journal of Coastal Research, v. 21, no. 3, p. 453–463. [Also available at https://doi.org/10.2112/03-0079.1.]

Sallenger, A.H., Jr., 2000, Storm impact scale for barrier islands: Journal of Coastal Research, v. 16, no. 3, p. 890–895. [Also available at https https://www.jstor.org/stable/4300099.]

Smith, C.G., Osterman, L.E., and Poore, R.Z., 2013, An examination of historical inorganic sedimentation and organic matter accumulation in several marsh types within the Mobile Bay and Mobile—Tensaw River delta region: Journal of Coastal Research, v. 63, no. sp1, p. 68–83. [Also available at https://doi.org/10.2112/SI63-007.1.]

Sweet, W.V., Kopp, R.E., Weaver, C.P., Obeysekera, J., Horton, R.M., Thieler, E.R., and Zervas, C., 2017, Global and regional sea level rise scenarios for the United States: National Oceanic and Atmospheric Administration Technical Report NOS CO-OPS 083, 56 p., accessed October 21, 2019, at https://tidesandcurrents.noaa.gov/publications/techrpt83_Global_and_Regional_SLR_Scenarios_for_the_US_final.pdf.

U.S. Army Corps of Engineers, 2014, Procedures to evaluate sea level change—Impacts, responses, and adaptation: U.S. Army Corps of Engineers Technical Letter no. 1100–2–1, 254 p., accessed June 3, 2019, at https://www.publications.usace.army.mil/Portals/76/Publications/EngineerTechnicalLetters/ETL_1100-2-1.pdf.

Vinent, O.D., and Moore, L.J., 2015, Barrier island bistability induced by biophysical interactions: Nature Climate Change, v. 5, no. 2, p. 158–162. [Also available at https://doi.org/10.1038/nclimate2474.]

Walters, D.C., and Kirwan, M.L., 2016, Optimal hurricane overwash thickness for maximizing marsh resilience to sea level rise: Ecology and Evolution, v. 6, no. 9, p. 2948–2956. [Also available at https://doi.org/10.1002/ece3.2024.]

Walters, D., Moore, L.J., Vinent, O.D., Fagherazzi, S., and Mariotti, G., 2014, Interactions between barrier islands and backbarrier marshes affect island system response to sea level rise—Insights from a coupled model: Journal of Geophysical Research. Earth Surface, v. 119, no. 9, p. 2013–2031. [Also available at https://doi.org/10.1002/2014JF003091.]

Weiss, A.D., 2001, Topographic position and landforms analysis: San Diego, Calif., Esri Users Conference, accessed September 19, 2016, at http://www.jennessent.com/downloads/tpi-poster-tnc_18x22.pdf.

Wernette, P., Houser, C., and Bishop, M.P., 2016, An automated approach for extracting barrier island morphology from digital elevation models: Geomorphology, v. 262, p. 1–7. [Also available at https://doi.org/10.1016/j.geomorph.2016.02.024.]

Williams, K., Pinzon, Z.S., Stumpf, R.P., and Raabe, E.A., 1999, Sea-level rise and coastal forests on the Gulf of Mexico: U.S. Geological Survey Open File Report 99–441, 122 p. [Also available at https://doi.org/10.3133/ofr99441.]

Woodroffe, C.D., Rogers, K., McKee, K.L., Lovelock, C.E., Mendelssohn, I.A., and Saintilan, N., 2016, Mangrove sedimentation and response to relative sea-level rise: Annual Review of Marine Science, v. 8, no. 1, p. 243–266. [Also available at https://doi.org/10.1146/annurev-marine-122414-034025.]

Young, D.R., Brantley, S.T., Zinnert, J.C., and Vick, J.K., 2011, Landscape position and habitat polygons in a dynamic coastal environment: Ecosphere, v. 2, no. 6, p. 1–15. [Also available at https://doi.org/10.1890/ES10-00186.1.]

Zinnert, J.C., Stallins, J.A., Brantley, S.T., and Young, D.R., 2017, Crossing scales—The complexity of barrier-island processes for predicting future change: Bioscience, v. 67, no. 1, p. 39–52. [Also available at https://doi.org/10.1093/biosci/biw154.]

Appendix A1. Maps of Model Results for the Pelican Island Southeast Nourishment (R2), Sand Island Platform Nourishment and Sand Bypassing (R3), Back-Barrier Tidal Flats and Marsh Habitat Restoration (R5), and West End Beach and Dune Nourishment (R6) Measures for the Barrier Island Restoration Feasibility Assessment, Dauphin Island, Alabama

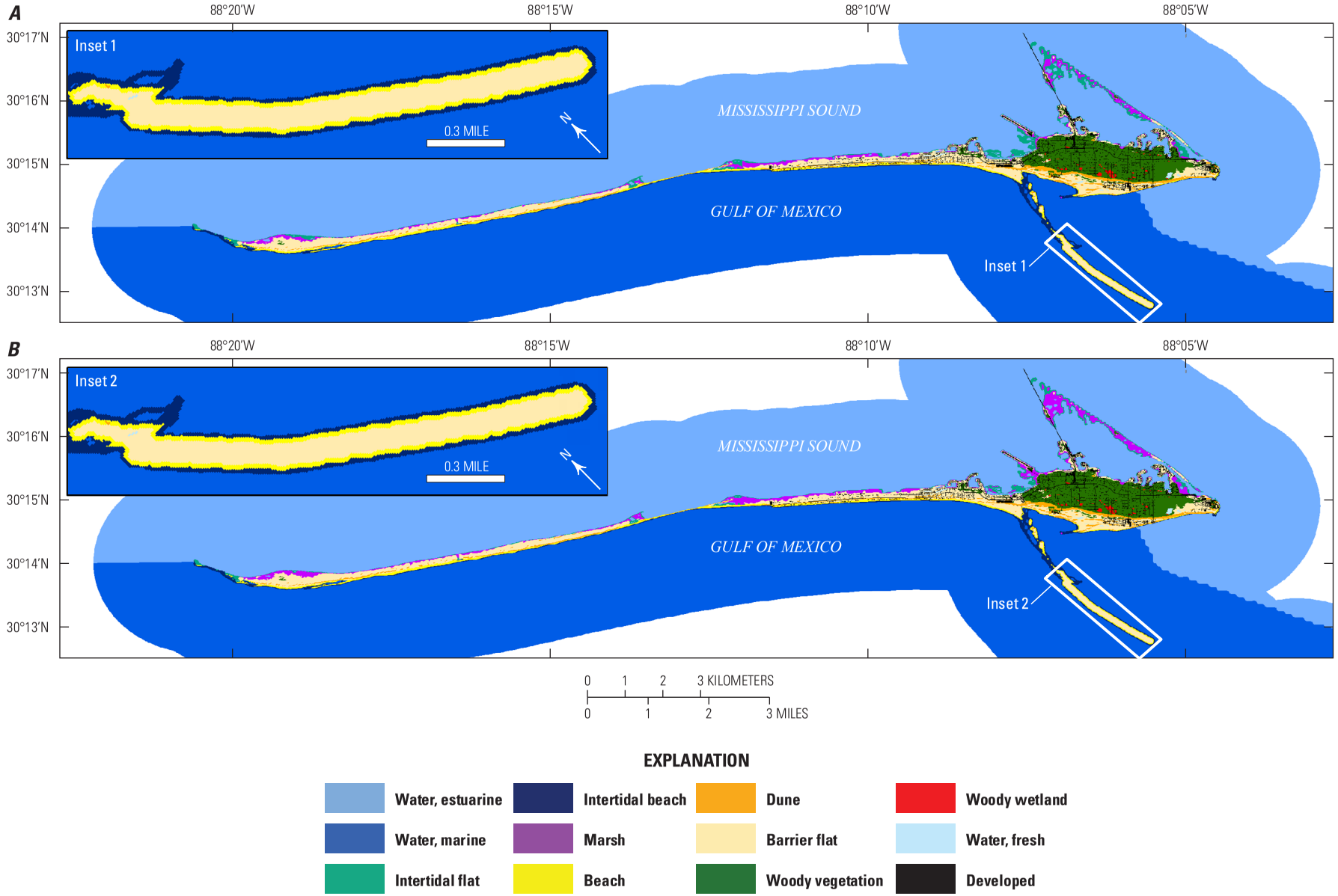

Figure A1.1. Habitat model results for the Pelican Island southeast nourishment restoration measure (R2) for the Barrier Island Restoration Feasibility Assessment project, Dauphin Island, Alabama. *A*, year 0 for "medium" storminess (ST2) and a sea level 0.3 meter (m) above the contemporary sea level (SL1) using the U.S. Army Corps of Engineers (USACE) high sea-level rise (SLR) curve (H); *B*, year 0 for ST2SL1 using the USACE intermediate SLR curve (I); *C*, year 10 for ST2SL1H; *D*, year 10 for ST2SL1I; *E*, year 0 for "high" storminess (ST3) and a sea level 0.96 m above the contemporary sea level (SL3) using the USACE high SLR curve (H); *F*, year 0 for ST3SL3 using the USACE intermediate SLR curve (I); *G*, year 10 for ST3SL3H; *H*, year 10 for ST3SL3I. The solid white box indicates the general area of the restoration measure.

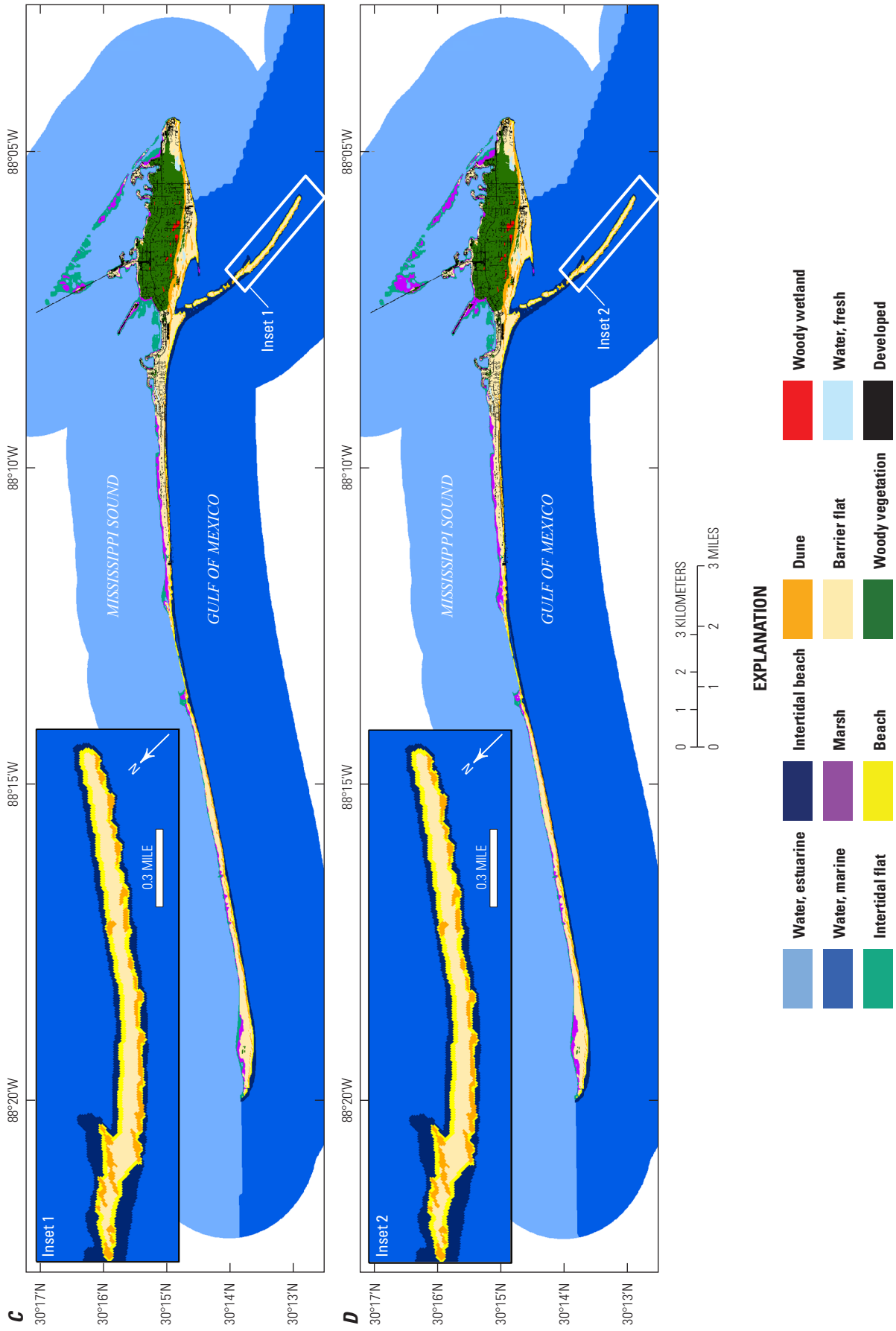

Figure A1.1. —Continued

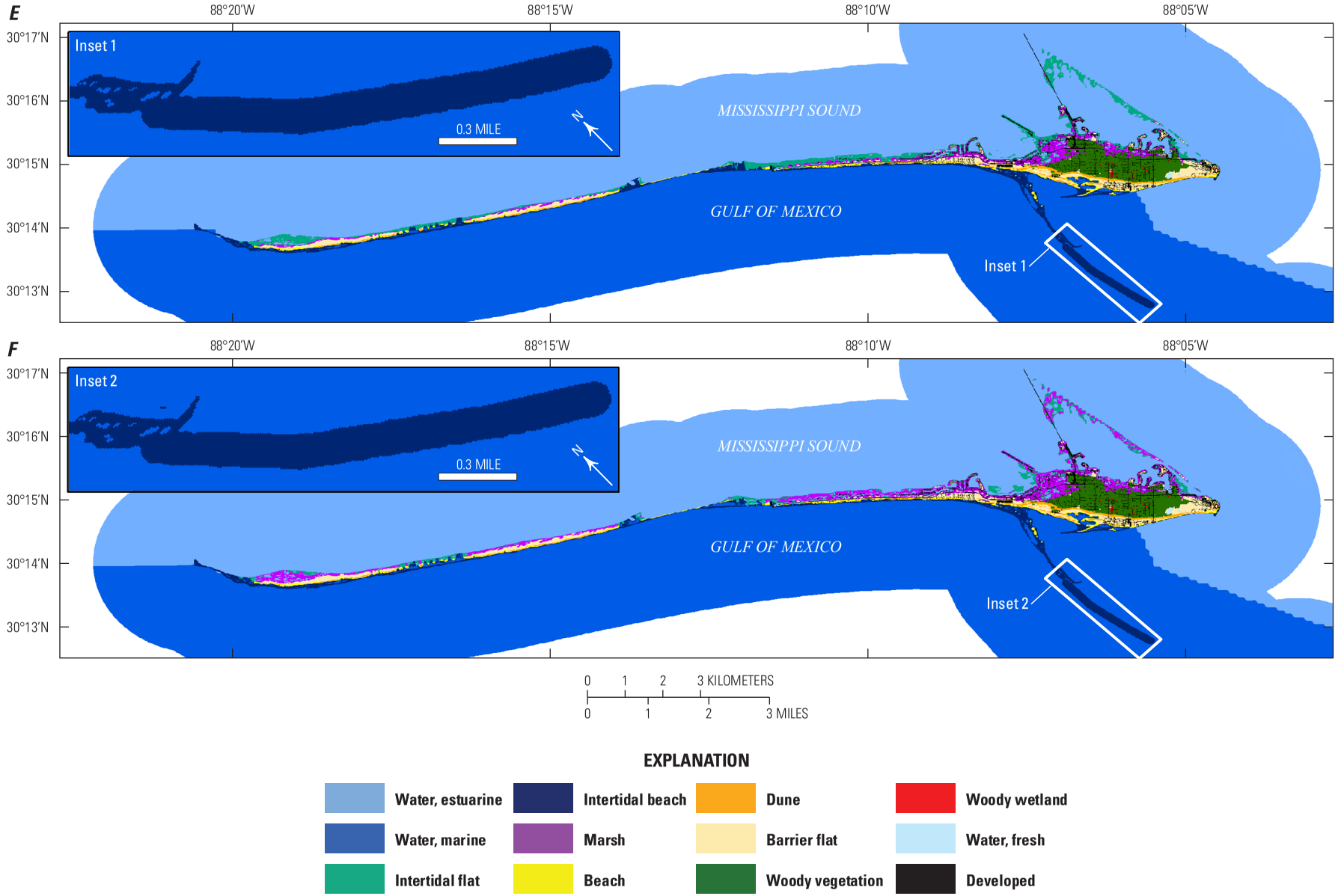

Figure A1.1. —Continued

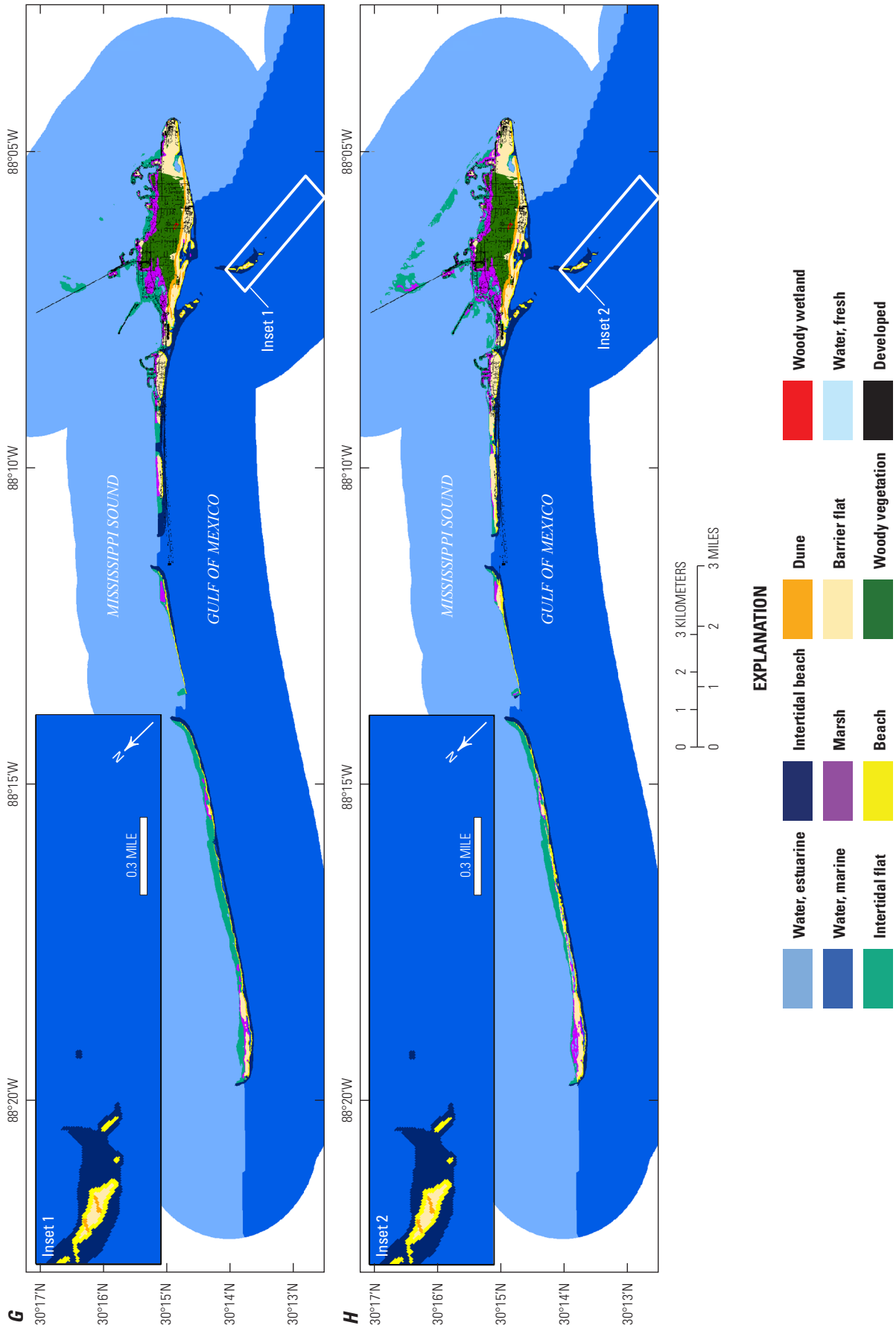

Figure A1.1. —Continued

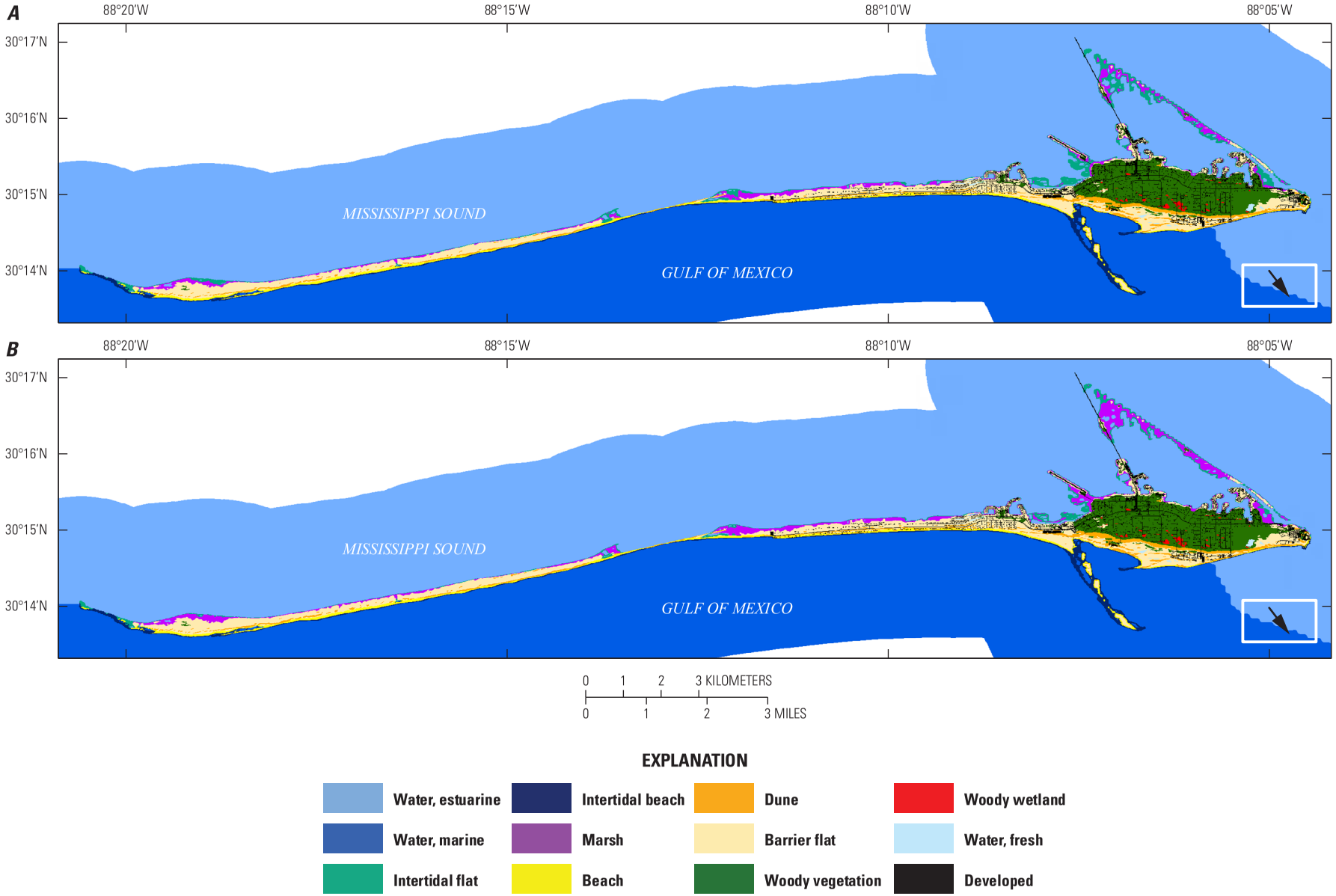

Figure A1.2. Habitat model results for the Sand Island platform nourishment and sand bypassing restoration measure (R3) for the Barrier Island Restoration Feasibility Assessment project, Dauphin Island, Alabama. *A*, year 0 for "medium" storminess (ST2) and a sea level 0.3 meter (m) above the contemporary sea level (SL1) using the U.S. Army Corps of Engineers (USACE) high sea-level rise (SLR) curve (H); *B*, year 0 for ST2SL1 using the USACE intermediate SLR curve (I); *C*, year 10 for ST2SL1H; *D*, year 10 for ST2SL1I; *E*, year 0 for "high" storminess (ST3) and a sea level 0.96 m above the contemporary sea level (SL3) using the USACE high SLR curve (H); *F*, year 0 for ST3SL3 using the USACE intermediate SLR curve (I); *G*, year 10 for ST3SL3H; *H*, year 10 for ST3SL3I. The solid white box indicates the general area of the restoration measure.

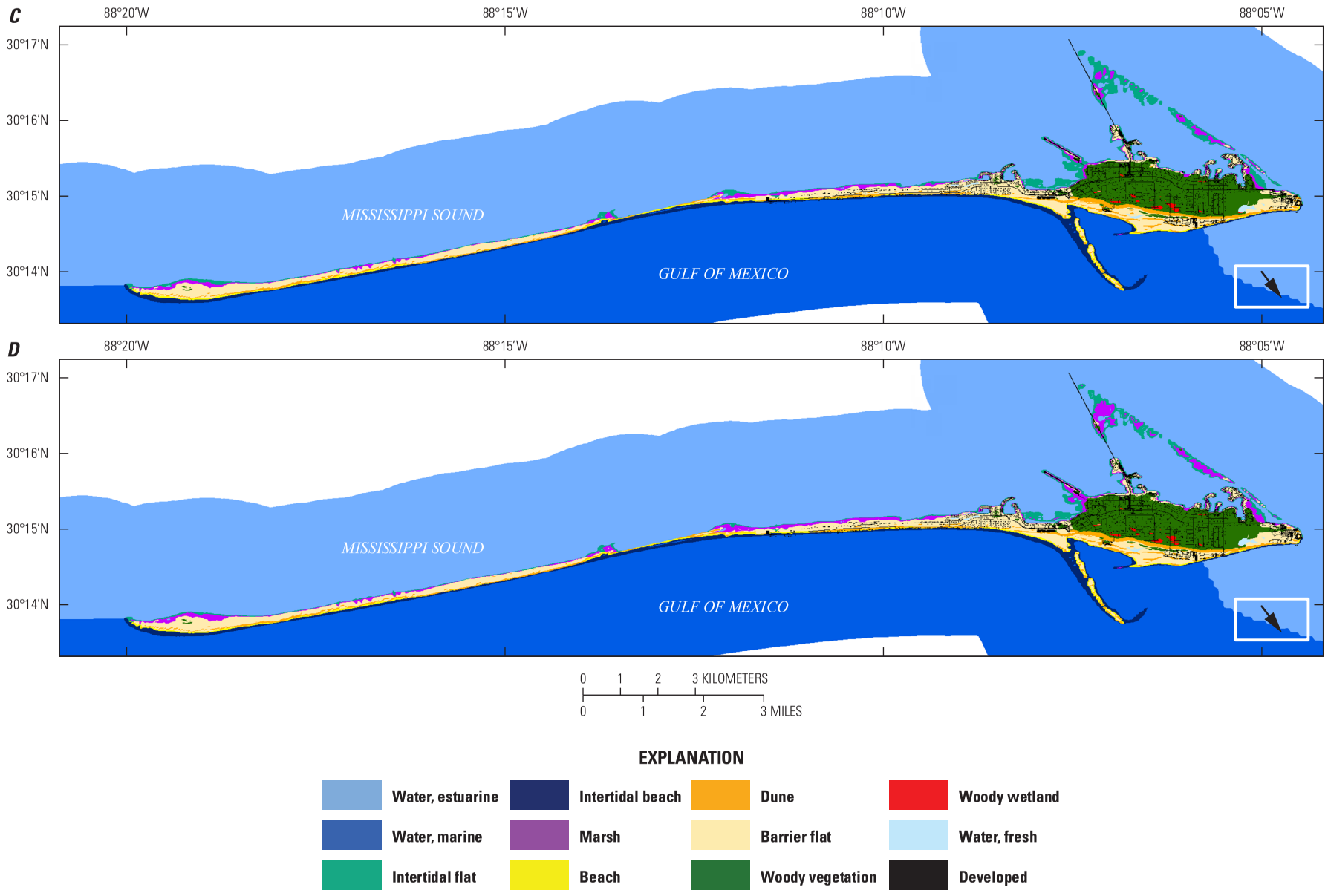

Figure A1.2. —Continued

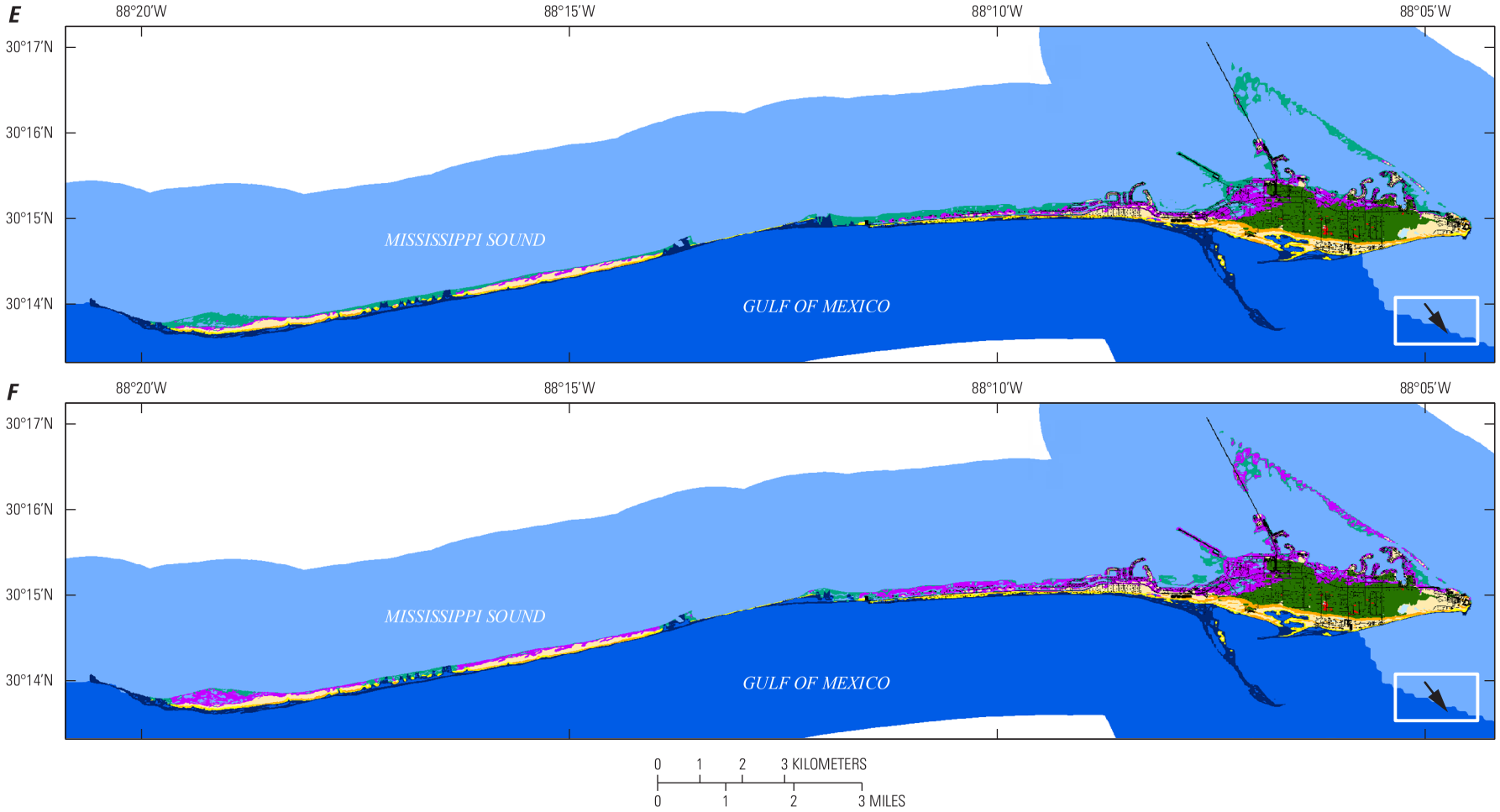

Figure A1.2. —Continued

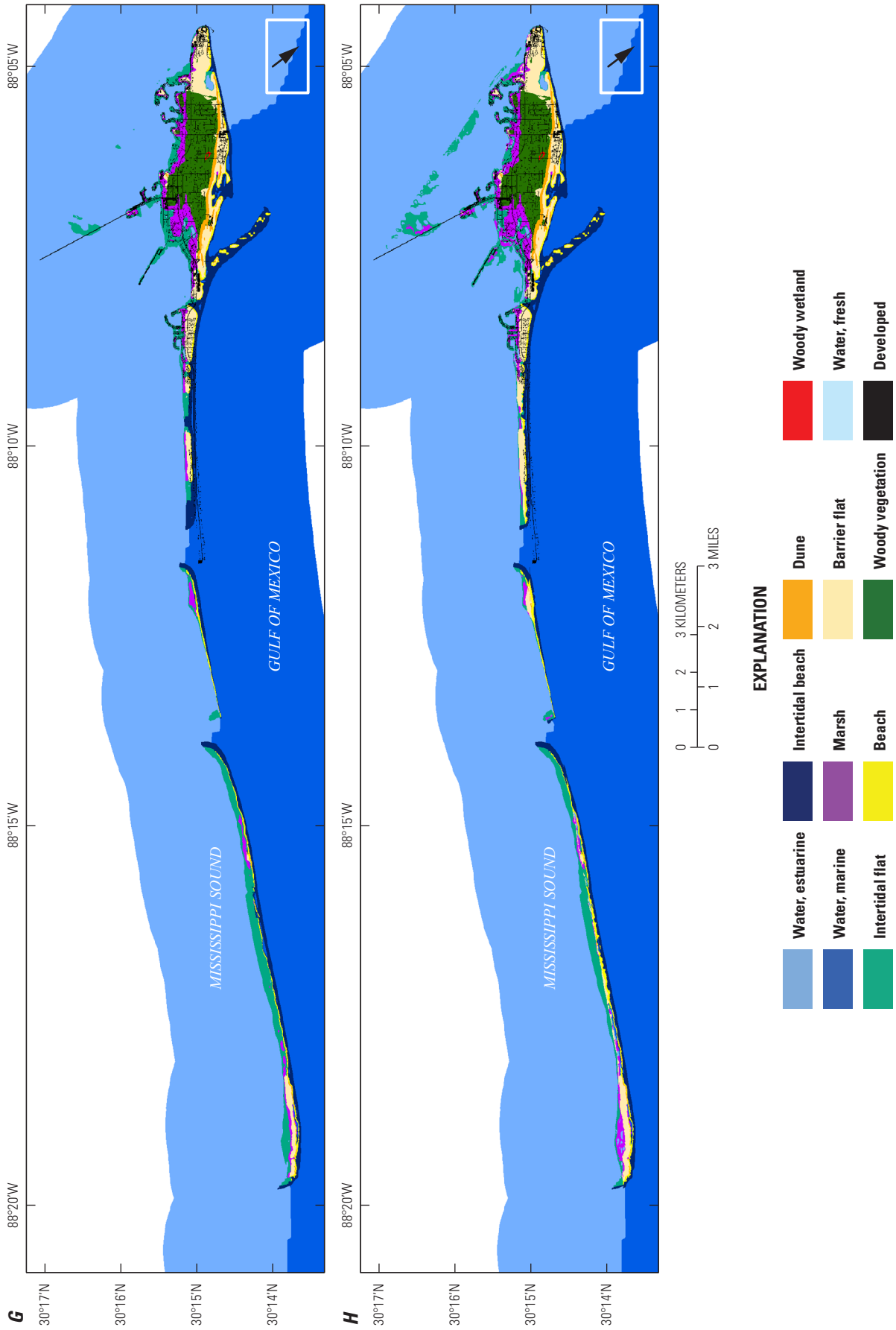

Figure A1.2. —Continued

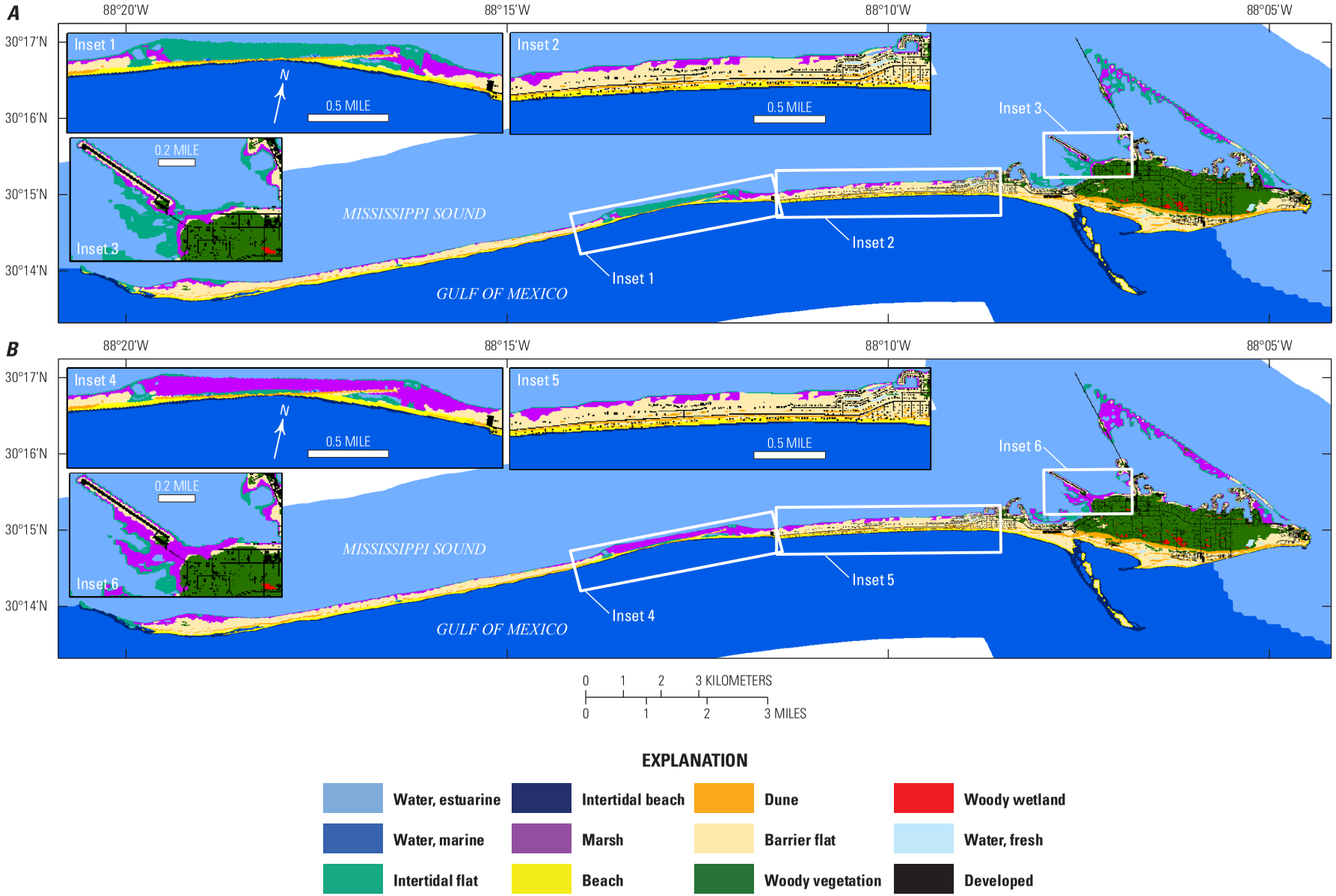

Figure A1.3. Habitat model results for the back-barrier tidal flats and marsh habitat restoration measure (R5) for the Barrier Island Restoration Feasibility Assessment project, Dauphin Island, Alabama. *A*, year 0 for "medium" storminess (ST2) and a sea level 0.3 meter (m) above the contemporary sea level (SL1) using the U.S. Army Corps of Engineers (USACE) high sea-level rise (SLR) curve (H); *B*, year 0 for ST2SL1 using the USACE intermediate SLR curve (I); *C*, year 10 for ST2SL1H; *D*, year 10 for ST2SL1I; *E*, year 0 for "high" storminess (ST3) and a sea level of about 1.0 m above the contemporary sea level (SL3) using the USACE high SLR curve (H); *F*, year 0 for ST3SL3 using the USACE intermediate SLR curve (I); *G*, year 10 for ST3SL3H; *H*, year 10 for ST3SL3I. The solid white box indicates the general area of the restoration measure.

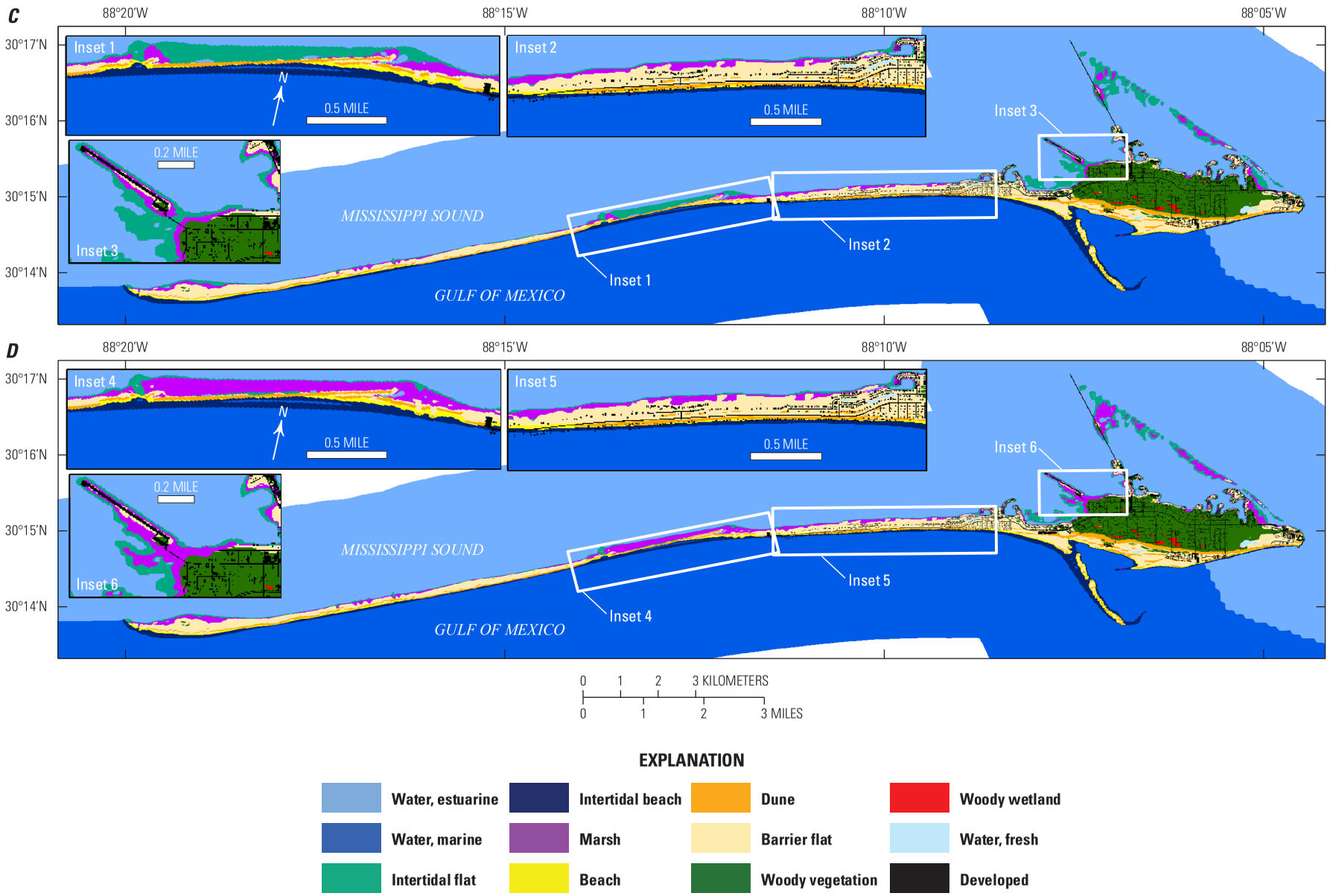

Figure A1.3. —Continued

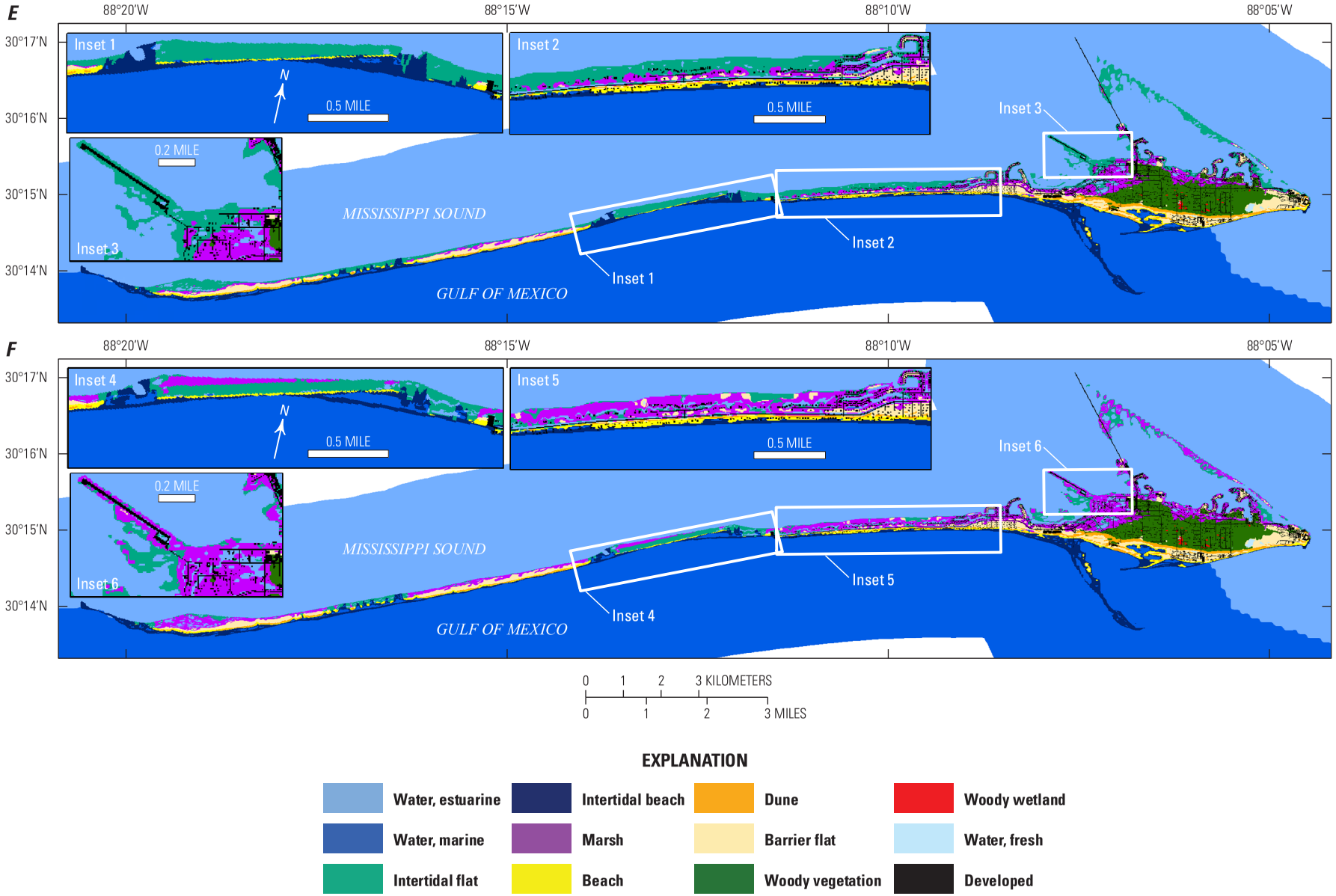

Figure A1.3. —Continued

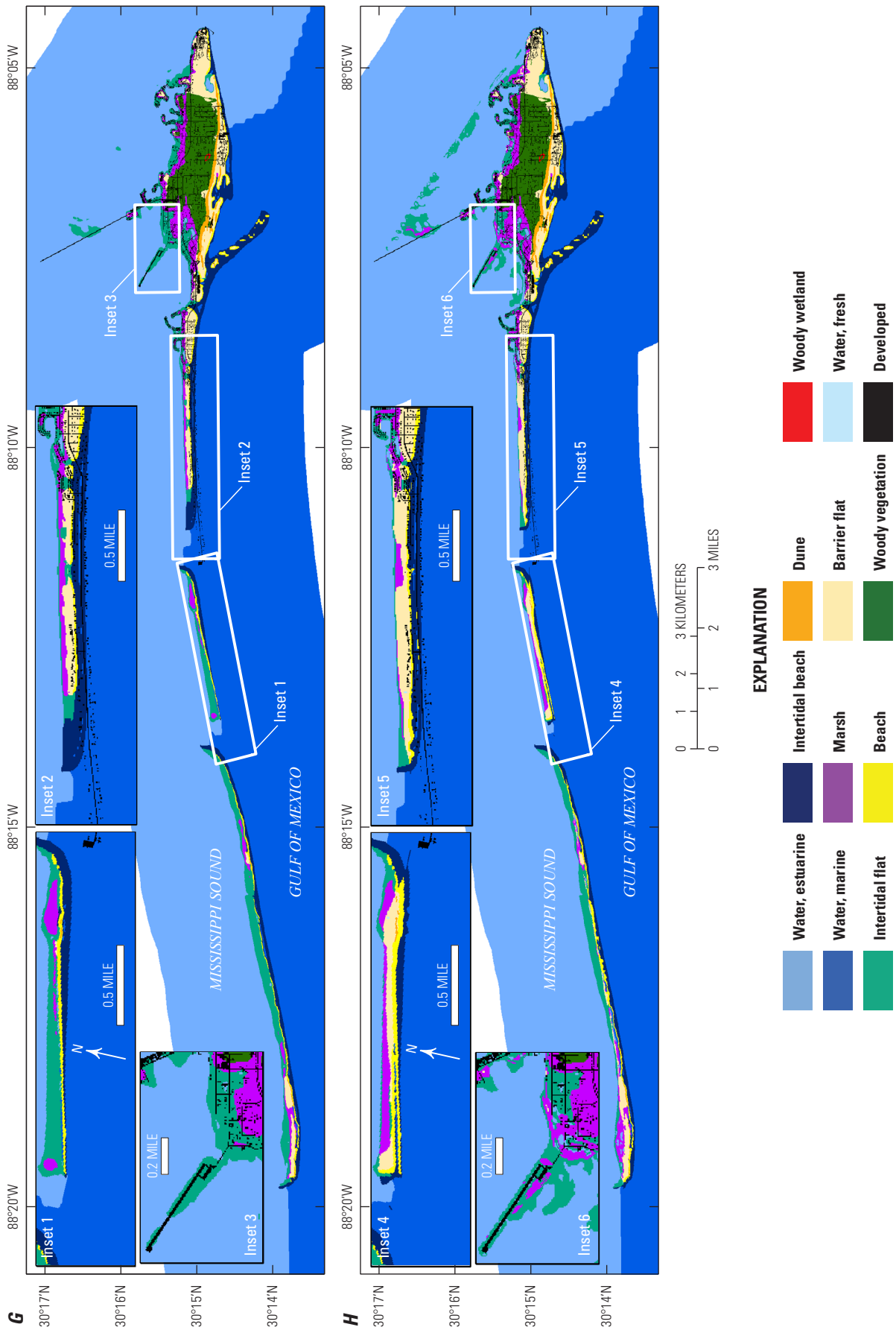

Figure A1.3. —Continued

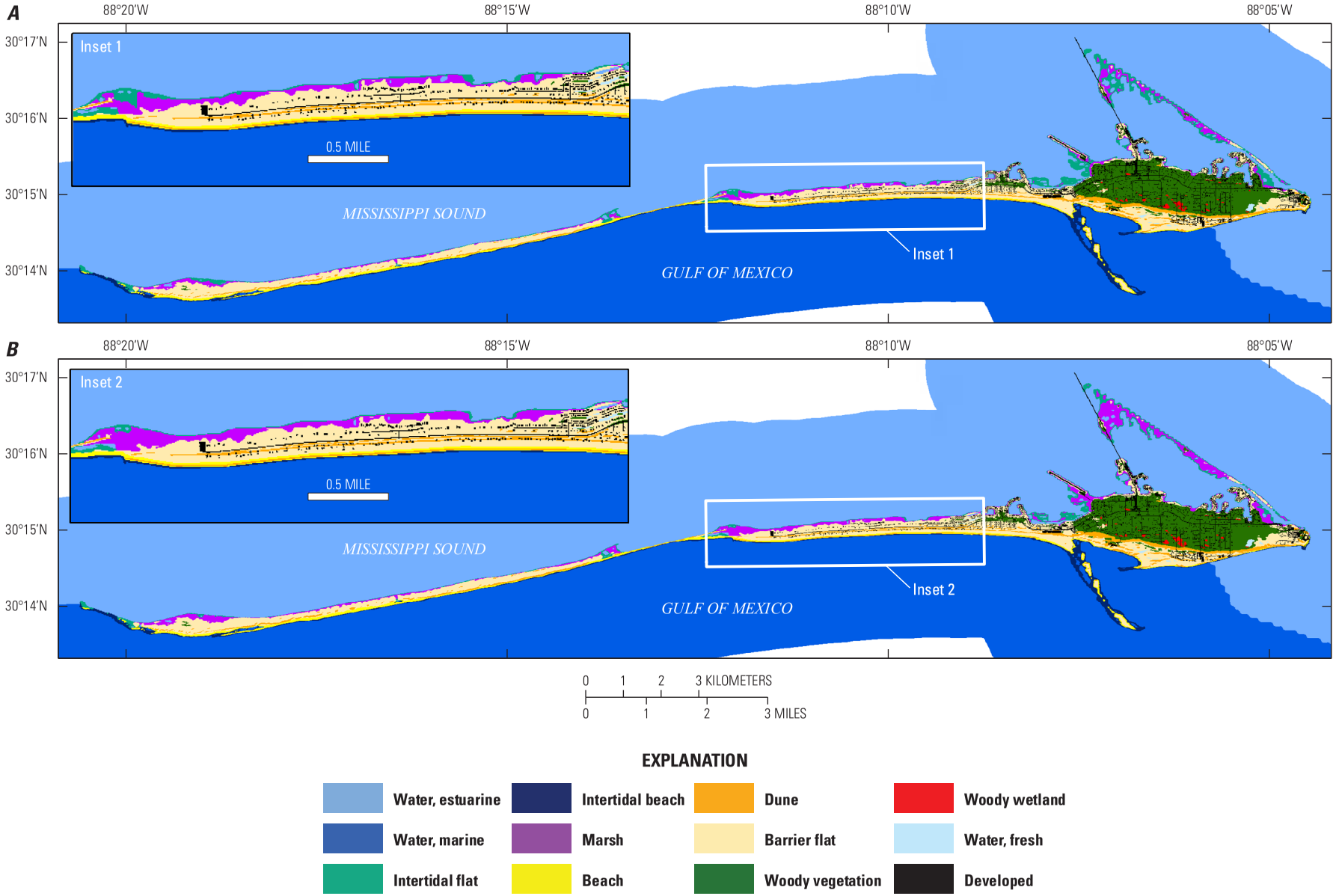

Figure A1.4. Habitat model results for the west end beach and dune restoration measure (R6) for the Barrier Island Restoration Feasibility Assessment project, Dauphin Island, Alabama. *A*, year 0 for "medium" storminess (ST2) and a sea level 0.3 meter (m) above the contemporary sea level (SL1) using the U.S. Army Corps of Engineers (USACE) high sea-level rise (SLR) curve (H); *B*, year 0 for ST2SL1 using the USACE intermediate SLR curve (I); *C*, year 10 for ST2SL1H; *D*, year 10 for ST2SL1I; *E*, year 0 for "high" storminess (ST3) and a sea level of about 1.0 m above the contemporary sea level (SL3) using the USACE high SLR curve (H); *F*, year 0 for ST3SL3 using the USACE intermediate SLR curve (I); *G*, year 10 for ST3SL3H; *H*, year 10 for ST3SL3I. The solid white box indicates the general area of the restoration measure.

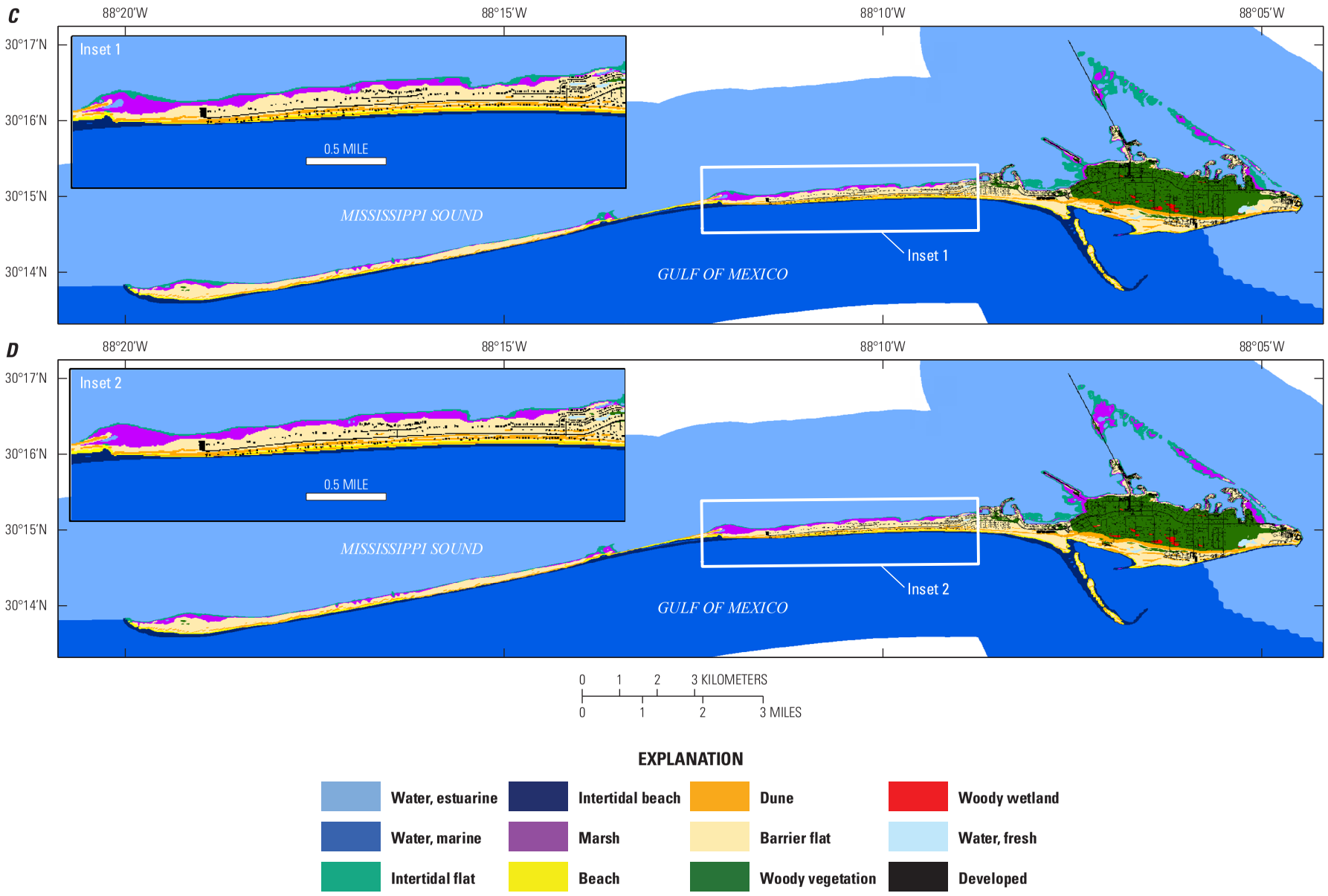

Figure A1.4. —Continued

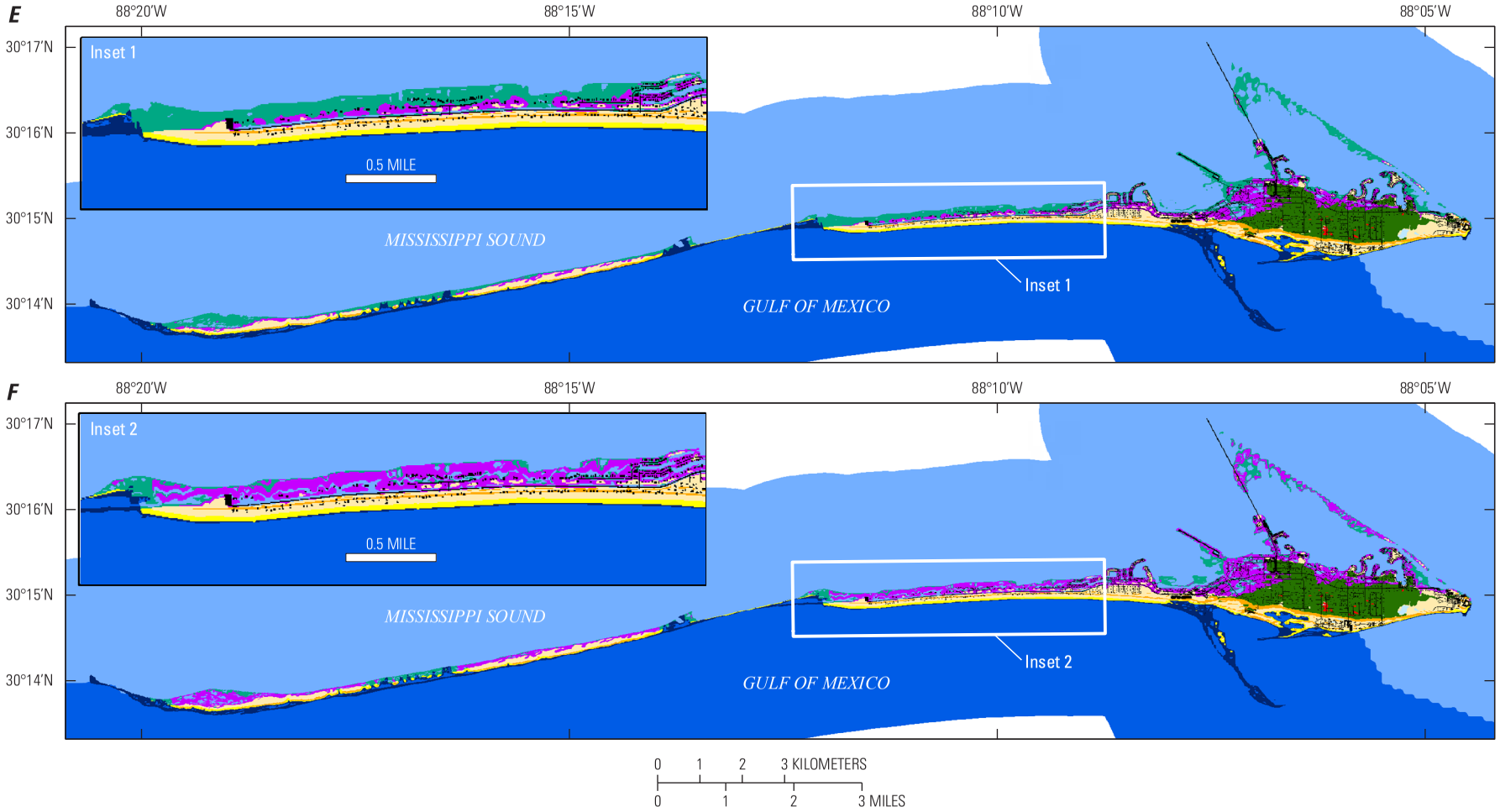

Figure A1.4. —Continued

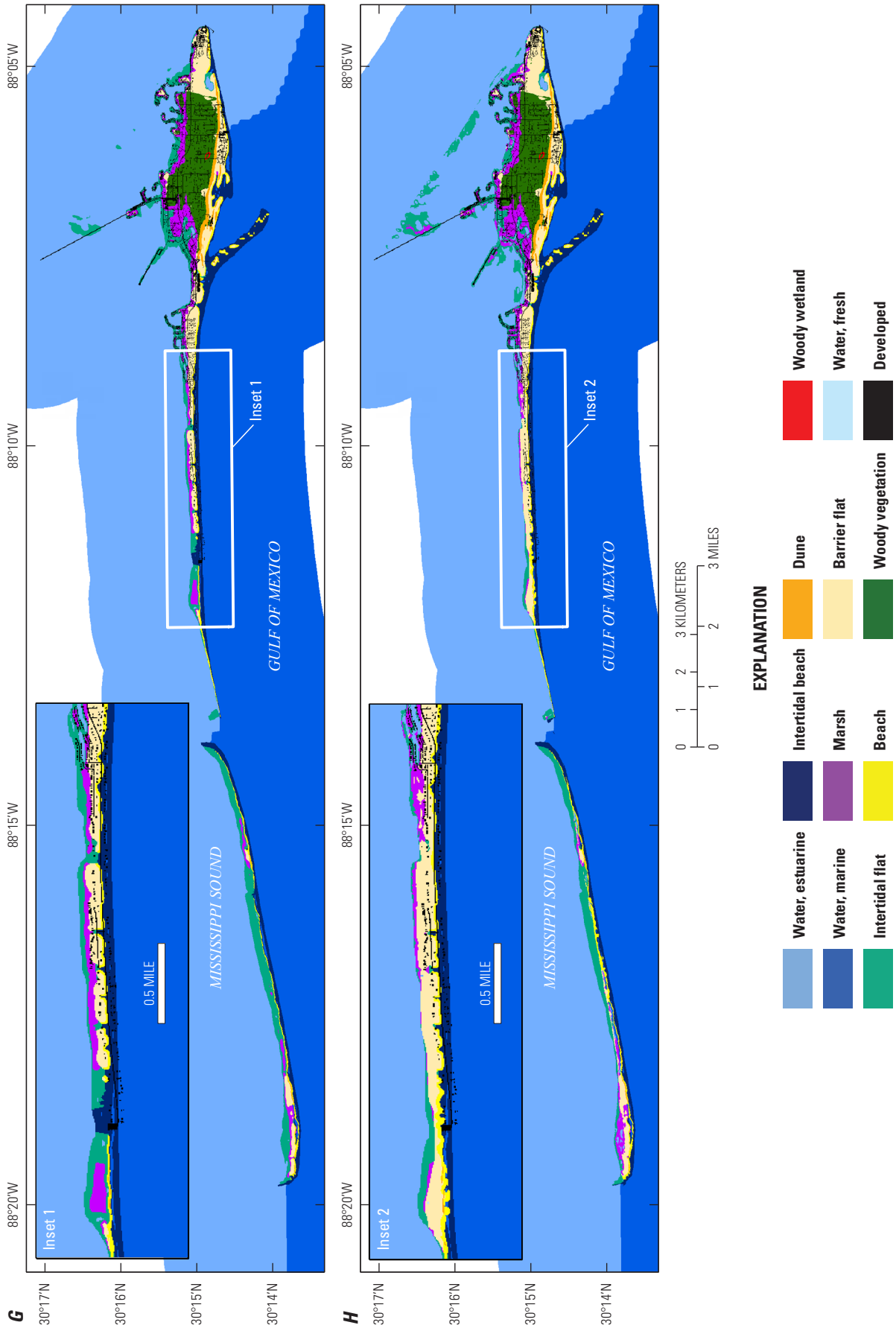

Figure A1.4. —Continued

Chapter B. Oyster Habitat Suitability Modeling for the Alabama Barrier Island Restoration Feasibility Assessment at Dauphin Island

By Hongqing Wang,[1] Nicholas M. Enwright,[1] Thomas M. Soniat,[2] Jason E. Herrmann,[3] Megan K. La Peyre,[1,4] Sung-Chan Kim,[5] Barry Bunch,[5] Spencer J. Stelly,[6] P. Soupy Dalyander,[1] and Rangley C. Mickey[1]

Abstract

Increasingly, natural resource managers are concerned with comprehensive coastal restoration actions that provide many ecosystem benefits, including reduction of shoreline loss; stabilization of marshes, beach, and dunes; enhancement of fishery habitat; and facilitation of seagrass colonization. Barrier island restoration can provide these benefits; however, the feasibility and success of the restoration effort should consider how specific restoration actions might affect or add to existing important habitat, such as eastern oyster reefs. In this study, a spatially explicit oyster habitat suitability index model driven by water quality variables was developed for estuarine waters near Dauphin Island, Alabama, to assess how habitat suitability for oysters changes for two potential future storminess and future sea-level conditions and a variety of restoration measures including beach and dune restoration, marsh restoration, placement of sand in the littoral zone, and the no-action measure. The habitat suitability index model was calibrated and validated using existing field data on oyster density and continuous water quality data. Habitat suitability modeling results indicated that the proposed Dauphin Island restoration projects tend to have little or no effects on oyster habitat under potential future conditions with "medium" storminess and a future sea-level rise of 0.3 meter by 2100. In contrast, beach/dune restoration in front of Katrina Cut could potentially increase the oyster area in the highly suitable class and decrease the area in the marginally suitable and suitable classes, while maintaining the total suitable area unchanged or slightly increased under potential future conditions with "high" storminess and a sea-level rise of about 1.0 meter by 2100. The HSI model could be improved by incorporating substrate and other biophysical parameters as data become available. Information from the oyster habitat suitability modeling results can be combined with information on island geomorphology and associated subaerial habitats, such as intertidal marsh, beach, and dune, to gauge the collective benefits and tradeoff of the various restoration actions being considered for Dauphin Island. This information can help land managers achieve the goal of holistic coastal restoration by improving barrier island geomorphology for resilience and also enhancing the habitat suitability for fishery species, including oysters.

Introduction

Dauphin Island, Alabama, provides buffering (for example, wave attenuation) and regulation of salinity to about one-third of the Mississippi Sound and estuarine habitats, including oysters, marshes, and seagrasses. Federal, State, and local agencies and organizations have invested in restoring Dauphin Island to enhance, maintain, and protect important coastal habitat and living resources damaged by recent hurricanes (for example, Hurricane Katrina) and the 2010 Deepwater Horizon oil spill. Past, current, and future potential habitat conditions and changes need to be monitored and predicted to effectively implement barrier island restoration projects; therefore, a habitat suitability index (HSI) model is a good approach to link the geophysical features of the barrier island and the water quality with habitat suitability for critical species, such as *Crassostrea virginica* (eastern oyster). The Alabama coast, including Mobile Bay and Dauphin Island surrounding waters, is among the major oyster farming areas in the Northern Gulf of Mexico (Gregalis and others, 2008); thus, it is critical to include the effect of Dauphin Island restoration on oyster habitat dynamics.

[1]U.S. Geological Survey.

[2]University of New Orleans.

[3]Alabama Department of Conservation and Natural Resources.

[4]Louisiana Fish and Wildlife Cooperative Research Unit.

[5]U.S. Army Corps of Engineers.

[6]Stelly Consulting at the U.S. Geological Survey.

Researchers have developed and applied oyster HSI models for coastal restoration and other management needs (Soniat and Brody, 1988; Barnes and others, 2007; Pollack and others, 2012; Soniat and others, 2013). Previous oyster life-cycle-based studies indicated that salinity, temperature, food availability, suspended sediment concentration, bottom type or substrate, and water depth are important physical factors regulating oyster population dynamics (Shumway, 1996; Livingston and others, 2000; Wang and others, 2008; La Peyre and others, 2009; La Peyre and others, 2013; Soniat and others, 2013; Wang and others, 2017). In addition, the model's relation between the HSI score and each physical parameter should be established based on field data and oyster biology. Suitable ranges for environmental factors should be specific to the study area to optimize model accuracy (Barnes and others, 2007; Leonhardt and others, 2017; Miller and others, 2017; Sehlinger and others, 2019) and accommodate phenotypic variation. Furthermore, variables selected for model inclusion might not have an equal effect on habitat quality when oyster density data and water quality variables are examined together, requiring the application of different weights. For example, Linhoss and others (2016) documented that the contributions of water quality variables to oyster habitat suitability model predictions in St. Louis Bay, Mississippi, were 67 percent for average salinity, 16 percent for mean water depth, 10 percent for minimum dissolved oxygen (DO), 5 percent for mean total suspended solids (TSS), 1.2 percent for minimum temperature, and 0.2 percent for maximum temperature based on the simulated hydrodynamic conditions across St. Louis Bay in the Mississippi Sound during 2011 using the Environmental Fluid Dynamics Code and the Water Quality Analysis and Simulation Program.

Purpose and Scope

The objectives of this study were to (1) develop a spatially explicit HSI model for oysters in estuarine waters near Dauphin Island by using data found in the literature to establish an initial model; (2) refine the model by using site-specific biological data and water quality data to calibrate and validate the HSI model; and (3) use the model to assess how habitat suitability for oysters changes for two potential future storminess and sea-level conditions and a variety of restoration measures including beach and dune restoration, marsh restoration, placement of sand in the littoral zone, and the no-action measure (for example, 7 decisions × 4 scenarios × 2 periods). Habitat suitability model results could help restoration and resources managers to make ecosystem-based decisions to achieve the goal of enhancing barrier island ecological functions (including resilience) and habitat for fishery species including oysters. This model could be modified to predict oyster habitat suitability for other estuaries and bays near barrier islands.

Methods

Study Area

The focus area for this effort is the estuarine water of the Mississippi Sound on the north (or back-barrier side) of Dauphin Island. These areas are subtidal aquatic habitat with salinity rarely greater than 30 parts per thousand (ppt) and are highly suitable habitat for oysters (Wallace and others, 1999). The Cedar Point reef (fig. B1) is the current and historic center of the Alabama oyster fishery (Gregalis and others, 2008). South of Dauphin Island is the Gulf of Mexico, which includes nearshore waters that are subject to high wave energy and occasionally experience salinity levels greater than or equal to 30 ppt, which makes this area unsuitable for oyster reef development. Tides near Dauphin Island are diurnal with a mean tidal amplitude of 0.43 meter (m). Mean annual salinity varies from 8 to 22 ppt at Cedar Point and from 10 to 26 ppt at sites near Little Dauphin Island (Scyphers and others, 2011). The study area for oyster habitat suitability modeling includes the estuarine and marine waters near Dauphin Island and Mobile Bay, Ala. (fig. B1). The center of Dauphin Island is an important, vulnerable area that has been severely affected by recent hurricanes (fig. B1). This area was breached during Hurricane Ivan (2004), and the breach expanded considerably during Hurricane Katrina (2005); in 2010, the breach (known as Katrina Cut) was closed with a rock wall during the response to the Deepwater Horizon oil spill (Froede, 2008; Webb and others, 2011).

Model Development

We developed an oyster HSI model for Dauphin Island based on previous oyster HSI models (Soniat and others, 2013; Miller and others, 2017) and oyster and water quality data in the Mississippi Sound. Salinity, temperature, TSS, DO, and depth are key factors regulating oyster growth and survival and are often used to develop habitat suitability models for oyster restoration (Pollack and others, 2012; Soniat and others, 2013; Patterson and others, 2014; Linhoss and others, 2016). Therefore, these water quality parameters were included in the model framework for this study. The relations between HSI score and each physical parameter in the Dauphin Island oyster HSI model were established based on existing models (Soniat and others, 2013; Linhoss and others, 2016), but scores and variable weights were modified with local data.

Model Parameters and Curves

The oyster HSI model includes seven water quality variables and their relations (curves) with habitat suitability. HSI scores for individual water quality variables were determined from these curves; then, a total suitability index score (scaled

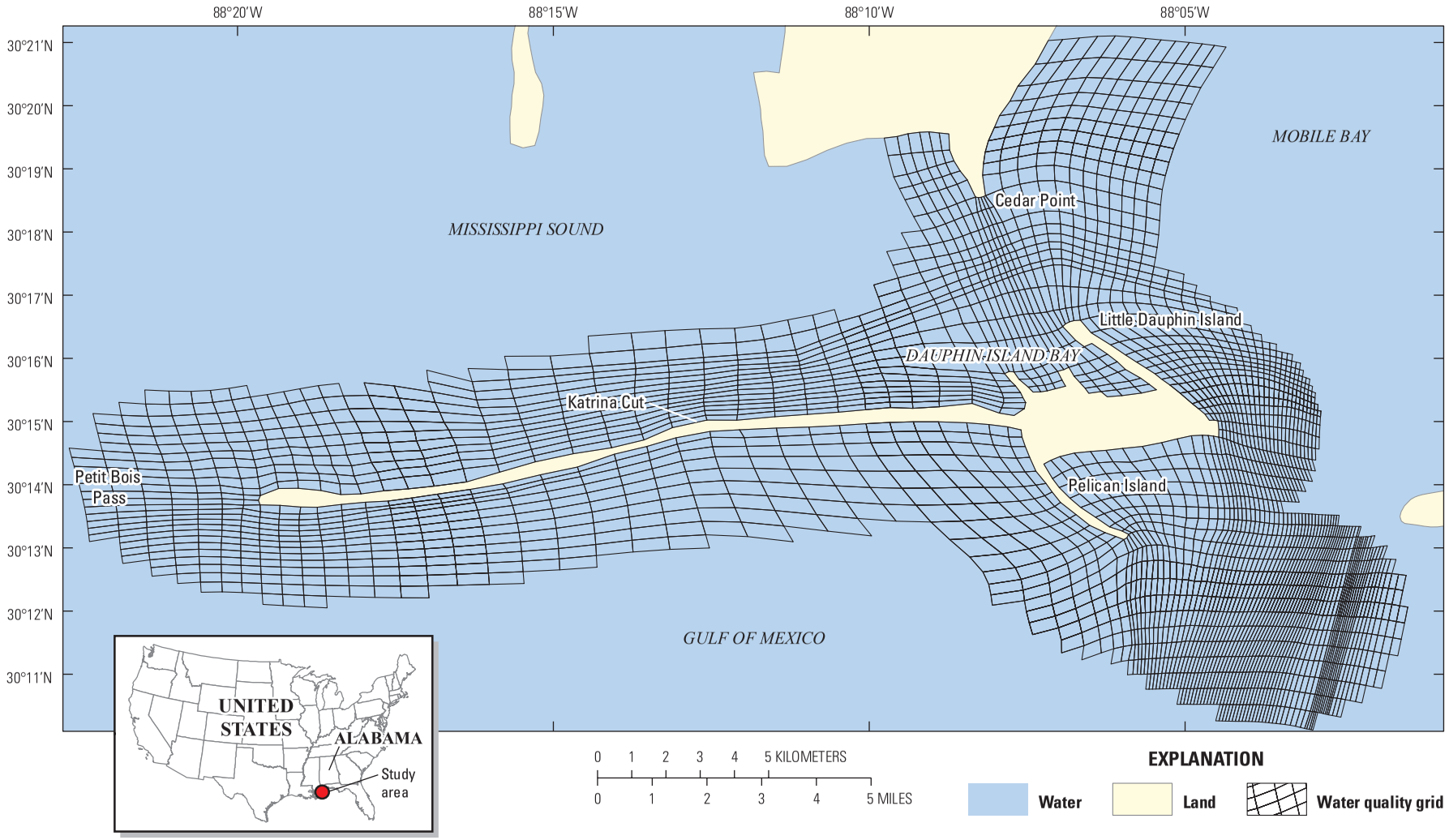

Figure B1. Study area of the oyster habitat suitability modeling near Dauphin Island, Alabama. Land and water areas are generalized from the water quality model grid.

0 to 1) was calculated from the index scores of the individual variables using a weighted geometric mean method. Details of the model parameters and curves are described in the following section.

Variable 1—Mean Salinity during May–September Spawning Period

The mean salinity-habitat relation was based on a habitat suitability study for oysters in Louisiana by Soniat and others (2013) and Denapolis (2018) in which the mean spawning-season salinities from 18 to 22 ppt were considered optimal, whereas salinities less than or equal to (≤) 5 ppt and greater than or equal to (≥) 40 ppt were unsuitable (that is, an HSI variable score of 0). This salinity-habitat relation was further modified based on oyster density data and the range of mean salinity collected at Cedar Point. The optimal mean spawning-season salinities were adjusted based on these data to be from 20 to 22 ppt and setting salinities ≤10 ppt and ≥40 ppt as unsuitable (fig. B2). The weights of each variable in the model were first determined based on information from previous studies, then updated, and a best value was given by model calibration. The weight of mean salinity during the spawning period was calibrated to be 6.

Variable 2—Minimum Monthly Mean Salinity

The minimum monthly mean salinity-habitat relation was also based on the suitability study for Louisiana oysters by Soniat and others (2013), Lavaud and others (2017), and Denapolis (2018). They found that extremely low salinities (≤2 ppt) caused mass mortalities of oysters. A single monthly mean of ≤2 ppt was unsuitable, yet a minimum mean salinity of ≥8 ppt was not considered detrimental (fig. B3). The cutoff salinity was set to 10 ppt based on oyster density and minimum monthly mean salinity data at Cedar Point. The weight of minimum monthly mean salinity was also calibrated to be 6.

Variable 3—Annual Mean Salinity

The annual mean salinity-habitat relation was also based on the oyster suitability index studies of Soniat and others (2013) and Denapolis (2018). In their efforts, the optimal annual mean salinity was between 10 and 15 ppt, and values ≤5 ppt and ≥40 ppt were unsuitable. This curve was further modified based on oyster density data and annual mean salinity data at Cedar Point. This modification involved setting the optimal annual mean salinity range to be from 17 to 20 ppt to reflect the relatively higher salinity for oysters in barrier island estuaries than those in river-dominated estuaries (fig. B4; La Peyre and others, 2009; Wang and others, 2017). The weight of annual mean salinity was also calibrated to be 6.

Variable 4—Annual Mean Dissolved Oxygen

An annual mean DO of 2 milligrams per liter (mg/L) was used in Linhoss and others (2016) and was set as the threshold for hypoxia (Patterson and others, 2014). Using heat shock protein 70 as a biomarker for environmental stress on oyster reefs near Dauphin Island, Patterson and others (2014) found that approximately 8 mg/L was the maximum level for which the oysters were not stressed as a result of DO levels. Suitability index values for DO from 2 to 8 mg/L were interpolated (fig. B5). The weight of annual mean DO was calibrated to be 1.

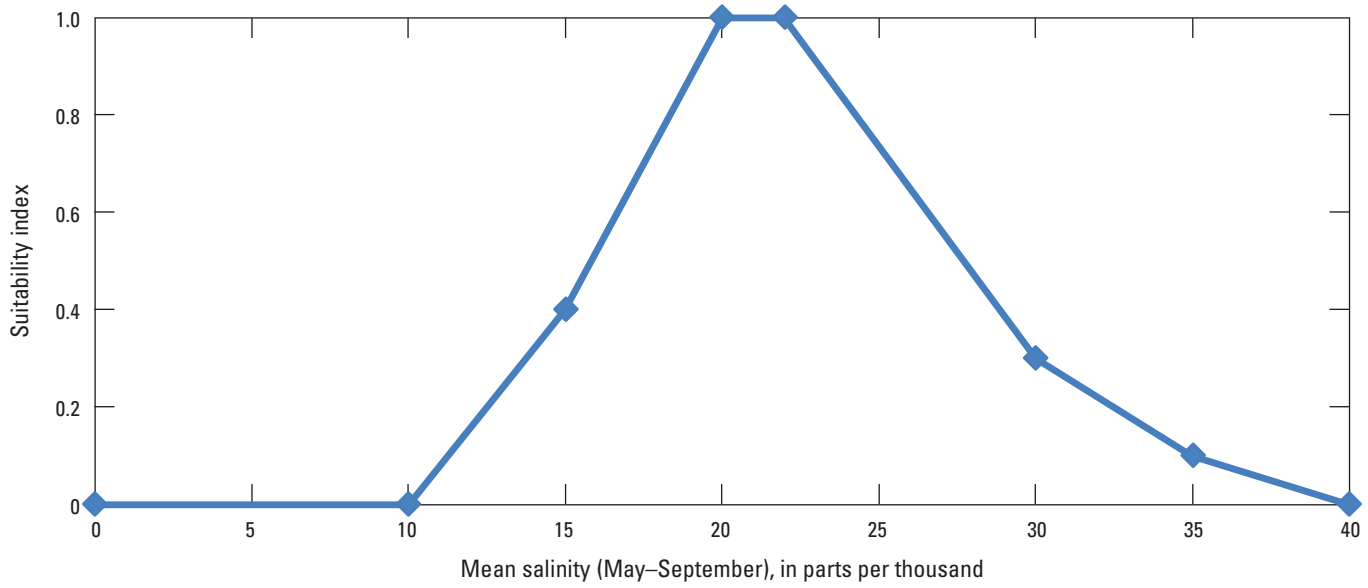

Figure B2. Relation between oyster habitat suitability index and mean spawning-season salinity (in parts per thousand) from May to September, for the area near Dauphin Island, Alabama.

Variable 5—Annual Mean Total Suspended Solids

The annual mean TSS-habitat relation (fig. B6) was based on the turbidity induced reduction of oyster filtration rate (Hofmann and others, 1992; Klinck and others, 1992; Powell and others, 1992; Wang and others, 2008, 2017) and the assumption that oyster habitat suitability would be reduced if filtration is diminished:

$$FR = FR\left[1 - 0.01\left(\frac{(\log_{10}(TSS/1,000) + 3.38)}{0.0418}\right)\right] \quad \text{(B1)}$$

where

FR is filtration rate (milliliters filtered per individual per min).

A similar relation was also included in the oyster HSI model for oysters in Chesapeake Bay, Maryland (Battista, 1999). Linhoss and others (2016) indicated that concentrations of TSS less than 22 mg/L (0.022 grams per liter) tended to be more suitable habitat. The weight of annual mean TSS was calibrated to be 2.

Variable 6—Annual Mean Water Depth

Oyster reefs in St. Louis Bay, Miss., are found in areas with a water depth that ranges from 0.1 to 6.9 m (Linhoss and others (2016). Optimal water depth there was found between 0.5 and 3 m (Barnes and others, 2007). This study used a similar approach and revised the optimal water depth from 2 to 3 m based on oyster density and minimum monthly mean

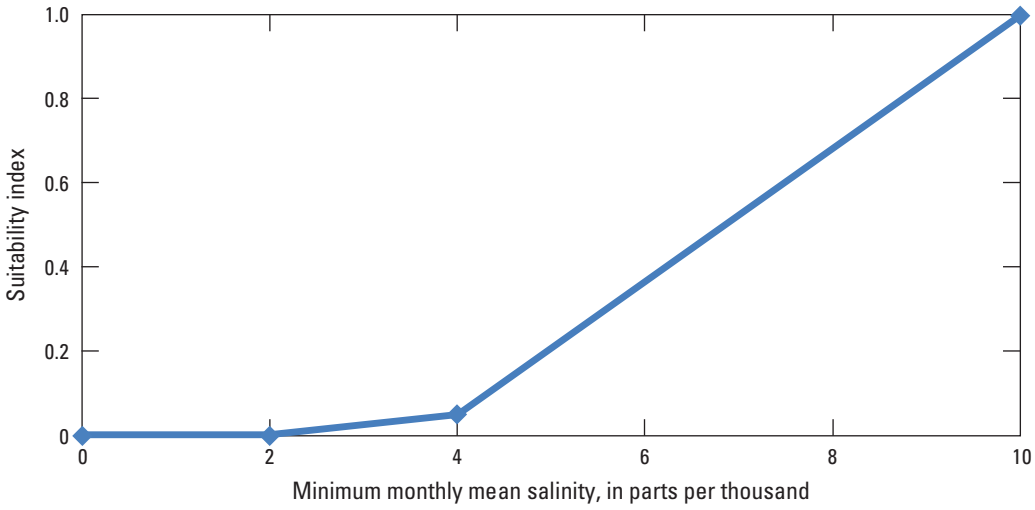

Figure B3. Relation between oyster habitat suitability index and minimum monthly mean salinity (in parts per thousand) for the area near Dauphin Island, Alabama.

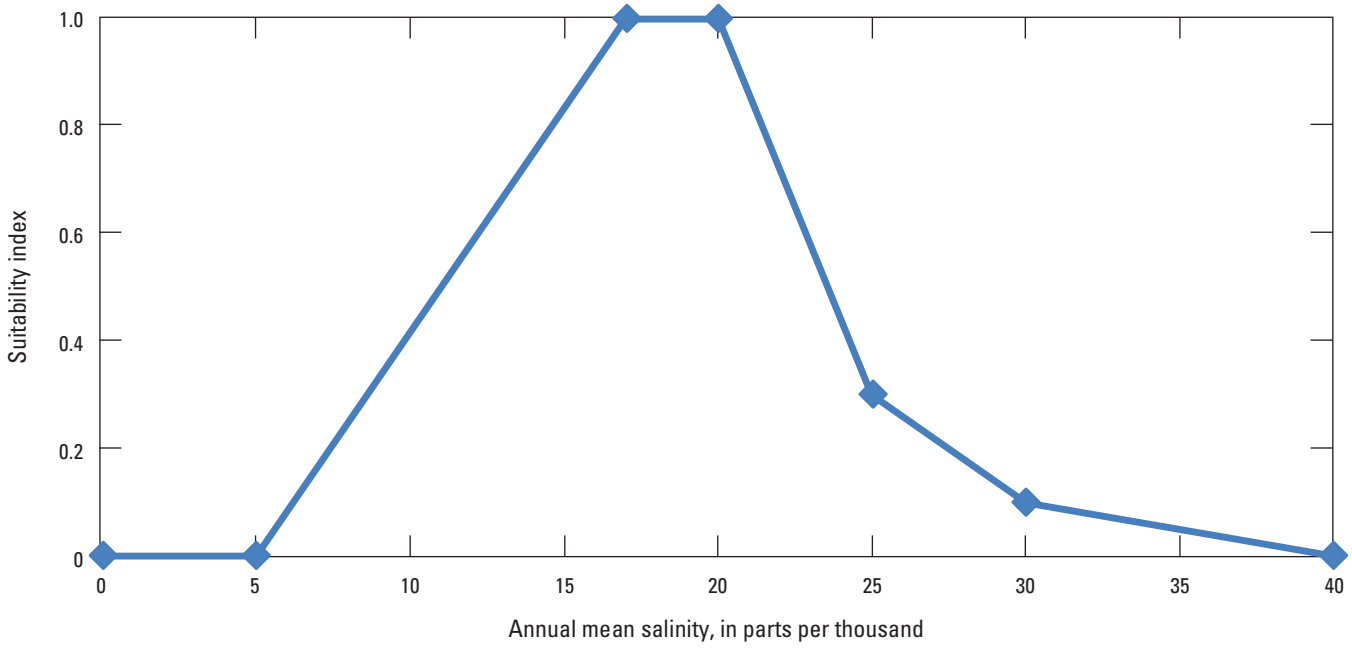

Figure B4. Relation between oyster habitat suitability index and annual mean salinity (in parts per thousand) for the area near Dauphin Island, Alabama.

salinity data at Cedar Point (fig. B7). The weight of annual mean water depth was calibrated to be 2.

Variable 7—Annual Mean Water Temperature

The temperature-habitat relation (fig. B8) was based on previous studies. Oyster feeding stops at less than (<) 6 degrees Celsius (°C), respiration and feeding could be disrupted when greater than (>) 32 °C (Kennedy, 1996), and physiological functions cease at >42 °C (Stanley and Sellers, 1986). Based on oyster growth and mortality data (Lowe and others, 2017), oysters along the Louisiana coast had a high survival rate between 18 and 32 °C with only a slight decrease with temperature. A similar relation was found for Gulf of Mexico oysters in Barnes and others (2007). The weight of temperature was calibrated to be 1.

The final total HSI score (HSI_{total}) was based on the seven variables given above. The final score was calculated using the weighted geometric mean method as follows:

$$HSI_{total} = \left(\prod_{i=1}^{n} V_i^{Wi}\right)^{(1/\sum_{i=1}^{n} Wi)} = \exp\left(\frac{\sum_{i=1}^{n} Wi \ln Vi}{\sum_{i=1}^{n} Wi}\right) \quad \text{(B2)}$$

where

Vi is the ith environmental variable,
Wi is the weight of Vi,
n is the number of variables (n=7) in the total HSI model, and $HSI_{total} = 0$, if any $V_i = 0$.

The calculated suitability index values were classified into the following groups based on Theuerkauf and Lipcius (2016) with modification: HSI_{total} >0.7 is highly suitable; HSI_{total} 0.5 to 0.7 is suitable; HSI_{total} 0.3 to 0.5 is marginally suitable; and HSI_{total} <0.3 is unsuitable.

Model Calibration and Validation

Higher oyster density and (or) rates of growth, size of oysters, and survival are generally assumed to be the results of highly suitable environmental conditions, which should also be represented by a higher suitability index score. The oyster

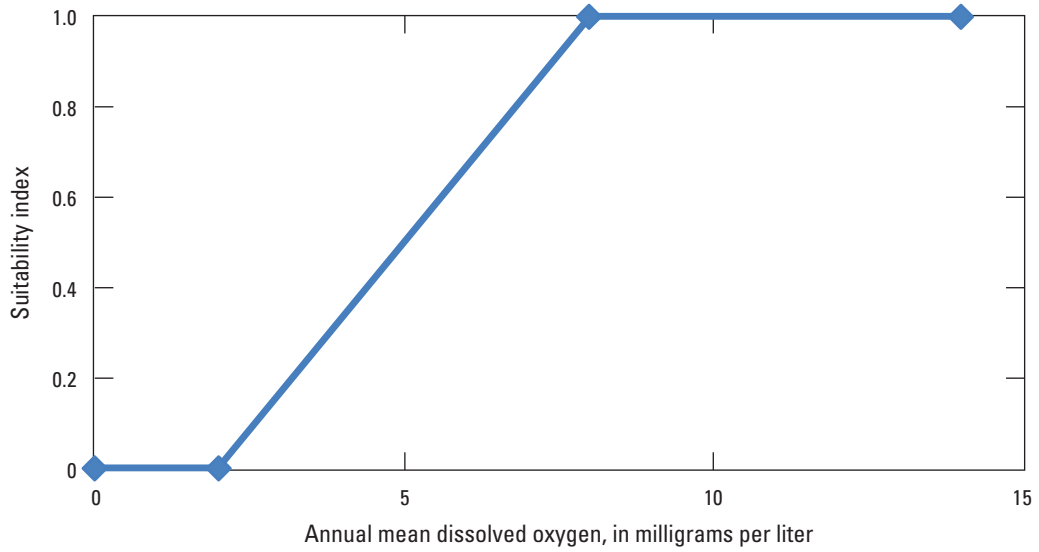

Figure B5. Relation between oyster habitat suitability index and annual mean dissolved oxygen (in milligrams per liter) for the area near Dauphin Island, Alabama.

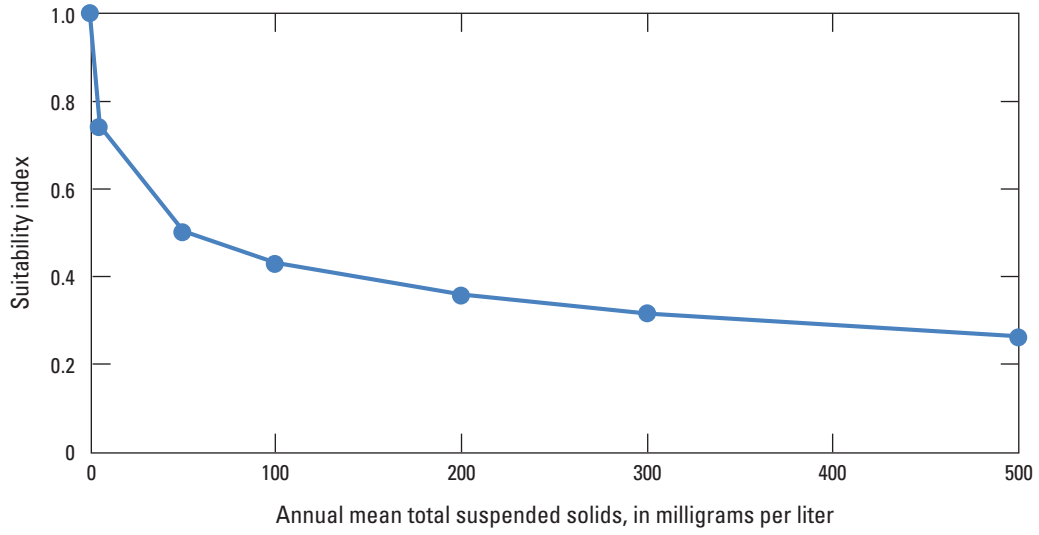

Figure B6. Relation between oyster habitat suitability index and annual mean total suspended solids (in milligrams per liter) for the area near Dauphin Island, Alabama.

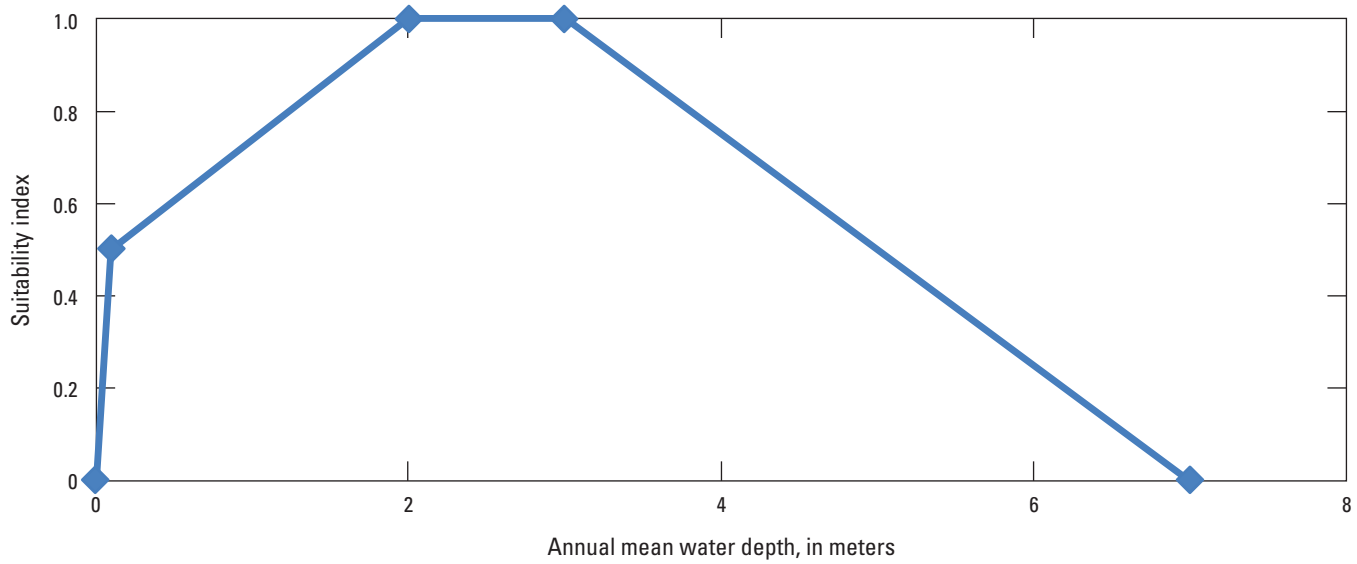

Figure B7. Relation between oyster habitat suitability index and annual mean water depth (in meters) for the area near Dauphin Island, Alabama.

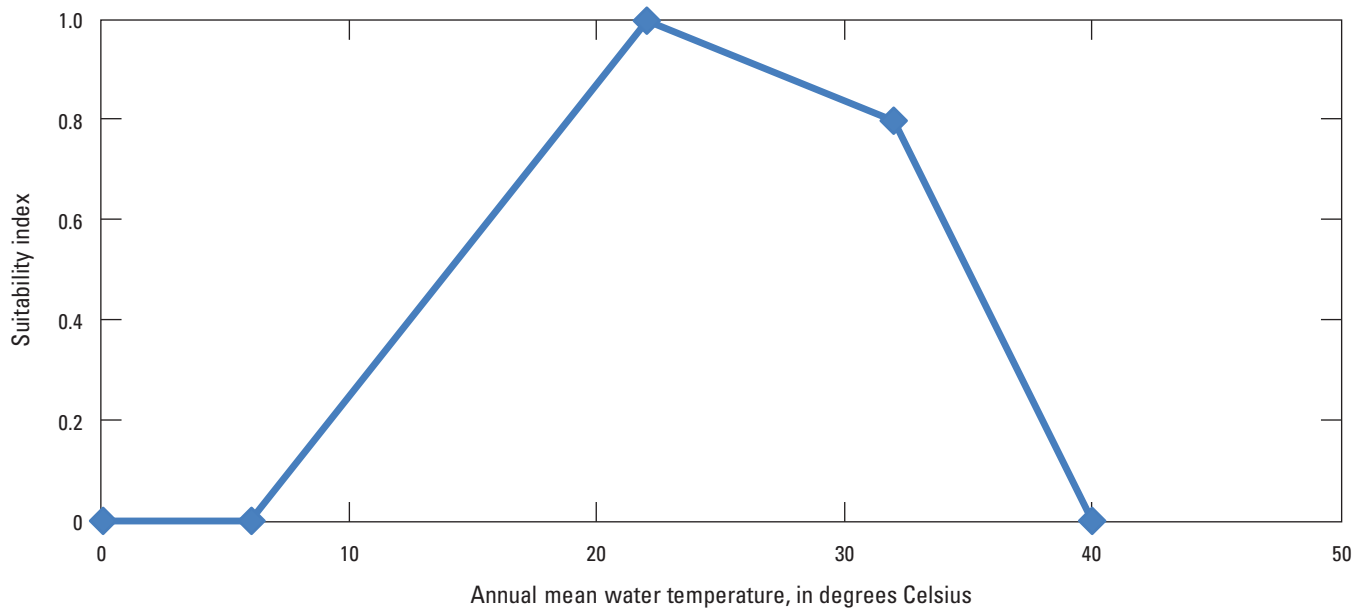

Figure B8. Relation between oyster habitat suitability index and annual mean water temperature (in degrees Celsius) for the area near Dauphin Island, Alabama.

density data used for suitability model calibration and validation were provided by Alabama Department of Conservation and Natural Resources (ADCNR) Marine Resources Division (MRD). Divers from ADCNR–MRD completed monthly surveys of 1-square-meter (m^2) quadrats during May to September from 1976 to 2017 at multiple oyster reefs near Dauphin Island and Mobile Bay. These data were paired with water quality data from the Mobile Bay National Estuary Program (https://arcos.disl.org/). Specifically, these data included half-hourly salinity, temperature, DO, water depth, and turbidity measurements from 2006 to 2017.

The habitat suitability model for oysters in the Dauphin Island estuary was calibrated using oyster density data and environmental data at Cedar Point in 2006 and from 2009 to 2011 (fig. B9). The calibration included the modification of each of seven habitat suitability curves (figs. B2–B8) and their weights in the total suitability model. The final curves and their weights were determined based on the best fit (highest coefficient of determination [R^2] value of the regression)

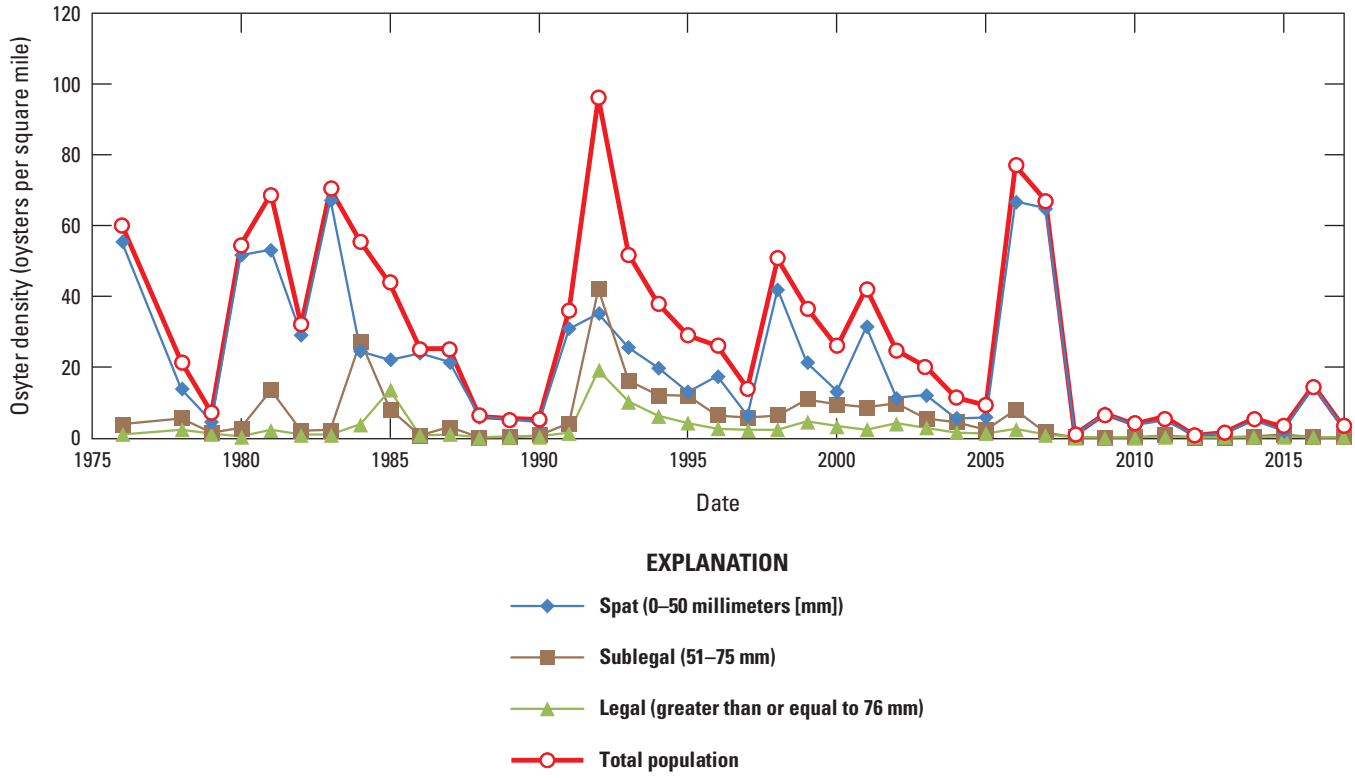

Figure B9. Oyster density by type at the Cedar Point reef in Alabama from 1975 to 2017.

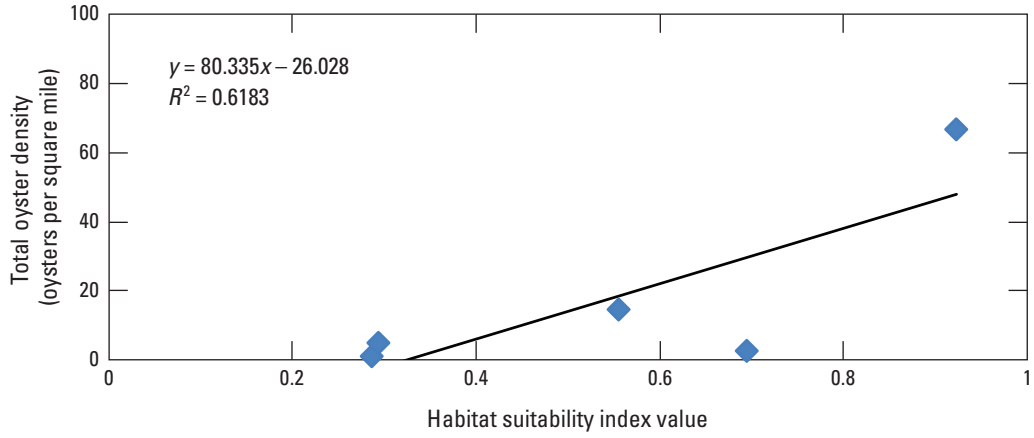

Figure B10. Results of habitat suitability index model validation for the area near Dauphin Island, Alabama, using oyster density data at Cedar Point, Alabama.

between the values of the total HSI and the total oyster density during the calibration years. Model validation was completed by regressing habitat suitability values (0 to 1) to measured total oyster density (oysters/m^2) at Cedar Point during 2007 and 2013–16 (fig. B10). The selection of calibration and validation periods was determined by the inclusion of high and low oyster density periods and associated water quality conditions in calibration as well as in validation.

Simulations for Restoration Measures

The restoration measures selected for the Alabama Barrier Island Restoration Feasibility Assessment project include beach nourishment and marsh restoration (table B1). The impacts of restoration measures were evaluated over a decadal period under various environmental forcing conditions including frequency of occurrence of tropical storms (that is, "storminess") and future sea level (Mickey and others, 2020) using the numerical model Delft3D (Mickey and others, 2020), an empirical dune growth model (Mickey and others,

Table B1. Restoration measures for the Alabama Barrier Island Restoration Feasibility Assessment project, Dauphin Island, Alabama.

[R, restoration measure; km, kilometer; m, meter; ~, approximate value]

Restoration measure	Description
Future without action (R0)	No restoration action.
Katrina Cut structure sand berm (R1)	Sensitivity testing related to the Katrina Cut structure (habitat suitability index modeling was not completed for this measure).
Pelican Island southeast nourishment (R2)	Pelican Island nourishment that extended the island by about 2.6 km to the south of the present tip of Pelican Island.
Sand Island platform nourishment and sand bypassing (R3)	Nourishment of the submerged Sand Island platform that is designed to increase the elevation to 2 m below mean sea level, which is 5 m higher than some current bed-elevation levels in this area.
West and east end beach and dune nourishment (R4)	Nourishment of the beach east of the Katrina Cut and the shorefront area east of Pelican Island to raise beach and dune elevations by a maximum of about 3.7 m.
Back-barrier tidal flats and marsh habitat restoration (R5)	Marsh restoration and filling of burrow pits along the back-barrier area of Dauphin Island.
West end beach and dune nourishment (R6)	Modified version of the R4 measure, which moved the restored dune area landward with no sediment nourishment east of Pelican Island.
West end and Katrina Cut beach and dune nourishment (R7)	Modified version of the R6 measure extends these changes west to the front side of the Katrina Cut rubble wall structure.

2020), and a landscape-position-based barrier island habitat model (chapter A). This assessment included seven restoration measures that were proposed and incorporated in the decadal simulations of barrier island geomorphology (Mickey and others, 2020; table B1). To quantify the effects of these restoration measures, changes in habitat suitability classes were compared to a future without action (R0) alternative.

The impacts of restoration measures were assessed under two potential scenarios with regard to storminess and future sea levels. The storminess bins included realizations with a "medium" storminess, which included one to three storms over a 10-year period (that is, ST2) and a "high" storminess, which included four to five storms over an equal period (that is, ST3). As previously mentioned, we predicted habitats under two future sea levels by 2100. These included a sea level of 0.3 m (that is, SL1) and a sea level of about 1.0 m (that is, SL3). Specifically, the medium storminess was paired with the 0.3 m above the contemporary sea level (that is, ST2SL1) and the "high" storminess bin was paired with the 1.0 m above the contemporary sea level (that is, ST3SL3). The storminess bins were determined by the number of storms that result in overwash of the representative profile given the dune characteristics at the time of the storm. For more information on how storminess and SLR bins were selected, see Mickey and others (2020).

Marsh accretion rates also determine landscape elevations to some extent, and it was important to include these in the scenarios. To account for intertidal marsh vertical accretion as a component of marsh morphology evolution, the Dauphin Island landscape-based habitat model (chapter A) considered two scenarios: the U.S. Army Corps of Engineers (USACE) high and intermediate SLR curves in which marsh kept pace with SLR through accretion (1 centimeter per year) through 2022 under the high SLR curve, whereas marsh kept pace with SLR by accretion for the entirety of the USACE intermediate curve (chapter A). Therefore, four future storminess and SLR scenarios were run for oyster habitat suitability modeling: (1) "medium" storminess and a 0.3-m sea level using the USACE high curve when intertidal marsh partially kept with SLR (ST2SL1H); (2) "medium" storminess and a 0.3-m sea level using the USACE intermediate curve when intertidal marsh completely kept with SLR (ST2SL1I); (3) "high" storminess and a 1.0-m sea level using the USACE high curve when intertidal marsh partially kept with SLR (ST3SL3H); and (4) "high" storminess and a 1.0-m sea level using the USACE intermediate curve when intertidal marsh completely kept with SLR (ST3SL3I).

Water Quality Model Data

The effects of the proposed restoration measures on estuarine and marine-water quality near Dauphin Island were simulated by the coupled hydrodynamic and water quality models. The U.S. Army Corp of Engineers three-dimensional model (Johnson and others, 1993), based on Curvilinear Hydrodynamics in 3 Dimensions—Waterway Experiment Station version (CH3D–WES), has been a successful management model for the U.S. Environmental Protection Agency Chesapeake Bay Program water quality modeling system (Kim, 2013). The CH3D–WES provides hydrodynamic flux across grid cell boundaries to a water quality model, the USACE Integrated Compartment Water Quality Model (CE–QUAL–ICM; Cerco and others, 2013), which has been used to manage the bay water quality by the Chesapeake Bay Program with simulation periods spanning decades. The hydrodynamic model, CH3D–WES, computes salinity, surface elevation, velocity, diffusivity, and bottom shear stress. Eutrophication

processes are computed by the CE–QUAL–ICM eutrophication model. The CE–QUAL–ICM model in this study incorporates 24 state variables in the water column including physical variables; multiple algal groups; 2 zooplankton groups; and multiple forms of carbon, nitrogen, phosphorus, and silica. For each variable, we used depth averaged water quality parameters. Because of limits of computational expense, water quality model outputs were not developed for each specific restoration measure. Instead, three general model outputs were developed. The first water quality model outputs included baseline 2015 geomorphology conditions with no island breaching (model name BASE). The second water quality model outputs included SL3 water levels with a single breach west of Katrina Cut. The third water quality model outputs included SL3 water levels and breaching on either side of the Katrina Cut, Little Dauphin Island, and Pelican Island (2BKC).

Water quality outputs were paired with each scenario (that is, combination of restoration measure along with storminess and future sea-level conditions). It was hypothesized that geomorphology would be the most sensitive factor when deciding which water quality output to use, then the presence/absence, location, and extent of breaching would be the most important factor in driving changes to estuarine water quality. This hypothesis was tested by assessing habitat suitability for ST3SL3 conditions using the BASE and 2BKC water quality outputs. It was noted that the presence of a breach near Katrina Cut for water quality models led to a reduction in suitability in plume-shaped areas extending northward from the "breached" areas into estuarine waters of the Mississippi Sound; thus, it is more important to properly match the breaching scenario compared to the sea-level scenario. The water quality data used for each restoration measure and storminess/sea-level combination are shown in table B2.

Habitat Suitability Index Model Spatial Framework and Processing

The domain of the HSI models generally matches the model domain for the landscape-position-based model (chapter A), which covered a 2.5-km buffer from Dauphin Island. One modification to the HSI domain was the addition of areas near Cedar Point in the northeastern edge of the landscape domain. The spatial resolution of the HSI varies

Table B2. Restoration measures for the Alabama Barrier Island Restoration Feasibility Assessment project, Dauphin Island, Alabama.

[SL, sea level; Y, year; BASE, baseline water quality model with no breaches; R, restoration measure; ST2SL1, "medium" storminess bin was paired with the 0.30-meter sea-level rise; ST3SL3, "high" storminess bin was paired with the 1.0-meter sea-level rise; 2BKC, water quality model with sea-level rise of about 1.0 meter and breaching on both sides of Katrina Cut; 1BSAL, water quality model with sea-level rise of about 1.0 meter and one breach on the western end of Katrina Cut]

Restoration measure	Water quality data				
	Storminess/ SL	Y0 High	Y10 High	Y0 Intermediate	Y10 Intermediate
Baseline[1]	SL0	BASE	BASE	BASE	BASE
Future without action (R0)	ST2SL1	BASE	BASE	BASE	BASE
	ST3SL3	BASE	2BKC	BASE	2BKC
Pelican Island southeast nourishment (R2)	ST2SL1	BASE	BASE	BASE	BASE
	ST3SL3	BASE	2BKC	BASE	2BKC
Sand Island platform nourishment and sand bypassing (R3)	ST2SL1	BASE	BASE	BASE	BASE
	ST3SL3	BASE	2BKC	BASE	2BKC
West and east end beach and dune nourishment (R4)	ST2SL1	BASE	BASE	BASE	BASE
	ST3SL3	BASE	1BSAL/2BKC	BASE	1BSAL/2BKC
Back-barrier tidal flats and marsh habitat restoration (R5)	ST2SL1	BASE	BASE	BASE	BASE
	ST3SL3	BASE	2BKC	BASE	2BKC
West end beach and dune nourishment (R6)	ST2SL1	BASE	BASE	BASE	BASE
	ST3SL3	BASE	1BSAL/2BKC	BASE	1BSAL/2BKC
West end and Katrina Cut beach and dune nourishment (R7)	ST2SL1	BASE	BASE	BASE	BASE
	ST3SL3	BASE	BASE[2]	BASE	BASE[2]

[1]Sea-level rise curves (that is, high and intermediate) and periods (that is, Y0 and Y10) are not applicable to the baseline condition. The baseline condition used the BASE model and the 2015 geomorphology data.

[2]2BKC used in the areas where breaching occurred near Little Dauphin Island and Pelican Island.

and is matched to the resolution of the water quality model. The area of the cells in this grid ranged from about 1 hectare (ha) in the Mobile River shipping channel to 56 ha in offshore estuarine and marine waters and had a median of 6.7 ha. Esri ArcMap 10.7.1 (Redlands, California) was used to calculate values of each habitat suitability variable (for example, annual mean salinity, DO, TSS, water depth, and water temperature) from water quality model monthly output for cells in the water quality grid for each scenario (table B2). The only variable that did not come directly from the water quality model outputs was mean water depth. The mean water depth variable was estimated using the geomorphic outputs for each scenario (that is, combination of restoration measure, storminess, and SLR). Landscape-position-based habitat model outputs (chapter A) were used to calculate the mean water depth. This water depth was relative to mean sea level based on observations during the most recent North American Tidal Datum Epoch (1983–2001) from a National Oceanic and Atmospheric Administration tide gauge (station identifier 8735180) on the eastern end of the island. Simulations were run for the initial year (Yr=0) and a period after 10 years (Yr=10) with the corresponding water quality input. A Python script (Python 2.7) was developed to read in the value of each habitat suitability parameter in spatial layers of the habitat suitability variables, calculate the individual suitability index based on the habitat suitability curves (figs. B2–B8) and determine the total HSI using the weighted geometric mean method, classify the suitability scores (0 to 1) into groups, and generate a spatial distribution map of oyster habitat suitability designations (that is, unsuitable, marginally suitable, suitable, and highly suitable).

The water quality grids (table B2) matched general island configurations related to breaching and (or) sea levels. We made a few minor modifications to the grids to enhance the comparability of the HSI outputs. First, we used the BASE grid for all the R7 simulations for the ST3SL3 scenarios, which matched the breaching scenario for Katrina Cut (that is, restoration prevented breaching along Katrina Cut); however, the geomorphology for the BASE grid is not correct for year 10 for Little Dauphin Island and Pelican Island (that is, does not contain breaching that was identified by geomorphic modeling). In order to account for the breaching at Little Dauphin Island and Pelican Island, we used the habitat suitability values that were determined for R0 for the ST3SL3 for year 10 for the missing water quality cells for Little Dauphin Island and Pelican Island. Second, the resolution of cells in each grid may differ, which can cause issues along the boundary of the model domain. For instance, the 2BKC water quality grid has areas where a single cell is made up of two cells. To enhance comparisons between each grid and avoid an issue with missing data, we merged two cells in 2BKC to match the grid registration of BASE for one boundary cell at the north-central portion of the model domain.

Habitat Suitability Index Model Results and Discussion

The following sections will include the results and discussion for the oyster habitat suitability under baseline conditions and future conditions. Data generated during this study are available from the ScienceBase (Wang and others, 2020).

Oyster Habitat Suitability Distribution under Baseline Condition

The baseline oyster habitat suitability distribution (that is, contemporary conditions without SLR) in estuarine waters of Dauphin Island is shown in figure B11. As expected, most suitable and highly suitable areas for oyster growth are to the north of Dauphin Island. Among the total area within the model domain (26,697.3 ha), the highly suitable area is about 46.4 percent, the suitable area is about 5.8 percent, the marginally suitable area is about 2.3 percent, and the unsuitable area is about 45.4 percent.

The HSI distribution is consistent with the current and historical oyster distribution around the Cedar Point area oyster reefs, where release and harvesting are prevalent, including adjacent intertidal waters 2–3 km southwest of Cedar Point where the largest expanse of oyster reefs in Alabama coastal waters was found (Gregalis and others, 2008). Our results also indicate suitability for areas that extend farther west from the current and historical oyster distribution for the area. Here, it is important to consider that the HSI model used for this study is solely based on water quality and, thus, does not factor in substrate suitability; therefore, oysters may not necessarily be present in areas that are identified as having good HSI.

The baseline oyster habitat suitability distribution map showed a spatial gradient of habitat for oyster growth and survivorship within estuarine waters near Dauphin Island; for example, there tends to be a gradient of highly suitable to suitable from the northwest (that is, close to Cedar Point) to the southeast of Little Dauphin Island and lower suitability near Petit Bois Pass (fig. B11). Field data from 1 year of sampling (Gregalis and others, 2008) also revealed that Cedar Point oyster reefs tend to have high numbers of spat, low numbers of dead spat, high numbers of oysters, and high natural recruitment. In contrast, the area south of Little Dauphin Island is suitable for oyster growth (for example, high number of oyster spat, moderate number of oysters), but this area tends to be less suitable than Cedar Point as indicated by a high number of dead spat because of the poor water quality or predation by oyster drills (Gregalis and others, 2008). It should be noted that the spatial patterns (locations) of oyster optimal suitability in the area may change or switch with changing physical environmental conditions; therefore, the area at or near Cedar Point may not always reflect the best place with highest oyster habitat suitability. Nevertheless, the agreement between the current and historical oyster reef distribution and the baseline

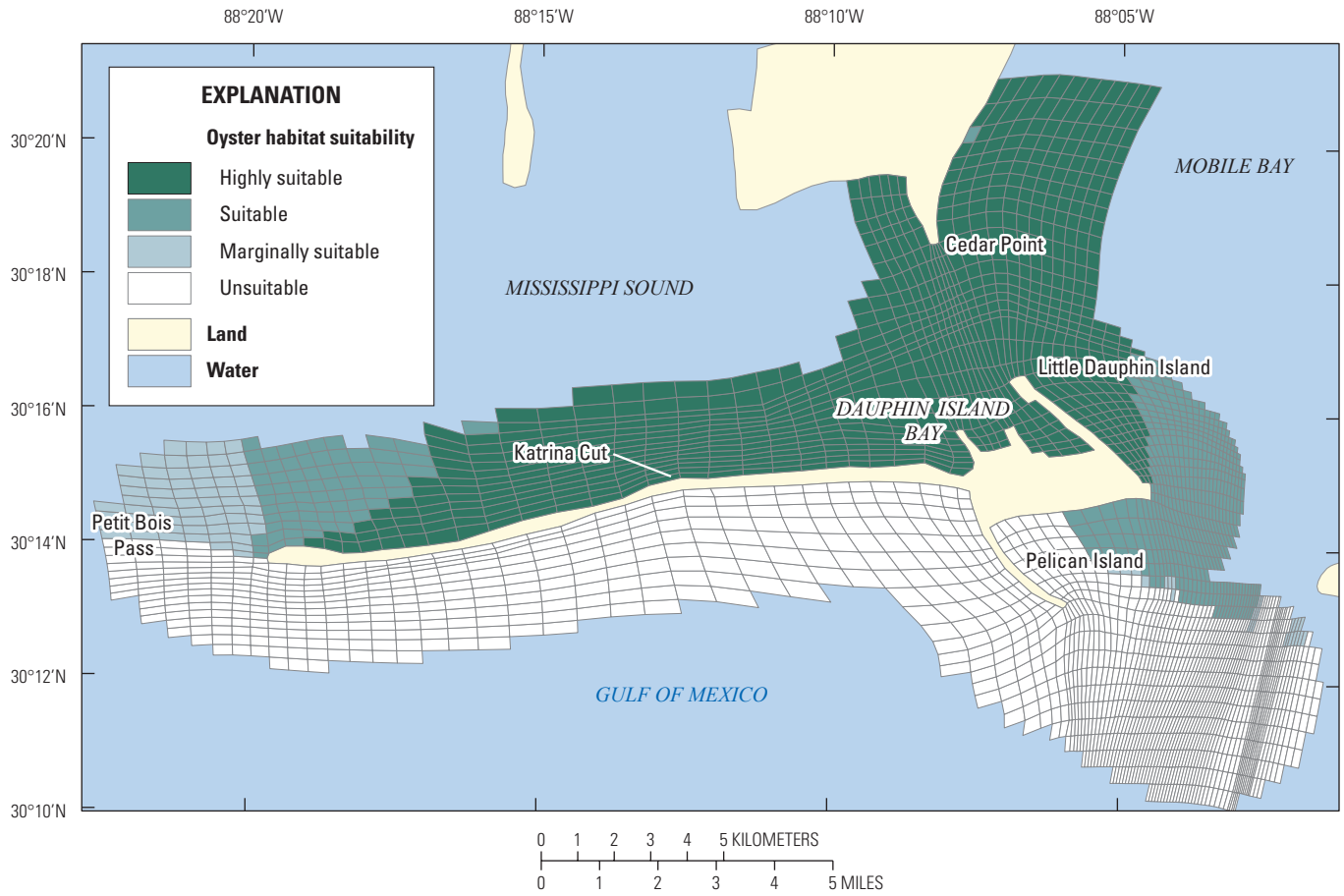

Figure B11. The distribution of oyster habitat suitability in estuarine waters near Dauphin Island, Alabama, for the baseline model (2015). Land and water areas are generalized areas from the water quality model grid.

habitat suitability map that was produced using the HSI model (fig. B11), as well as model validation, indicates that the habitat suitability model for estuarine waters near Dauphin Island can be used for prediction of oyster habitat suitability change under restoration measures and storminess and future sea-level conditions.

Oyster Habitat Suitability Distribution for Restoration Measures, Future Storminess, and Sea-Level Rise

Included in table B3 is a summary of the areal coverage of habitat quality bins and the proposed barrier island restoration measures including the future without action for the selected storminess and sea-level conditions at the initial year and for year 10. Presented in table B3 are 2 scenarios of marsh accretion and 2 periods after restoration. This table (table B3) also includes the percentage change per habitat suitability bin compared to the future without action measure.

For the initial year simulations with the USACE high SLR curve, it seemed that these restoration measures tended not to affect oyster habitat suitability (table B3). Similarly, many major differences were not seen in the results for year 0 for the USACE intermediate curve (with the assumption of intertidal marsh keeping pace with SLR). However, one exception was the back-barrier tidal flats and marsh habitat restoration (R5) for ST2SL1, which had a 7.8-percent increase in marginally suitable areas with much of that area coming from cells that were previously unsuitable (table B3). This change was more related to uncertainty and sensitivity along edges of classes rather than a change that resulted from the restoration measure. In contrast, the barrier island restoration measures were found to have large and positive effects on oyster habitat suitability distribution for year 10. Results under the USACE high and intermediate SLR curves had a similar trend and magnitude of change; therefore, results for the high USACE SLR curve were used to examine the impact of the various restoration efforts under future storm and sea-level conditions.

The oyster HSI distribution under the future without action for year 10 for the USACE high SLR curve is shown in figure B12. The ST2SL1 scenario did not show much change in oyster habitat distribution (location and extent) compared to the distribution without SLR except for a slight reduction in highly suitable area converting to suitable class in the estuarine waters near the south tip of Little Dauphin Island

Table B3. The areal coverage of oyster habitat suitability bins under various restoration, storminess, and sea-level conditions and percentage change of these habitat categories compared to baseline conditions.

[SL, sea level; ha, hectare; unsuitable, total habitat suitability index score (HSI_{total}) less than 0.3; marginally suitable, HSI_{total} 0.3–0.5; suitable, HSI_{total} 0.5–0.7; highly suitable, HSI_{total} greater than 0.7; USACE, U.S. Army Corps of Engineers; SLR, sea-level rise; R, restoration measure; ST2SL1, "medium" storminess bin was paired with the 0.30-meter SLR; ST3SL3, "high" storminess bin was paired with the 1.0 meter-SLR]

Restoration measure	Storminess/SL	Area (ha)				Percentage change compared to future without action			
		Unsuitable	Marginally suitable	Suitable	Highly suitable	Unsuitable	Marginally suitable	Suitable	Highly suitable
Year 0 with the USACE high SLR curve									
Future without action (R0)	ST2SL1	12,123.6	1,227.1	2,999.1	10,347.6	--	--	--	--
	ST3SL3	12,066.0	1,468.8	3,159.2	10,003.3	--	--	--	--
Pelican Island southeast nourishment (R2)	ST2SL1	12,123.6	1,227.1	2,999.1	10,347.6	0.00	0.00	0.00	0.00
	ST3SL3	12,066.0	1,468.8	3,159.2	10,003.3	0.00	0.00	0.00	0.00
Sand Island platform nourishment and sand bypassing (R3)	ST2SL1	12,123.6	1,227.1	2,999.1	10,347.6	0.00	0.00	0.00	0.00
	ST3SL3	12,082.8	1,455.2	3,156.0	10,003.3	0.14	−0.93	−0.10	0.00
West and east end beach and dune nourishment (R4)	ST2SL1	12,123.6	1,227.1	2,999.1	10,347.6	0.00	0.00	0.00	0.00
	ST3SL3	12,066.0	1,468.8	3,159.2	10,003.3	0.00	0.00	0.00	0.00
Back-barrier tidal flats and marsh habitat restoration (R5)	ST2SL1	12,123.6	1,227.1	2,999.1	10,347.6	0.00	0.00	0.00	0.00
	ST3SL3	12,066.0	1,468.8	3,159.2	10,003.3	0.00	0.00	0.00	0.00
West end beach and dune nourishment (R6)	ST2SL1	12,123.6	1,227.1	2,999.1	10,347.6	0.00	0.00	0.00	0.00
	ST3SL3	12,066.0	1,468.8	3,159.2	10,003.3	0.00	0.00	0.00	0.00
West end and Katrina Cut beach and dune nourishment (R7)	ST2SL1	12,123.6	1,227.1	2,999.1	10,347.6	0.00	0.00	0.00	0.00
	ST3SL3	12,066.0	1,473.0	3,155.0	10,347.6	0.00	0.29	−0.13	0.00
Year 0 with the USACE intermediate SLR curve									
Future without action (R0)	ST2SL1	12,123.6	1,227.1	2,999.1	10,347.6	--	--	--	--
	ST3SL3	12,066.0	1,468.8	3,159.2	10,003.3	--	--	--	--
Pelican Island southeast nourishment (R2)	ST2SL1	12,123.6	1,227.1	2,999.1	10,347.6	0.00	0.00	0.00	0.00
	ST3SL3	12,066.0	1,468.8	3,159.2	10,003.3	0.00	0.00	0.00	0.00
Sand Island platform nourishment and sand bypassing (R3)	ST2SL1	12,123.6	1,227.1	2,999.1	10,347.6	0.00	0.00	0.00	0.00
	ST3SL3	12,066.0	1,468.8	3,159.2	10,003.3	0.00	0.00	0.00	0.00
West and east end beach and dune nourishment (R4)	ST2SL1	12,123.6	1,227.1	2,999.1	10,347.6	0.00	0.00	0.00	0.00
	ST3SL3	12,041.7	1,496.4	3,156.0	10,003.3	−0.20	1.88	−0.10	0.00
Back-barrier tidal flats and marsh habitat restoration (R5)	ST2SL1	12,078.7	1,275.2	2,995.9	10,347.6	−0.37	3.92	−0.11	0.00
	ST3SL3	12,066.0	1,468.8	3,159.2	10,003.3	0.00	0.01	0.00	0.00
West end beach and dune nourishment (R6)	ST2SL1	12,123.6	1,227.1	2,999.1	10,347.6	0.00	0.00	0.00	0.00
	ST3SL3	12,066.0	1,468.8	3,159.2	10,003.3	0.00	0.00	0.00	0.00
West end and Katrina Cut beach and dune nourishment (R7)	ST2SL1	12,123.6	1,227.1	2,999.1	10,347.6	0.00	0.00	0.00	0.00
	ST3SL3	12,066.0	1,473.0	3,155.0	10,003.3	0.00	0.29	−0.13	0.00

Table B3. The areal coverage of oyster habitat suitability bins under various restoration, storminess, and sea-level conditions and percentage change of these habitat categories compared to baseline conditions.—Continued.

[SL, sea level; ha, hectare; unsuitable, total habitat suitability index score (HSI_{total}) less than 0.3; marginally suitable, HSI_{total} 0.3–0.5; suitable, HSI_{total} 0.5–0.7; highly suitable, HSI_{total} greater than 0.7; USACE, U.S. Army Corps of Engineers; SLR, sea-level rise; R, restoration measure; ST2SL1, "medium" storminess bin was paired with the 0.30-meter SLR; ST3SL3, "high" storminess bin was paired with the 1.0 meter-SLR]

Restoration measure	Storminess/SL	Area (ha)				Percentage change compared to future without action			
		Unsuitable	Marginally suitable	Suitable	Highly suitable	Unsuitable	Marginally suitable	Suitable	Highly suitable
Year 10 with the USACE high SLR curve									
Future without action (R0)	ST2SL1	11,984.6	1,366.0	2,999.1	10,347.6	--	--	--	--
	ST3SL3	12,112.0	1,704.7	5,773.9	7,324.9	--	--	--	--
Pelican Island southeast nourishment (R2)	ST2SL1	11,988.6	1,363.9	2,997.2	10,347.6	0.03	−0.15	−0.06	0.00
	ST3SL3	12,070.4	1,746.2	5,773.9	7,324.9	−0.34	2.43	0.00	0.00
Sand Island platform nourishment and sand bypassing (R3)	ST2SL1	11,984.6	1,366.0	2,999.1	10,347.6	0.00	0.00	0.00	0.00
	ST3SL3	12,152.1	1,723.0	5,715.6	7,324.9	0.33	1.07	−1.01	0.00
West and east end beach and dune nourishment (R4)	ST2SL1	11,984.6	1,366.0	2,999.1	10,347.6	0.00	0.00	0.00	0.00
	ST3SL3	12,078.8	1,644.1	4,940.2	8,252.4	−0.27	−3.55	−14.44	12.66
Back-barrier tidal flats and marsh habitat restoration (R5)	ST2SL1	11,984.6	1,366.0	2,999.1	10,347.6	0.00	0.00	0.00	0.00
	ST3SL3	12,095.0	1,737.0	5,758.7	7,324.9	−0.14	1.90	−0.26	0.00
West end beach and dune nourishment (R6)	ST2SL1	11,984.6	1,366.0	2,999.1	10,347.6	0.00	0.00	0.00	0.00
	ST3SL3	12,097.1	1,625.9	4,940.2	8,252.4	−0.12	−4.62	−14.44	12.66
West end and Katrina Cut beach and dune nourishment (R7)	ST2SL1	11,984.6	1,366.0	2,999.1	10,347.6	0.00	0.00	0.00	0.00
	ST3SL3	12,073.8	1,567.0	3,175.0	10,053.8	−0.32	−8.08	−45.01	37.26
Year 10 with the USACE intermediate SLR curve									
Future without action (R0)	ST2SL1	11,984.6	1,366.0	2,999.1	10,347.6	--	--	--	--
	ST3SL3	12,103.5	1,713.2	5,773.9	7,324.9	--	--	--	--
Pelican Island southeast nourishment (R2)	ST2SL1	11,984.6	1,366.0	2,999.1	10,347.6	0.00	0.00	0.00	0.00
	ST3SL3	12,062.7	1,746.2	5,781.7	7,324.9	−0.34	1.93	0.14	0.00
Sand Island platform nourishment and sand bypassing (R3)	ST2SL1	11,984.6	1,366.0	2,999.1	10,347.6	0.00	0.00	0.00	0.00
	ST3SL3	12,093.7	1,723.0	5,773.9	7,324.9	−0.08	0.57	0.00	0.00
West and east end beach and dune nourishment (R4)	ST2SL1	11,984.6	1,366.0	2,999.1	10,347.6	0.00	0.00	0.00	0.00
	ST3SL3	12,078.1	1,646.2	4,942.1	8,249.1	−0.21	−3.91	−14.41	12.62
Back-barrier tidal flats and marsh habitat restoration (R5)	ST2SL1	11,984.6	1,366.0	2,999.1	10,347.6	0.00	0.00	0.00	0.00
	ST3SL3	12,112.0	1,704.7	5,773.9	7,324.9	0.07	−0.50	0.00	0.00
West end beach and dune nourishment (R6)	ST2SL1	11,984.6	1,366.0	2,999.1	10,347.6	0.00	0.00	0.00	0.00
	ST3SL3	12,090.0	1,633.0	4,940.2	8,252.4	−0.11	−4.68	−14.44	12.66
West end and Katrina Cut beach and dune nourishment (R7)	ST2SL1	11,984.6	1,366.0	2,999.1	10,347.6	0.00	0.00	0.00	0.00
	ST3SL3	11,984.6	1,567.0	3,175.0	10,053.8	−0.25	−8.53	−45.01	37.26

as a result of the storms and sea level (fig. B12*A*). However, the highly suitable areas would be greatly reduced under ST3SL3 conditions with most of the reduction occurring in the back-barrier areas in the Mississippi Sound because of the breaching of the island near the Katrina Cut (fig. B12*B*). This reduction in oyster habitat suitability can be attributed to the increased salinity and increased water depth under increased storminess and sea level.

Modeling results indicated that proposed restoration measures would have little or no impacts on oyster habitat suitability distribution under the ST2SL1 scenario (table B3). In contrast, under the ST3SL3 scenario, restoration measures should generally increase the percentage change in highly suitable oyster areas from 12.6 percent to 37.3 percent compared to the future without action scenario (table B3, fig. B13). The west and east end beach and dune nourishment (R4), west end beach and dune nourishment (R6), and west end and Katrina Cut beach and dune nourishment (R7; table B1) could increase highly suitable area by 12.6 percent, 12.6 percent, and 37.3 percent, respectively (table B3, fig. B13). For example, beach/dune restoration in front of Katrina Cut (R7) reduced unsuitable, marginally suitable, and suitable area from 12,103.5 ha to 11,984.6 ha, from 1,713.2 ha to 1,567.0 ha, and from 5,773.9 ha to 3,175.0 ha, respectively, and increased the highly suitable area from 7,324.9 ha to 10,053.8 ha, (that is, an increase of 2,728.9 ha; table B3). There is a net increase of 130 ha in suitable groups (suitable and highly suitable) with this restoration measure under ST3SL3. Compared to the future without action, the total area of unsuitable class would all have minor reductions (about 1 percent); most of the oyster habitat suitability changes are because of restoration associated with the switches among the marginally suitable, suitable, and highly suitable classes. It should be noted that the future without action measure (R0) under the ST3SL3 condition has two breaches on either side of Katrina Cut, R5 similarly has two breaches, R4 and R6 have one breach (to the west of Katrina Cut), and R7 has no breaching.

The changes in oyster habitat suitability under restoration measures highlight the large and potentially positive effects of a barrier island geomorphology on oyster habitat suitability distribution in nearby estuarine waters. This point underscores the importance of a healthy barrier island for salinity regulation in the Mississippi Sound (Mickey and others, 2020). Barrier island breaching would likely have adverse impacts on oyster habitat suitability within Little Dauphin Island Bay because it is in the highly suitable class, and salinity may become higher than optimal (Gregalis and others, 2008). The seven restoration measures assessed in this study are expected to have slight positive effects on habitat near Little Dauphin Island. The U.S. Geological Survey and USACE are initiating a National Fish and Wildlife Foundation-funded project focused on Little Dauphin Island. This project will enhance the hydrodynamic modeling effort for this island and integrate management decisions specific for this area.

Future Studies

In this study, the oyster habitat suitability model was calibrated and validated using field data at the Cedar Point reef. Although the reef dataset we used for calibration included oyster reef observations, it did not have continuous water quality monitoring nearby to couple with these data; thus, the lack of data from other locations for model calibration and validation could affect the habitat suitability model's applicability in other barrier island-dominated estuaries. Furthermore, many of the relations between habitat suitability and water quality variables were based on work for different regions/oyster populations and there is increasing evidence of local population adaptations. Populations may have differential response to water quality conditions that we are not capturing. Therefore, additional water quality and oyster biological data from a well-planned and distributed monitoring regime are needed to improve the habitat suitability model's applicability for the assessment and prediction of habitat change under various future environmental conditions to identify optimal habitat for barrier island restoration and oyster reef restoration (Soniat and Brody, 1988; Theuerkauf and Lipcius, 2016).

Simulated habitat suitability scores may be overestimated because of underestimated TSS from the water quality model related to (1) the organic part not being entirely incorporated, TSS was only inorganic based; and (2) wind waves not being incorporated in the coupled hydrodynamic and water quality model (Kim, 2013) that provided simulated water quality conditions under various scenarios to the oyster HSI model; furthermore, the highest habitat suitability score was given when TSS was at or close to zero (no food in the water column). However, the experimental results indicated that increasing TSS or turbidity may increase the oyster clearance rate (the volume of water completely cleared of suspended particles per unit of time) because they must filter more to get enough food; but it also costs more energy, which could slow somatic growth (Hofmann and others, 1992; Powell and others, 1992). It was found that the oyster clearance rate may not change with turbidity in 0–400 mg/L^{-1} (La Peyre, Louisiana Fish and Wildlife Cooperative Research Unit, unpub. data, 2015). Other studies indicated a compensatory response, increased clearance rate with increasing TSS (Shumway, 1996; Bayne, 2017), but there is also evidence of local adaptation; therefore, further modification of TSS with oyster habitat quality using local data is needed for model improvement. Nevertheless, TSS was calibrated to have a lower weight; TSS data used in the modeling were larger than 22 mg/L with less variability, thus having little impact on total oyster habitat suitability scores compared to other critical variables such as those of salinity derived ones.

The oyster habitat suitability model could also be improved by adding other biophysical parameters. Previous oyster habitat suitability models have included cultch materials, such as oyster or clam shell, which provide suitable hard bottom for spat settling (Cake, 1983; Soniat and Brody, 1988; Barnes and others, 2007; Soniat and others, 2013; Denapolis,

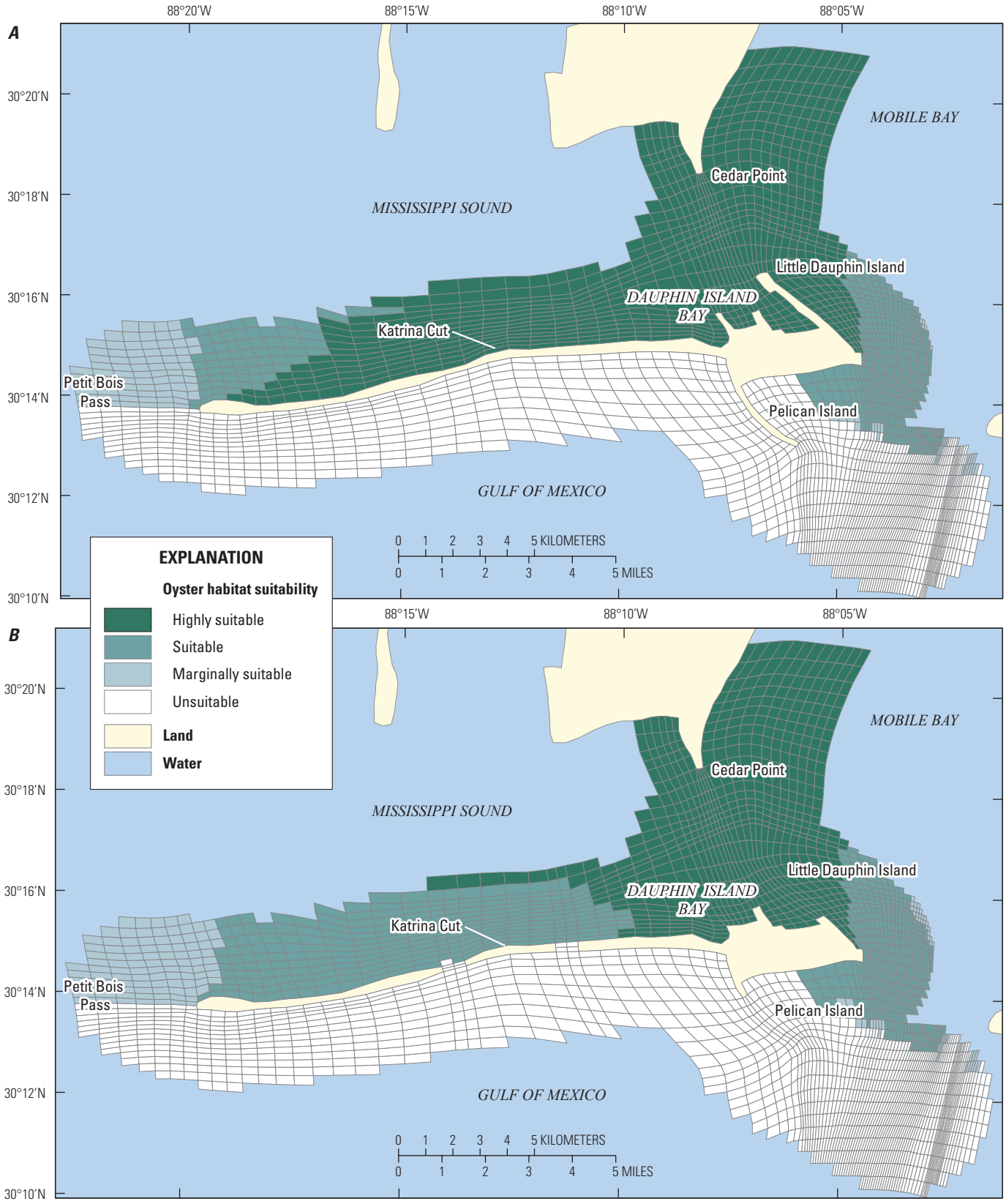

Figure B12. The distribution of oyster total habitat suitability index score under the future without action restoration measure (R0) in estuarine waters near Dauphin Island, Alabama, for year 10 using the U.S. Army Corps of Engineers high sea-level rise curve. *A*, with "medium" storminess and sea level (ST2SL1); *B*, with "high" storminess and sea level (ST3SL3). Land and water areas are generalized areas from the water quality model grid.

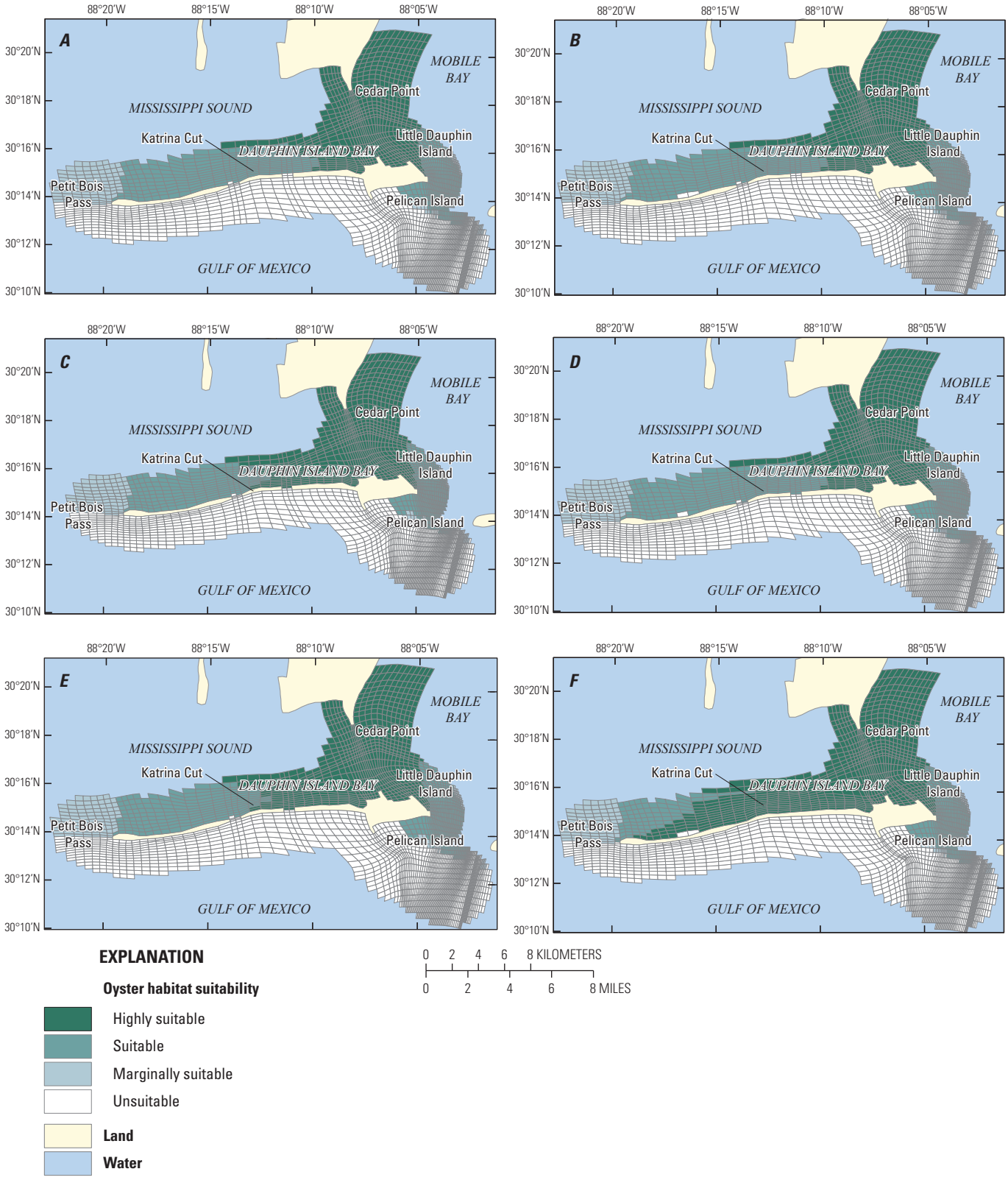

Figure B13. The distribution of oyster total habitat suitability index score with restoration measures under high storminess and sea level (ST3SL3) in estuarine waters near Dauphin Island, Alabama, for year 10 with the U.S. Army Corps of Engineers high sea-level rise curve. *A*, with restoration measure R2; *B*, with restoration measure R3; *C*, with restoration measure R4; *D*, with restoration measure R5; *E*, with restoration measure R6; *F*, with restoration measure R7. Land and water areas are generalized areas from the water quality model grid.

2018). Substrate was not included in this HSI model because of a lack of data on substrate distribution in estuarine waters near Dauphin Island. In its present form, the model results can be used to locate areas where water quality parameters are suitable for oysters and substrate should be placed. The rationale is that areas with a high HSI value should promote spat settlement and survival and be candidates for the implementation of oyster reef restoration projects. Moreover, water flow rate (current velocity) is also a key factor on oyster filtration, growth, and spat settlement and should be incorporated to reflect this habitat requirement (Lenihan and others, 1996; La Peyre and others, 2015; Theuerkauf and Lipcius, 2016; Wang and others, 2017). Additionally, we used mean salinity during the May–September spawning period in the Dauphin Island oyster HSI model; nevertheless, lots of evidence of significant spawning in October and even November in recent decades was found (La Peyre and others, 2009, 2013; Sehlinger and others, 2019); therefore, spawning in late fall until November should be incorporated in the model.

Although HSI models are useful in determining locations for oyster reef restoration, population dynamic modeling is needed to determine the interaction between oyster population growth, mortality, and physical environmental conditions. In this study, the oyster habitat suitability model was developed based solely on estuarine water quality conditions. It did not explicitly consider onsite biotic interactions such as diseases, predation, and competition on oyster population dynamics, although they are largely salinity dependent (Miller and others, 2017). Furthermore, important processes such as the feedback between oyster filtration, growth, and water quality parameters such as oyster density and velocity on food (chlorophyll *a*) reduction are not explicitly modeled (Wang and others, 2017). Therefore, the HSI model provides the broad landscape for potential sites for oyster habitat restoration, but the choice for specific locations for restoration should consider factors not explicitly included in the model (for example, bottom firmness, current speed) to achieve optimal oyster production. The infeasibility of including additional but important variables may explain some of the discrepancy between habitat suitability scores and oyster densities in the model validation (fig. B10). A better understanding of the effects of barrier island restoration on oyster population dynamics (recruitment, growth, mortality, and reproduction) requires a model that integrates hydrodynamic, water quality, oyster population, and species interaction (Wang and others, 2008, 2017).

Restored reefs can diminish shoreline erosion, stabilize marshes, enhance fishery habitat, and facilitate seagrass colonization (Scyphers and others, 2011; La Peyre and others, 2015). At Cedar Point and near Little Dauphin Island, oyster reefs have been constructed under ADCNR's oyster restoration program as large subtidal reefs, breakwater reefs, and unfished ecosystem services study reefs (Wallace and others, 1999; Gregalis and others, 2008). Constructed oyster reefs may benefit the seagrass beds, such as by increasing seagrass abundance between the reefs and the shoreline (Sharma and others, 2016). The ADCNR will incorporate a living shoreline for the restoration of Dauphin Island to protect shorelines, maintain island geomorphology, and enhance habitat for oysters and seagrasses.

Conclusions

A spatially explicit oyster HSI model was developed for estuarine waters near Dauphin Island based on previous studies on oysters along the Gulf of Mexico. The HSI model was calibrated and validated using existing site-specific field data on oyster density and water quality variables. The habitat suitability model was shown to be useful for the assessment and prediction of the impacts of barrier island restoration measures on oyster habitat under various scenarios of future storminess and future sea level. Suitable oyster areas are identified in the estuarine waters north of Dauphin Island, especially near Cedar Point where oyster harvest has traditionally occurred. Modeling results indicated that the impacts of each of the individual restoration measures would be localized and that the restoration projects would yield a positive effect on oyster habitat under high storminess and sea level (ST3SL3 conditions) but not under ST2SL1 conditions. Study results suggest that such restorations could maintain barrier island integrity while enhancing oyster habitat, growth, and distribution.

References Cited

Barnes, T.K., Volety, A.K., Chartier, K., Mazzotti, F.J., and Pearlstine, L., 2007, A habitat suitability model for the eastern oyster (*Crassostrea virginica*), a tool for restoration of the Caloosahatchee Estuary, Florida: Journal of Shellfish Research, v. 26, no. 4, p. 949–959. [Also available at https://doi.org/10.2983/0730-8000(2007)26[949:AHSIMF]2.0.CO;2.]

Battista, T.A., 1999, Habitat suitability index model for the eastern oyster, *Crassostrea virginica*, in the Chesapeake Bay—A geographic information system approach: College Park, Md., University of Maryland, master thesis, 125 p.

Bayne, B., 2017, Biology of oysters (1st ed., v. 41): Cambridge, Mass., Academy Press, 860 p.

Cake, E.W., 1983, Habitat suitability index models: Gulf of Mexico American oyster: U.S. Department of Interior, Fish and Wildlife Service, FWS/OBS-82/10.57, 37 p. [Also available at https://archive.usgs.gov/archive/sites/www.nwrc.usgs.gov/wdb/pub/hsi/hsi-057.pdf.]

Cerco, C.F., Kim, S.C., and Noel, M.R., 2013, Management modeling of suspended solids in the Chesapeake Bay, USA: Estuarine, Coastal and Shelf Science, v. 116, p. 87–98. [Also available at https://doi.org/10.1016/j.ecss.2012.07.009.]

Denapolis, T.V., 2018, Legacy habitat suitability of eastern oysters (*Crassostrea virginica*) in Louisiana—A prelude to Mississippi River Delta freshwater diversions: University of New Orleans, master thesis, 139 p.

Froede, C.R., Jr., 2008, Changes to Dauphin Island, Alabama, brought about by Hurricane Katrina (August 29, 2005): Journal of Coastal Research, v. 24, no. sp3, p. 110–117. [Also available at https://doi.org/10.2112/06-0782.1.]

Gregalis, K.C., Powers, S.P., and Heck, K.L., Jr., 2008, Restoration of oyster reefs along a bio-physical gradient in Mobile Bay, Alabama: Journal of Shellfish Research, v. 27, no. 5, p. 1163–1169. [Also available at https://doi.org/10.2983/0730-8000-27.5.1163.]

Hofmann, E.E., Powell, E.N., Klinck, J.M., and Wilson, E.A., 1992, Modeling oyster populations. III. Critical feeding periods, growth and reproduction: Journal of Shellfish Research, v. 11, no. 2, p. 399–416.

Johnson, B.H., Kim, K.W., Heath, R.E., Hsieh, B.B., and Butler, H.L., 1993, Validation of a three-dimensional hydrodynamic model of Chesapeake Bay: Journal of Hydraulic Engineering, v. 119, no. 1, p. 2–20. [Also available at https://doi.org/10.1061/(ASCE)0733-9429(1993)119:1(2).]

Kennedy, V.S., 1996, The ecological role of the eastern oyster, *Crassostrea virginica*, with remarks on disease: Journal of Shellfish Research, v. 15, p. 177–183.

Kim, S.C., 2013, Evaluation of a three-dimensional hydrodynamic model applied to Chesapeake Bay through long-term simulation of transport processes: Journal of the American Water Resources Association, v. 49, no. 5, p. 1078–1090. [Also available at https://doi.org/10.1111/jawr.12113.]

Klinck, J.M., Powell, E.N., Hofmann, E.E., Wilson, E.A., and Ray, S.M., 1992, Modeling oyster populations—The effect of density and food supply on production: Proceedings of Advanced Marine Technology Conference 5, p. 85–105.

La Peyre, M.K., Eberline, B.S., Soniat, T.M., and La Peyre, J.F., 2013, Differences in extreme low salinity timing and duration differentially affect eastern oyster (*Crassostrea virginica*) size class growth and mortality in Breton Sound, LA: Estuarine, Coastal and Shelf Science, v. 135, p. 146–157. [Also available at https://doi.org/10.1016/j.ecss.2013.10.001.]

La Peyre, M.K., Gossman, B., and LaPeyre, J.F., 2009, Defining optimal freshwater flow for oyster production—Effects of freshet rate and magnitude of change and duration on eastern oysters and *Perkinsus marinus* infection: Estuaries and Coasts, v. 32, no. 3, p. 522–534. [Also available at https://doi.org/10.1007/s12237-009-9149-9.]

La Peyre, M.K., Serra, K., Joyner, T.A., and Humphries, A., 2015, Assessing shoreline exposure and oyster habitat suitability maximizes potential success for sustainable shoreline protection using restored oyster reefs: PeerJ, v. 3, p. e1317. [Also available at https://doi.org/10.7717/peerj.1317.]

Lavaud, R., La Peyre, M.K., Casas, S.M., Bacher, C., and La Peyre, J.F., 2017, Integrating the effects of salinity on the physiology of the eastern oyster, *Crassostrea virginica*, in the northern Gulf of Mexico through a Dynamic Energy Budget model: Ecological Modelling, v. 363, no. 10, p. 221–233. [Also available at https://doi.org/10.1016/j.ecolmodel.2017.09.003.]

Lenihan, H.S., Peterson, C.H., and Allen, J.M., 1996, Does flow speed also have a direct effect on growth of active suspension-feeders—An experimental test on oyster: Limnology and Oceanography, v. 41, no. 6, p. 1359–1366. [Also available at https://doi.org/10.4319/lo.1996.41.6.1359.]

Leonhardt, J.M., Casas, S., Supan, J.E., and La Peyre, J.F., 2017, Stock assessment for eastern oyster seed production and field grow-out in Louisiana: Aquaculture (Amsterdam, Netherlands), v. 466, p. 9–19. [Also available at https://doi.org/10.1016/j.aquaculture.2016.09.034.]

Linhoss, A.C., Camacho, R., and Ashby, S., 2016, Oyster habitat suitability in the Northern Gulf of Mexico: Journal of Shellfish Research, v. 35, no. 4, p. 841–849. [Also available at https://doi.org/10.2983/035.035.0412.]

Livingston, R.J., Lewis, F.G., Woodsum, G.C., Niu, X.F., Galperin, B., Huang, W., Christensen, J.D., Monaco, M.E., Battista, T.A., Klein, C.J., Howell, R.L., IV, and Ray, G.L., 2000, Modeling oyster population response to variation in freshwater input: Estuarine, Coastal and Shelf Science, v. 50, no. 5, p. 655–672. [Also available at https://doi.org/10.1006/ecss.1999.0597.]

Lowe, M.R., Sehlinger, T., Soniat, T.M., and La Peyre, M.K., 2017, Interactive effects of water temperature and salinity on growth and mortality of eastern oysters, *Crassostrea virginica*—A meta-analysis using 40 years of monitoring data: Journal of Shellfish Research, v. 36, no. 3, p. 683–697. [Also available at https://doi.org/10.2983/035.036.0318.]

Mickey, R.C., Godsey, E., Dalyander, P.S., Gonzalez, V., Jenkins, R.L., III, Long, J.W., Thompson, D.M., and Plant, N.G., 2020, Application of decadal modeling approach to forecast barrier island evolution, Dauphin Island, Alabama: U.S. Geological Survey Open-File Report 2020–1001, 45 p., https://doi.org/10.3133/ofr20201001.

Miller, L.S., La Peyre, J., and La Peyre, M., 2017, Suitability of oyster restoration sites along the Louisiana Coast—Examining site and stock × site interaction: Journal of Shellfish Research, v. 36, no. 2, p. 341–351. [Also available at https://doi.org/10.2983/035.036.0206.]

Patterson, H.K., Boettcher, A., and Carmichael, R.H., 2014, Biomarkers of dissolved oxygen stress in oysters—A tool for restoration and management efforts: PLoS One, v. 9, no. 8, p. e104440. [Also available at https://doi.org/10.1371/journal.pone.0104440.]

Pollack, J.B., Cleveland, A., Palmer, T.A., Reisinger, A.S., and Montagna, P.A., 2012, A restoration suitability index model for the eastern oyster (*Crassostrea virginica*) in the Mission-Aransas Estuary, TX, USA: PLoS One, v. 7, no. 7, p. e40839. [Also available at https://doi.org/10.1371/journal.pone.0040839.]

Powell, E.N., Hofmann, E.E., Klinck, J.M., and Ray, S.M., 1992, Modeling oyster populations. I. A commentary on filtration rate. Is faster always better?: Journal of Shellfish Research, v. 11, no. 2, p. 387–398.

Scyphers, S.B., Powers, S.P., Heck, K.L., Jr., and Byron, D., 2011, Oyster reefs as natural breakwaters mitigate shoreline loss and facilitate fisheries: PLoS One, v. 6, no. 8, p. e22396. [Also available at https://doi.org/10.1371/journal.pone.0022396.]

Sehlinger, T., Lowe, M.R., La Peyre, M.K., and Soniat, T.M., 2019, Differential effects of temperature and salinity on growth and mortality of oysters (*Crassostrea virginica*) in Barataria Bay and Breton Sound, Louisiana: Journal of Shellfish Research, v. 38, no. 2, p. 317–326. [Also available at https://doi.org/10.2983/035.038.0212.]

Sharma, S., Goff, J., Moody, R.M., Byron, D., Heck, K.L., Jr., Powers, S.P., Ferraro, C., and Cebrian, J., 2016, Do restored oyster reefs benefit seagrasses? An experimental study in the Northern Gulf of Mexico: Restoration Ecology, v. 24, no. 3, p. 306–313. [Also available at https://doi.org/10.1111/rec.12329.]

Shumway, S.E., 1996, Natural environmental factors, *in* Kennedy, V.S., Newell, R.I.E., and Eble, A.F., eds., The Eastern Oyster *Crassostrea virginica*: College Park, Maryland Sea Grant College, p. 467–513.

Soniat, T.M., and Brody, M.S., 1988, Field validation of a habitat suitability index model for the American oyster: Estuaries, v. 11, no. 2, p. 87–95. [Also available at https://doi.org/10.2307/1351995.]

Soniat, T.M., Conzelmann, C.P., Byrd, J.D., Roszell, D.P., Bridevaux, J.L., Suir, K.J., and Colley, S.B., 2013, Predicting the effects of proposed Mississippi River diversions on oyster habitat quality—Application of an oyster habitat suitability index model: Journal of Shellfish Research, v. 32, no. 3, p. 629–638. [Also available at https://doi.org/10.2983/035.032.0302.]

Stanley, J.G., and Sellers, M.A., 1986, Species profiles—Life histories and environmental requirements of coastal fishes and invertebrates (Gulf of Mexico)—Eastern oyster: Slidell, La., National Wetlands Research Center, Biological Report no. 82 (11.64), 27 p.

Theuerkauf, S.J., and Lipcius, R.N., 2016, Quantitative validation of a habitat suitability index for oyster restoration: Frontiers in Marine Science, v. 3, no. 64, 9 p. [Also available at https://doi.org/10.3389/fmars.2016.00064.]

Wallace, R.K., Heck, K., and Van Hoose, M., 1999, Oyster restoration in Alabama, chap. 6 *of* Luckenbach, M.W., Mann, R., and Wesson, J.A. (eds.), Oyster reef habitat restoration—A synopsis and synthesis of approaches, Williamsburg, Va., April 1995, Symposium proceedings: Virginia Institute of Marine Science, College of William and Mary, 373 p.

Wang, H., Chen, Q., La Peyre, M.K., Hu, K., and LaPeyre, J.F., 2017, Predicting the impacts of Mississippi River diversions and sea-level rise on spatial patterns of eastern oyster growth rate and production: Ecological Modelling, v. 352, p. 40–53. [Also available at https://doi.org/10.1016/j.ecolmodel.2017.02.028.]

Wang, H., Enwright, N.M., Soniat, T., Hermann, J., LaPeyre, M.K., Kim, S.-C., Bunch, B., Stelly, S., Dalyander, S., and Mickey, R.C., 2020, Oyster habitat suitability modeling for the Alabama Barrier Island restoration assessment at Dauphin Island: U.S. Geological Survey data release, https://doi.org/10.5066/P9O30XMZ.

Wang, H., Huang, W., Harwell, M.A., Edmiston, L., Johnson, E., Hsieh, P., Milla, K., Christensen, J., Stewart, J., and Liu, X., 2008, Modeling oyster growth rate by coupling oyster population and hydrodynamic models for Apalachicola Bay, Florida, USA: Ecological Modelling, v. 211, no. 1–2, p. 77–89. [Also available at https://doi.org/10.1016/j.ecolmodel.2007.08.018.]

Webb, B.M., Douglass, S.L., Dixon, C.R., and Buhring, B., 2011, Application of coastal engineering principles in response to the Deepwater Horizon disaster—Lessons learned in coastal Alabama: Coastal Engineering Practice, v. 2011, p. 359–372. [Also available at https://doi.org/10.1061/41190(422)30.]

Chapter C. Seagrass Habitat Suitability Modeling for the Alabama Barrier Island Restoration Feasibility Assessment at Dauphin Island

By Hongqing Wang,[1] Nicholas M. Enwright,[1] Kelly M. Darnell,[2] Megan K. La Peyre,[1,3] Just Cebrian,[4] Sung-Chan Kim,[5] Barry Bunch,[5] Spencer J. Stelly,[6] Brady R. Couvillion,[1] P. Soupy Dalyander,[1] Rangley C. Mickey,[1] and Martha Segura[7]

Abstract

Seagrass beds provide critical ecosystem services, such as structural habitat, foraging sites for finfish and shellfish, improvement of water quality, blue carbon sequestration, sediment stabilization, and reduction of coastal erosion. Seagrass beds near barrier islands are particularly vulnerable to natural and anthropogenic disturbances and are easily affected by tidal, wind, and wave energy and overwash because of their location along the leeward side of dynamic barrier islands. The sensitive nature of these seagrass beds makes it critical to understand how a specific barrier island restoration effort may positively or negatively affect the preservation of these resources. In this study, a spatially explicit seagrass habitat suitability index model was developed for estuarine waters near Dauphin Island, Alabama. This model was used to assess how habitat suitability for seagrass changes following two potential future storminess and sea-level change scenarios and a variety of restoration measures including beach and dune restoration, marsh restoration, placement of sand in the littoral zone, and a no-action alternative. The habitat suitability index model was calibrated and validated using available in situ seagrass monitoring data and continuous water quality data. Model results indicated the areal coverage of the suitable class increased more than 12 percent, most notably, in areas behind beach/dune restoration at Katrina Cut. The reason for this increase is because of the restoration preventing breaching near Katrina Cut under future conditions with moderate storminess. Barrier island restoration measures that did not prevent breaching generally did not affect the seagrass overall habitat suitability and distribution relative to a no-action alternative. Information from the seagrass habitat suitability modeling results can be combined with information on island geomorphology and associated various subaerial habitats, such as intertidal marsh, beach, and dunes, to gauge the collective benefits and tradeoffs of the various restoration actions being considered for Dauphin Island. This information can help land managers achieve the goal of holistic coastal restoration by improving barrier island geomorphology for resilience and also enhancing the habitat suitability for seagrass.

Introduction

Seagrass beds in marine and estuarine environments provide critical ecosystem services, such as the provision of structural habitat and foraging area for finfish and shellfish, improvement of water quality by adding oxygen to the water column and filtering nutrients and contaminants, sediment stabilization, and the reduction of coastal erosion through accumulating fine particle sediment and attenuating waves and current energy (Koch, 2001; Millet and others, 2010). The spatial extent of seagrass coverage along the northern Gulf of Mexico, including barrier islands within the Mississippi Sound region, has declined substantially in recent years (Pham and others, 2014). For example, along the Petit Bois Island (not shown) in the Mississippi Sound, seagrass spatial extent declined from 650 hectares (ha) in 1969 to 219 ha in 2010, a reduction of greater than (>) 66 percent (Pham and others, 2014). The large decline in seagrass habitat is largely attributed to natural disturbances (for example, hurricanes, tropical storms, rising sea levels, changes in rainfall pattern, and freshwater inflow) and human activities (for example, land

[1]U.S. Geological Survey.

[2]The University of Southern Mississippi.

[3]Louisiana Fish and Wildlife Cooperative Research Unit.

[4]Mississippi State University.

[5]U.S. Army Corps of Engineers.

[6]Stelly Consulting at the U.S. Geological Survey.

[7]National Park Service.

development, freshwater and sediment management). Seagrass beds in estuarine waters near barrier islands are particularly vulnerable to these natural and anthropogenic disturbances because they are located on the lee side of dynamic barrier islands and they are easily affected by tidal, wind, and wave energy. Seagrass species often lack traits to quickly colonize previously occupied areas; therefore, once impacted, it is likely to take a long time (for example, >3 years) for seagrass habitats to recover via natural processes (Bell and others, 2008). Also, the success rate of restoration of seagrass habitats relative to reference conditions is highly variable and often low. Researchers have determined that about 50 percent of seagrass restoration projects have failed to meet success criteria (for example, the survival rate of planting and growth rate of bottom coverage) because the reestablishment of seagrass beds tends to work the best in areas that were previously occupied by seagrass (Fonseca and Bell, 1998; Bell and others, 2008). Therefore, natural resource managers should take the slow recovery of seagrass habitat into account when planning, designing, and implementing barrier island restoration projects.

Habitat suitability index (HSI) models can be used as a screening or risk assessment tool by coastal restoration and resource managers to efficiently manage restoration activities to achieve barrier island restoration, reduction in degradation, and enhancement of habitat suitability for critical estuarine and marine species. Nevertheless, there are few HSI models that address habitat changes of wetland, estuarine, and marine species including seagrass near barrier islands.

Purpose and Scope

The objectives of this study were to (1) develop a spatially explicit HSI model for seagrass in the estuarine waters near Dauphin Island, Alabama, by using literature to establish an initial model; (2) refine the model by using site-specific biological and water quality data to calibrate and validate the HSI model; and (3) use the model to assess how habitat suitability for seagrass changes for two potential future storminess (decadal-scale variation in storm frequency and intensity) and sea-level scenarios and a variety of restoration actions including beach and dune restoration, marsh restoration, placement of sand in the littoral zone or nearshore, and the no-action alternative. Habitat suitability model results could help restoration and resources managers make ecosystem-based decisions to achieve the goal of enhancing barrier island resiliency through improving ecological functions and seagrass habitat. This model could be modified to predict seagrass habitat suitability for other estuaries and bays near barrier islands.

Methods

Study Area

The study area is mainly the shallow water areas with depths less than (<) 2.5 meters (m) near Dauphin Island and Mobile Bay, Ala. (fig. C1). The focus area for this effort is the estuarine waters of the Mississippi Sound on the north (or back-barrier side) of Dauphin Island, where seagrass beds are historically found in abundance (Pham and others, 2014; Vittor and Associates, Inc., 2015). Shallow waters to the south of Dauphin Island facing the northern Gulf of Mexico are unsuitable for seagrass bed development because of their exposure to high wave energy. Tides in this area are diurnal with mean tidal amplitude of 0.4 m and with salinity varying from 20 to 27 parts per thousand (ppt; Sharma and others, 2016).

Model Development

Along the Mississippi Sound and coastal Alabama, *Halodule wrightii* (shoal grass) is an opportunistic mesohaline to polyhaline species of seagrass (Hall and others, 2006). This species is the dominant species (>62 percent) of seagrass communities in this area because of its rapid growth and tolerance to a wide range of salinity (Eleuterius, 1989; Dunton, 1994; Vittor and Associates, Inc., 2004; Pham and others, 2014). *H. wrightii* was found to be an early successional pioneer species that can occupy areas recently disturbed or areas with a fluctuating physical environment (Santos and Lirman, 2012). As a result, *H. wrightii* was the species chosen on which to focus the HSI model. This was done by linking the biological and ecological characteristics (percent coverage, aboveground biomass, and height) of this species to environmental factors. Previous studies found that *H. wrightii* and other seagrass species are highly susceptible to changes in water quality variables (salinity, water depth, and turbidity), geomorphological variables (water depth), and hydrodynamic variables (exposure to wind waves) (Koch, 2001; Santos and Lirman, 2012; Hillmann and others, 2016; Shafer and others, 2016a; La Peyre and others, 2017; DeMarco and others, 2018). These findings were considered for determining estuarine water quality parameters and geomorphological parameters that could be used in the seagrass HSI model developed in this study.

Data Collection

The U.S. Geological Survey (USGS) Louisiana Fish and Wildlife Cooperative Research Unit and Louisiana State University (LSU) Agricultural Center completed seagrass monitoring across the northern Gulf of Mexico during the peak of the growing season in mid-June through early September in 2013, 2014, and 2015 (Hillmann and others, 2016; La Peyre and others, 2017; DeMarco and others,

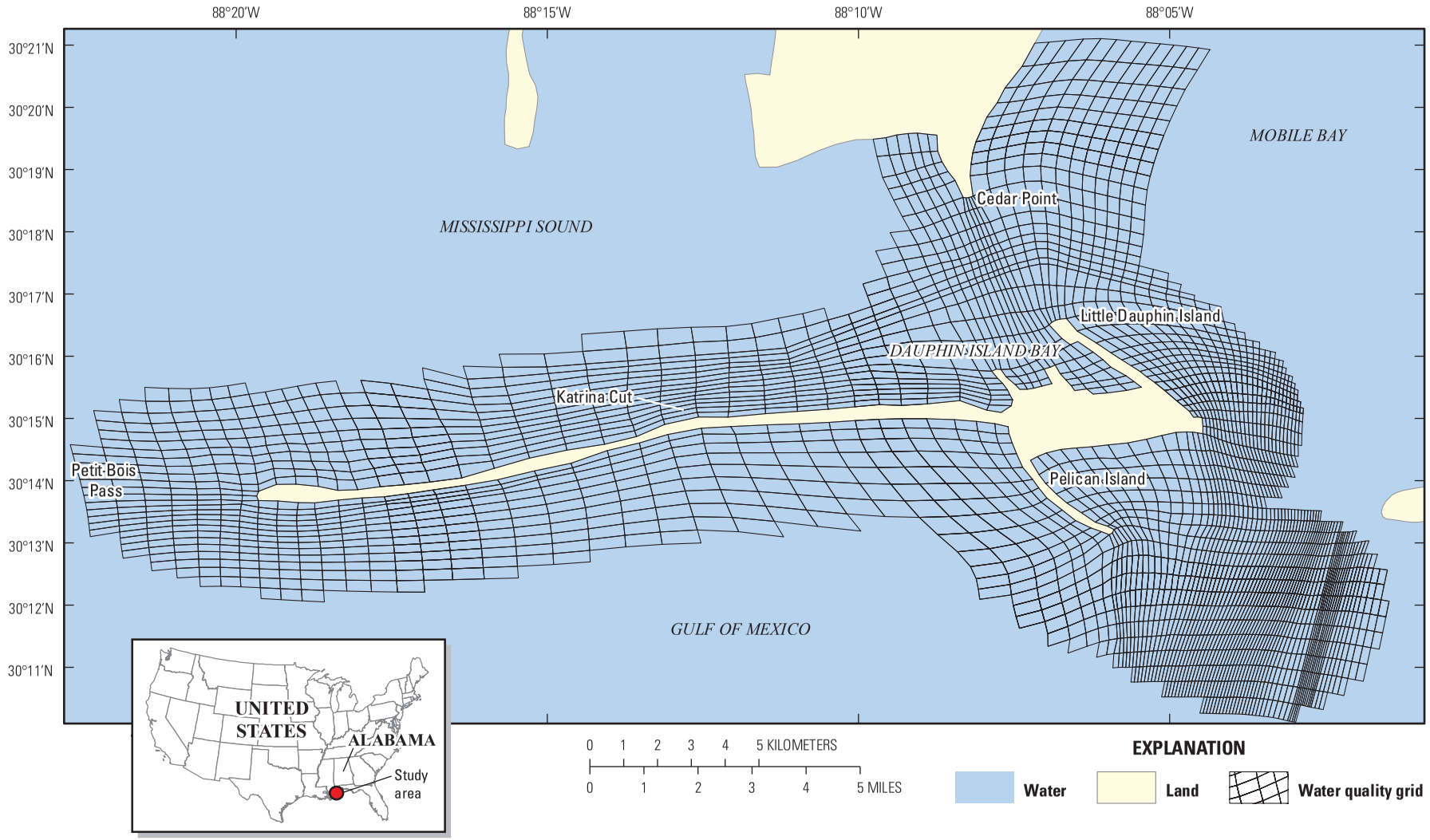

Figure C1. Study area of the seagrass habitat suitability modeling for Dauphin Island, Alabama. Land and water areas are generalized areas from the water quality model grid.

2018). Data were collected at a total of 384 sites (see fig. 1 in Hillmann and others, 2016). This collection included seagrass data on vegetation coverage, aboveground biomass, and discrete water quality (temperature, turbidity, dissolved oxygen [DO], and pH) for 14 submerged aquatic vegetation species including *H. wrightii*. Salinity, temperature, and water depth differed substantially by salinity zones (that is, fresh, intermediate, brackish, and saline) across the northern Gulf of Mexico (Hillmann and others, 2016). The coverage and biomass for *H. wrightii* were used in model development.

From 2011 to 2016, the National Park Service (NPS) Gulf Coast Inventory and Monitoring Network (GULN) conducted long-term seagrass monitoring at 170 permanent stations (https://irma.nps.gov/DataStore/DownloadFile/610650) including locations at four of the islands in the Mississippi-Alabama barrier island chain (Cat Island, Ship Island, Horn Island, and Petit Bois Island). NPS GULN seagrass monitoring data include seagrass metrics (species composition, canopy height, percent coverage) and water quality measures (temperature, pH, DO, salinity, turbidity, chlorophyll *a*, and Secchi depth). These field data for *H. wrightii* were also used in model development and model validation.

Model Parameters and Curve

Variable 1—Mean Salinity during the Summer Growing Season (April–August)

Seagrass peak presence occurs from the spring to summer, and the highest likelihood of seagrass occurrence is during summer months (Visser and others, 2013). Thus, the mean salinity during the summer months (April to August) was used for developing the relation between salinity and the habitat suitability score. The model curve was based on the relation between salinity and seagrass coverage and biomass using salinity observations (range: 9–35 ppt; optimal: 30–33 ppt) from La Peyre and others (2017) and analyzed with in situ seagrass monitoring data from NPS GULN (percent coverage, seagrass height, and water quality) (see "Data Collection") (fig. C2).

Variable 2—Mean Temperature during the Growing Season (April–August)

Previous studies have indicated that temperature affects seagrass growth and survival (Mazzotti and others, 2008) and is most limiting in the winter (Koch, 2001). The temperature-habitat score curve was derived from seagrass coverage, biomass, and temperature data from La Peyre and others (2017). Parameters used included a minimum temperature of 22 degrees Celsius (°C), an optimal range of 28–32 °C, and analyzed with in situ seagrass monitoring data from NPS GULN (percent coverage, seagrass height, and water quality; fig. C3).

Variable 3—Annual Mean Water Depth

Light availability is often determined as one of the main factors controlling the distribution and production of seagrass in shallow systems (Dunton, 1994; Millet and others, 2010). In this study, water depth and total suspended solids (TSS)/turbidity were used as a proxy for light availability because the water quality models that were used for this study do not output light information. Normally, the vertical distribution of seagrass beds is limited by upper (determined by tides and

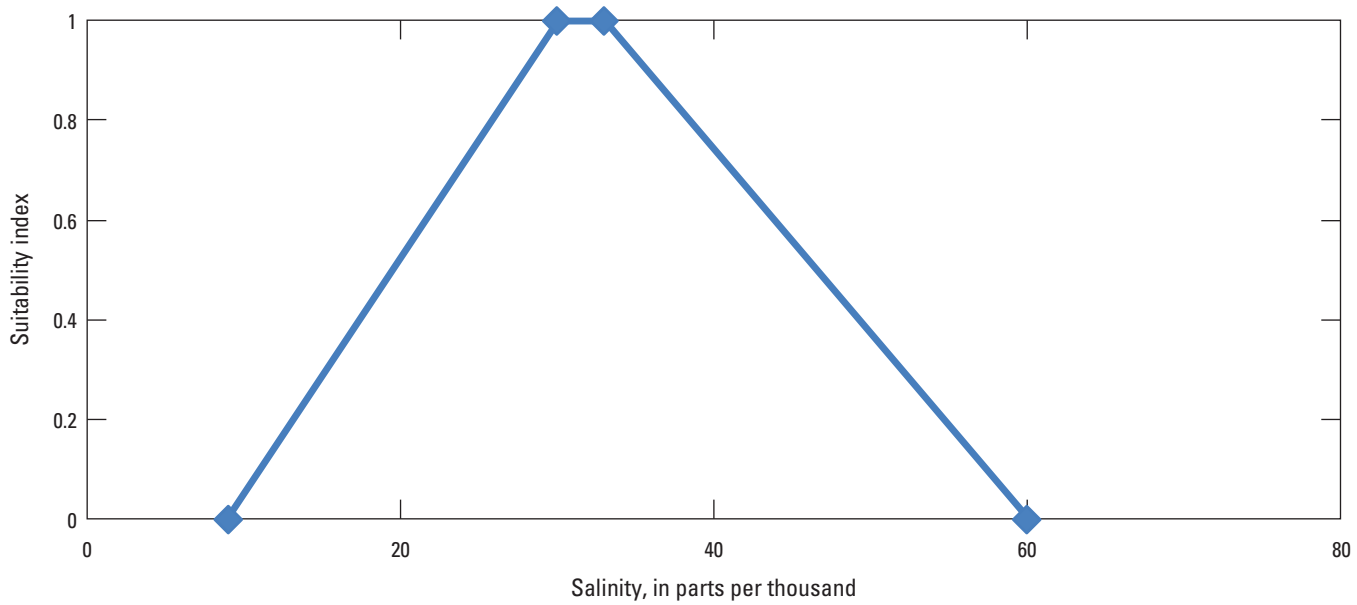

Figure C2. Relation between seagrass habitat suitability index and mean growing season salinity (in parts per thousand) from April to August for Dauphin Island, Alabama.

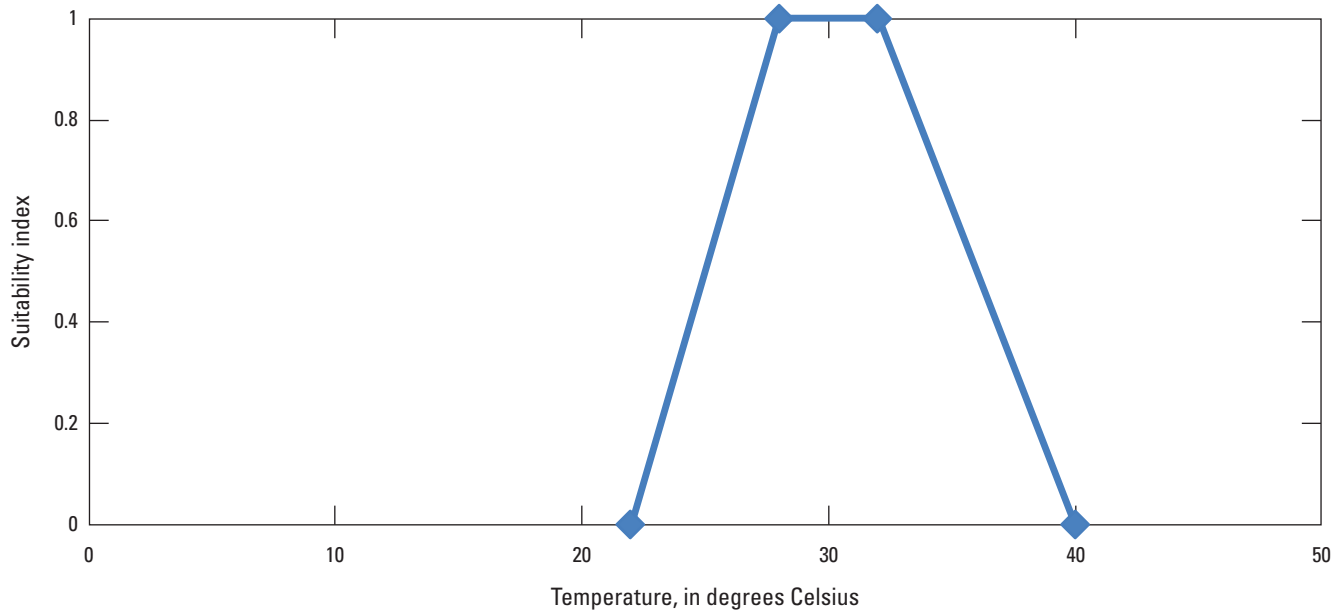

Figure C3. Relation between seagrass habitat suitability index and mean growing season water temperature (in degrees Celsius) from April to August for Dauphin Island, Alabama.

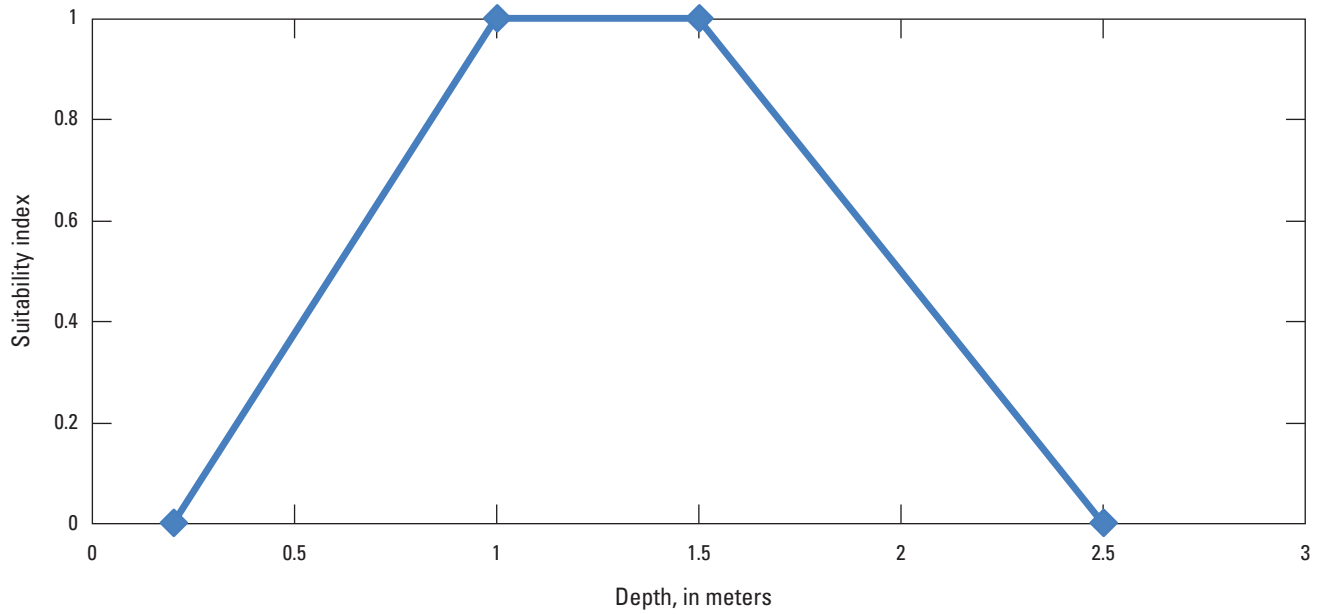

Figure C4. Relation between seagrass habitat suitability index and annual mean water depth (in meters) for Dauphin Island, Alabama.

waves) and lower (determined by light penetration) depths (Koch, 2001). Seagrass coverage and biomass from La Peyre and others (2017) were plotted with water depth, and the curve was then revised based on the coverage and height data from in situ seagrass monitoring data with depth from NPS GULN (fig. C4). The maximum depth was determined to be 2.5 m, with the optimal depth of 1.0 to 1.5 m, based on the observed occurrence of *H. wrightii* with depth near Dauphin Island and previous studies on seagrass along the barrier islands within the Mississippi Sound (Heck and others, 1994).

Variable 4—Mean Total Suspended Solids/Turbidity during the Growing Season (April–August)

Turbidity was used with water depth to indicate the level of light availability. It was found that turbidity could be

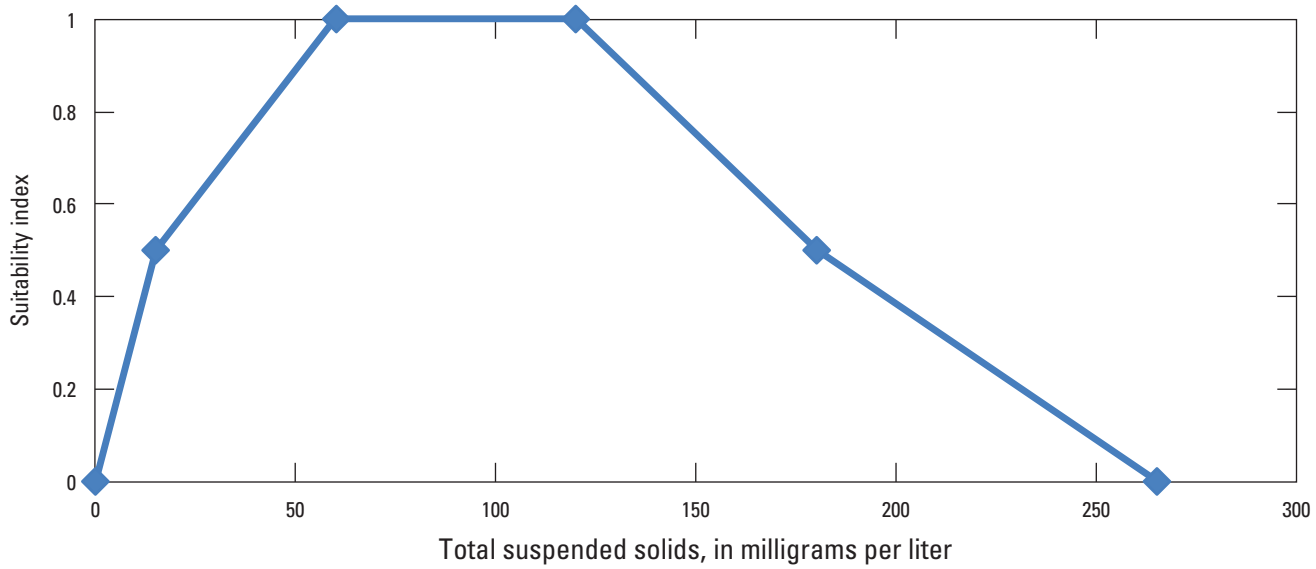

Figure C5. Relation between seagrass habitat suitability index and annual mean total suspended solids (in milligrams per liter) for Dauphin Island, Alabama.

used to supplement light attenuation in determining seagrass response to sedimentation associated with dredging activities (Newell and Koch, 2004; Lawson and others, 2007; Shafer and others, 2016b). An increase in turbidity is associated with reduction in available light, which can lead to a decline in seagrass coverage and density (DeMarco and others, 2018). The TSS/turbidity-habitat curve was developed from seagrass coverage and biomass data during 2013–15 (La Peyre and others, 2017). The optimal TSS concentrations were determined between 60 and 120 milligrams per liter (mg/L) when peak biomasses with large coverage occurred. TSS greater than 265 mg/L would not support seagrass survival and growth (fig. C5).

Variable 5—Exposure to Wind and Waves—Relative Wave Exposure Index

Researchers have found that physical settings of seagrass beds, as measured by the relative (wave) exposure index (REI), along with information on tidal current velocity and water depth, could account for some of the variation in seagrass composition, coverage, shoot density, and belowground biomass (Fonseca and Bell, 1998). Seagrass beds can be forced into deeper waters because of wave exposure from increased wind velocity and reduced light availability from sediment resuspension (Fonseca and Bell, 1998; Koch, 2001; Millet and others, 2010; Carr and others, 2016; DeMarco and others, 2018). Seagrass has generally not been found on the gulf-facing beaches of the island chain in the Mississippi Sound because of high wave energy (Pham and others, 2014). The impact of wind and wave energy on coastal seagrass distribution and growth is rarely incorporated in HSI modeling, but it has been found to be critical and significant in many studies (Newell and Koch, 2004; Cho and Biber, 2016; Saunders and others, 2017; DeMarco and others, 2018). A linear decrease in the probability of seagrass occurrence with exposure was found by DeMarco and others (2018). The relation between REI and seagrass percent coverage for the Dauphin Island area was developed using in situ seagrass monitoring data from NPS GULN. The process followed for this study was used by Fonseca and Bell (1998) to calculate REI. Wind climatology data were acquired from the U.S. Army Corps of Engineers (USACE) Wave Information Studies Gulf of Mexico station 73151. These data were collected at a height of 5 m just south of Dauphin Island from 1980 to 2014. From these data, we extracted the winds that exceeded the 95th percentile wind speed. Next, we calculated the grand mean (that is, mean of monthly means of daily maximum winds) for wind speed for eight vectors from 0 to 360 degrees (°) in 45 ° increments. The equation for REI is as follows:

$$REI = \sum_{i=1}^{8}(V_i \times P_i \times F_i) \quad \text{(C1)}$$

where

i is each of the vectors discussed previously,
V is the grand mean for wind speed in each respective vector,
P is the percentage of frequency that wind occurred in this vector (i), and
F is the effective fetch, in meters.

Fetch is the distance between a point in a water body to a land mass (that is, subaerial land). Effective fetch is calculated by determining fetch in nine 11.25 ° increments for a given vector weighted by the cosine of the angle; for example, the effective fetch for 0 to 45 ° would include weighted fetch

calculations for vectors from 315 to 45 ° in 11.25 ° increments. The use of effective fetch allows for the ability to capture minor irregularities that could be missed by using a single fetch vector for a given zone (that is, 22.5 ° for the vector from 0 to 45 °). To reduce computational complexity, we restricted the REI calculations to estuarine unconsolidated bottom wetlands from the U.S. Fish and Wildlife Service's National Wetlands Inventory data that had water depths less than about 2.5 m.

For the REI for the initial model calibration (fig. C5) and land areas other than Dauphin Island (that is, Petit Bois Island and other islands and mainland areas to the north), water depth was extracted from the 3-m USGS Coastal National Elevation Database (CoNED) topobathymetric digital elevation model (TBDEM; Thatcher and others, 2016) for the northern Gulf of Mexico. This TBDEM includes historical bathymetric and topographic data from various periods between 1917 and 2011. The vertical datum of the CoNED TBDEM was transformed from the North American Vertical Datum of 1988 to local mean sea level based on observations during the most recent North American Tidal Datum Epoch (1983 to 2001) from a National Oceanic and Atmospheric Administration tide gauge (station identifier 8735180) on the eastern end of Dauphin Island. Next, Monte Carlo simulations with 100 iterations were used to develop a probabilistic surface related to an area being subtidal using bathymetric data uncertainty assumptions from Byrnes and others (2002). For more information on this process, see Enwright and others (2019). This probability surface was used to extract nonsubtidal areas (that is, subaerial or land areas for fetch estimation). For modeled outputs including the baseline 2015 geomorphology conditions and various restoration measures under storminess and future sea-level conditions, the subaerial area (that is, intertidal and supratidal/upland areas) for Dauphin Island was extracted from the geomorphic TBDEMs (Mickey and others, 2020) as outlined in the landscape-position habitat model results (chapter A). For future conditions for areas outside the Dauphin Island habitat modeling domain (chapter A), we used the CoNED data, but opted to leave the shorelines static (that is, did not incorporate sea-level rise [SLR]) because these areas were not modeled in our effort. The rationale for this was that we preferred to not make assumptions as to whether or not these areas may keep pace with SLR. In other words, only the Dauphin Island shoreline was dynamic with regard to sea level and storminess. This is a reasonable assumption because we would mainly expect the seagrass impacts related to exposure to be localized to Dauphin Island. The spatial resolution of the REI was 250 m. REI was normalized to range from 0 to 1. The cutoff point of the normalized REI at which seagrass is not present was set at 0.85 based on in situ seagrass monitoring data (fig. C6).

The final total HSI score (HSI_{total}) is based on these five variables. The final score was calculated using the weighted geometric mean method as follows:

$$HSI_{total} = \left(\prod_{i=1}^{n} V_i^{Wi}\right)^{(1/\sum_{i=1}^{n} Wi)} = \exp\left(\frac{\sum_{i=1}^{n} Wi \ln Vi}{\sum_{i=1}^{n} Wi}\right) \quad \text{(C2)}$$

where

V_i is the ith environmental variable,
W_i is the weight of V_i,
n is the number of variables in the total HSI model, and HSI_{total}=0, if any V_i=0.

The calculated suitability index values were classified into the following groups based on Theuerkauf and Lipcius (2016) with modification: HSI_{total} >0.7 is highly suitable; HSI_{total} 0.5–0.7 is suitable; HSI_{total} 0.3–0.5 is marginally suitable; and HSI_{total} <0.3 is unsuitable.

Model Calibration and Validation

Seagrass height, percent coverage, and water quality variables collected at stations on two islands across Mississippi Sound (Horn Island and Petit Bois Island) from the NPS GULN seagrass monitoring data were used for the refinement of the curves derived from the LSU dataset (La Peyre and others, 2017) and modification of variable weights. TSS data were not available in the GULN dataset, so this information was derived from light attenuation at measurement depth using the relation between light attenuation and TSS that was derived from field data collected at Dauphin Island Bridge in summer of 1977 (fig. C7; Crozier and Schroeder, 1978).

During the calibration, which included curve refinement and weight adjustment, the total HSI scores for *H. wrightii* across the 18 LSU sites from 2013 to 2015 were compared with the average percentage of coverage and aboveground biomass to determine the optimal curve and weight for each variable in the model. The values of exposure to wind and waves at 3 of the 18 LSU sites were estimated using the methods described above. The final weights of variables were determined in the order of salinity (5) > depth (4) > wave exposure (3) > temperature (2) > TSS/turbidity (1) based on a literature review, expert opinion, and model calibration.

We used seagrass height and water quality data collected during the summer (August–September) from the NPS GULN stations on two islands in the Mississippi Sound (Cat Island and Ship Island, which were not used in model calibration) during 2011–16 for model validation. The values of exposure to wind and waves at GULN stations were estimated using the methods described above. Seagrass height rather than percent coverage was used in model validation. The rationale for this decision was that once seagrass presence occurs, the growth, biomass, and health measured by height and (or) aboveground biomass should be closely related to habitat quality.

Simulations for Restoration Measures

This Alabama Barrier Island Restoration Feasibility Assessment project included seven potential restoration measures that were incorporated into the simulations of long-term barrier island geomorphology (Mickey and others, 2020;

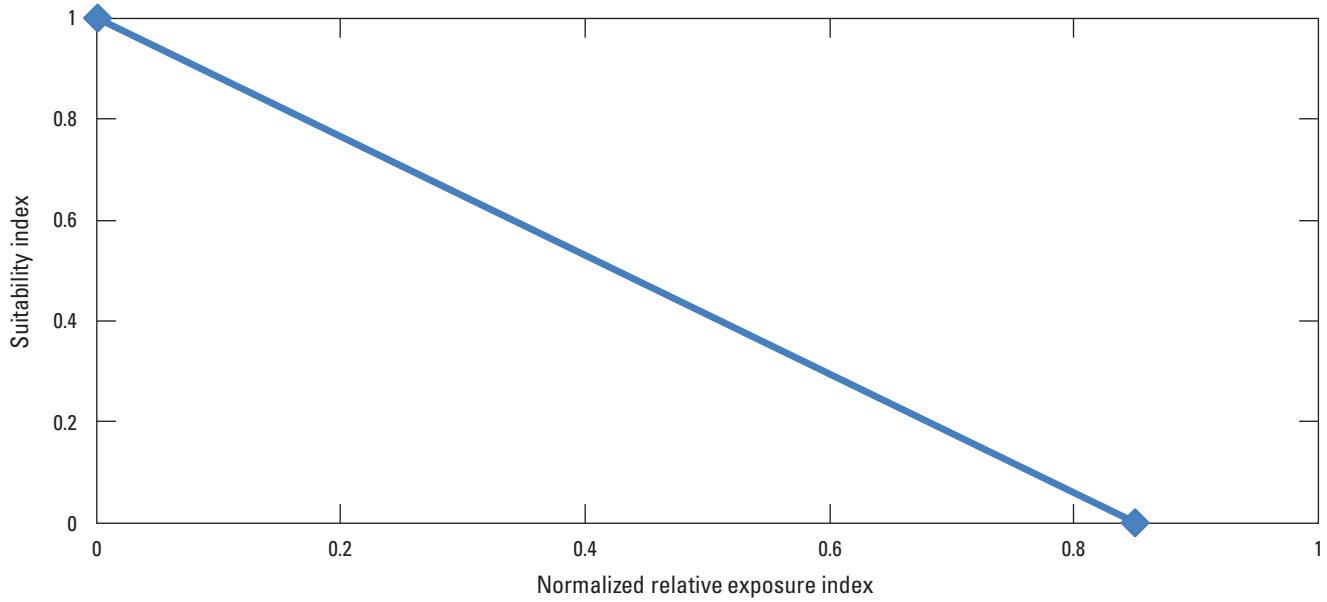

Figure C6. Relation between seagrass habitat suitability index and the normalized relative exposure index for Dauphin Island, Alabama.

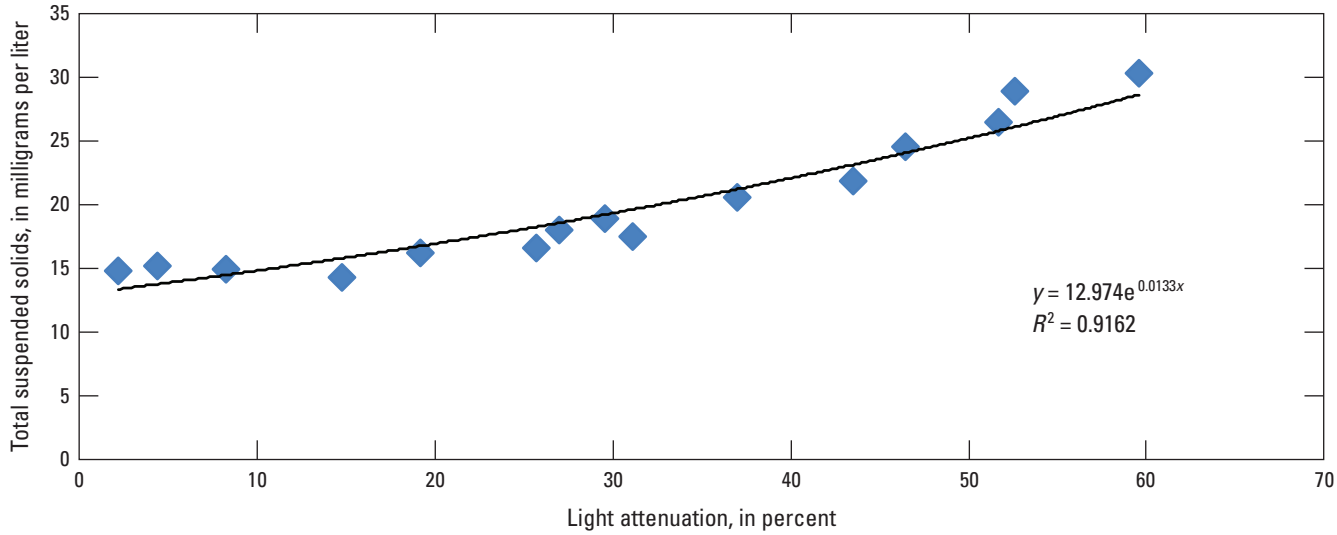

Figure C7. Relation between total suspended solids (in milligrams per liter) and light attenuation (as a percentage) using data from Crozier and Schroeder (1978).

table C1). The evolution of restoration assessments was evaluated over a decadal period and under various future conditions related to storminess and future sea level (Mickey and others, 2020) using the numerical model Delft3D (Mickey and others, 2020), an empirical dune growth model (Mickey and others, 2020), and a landscape-position-based barrier island habitat model (chapter A). To quantify the effects of these restoration measures, changes in habitat suitability classes were compared to a future without action (R0) alternative.

We assessed the impacts of restoration measures under two potential scenarios with regard to storminess and sea level. The storminess bins included realizations with a "medium" storminess, which included one to three storms over a 10-year period (that is, ST2), and a "high" storminess, which included four to five storms over an equal period (that is, ST3). As previously mentioned, we predicted habitats under two future sea levels. These included a sea level of 0.3 m (that is, SL1) and a sea level of about 1.0 m (that is, SL3). Specifically, the medium storminess bin was paired with the 0.3 m sea level (that is, ST2SL1) and the "high" storminess bin was paired with the 1.0 m sea level (that is, ST3SL3). For

Table C1. Restoration measures for the Alabama Barrier Island Restoration Feasibility Assessment project, Dauphin Island, Alabama. For more information see Mickey and others (2020).

[R, restoration measure; km, kilometer; m, meter; ~, approximate value]

Restoration measure	Description
Future without action (R0)	No restoration action.
Katrina Cut structure sand berm (R1)	Sensitivity testing related to the Katrina Cut structure (habitat suitability index modeling was not completed for this measure).
Pelican Island southeast nourishment (R2)	Pelican Island nourishment that extended the island by about 2.6 km to the south of the present tip of Pelican Island.
Sand Island platform nourishment and sand bypassing (R3)	Nourishment of the submerged Sand Island platform that is designed to increase the elevation to 2 m below mean sea level, which is 5 m higher than some current bed-elevation levels in this area.
West and east end beach and dune nourishment (R4)	Nourishment of the beach east of the Katrina Cut and the shorefront area east of Pelican Island to raise beach and dune elevations by a maximum of about 3.7 m.
Back-barrier tidal flats and marsh habitat restoration (R5)	Marsh restoration and filling of burrow pits along the back-barrier area of Dauphin Island.
West end beach and dune nourishment (R6)	Modified version of the R4 measure, which moved the restored dune area landward with no sediment nourishment east of Pelican Island.
West end and Katrina Cut beach and dune nourishment (R7)	Modified version of the R6 measure extends these changes west to the front side of the Katrina Cut rubble wall structure.

more information on how these storminess and sea-level bins were selected, see Mickey and others (2020).

To account for intertidal marsh vertical accretion as a component of marsh morphology evolution, the Dauphin Island landscape-based habitat model (chapter A) determined two situations: the USACE high and intermediate SLR curves. Marsh would keep pace with SLR through accretion (1 centimeter per year) until 2022 under the USACE high SLR curve, whereas marsh would keep pace with SLR by accretion for the entirety of the USACE intermediate SLR curve (chapter A). Therefore, four future storminess and sea-level scenarios were run for seagrass habitat suitability modeling: (1) "medium" storminess and a 0.3-m sea level using the USACE high curve when intertidal marsh did not keep with SLR for much of the SLR curve (ST2SL1H); (2) "medium" storminess and a 0.3-m sea level using the USACE intermediate curve when intertidal marsh largely kept pace with sea level (ST2SL1I); (3) "high" storminess and about a 1.0-m sea level using the USACE high curve when intertidal marsh did not keep with SLR for much of the SLR curve (ST3SL3H); and (4) "high" storminess and about a 1.0-m sea level using the USACE intermediate curve when intertidal marsh largely kept pace with SLR (ST3SL3I). For more information about the storminess scenarios and SLR curves, see Mickey and others (2020) and chapter A, respectively.

Water Quality Model Data

The impacts of the proposed restoration measures on estuarine and marine-water quality near Dauphin Island were simulated by the coupled hydrodynamic and water quality models. The USACE three-dimensional model (Johnson and others, 1993), based on Curvilinear Hydrodynamics in 3 Dimensions—Waterway Experiment Station version (CH3D–WES) has been proven to be a successful management model for the U.S. Environmental Protection Agency Chesapeake Bay Program water quality modeling system (Kim, 2013). The CH3D–WES provides transport to a water quality model, the USACE Integrated Compartment Water Quality Model (CE–QUAL–ICM; Cerco and others, 2013), which has been used to manage the bay's water quality by the Chesapeake Bay Program and, thus, the simulation period spans over decades. The hydrodynamic model, CH3D–WES, computes salinity, surface elevation, velocity, diffusivity, and bottom shear stress. Eutrophication processes are computed by the CE–QUAL–ICM eutrophication model. The CE–QUAL–ICM model in this study incorporates 24 state variables in the water column including physical variables; multiple algal groups; two zooplankton groups; and multiple forms of carbon, nitrogen, phosphorus, and silica. For each variable, we used depth averaged water quality parameters. Because of feasibility limitations, water quality model outputs were not developed for each specific restoration measure. Instead, three general models were developed. The first water quality model included baseline 2015 geomorphology conditions with no island breaching (model name BASE). The second water quality model included SL3 water levels with a single breach west of Katrina Cut. The third water quality model included SL3 water levels and breaching on either side of the Katrina Cut (2BKC).

One challenge was to determine how water quality outputs should be paired with each scenario (that is, combination of restoration measure along with storminess and sea-level conditions). It was hypothesized that geomorphology (that is, if island breaching is present) would be the most sensitive factor when deciding which water quality output to use. In other words, an absence of breaches would lead to the use of the BASE water quality outputs even when assessing habitat suitability for potential realizations with the ST3SL3 conditions. This hypothesis was tested by assessing habitat suitability for ST3SL3 conditions using the BASE and 2BKC water quality outputs. It was noted that the presence of a breach near Katrina Cut for water quality models led to a reduction in suitability in plume-shaped areas extending northward from the "breached" areas into estuarine waters of the Mississippi Sound; thus, it is more important to properly match the breaching scenario compared to the sea-level scenario. The water quality data used for each restoration measure and storminess/sea-level combination are shown in table C2.

Habitat Suitability Index Model Spatial Framework and Processing

The domain of the HSI models generally matches the model domain for the landscape-position-based model (chapter A), which covered a 2.5-km buffer from Dauphin Island. One modification to the HSI domain was the addition of areas near Cedar Point in the northeastern edge of the landscape domain. The spatial resolution of the HSI varies and is matched to the resolution of the water quality model. The area of the cells in this grid ranged from about 1 hectare (ha) in the Mobile River shipping channel to 56 ha in offshore estuarine and marine waters and had a median of 6.7 ha. Esri ArcMap 10.7.1 (Redlands, California) was used to calculate values of each habitat suitability variable (for example, mean growing season salinity and mean growing season water temperature) from water quality model monthly output for cells in the water quality grid for each scenario (table C2). Similar to chapter B, the mean water depth variable was estimated using the geomorphic outputs for each scenario (that is, combination of restoration measure, storminess, and SLR). Landscape-position-based habitat model outputs (chapter A) were used to calculate the mean water depth. This water depth was relative to mean sea level based on observations during the most recent North

Table C2. Restoration measures for the Alabama Barrier Island Restoration Feasibility Assessment project, Dauphin Island, Alabama.

[SL, sea level; Y, year; BASE, baseline water quality model with no breaches; ST2SL1, "medium" storminess bin was paired with the 0.30-meter sea-level rise; ST3SL3, "high" storminess bin was paired with the 1.0-meter sea-level rise; 2BKC, water quality model with sea level of about 1.0 meter and breaching on both sides of Katrina Cut; 1BSAL, water quality model with sea level of 0.96 meter and one breach on the western end of Katrina Cut]

Restoration measure	Storminess/SL	Water quality data			
		Y0 high	Y10 high	Y0 intermediate	Y10 intermediate
Baseline[1]	SL0	BASE	BASE	BASE	BASE
Future without action (R0)	ST2SL1	BASE	BASE	BASE	BASE
	ST3SL3	BASE	2BKC	BASE	2BKC
Pelican Island southeast nourishment (R2)	ST2SL1	BASE	BASE	BASE	BASE
	ST3SL3	BASE	2BKC	BASE	2BKC
Sand Island platform nourishment and sand bypassing (R3)	ST2SL1	BASE	BASE	BASE	BASE
	ST3SL3	BASE	2BKC	BASE	2BKC
West and east end beach and dune nourishment (R4)	ST2SL1	BASE	BASE	BASE	BASE
	ST3SL3	BASE	1BSAL/2BKC	BASE	1BSAL/2BKC
Back-barrier tidal flats and marsh habitat restoration (R5)	ST2SL1	BASE	BASE	BASE	BASE
	ST3SL3	BASE	2BKC	BASE	2BKC
West end beach and dune nourishment (R6)	ST2SL1	BASE	BASE	BASE	BASE
	ST3SL3	BASE	1BSAL/2BKC	BASE	1BSAL/2BKC
West end and Katrina Cut beach and dune nourishment (R7)	ST2SL1	BASE	BASE	BASE	BASE
	ST3SL3	BASE	BASE[2]	BASE	BASE[2]

[1]Sea-level rise curves (that is, high and intermediate) and periods (that is, Y0 and Y10) are not applicable to the baseline condition. The baseline condition used the BASE model and the 2015 geomorphology data.

[2]2BKC was used in the areas where breaching occurred near Little Dauphin Island and Pelican Island.

American Tidal Datum Epoch (1983–2001) from a National Oceanic and Atmospheric Administration tide gauge (station identifier 8735180) on the eastern end of the island. Simulations were run for the initial year (Yr=0) and a period after 10 years (Yr=10) with the corresponding water quality input. A Python script (Python 2.7) was developed to read in the value of each habitat suitability parameter in spatial layers of the habitat suitability variables, calculate the individual suitability index based on the habitat suitability curves (figs. B2–B6) and determine the total HSI using the weighted geometric mean method, classify the suitability scores (0 to 1) into groups, and generate a spatial distribution map of oyster habitat suitability designations (that is, unsuitable, marginally suitable, suitable, and highly suitable).

The water quality grids (table C2) matched general island configurations related to breaching and (or) sea levels. We made a few minor modifications to the grids to enhance the comparability of the HSI outputs. First, we used the BASE grid for all the R7 simulations for the ST3SL3 scenarios, which matched the breaching scenario for Katrina Cut (that is, restoration prevented breaching along Katrina Cut); however, the geomorphology for the BASE grid is not correct for year 10 for Little Dauphin Island and Pelican Island (that is, does not contain breaching that was identified by geomorphic modeling). In order to account for the breaching at Little Dauphin Island and Pelican Island, we used the habitat suitability values that were determined for R0 for the ST3SL3 for year 10 for the missing water quality cells for Little Dauphin Island and Pelican Island. Second, the resolution of cells in each grid may differ, which can cause issues along the boundary of the model domain. For instance, the 2BKC water quality grid has areas where a single cell is made up of two cells. To enhance comparisons between each grid and avoid an issue with missing data, we merged two cells in 2BKC to match the grid registration of BASE for one boundary cell at the north-central portion of the model domain.

Habitat Suitability Index Model Results and Discussion

The following sections will include the results and discussion for the seagrass habitat suitability under baseline conditions and future conditions. Data generated during this study are available from the ScienceBase (Wang and others, 2020).

Seagrass Habitat Suitability Model Validation

There was a significant and positive correlation between habitat suitability score and seagrass height (fig. C8), indicating that the seagrass habitat suitability model is related to habitat quality for seagrass distribution and growth. The low coefficient of determination (R^2; <0.5) is attributed to (1) the uncertainty in the relation between water quality variables and habitat suitability, (2) the lack of other critical biophysical parameters such as substrate type and nutrients (nitrogen and phosphorus) and historical seagrass presence or absence onsite, (3) the lack of a commonly used light availability parameter (for example, photosynthetically active radiation), and (4) variability in the water quality parameters over space and time (Kemp and others, 2004; Zajac and others, 2015; Cho and Biber, 2016).

Seagrass Habitat Suitability Distribution under Baseline Condition

The baseline seagrass suitability distribution (that is, 2015 geomorphology contemporary conditions without SLR) in estuarine waters of Dauphin Island is shown in figure C9. Generally, the estuarine waters on the leeward side of the barrier island with a water depth of <2 m are suitable for seagrass presence, and the suitability is classified as marginal (0.3–0.5). Areas with suitable to highly suitable HSI scores were found in the shallow waters in the middle and northeast of Dauphin Island. Seagrass mapping efforts over the past 15 years have found that seagrass beds were distributed mostly in shallow waters on the leeward side of Dauphin Island and, more specifically, west of Katrina Cut (Vittor and Associates, Inc., 2004, 2005, 2009, 2015), where they were protected from high wind and wave energy of the Gulf of Mexico. For these mapping efforts, there were no seagrass beds found in shallow waters on the high wave energy gulf-facing side of Dauphin Island. Although our HSI model has successfully identified the suitable areas where seagrass has been found over the past 15 years, there were some areas, such as Dauphin Island Bay, Graveline Bay, and Aloe Bay (west of Dauphin Island Bay and north of Dauphin Island), that the model considered to have some level of suitability, yet seagrass has not historically been detected there. Although these areas do have shallow water and are generally sheltered, it is possible that seagrass beds have not thrived here because of the impact of human activities on water quality. These impacts could be potentially associated with a wastewater treatment outflow in the area, which could impact nutrient levels. As a reminder, nutrients were not incorporated in the HSI model. For all scenarios, including the baseline, we did not have any areas with a highly suitable score. We suspect this is related to the previously mentioned limitations to the HSI model related to nutrients. These issues certainly point to room for improvement in the model; however, despite these limitations, the model can still be used to capture the relative impact to seagrass habitat suitability for various restoration measures under future conditions with regard to storminess and sea level.

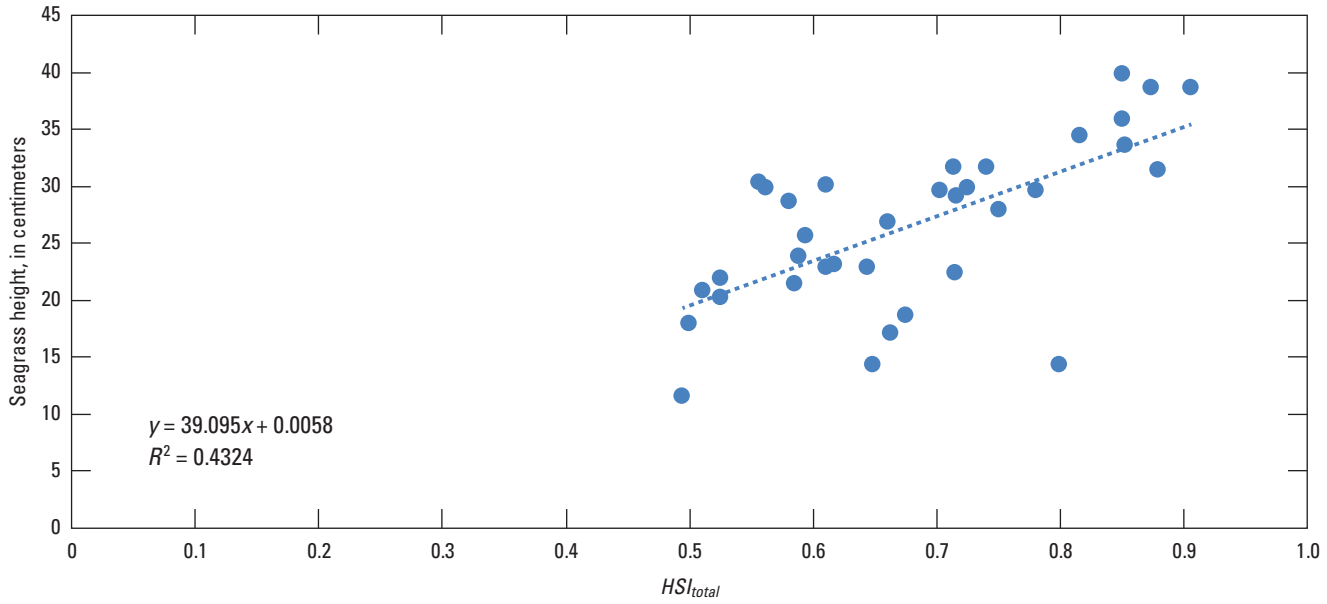

Figure C8. Validation result of the seagrass habitat suitability index model for Dauphin Island, Alabama, using seagrass height data from the National Park Service Gulf Coast Inventory and Monitoring Network.

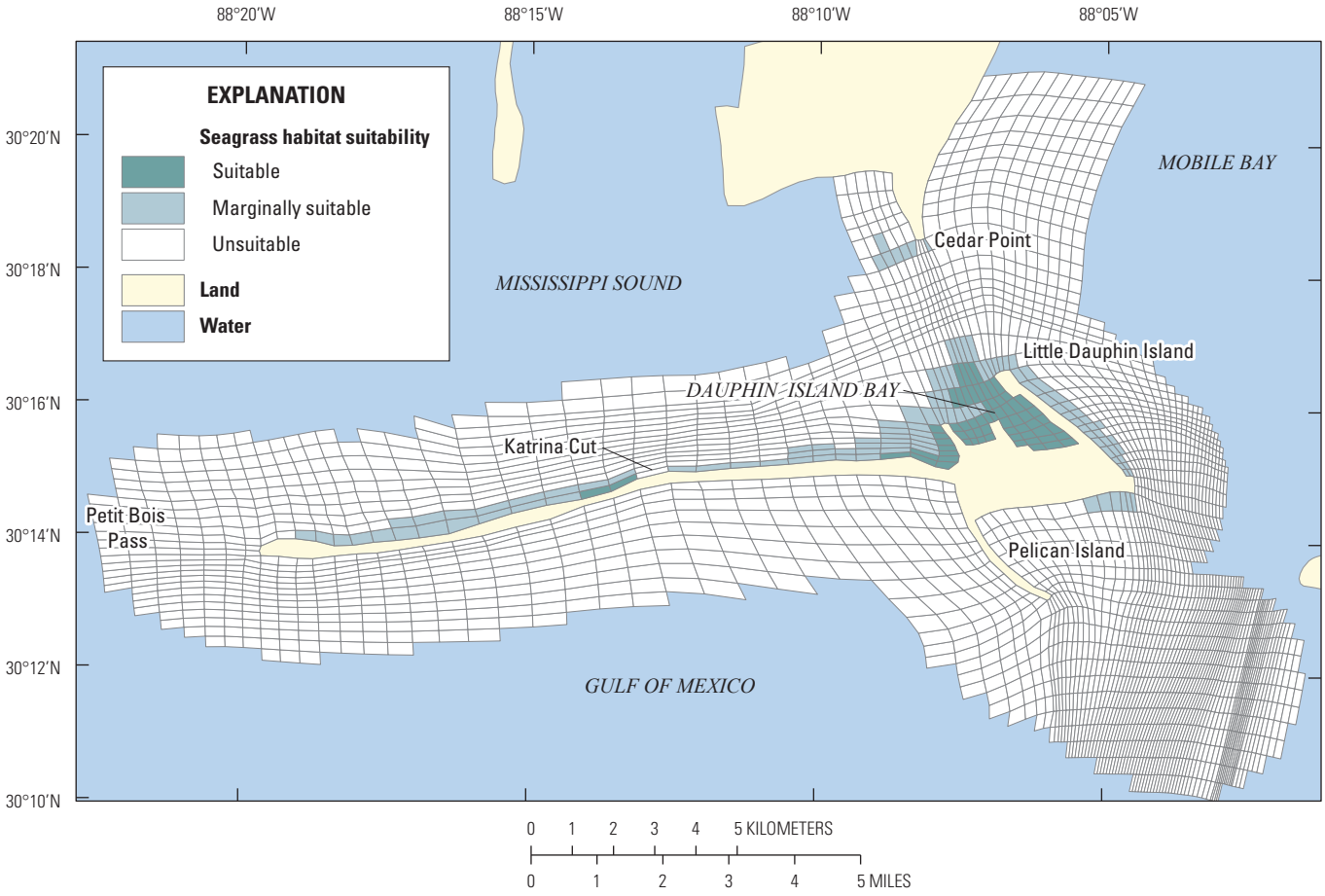

Figure C9. The distribution of seagrass habitat suitability in estuarine waters near Dauphin Island, Alabama, for the baseline model (2015). Land and water areas are generalized areas from the water quality model grid.

Seagrass Habitat Suitability Distribution for Various Restoration Measures, Future Storminess, and Sea-Level Rise

Included in table C3 is a summary of the areal coverage of seagrass HSI bins for the proposed barrier island restoration measures including the future without action conditions (R0) for the previously described storminess, sea level, and SLR rate combinations for year 0 and year 10. These tables also include the percentage change per habitat suitability bin compared to R0. The seagrass HSI distribution under the R0 is shown in figure C10 for year 10 for the ST2SL1 scenario (fig. C10*A*) and for the ST3SL3 scenario (fig. C10*B*) for the high USACE SLR curve. Compared to HSI distribution under the baseline condition (fig. C9), the ST2SL1 scenario would slightly reduce the seagrass suitable areas, but the general pattern and distribution of suitability would not change (fig. C10*A*); however, under the ST3SL3 scenario, the area and pattern in seagrass suitable areas would change dramatically via a reduction and fragmentation of suitable areas (fig. C10*B*). This is likely because of the increased water depth and increased salinity because of island breaching (chapter A). Along those lines, researchers have noted a substantial drop in vegetated seagrass area for Ship Island in the Mississippi Sound after major breaching during Hurricane Camille in 1969 (Pham and others, 2014). The results of this study indicated that breaching in the Katrina Cut area of Dauphin Island would certainly impact local seagrass distribution and growth. The results highlighted in figure C10*B* suggest that, in the absence of restoration, breaching combined with deeper waters associated with SLR would impact the ability for seagrass beds to provide ecosystem services, such as trapping of sediment to maintain barrier island morphology, enhancing habitat for critical fish and other species, and adding blue carbon to the system.

For the initial year simulation, under the ST2SL1 scenario with the high USACE SLR curve for the R0, most of the estuarine waters in this study that are near Dauphin Island (25,291.7 ha, 94.7 percent) are not suitable for seagrass distribution and growth with 1,005.6 ha (3.8 percent) being marginally suitable and 400.1 ha (1.5 percent) being suitable (table C3). With the increase in storminess and sea level (ST3SL3), the area in the unsuitable class increased to 26,107.9 ha (97.8 percent), whereas the marginally suitable and suitable areas decreased to 415.6 ha (1.6 percent) and 173.8 ha (0.7 percent), respectively (table C3). Several restoration measures, including R2, R3, and R4, did not tend to affect the seagrass habitat distribution regardless of the storminess and SLR conditions. The areal change percentages under these restoration measures were close to zero, except for an increase of about 0.2 percent for the suitable class under R4 for the ST3SL3 scenario (table C3). This increase of suitable area with R4 could be attributed to a reduction in breaching (that is, there was only a breach on the western side of Katrina Cut). Small increases (>1 percent) in the areas of marginally suitable and suitable classes can be reached with the R5, R6, and R7 restoration measures for the ST2SL1 scenario (table C3). The most notable increase was for R7 where the suitable area increased by 7.8 percent with ST2SL1 (table C3).

For the initial year under both storminess and sea-level scenarios using the intermediate USACE SLR curve, restoration measures R2 through R6 tended to not affect seagrass habitat suitability. In contrast, R7 increased the area in the suitable class by about 11.0 percent under the ST3SL3 scenario for the intermediate USACE SLR curve. These increases were offset with a slight decline in the marginally suitable class (table C3). It is important to note that these minor increases in suitable areas seem to be attributed to the arbitrary bin breaks and minor changes in input parameters. In other words, this difference is a result of one to two cells changing from marginally suitable to suitable as a result of minor changes in REI and water depth. The net change led to the cell being in another bin, but the magnitude of the change in the HSI score may be negligible. As a result, we suggest that these changes are more related to noise and uncertainty instead of an impact from the restoration measure.

Model simulations indicated that the restoration activities tend to result in positive and negative impacts on seagrass habitat in year 10, depending on the severity of the storminess and the rate of SLR. The area of the suitable class under the ST2SL1 scenario with the USACE high SLR curve tended not to be affected by any of these restoration measures, although there was a slight increase (<0.1 percent) for the unsuitable class and a small decrease (<2.1 percent) in the marginally suitable class (table C3, fig. C11*A–E*). In comparison, R5 had an increase of about 2.8 percent for the marginally suitable area, and a decrease of <0.1-percent area for the unsuitable class (table C3, fig. C11*D*). Finally, R7 had an increase in the marginally suitable areas of about 2.1 percent and an increase in suitable area of more than 12 percent, with a slight decrease in the unsuitable and suitable classes (table C3, fig. C11*F*). The large change associated with R7 is related to breaching conditions. The breaching condition varies under the ST3SL3 condition: R0 and R5 have breaches on either side of Katrina Cut and along Little Dauphin Island and Pelican Island), R4 and R6 have one breach on the west side of Katrina Cut and along Little Dauphin Island and Pelican Island, and R7 has no breaching along Katrina Cut but breaches along Little Dauphin Island and Pelican Island. The changes associated with R5 are similar to the changes noted earlier with regard to change of a single cell, are most likely noise, and should not be attributed to the restoration measure.

Similarly, for year 10 using the USACE intermediate SLR curve, R2 and R3 did not affect seagrass habitat under ST2SL1 (table C3). R4, R6, and R7 tended to result in a slight increase (<0.1 percent) in the unsuitable class and a decrease (<2.2 percent) in the marginally suitable class (table C3). R5 could slightly reduce (<2.7 percent) the suitable area while slightly increasing unsuitable and suitable classes (table C3). For the ST3SL3 scenario, R7 increases the area in the marginally suitable class by 5.4 percent and the area in the suitable

Table C3. The areal coverage of seagrass habitat suitability bins under various restoration, storminess, and sea-level conditions and percentage change of these habitat categories compared to baseline conditions for estuarine areas near Dauphin Island, Alabama.

[SL, sea level; ha, hectare; unsuitable, total habitat suitability index score (HSI_{total}) less than 0.3; marginally suitable, HSI_{total} 0.3–0.5; suitable, HSI_{total} 0.5–0.7; highly suitable, HSI_{total} greater than 0.7; USACE, U.S. Army Corps of Engineers; SLR, sea-level rise; R, restoration; ST2SL1, "medium" storminess bin was paired with the 0.30-meter SLR; ST3SL3, "high" storminess bin was paired with the 0.96-meter SLR]

Restoration measure	Storminess/SL	Area (ha)				Percentage change compared to future without action			
		Unsuitable	Marginally suitable	Suitable	Highly suitable	Unsuitable	Marginally suitable	Suitable	Highly suitable
Year 0 with the USACE high SLR curve									
Future without action (R0)	ST2SL1	25,291.7	1,005.6	400.1	0.00	--	--	--	--
	ST3SL3	26,107.9	415.6	173.8	0.00	--	--	--	--
Pelican Island southeast nourishment (R2)	ST2SL1	25,291.7	1,005.6	400.1	0.00	0.00	0.00	0.00	0.00
	ST3SL3	26,107.9	415.6	173.8	0.00	0.00	0.00	0.00	0.00
Sand Island platform nourishment and sand bypassing (R3)	ST2SL1	25,291.7	1,005.6	400.1	0.00	0.00	0.00	0.00	0.00
	ST3SL3	26,107.9	415.6	173.8	0.00	0.00	0.00	0.00	0.00
West and east end beach and dune nourishment (R4)	ST2SL1	25,289.7	1,007.5	400.1	0.00	−0.01	0.19	0.00	0.00
	ST3SL3	26,107.9	415.6	173.8	0.00	0.00	0.00	0.00	0.00
Back-barrier tidal flats and marsh habitat restoration (R5)	ST2SL1	25,267.5	1,018.9	411.0	0.00	−0.10	1.32	2.72	0.00
	ST3SL3	26,094.7	428.9	173.8	0.00	−0.05	3.20	0.00	0.00
West end beach and dune nourishment (R6)	ST2SL1	25,280.9	1,016.4	400.1	0.00	−0.04	1.07	0.00	0.00
	ST3SL3	26,107.9	415.6	173.8	0.00	0.00	0.00	0.00	0.00
West end and Katrina Cut beach and dune nourishment (R7)	ST2SL1	25,280.9	985.3	431.1	0.00	−0.04	−2.02	7.75	0.00
	ST3SL3	26,107.9	415.6	173.8	0.00	0.00	0.00	0.00	0.00
Year 0 with the USACE intermediate SLR curve									
Future without action (R0)	ST2SL1	25,272.1	1,025.1	400.1	0.00	--	--	--	--
	ST3SL3	26,047.3	494.2	155.8	0.00	--	--	--	--
Pelican Island southeast nourishment (R2)	ST2SL1	25,272.1	1,025.1	400.1	0.00	0.00	0.00	0.00	0.00
	ST3SL3	26,047.3	494.2	155.8	0.00	0.00	0.00	0.00	0.00
Sand Island platform nourishment and sand bypassing (R3)	ST2SL1	25,272.1	1,025.1	400.1	0.00	0.00	0.00	0.00	0.00
	ST3SL3	26,047.3	494.2	155.8	0.00	0.00	0.00	0.00	0.00
West and east end beach and dune nourishment (R4)	ST2SL1	25,281.0	1,016.3	400.1	0.00	0.04	−0.86	0.00	0.00
	ST3SL3	26,047.3	494.2	155.8	0.00	0.00	0.00	0.00	0.00
Back-barrier tidal flats and marsh habitat restoration (R5)	ST2SL1	25,272.1	1,025.1	400.1	0.00	0.00	0.00	0.00	0.00
	ST3SL3	26,047.3	494.2	155.8	0.00	0.00	0.00	0.00	0.00
West end beach and dune nourishment (R6)	ST2SL1	25,272.1	1,025.1	400.1	0.00	0.00	0.00	0.00	0.00
	ST3SL3	26,047.3	494.2	155.8	0.00	0.00	0.00	0.00	0.00
West end and Katrina Cut beach and dune nourishment (R7)	ST2SL1	25,282.9	1,014.3	400.1	0.00	0.04	−1.05	0.00	0.00
	ST3SL3	26,047.3	477.1	172.9	0.00	0.00	−3.46	10.98	0.00

Table C3. The areal coverage of seagrass habitat suitability bins under various restoration, storminess, and sea-level conditions and percentage change of these habitat categories compared to baseline conditions for estuarine areas near Dauphin Island, Alabama—Continued.

[SL, sea level; ha, hectare; unsuitable, total habitat suitability index score (HSI_{total}) less than 0.3; marginally suitable, HSI_{total} 0.3–0.5; suitable, HSI_{total} 0.5–0.7; highly suitable, HSI_{total} greater than 0.7; USACE, U.S. Army Corps of Engineers; SLR, sea-level rise; R, restoration; ST2SL1, "medium" storminess bin was paired with the 0.30-meter SLR; ST3SL3, "high" storminess bin was paired with the 0.96-meter SLR]

Restoration measure	Storminess/SL	Area (ha)				Percentage change compared to future without action			
		Unsuitable	Marginally suitable	Suitable	Highly suitable	Unsuitable	Marginally suitable	Suitable	Highly suitable
Year 10 with the USACE high SLR curve									
Future without action (R0)	ST2SL1	25,285.5	1,000.9	411.0	0.00	--	--	--	--
	ST3SL3	26,304.80	482	128.7	0.00	--	--	--	--
Pelican Island southeast nourishment (R2)	ST2SL1	25,280.4	1,006.0	411.0	0.00	−0.02	0.51	0.00	0.00
	ST3SL3	26,310.60	476.2	128.7	0.00	0.02	−1.20	0.00	0.00
Sand Island platform nourishment and sand bypassing (R3)	ST2SL1	25,285.5	1,000.9	411.0	0.00	0.00	0.00	0.00	0.00
	ST3SL3	26,331	455.8	128.7	0.00	0.10	−5.40	0.00	0.00
West and east end beach and dune nourishment (R4)	ST2SL1	25,306.4	980.0	411.0	0.00	0.08	−2.09	0.00	0.00
	ST3SL3	26,314.90	471.9	128.7	0.00	0.04	− 2.10	0.00	0.00
Back-barrier tidal flats and marsh habitat restoration (R5)	ST2SL1	25,272.1	1,014.3	411.0	0.00	−0.05	1.34	0.00	0.00
	ST3SL3	26,291.50	495.3	128.7	0.00	−0.05	2.7	0.00	0.00
West end beach and dune nourishment (R6)	ST2SL1	25,297.6	988.7	411.0	0.00	0.05	−1.22	0.00	0.00
	ST3SL3	26,292.60	497.5	125.4	0.00	− 0.05	3.22	−2.56	0.00
West end and Katrina Cut beach and dune nourishment (R7)	ST2SL1	25,297.6	988.7	411.0	0.00	0.05	−1.22	0.00	0.00
	ST3SL3	26,232.90	492.1	144.6	0.00	−0.27	2.10	12.35	0.00
Year 10 with the USACE intermediate SLR curve									
Future without action (R0)	ST2SL1	25,285.5	1,000.9	411.0	0.00	--	--	--	--
	ST3SL3	26,123.5	567.9	224.2	0.00	--	--	--	--
Pelican Island southeast nourishment (R2)	ST2SL1	25,285.5	1,000.9	411.0	0.00	0.00	0.00	0.00	0.00
	ST3SL3	26,123.5	567.9	224.2	0.00	0.00	0.00	0.00	0.00
Sand Island platform nourishment and sand bypassing (R3)	ST2SL1	25,285.5	1,000.9	411.0	0.00	0.00	0.00	0.00	0.00
	ST3SL3	26,123.5	567.9	224.2	0.00	0.00	0.00	0.00	0.00
West and east end beach and dune nourishment (R4)	ST2SL1	25,307.4	979.0	411.0	0.00	0.09	−2.19	0.00	0.00
	ST3SL3	26,230.0	462.3	223.3	0.00	0.41	−18.59	−0.40	0.00
Back-barrier tidal flats and marsh habitat restoration (R5)	ST2SL1	25,295.2	1,002.0	400.1	0.00	0.04	0.11	−2.65	0.00
	ST3SL3	26,111.2	584.3	220	0.00	−0.05	2.89	−1.87	0.00
West end beach and dune nourishment (R6)	ST2SL1	25,307.4	979.0	411.0	0.00	0.09	−2.19	0.00	0.00
	ST3SL3	26,182.0	509.4	224.2	0.00	0.22	−10.30	0.00	0.00
West end and Katrina Cut beach and dune nourishment (R7)	ST2SL1	25,307.4	979.0	411.0	0.00	0.09	−2.19	0.00	0.00
	ST3SL3	26,162.3	598.4	281.2	0.00	0.15	5.37	25.42	0.00

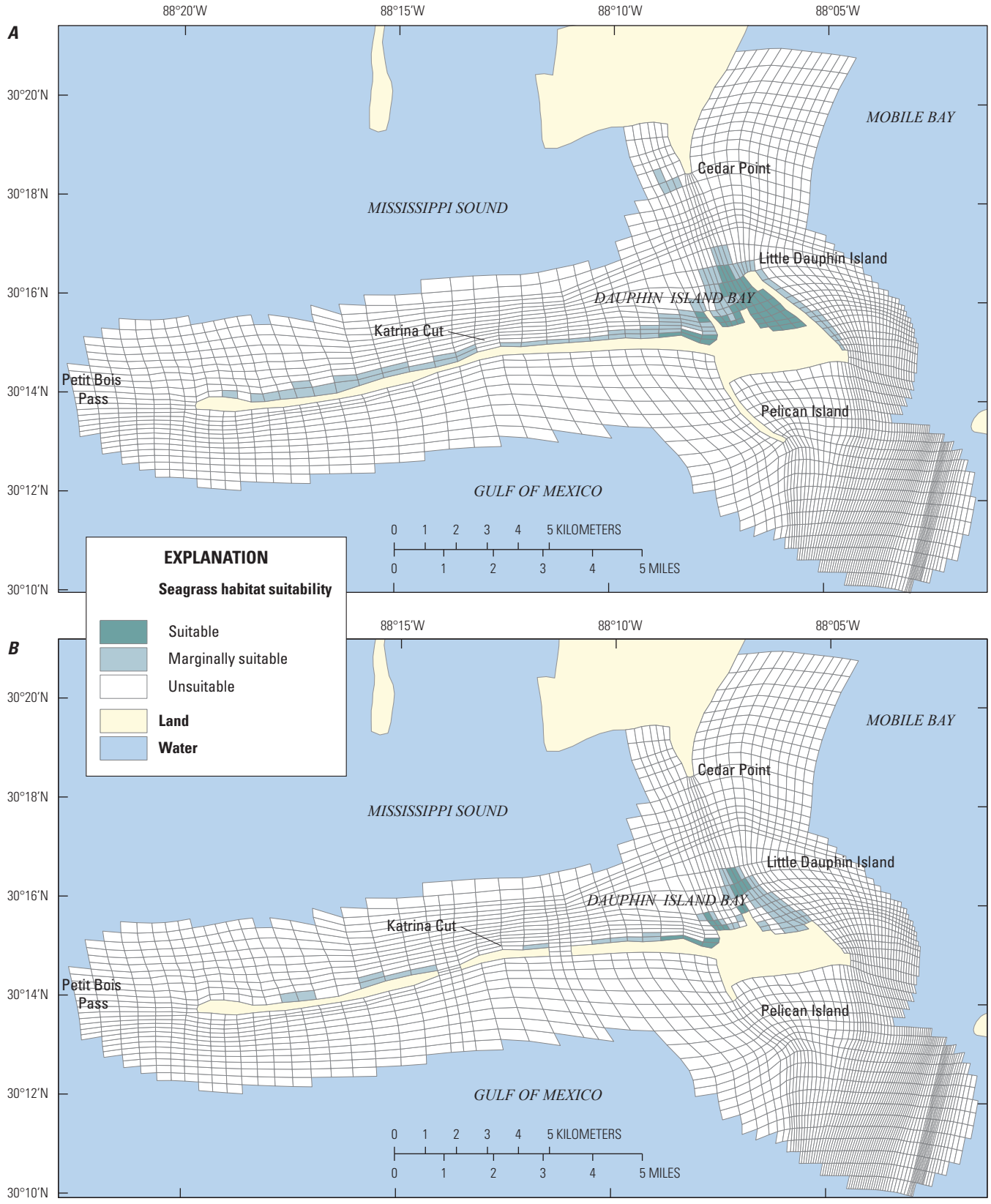

Figure C10. The distribution of the seagrass total habitat suitability index score under the future without action restoration measure (R0) in estuarine waters near Dauphin Island, Alabama, for year 10 using the U.S. Army Corps of Engineers high sea-level rise curve. *A*, with "medium" storminess and sea level (ST2SL1); *B*, with "high" storminess and sea level (ST3SL3). Land and water areas are generalized areas from the water quality model grid.

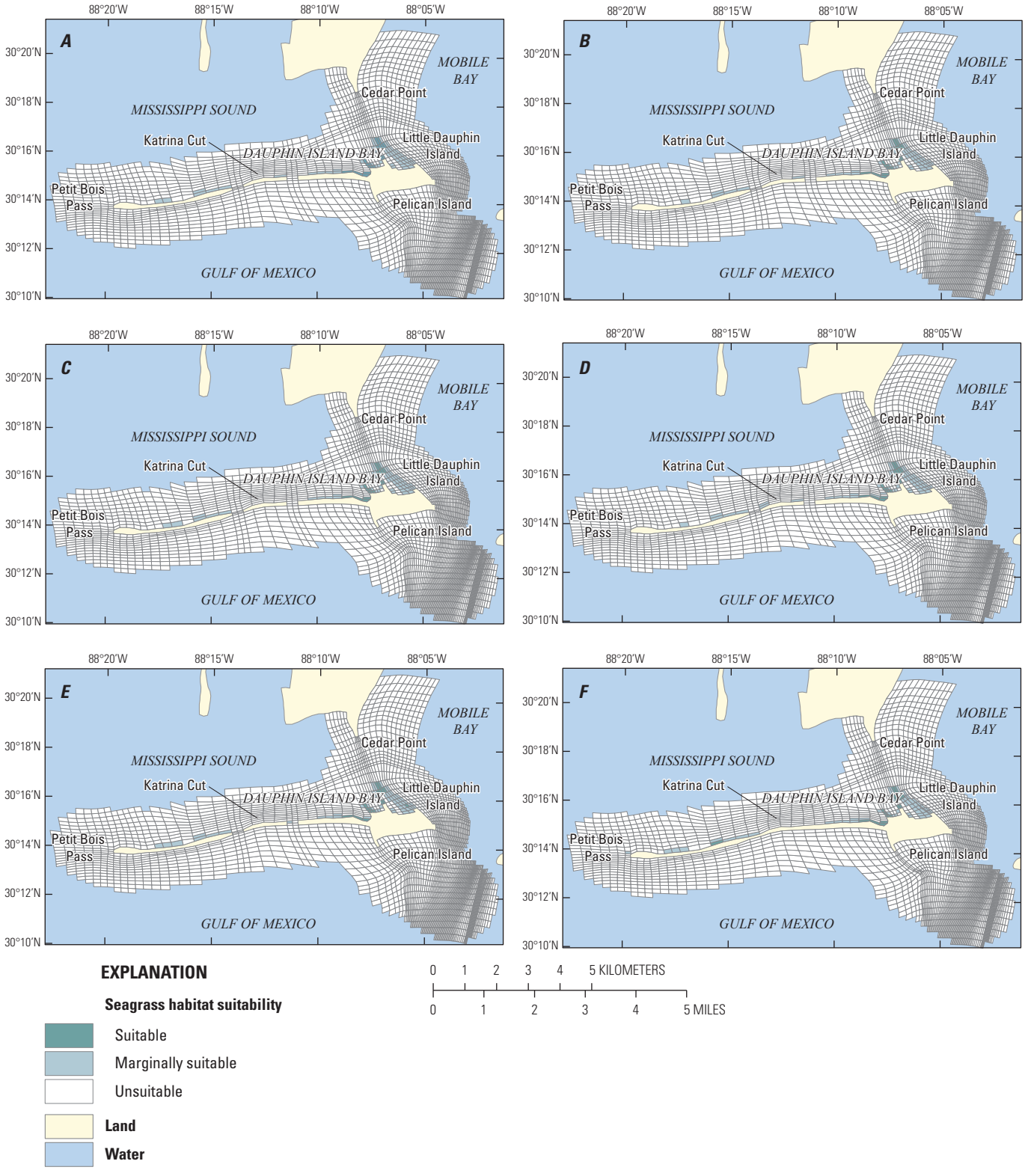

Figure C11. The distribution of seagrass total habitat suitability in Dauphin Island, Alabama, estuarine waters over the 10-year simulation under various restoration actions with high storminess and sea-level rise conditions (ST3SL3) using the U.S. Army Corps of Engineers high sea-level rise curve. *A*, with restoration measure R2; *B*, with restoration measure R3; *C*, with restoration measure R4; *D*, with restoration measure R5; *E*, with restoration measure R6; *F*, with restoration measure R7. Land and water areas are generalized areas from the water quality model grid.

class by 25.4 percent (table C3). Other restoration measures tended to result in decreases in the marginally suitable and suitable classes with no or little change in the unsuitable class. For example, the suitable class tended to reduce by 0.4–1.9 percent with R4 to R6, the marginally suitable class increased by 2.9 percent with R5 and reduced by 10.3–18.6 percent with R4 and R6 compared to the future with no action (table C3). Similar to the results for the USACE high curve, the loss of seagrass suitable areas under these restoration measures could likely be related to breaching. Collectively, these results indicate that, among the studied restoration measures, R7 could lessen the chance of breaching and enhance and preserve seagrass habitat suitability.

Discussion

Salinity, light availability, and other water quality parameters could change significantly at smaller time scales (for example, daily and weekly) as a result of wind, storm events, or human-induced events, such as eutrophication, biotic disturbances, and salinity fluctuation (Millet and others, 2010). If the changes in these critical factors exceed the tolerance of seagrasses, then the vegetation could die off and not recover; for example, high light attenuation may prevent the establishment or maintenance of seagrass beds (Millet and others, 2010). A possible impact from this could be that the habitat suitability values will not detect these episodic and extreme changes because the monthly or annual averages of these variables are used. Therefore, as more data become available, future efforts should explore the development of within-year HSI models (for example, monthly or even weekly) to avoid the missing impacts from short-term, extreme environmental condition change.

Researchers have found that water depth, suspended sediment, phytoplankton biomass, and colored dissolved organic matter affect light availability in shallow estuaries (Ganju and others, 2014; Carr and others, 2016). With more and more nutrient loading into the estuary, eutrophication and algal blooms could affect seagrass beds; thus, water quality variables, such as chlorophyll *a* concentration, may also need to be added to the habitat suitability model along with water depth and TSS to explain the spatial and temporal variability in light availability for seagrass distribution and production. Chlorophyll *a* concentration represents the abundance of phytoplankton in estuaries and is a function of nutrient loading, residence time, advection, grazing by zooplankton, and other factors (for example, Kemp and others, 2004). Another potential issue with this study is that our TSS values were low. This was because of two factors: (1) the organic part was not entirely incorporated; and (2) wind waves were not incorporated in the coupled hydrodynamic and water quality model (Kim, 2013). It was found that wind-driven sediment suspension controls light availability in a shallow coastal lagoon (Newell and Koch, 2004; Lawson and others, 2007); moreover, wave climate, such as significant wave height, was found to be the best predictor of seagrass occurrence and used in seagrass habitat suitability modeling (Saunders and others, 2017; DeMarco and others, 2018). Besides process-driven estuarine water quality models, wind/wave and sediment transport models and simulation results in barrier island regions should be used for future habitat suitability modeling, if they are readily available. For instance, bathymetric data could be combined with the fetch data to provide wave energy information using models such as the National Oceanic and Atmospheric Administration's Wave Exposure Model (Fonseca and Malhotra, 2008).

In the future, mechanistic models that predict seagrass growth and persistence under various environmental conditions and human management are needed to not only know the distribution and abundance of seagrass but also enhance ecosystem services, such as capturing and storing more "blue carbon" (carbon stored and sequestered in coastal ecosystems such as mangrove forests, seagrass meadows, or intertidal saltmarshes) through continuous and persistent growth of seagrass communities (Hillmann and others, 2016; DeMarco and others, 2018). Seagrass mechanistic models use photosynthetically active radiation at short time scales to simulate seagrass growth and respiration with other environmental variables, such as TSS and DO (Dunton, 1994; Millet and others, 2010). Habitat suitability models often do not incorporate the feedback effects of seagrass on physical conditions; for example, the positive feedback effect of seagrass on wave attenuation. Thus, the impact of reduced sediment resuspension on seagrass biomass (Newell and Koch, 2004) was not included in the habitat suitability modeling. Furthermore, the interaction among physical, geological, and geochemical factors that control seagrass distribution and growth cannot be reflected in the habitat suitability model and require coupled process-driven models.

Conclusions

HSI models can assist with the assessment and prediction of the effect of barrier island restoration on seagrass habitat. Among the seven restoration measures assessed, west end and Katrina Cut beach and dune nourishment (R7) seemed to be a major restoration activity that can have a large positive effect on seagrass habitat suitability near Dauphin Island. The positive influence of this restoration action could be attributed to its potential to stop the inflow of high salinity saltwater and lower exposure to wave energy by preventing breaching around Katrina Cut. In general, other barrier island restoration measures did not affect the seagrass overall habitat suitability and distribution. For future efforts, the improvement of this seagrass habitat suitability model would require more field data on seagrass biology and water quality from well-distributed stations along with additional model parameters, such as substrate and nutrients.

References Cited

Bell, S.S., Tewfik, A., Hall, M.O., and Fonseca, M.S., 2008, Evaluation of seagrass planting and monitoring techniques—Implications for assessing restoration success and habitat equivalency: Restoration Ecology, v. 16, no. 3, p. 407–416. [Also available at https://doi.org/10.1111/j.1526-100X.2007.00308.x.]

Byrnes, M.R., Baker, J.L., and Li, F., 2002, Quantifying potential measurement errors and uncertainties associated with bathymetric change analysis: Vicksburg, Miss., U.S. Army Corps of Engineers, ERDC/CHL CHETN–IV–50, 17 p.

Carr, J.A., D'Odorico, P., McGlathery, K.J., and Wiberg, P.L., 2016, Spatially explicit feedbacks between seagrass meadow structure, sediment and light—Habitat suitability for seagrass growth: Advances in Water Resources, v. 93, part B, p. 315–325. [Also available at https://doi.org/10.1016/j.advwatres.2015.09.001.]

Cerco, C.F., Kim, S.C., and Noel, M.R., 2013, Management modeling of suspended solids in the Chesapeake Bay, USA: Estuarine, Coastal and Shelf Science, v. 116, p. 87–98. [Also available at https://doi.org/10.1016/j.ecss.2012.07.009.]

Cho, H.J., and Biber, P.D., 2016, Habitat characterization for submerged and floating-leaved aquatic vegetation in coastal river deltas of Mississippi and Alabama: Southeastern Geographer, v. 56, no. 4, p. 454–472. [Also available at https://doi.org/10.1353/sgo.2016.0046.]

Crozier, G.F., and Schroeder, W.W., 1978, Mobile Bay turbidity study: Dauphin Island, Ala., Marine Environmental Sciences Consortium NASA–CB–150711, 60 p.

DeMarco, K., Couvillion, B., Brown, S., and La Peyre, M., 2018, Submerged aquatic vegetation mapping in coastal Louisiana through development of a spatial likelihood occurrence (SLOO) model: Aquatic Botany, v. 151, p. 87–97. [Also available at https://doi.org/10.1016/j.aquabot.2018.08.007.]

Dunton, K.H., 1994, Seasonal growth and biomass of the subtropical seagrass *Halodule wrightii* in relation to continuous measurements of underwater irradiance: Marine Biology, v. 120, no. 3, p. 479–489. [Also available at https://doi.org/10.1007/BF00680223.]

Eleuterius, L.N., 1989, Catastrophic loss of seagrasses in Mississippi Sound: Proceedings of Tenth Annual Minerals Management Service, USDI, Gulf of Mexico, OCS Region, Information Transfer Meeting, December 6–7, 1989, New Orleans, La.

Enwright, N.M., Wang, L., Wang, H., Osland, M.J., Feher, L.C., Borchert, S.M., and Day, R.H., 2019, Modeling barrier island habitats using landscape position information: Remote Sensing, v. 11, no. 8, 24 p. [Also available at https://doi.org/10.3390/rs11080976.]

Fonseca, M.S., and Bell, S.S., 1998, Influence of physical setting on seagrass landscapes near Beaufort, North Carolina, USA: Marine Ecology Progress Series, v. 171, p. 109–121. [Also available at https://doi.org/10.3354/meps171109.]

Fonseca, M.S., and Malhotra, A., 2008, WEMo (Wave Exposure Model) user manual (version 3.1): Beaufort, N.C., National Oceanic and Atmospheric Administration, National Centers for Coastal Ocean Science, 70 p. [Also available at https://cdn.coastalscience.noaa.gov/page-attachments/products/WEMo/WEMo_V31_manual.pdf.]

Ganju, N.K., Miselis, J.L., and Aretxabaleta, A.L., 2014, Physical and biogeochemical controls on light attenuation in a eutrophic, back-barrier estuary: Biogeosciences, v. 11, no. 24, p. 7193–7205. [Also available at https://doi.org/10.5194/bg-11-7193-2014.]

Hall, L.M., Hanisak, M.D., and Virnstein, R.W., 2006, Fragments of the seagrasses *Halodule wrightii* and *Halophila johnsonii* as potential recruits in Indian River Lagoon, Florida: Marine Ecology Progress Series, v. 310, p. 109–117. [Also available at https://doi.org/10.3354/meps310109.]

Heck, K.L., Sullivan, M.J., and Moncreiff, C.A., 1994, An ecological analysis of seagrass meadows of the Gulf Islands National Seashore, years one and two—National Park Service. Gulf Islands National Seashore, 63 p.

Hillmann, E.R., DeMarco, K., and La Peyre, M.K., 2016, Establishing a baseline of estuarine submerged aquatic vegetation resources across salinity zones within coastal areas of the northern Gulf of Mexico: Journal of the Southeastern Association of Fish and Wildlife Agencies, v. 3, p. 25–32.

Johnson, B.H., Kim, K.W., Heath, R.E., Hsieh, B.B., and Butler, H.L., 1993, Validation of a three-dimensional hydrodynamic model of Chesapeake Bay: Journal of Hydraulic Engineering, v. 119, no. 1, p. 2–20. [Also available at https://doi.org/10.1061/(ASCE)0733-9429(1993)119:1(2).]

Kemp, W.M., Batleson, R., Bergstrom, P., Carter, V., Gallegos, C.L., Hunley, W., Karrh, L., Koch, E.W., Landwehr, J.M., Moore, K.A., Murray, L., Naylor, M., Rybicki, N.B., Stevenson, J.C., and Wilcox, D.J., 2004, Habitat requirements for submerged aquatic vegetation in Chesapeake Bay—Water quality, light regime, and physical-chemical factors: Estuaries, v. 27, no. 3, p. 363–377. [Also available at https://doi.org/10.1007/BF02803529.]

Kim, S.C., 2013, Evaluation of a three-dimensional hydrodynamic model applied to Chesapeake Bay through long-term simulation of transport processes: Journal of the American Water Resources Association, v. 49, no. 5, p. 1078–1090. [Also available at https://doi.org/10.1111/jawr.12113.]

Koch, E.W., 2001, Beyond light—Physical, geological, and geochemical parameters as possible submersed aquatic vegetation habitat requirements: Estuaries, v. 24, no. 1, p. 1–17. [Also available at https://doi.org/10.2307/1352808.]

La Peyre, M., DeMarco, K., and Hillmann, E., 2017, Submerged aquatic vegetation and environmental data for coastal areas from Texas through Alabama, 2013–2015: U.S. Geological Survey data release, accessed September 2018 at https://doi.org/10.5066/F7GH9G44.

Lawson, S.E., Wiberg, P.L., McGlathery, K.J., and Fugate, D.C., 2007, Wind-driven sediment suspension controls light availability in a shallow coastal lagoon: Estuaries and Coasts, v. 30, no. 1, p. 102–112. [Also available at https://doi.org/10.1007/BF02782971.]

Mazzotti, F.J., Pearlstine, L.G., Chamberlain, R.H., Hunt, M.J., Barnes, T., Chartier, K., and DeAngelis, D., 2008, Stressor response model for tape grass (*Vallisneria americana*): University of Florida Circular 1524, 10 p., accessed October 2018 at http://edis.ifas.ufl.edu/pdffiles/UW/UW28100.pdf.

Mickey, R.C., Godsey, E., Dalyander, P.S., Gonzalez, V., Jenkins, R.L., III, Long, J.W., Thompson, D.M., and Plant, N.G., 2020, Application of decadal modeling approach to forecast barrier island evolution, Dauphin Island, Alabama: U.S. Geological Survey Open-File Report 2020–1001, 45 p., https://doi.org/10.3133/ofr20201001.

Millet, B., Robert, C., Grillas, P., Coughlan, C., and Banas, D., 2010, Numerical modelling of vertical suspended solids concentrations and irradiance in a turbid shallow system (Vaccares, Se France): Hydrobiologia, v. 638, no. 1, p. 161–179. [Also available at https://doi.org/10.1007/s10750-009-0038-9.]

Newell, R.I.E., and Koch, E.W., 2004, Modeling seagrass density and distribution in response to changes in turbidity stemming from bivalve filtration and seagrass sediment stabilization: Estuaries, v. 27, no. 5, p. 793–806. [Also available at https://doi.org/10.1007/BF02912041.]

Pham, L.T., Biber, P.D., and Carter, G.A., 2014, Seagrass in the Mississippi and Chandeleur Sounds and problems associated with decadal-scale change detection: Gulf of Mexico Science, v. 32, no. 1, p. 24–43. [Also available at https://doi.org/10.18785/goms.3201.03.]

Santos, R.O., and Lirman, D., 2012, Using habitat suitability models to predict changes in seagrass distribution caused by water management practices: Canadian Journal of Fisheries and Aquatic Sciences, v. 69, no. 8, p. 1380–1388. [Also available at https://doi.org/10.1139/f2012-018.]

Saunders, M.I., Atkinson, S., Klein, C.J., Weber, T., and Possingham, H.P., 2017, Increased sediment loads cause non-linear decreases in seagrass suitability habitat extent: PLoS One, v. 12, no. 11, p. e0187284. [Also available at https://doi.org/10.1371/journal.pone.0187284.]

Shafer, D.J., Maglio, C.K., McConnell, K., Beck, T.M., and Pollock, C.B., 2016b, Characterizing seagrass exposure to light attenuation and turbidity associated with dredging activity in the Gulf Intracoastal Waterway, Sarasota Bay, Florida: Vicksburg, Miss., U.S. Army Corps of Engineers, ERDC TN–DOER–E39, 12 p.

Shafer, D.J., Swannack, T.M., Saltus, C., Kaldy, J.E., and Davis, A., 2016a, Development and validation of a habitat suitability model for the non-indigenous seagrass *Zostera japonica* in North America: Management of Biological Invasions, v. 7, no. 2, p. 141–155. [Also available at https://doi.org/10.3391/mbi.2016.7.2.02.]

Sharma, S., Goff, J., Moody, R.M., Byron, D., Heck, K.L., Jr., Powers, S.P., Ferraro, C., and Cebrian, J., 2016, Do restored oyster reefs benefit seagrasses? An experimental study in the Northern Gulf of Mexico: Restoration Ecology, v. 24, no. 3, p. 306–313. [Also available at https://doi.org/10.1111/rec.12329.]

Thatcher, C.A., Brock, J.C., Danielson, J.J., Poppenga, S.K., Gesch, D.B., Palaseanu-Lovejoy, M., Barras, J.A., Evans, G.A., and Gibbs, A.E., 2016, Creating a Coastal National Elevation Database (CoNED) for science and conservation applications: Journal of Coastal Research, v. SI, no. 76, p. 64–74. [Also available at https://doi.org/10.2112/SI76-007.]

Theuerkauf, S.J., and Lipcius, R.N., 2016, Quantitative validation of a habitat suitability index for oyster restoration: Frontiers in Marine Science, v. 3, no. 64, 9 p. [Also available at https://doi.org/10.3389/fmars.2016.00064.]

Visser, J.M., Duke-Sylvester, S.M., Carter, J., and Broussard, W.P., III, 2013, A computer model to forecast wetland vegetation changes resulting from coastal restoration and protection in coastal Louisiana: Journal of Coastal Research, v. 67, no. sp1, p. 51–59. [Also available at https://doi.org/10.2112/SI_67_4.]

Vittor, B.A., and Associates, Inc., 2004, Mapping of submerged aquatic vegetation in Mobile Bay and adjacent waters of coastal Alabama in 2002: Mobile, Ala., Mobile Bay National Estuary Program, 63 p.

Vittor, B.A., and Associates, Inc., 2005, Historical SAV distribution in the Mobile Bay National Estuary Program area and ranking analysis of potential SAV restoration sites: Mobile, Ala., Mobile Bay National Estuary Program, 17 p.

Vittor, B.A., and Associates, Inc., 2009, Submerged aquatic vegetation mapping in Mobile Bay and adjacent waters of coastal Alabama in 2008 and 2009: Mobile, Ala., Mobile Bay National Estuary Program, 28 p.

Vittor, B.A., and Associates, Inc., 2015, Mapping of submerged aquatic vegetation in Mobile Bay and adjacent waters of coastal Alabama in 2015: Mobile, Ala., Mobile Bay National Estuary Program, 31 p.

Wang, H., Enwright, N.M., Darnell, K.M., LaPeyre, M.K., Cebrian, J., Kim, S.-C., Bunch, B., Stelly, S.J., Couvillion, B.R., Dalyander, P.S., Mickey, R.C., and Segura, M., 2020, Seagrass habitat suitability modeling for the Alabama Barrier Island restoration assessment at Dauphin Island: U.S. Geological Survey data release, https://doi.org/10.5066/P9B32VTE.

Zajac, Z., Stith, B., Bowling, A.C., Langtimm, C.A., and Swain, E.D., 2015, Evaluation of habitat suitability index models by global sensitivity and uncertainty analyses—A case study for submerged aquatic vegetation: Ecology and Evolution, v. 5, no. 13, p. 2503–2517. [Also available at https://doi.org/10.1002/ece3.1520.]

For additional information, contact:
Director, Wetland and Aquatic Research Center
U.S. Geological Survey
700 Cajundome Blvd.
Lafayette, LA 70506

For additional information, visit
https://www.usgs.gov/centers/wetland-and-aquatic-research-center-warc

Publishing support provided by the Rolla Publishing Service Center

ISSN 2331-1258 (online)
https://doi.org/10.3133/ofr20201003